Robust Tracking Control and Signal Estimation for Networked Control Systems

by

Hui Zhang

B.Sc., Harbin Institute of Technology, 2006

M.Sc., Jilin University, 2008

A Dissertation Submitted in Partial Fulfillment of the

Requirements for the Degree of

DOCTOR OF PHILOSOPHY

in the Department of Mechanical Engineering

Robust Tracking Control and Signal Estimation for Networked Control Systems

by

Hui Zhang

B.Sc., Harbin Institute of Technology, 2006

M.Sc., Jilin University, 2008

Supervisory Committee

Dr. Yang Shi, Supervisor

(Department of Mechanical Engineering)

Dr. Afzal Suleman, Departmental Member

(Department of Mechanical Engineering)

Dr. Xiaodai Dong, Outside Member

(Department of Electrical & Computer Engineering)

Supervisory Committee

Dr. Yang Shi, Supervisor

(Department of Mechanical Engineering)

Dr. Afzal Suleman, Departmental Member

(Department of Mechanical Engineering)

Dr. Xiaodai Dong, Outside Member

(Department of Electrical & Computer Engineering)

ABSTRACT

Networked control systems (NCSs) are known as distributed control systems (DCSs) which are based on traditional feedback control systems but closed via a real-time communication channel. In an NCS, the control and feedback signals are exchanged among the system's components in the form of information packages through the communication channel. The research of NCSs is important from the application perspective due to the significant advantages over the traditional point-to-point control. However, the insertion of the communication links would also bring challenges and constraints such as the network-induced delays, the missing packets, and the inter symbol interference (ISI) into the system design. In order to tackle these issues and move a step further toward industry applications, two important design problems are

investigated in the control areas: Tracking Control (Chapter 2–Chapter 5) and Signal Estimation (Chapter 6–Chapter 8).

With the fact that more than 90% of control loops in industry are controlled by proportional-integral-derivative (PID) controllers, the first work in this thesis aims to propose the design algorithm on PID controllers for NCSs. Such a design will not require the change or update of the existing industrial hardware, and it will enjoy the advantages of the NCSs. The second motivation is that, due to the network-induced constraints, there is no any existing work on tuning the PID gains for a general NCS with a state-space model. In Chapter 2, the PID tracking control for multi-variable NCSs subject to time-varying delays and packet dropouts is exploited. The $\mathcal{H}_\infty$ control is employed to attenuate the load disturbance and the measurement noise.

In Chapter 3, the probabilistic delay model is used to design the delay-scheduling tracking controllers for NCSs. The tracking control strategy consists of two parts: (1) the feedforward control can enhance the transient response, and (2) the feedback control is the digital PID control. In order to compensate for the delays on both communication links, the predictive control scheme is adopted.

To make full use of the delay information, it is better to use the Markov chain to model the network-induced delays and the missing packets. A common assumption on the Markov chain model in the literature is that the probability transition matrix is precisely known. However, the assumption may not hold any more when the delay is time-varying in a large set and the statistics information on the delays is inadequate. In Chapter 4, it is assumed that the transition matrices are with partially unknown elements. An observer-based robust energy-to-peak tracking controller is designed for the NCSs.

In Chapter 5, the step tracking control problem for the nonlinear NCSs is investigated. The nonlinear plant is represented by Takagi-Sugeno (T-S) fuzzy linear

model. The control strategy is a modified PI control. With an augmentation technique, the tracking controller design problem is converted into an $\mathcal{H}_\infty$ optimization problem. The controller parameters can be obtained by solving non-iterative linear matrix inequality conditions.

The state estimation problem for networked systems is explored in Chapter 6. At the sensor node, the phenomenon of multiple intermittent measurements is considered for a harsh sensing environment. It is assumed that the network-induced delay is time-varying within a bounded interval. To deal with the delayed external input and the non-delayed external input, a weighted $\mathcal{H}_\infty$ performance is defined. A Lyapunov-based method is employed to deal with the estimator design problem. When the delay is not large, the system with delayed state can be transformed into delay-free systems. By using the probabilistic delay model and the augmentation, the $\mathcal{H}_\infty$ filter design algorithm is proposed for networked systems in Chapter 7. Considering the phenomenon of ISI, the signals transmitted over the communication link would distort, that is, the output of the communication link is not the same with the input to the communication link. If the phenomenon occurs in the NCSs, it is desired to reconstruct the signal. In Chapter 8, a robust equalizer design algorithm is proposed to reconstruct the input signal, being robust against the measurement noise and the parameter variations.

Finally, the conclusions of the dissertation are summarized and future research topics are presented.

Contents

List of Tables

List of Figures

ACKNOWLEDGEMENTS

First of all, I would like to express my sincere gratitude to my supervisor Dr. Yang Shi for all his support, guidance and help not only in my research work but also in my personal life. During the past four years, he has been continuously providing me with his inspiration, patience, passion, vision, encouragement, and great freedom in my research. He is an excellent researcher and always targeting at doing world-class research which triggers me to do better and better. He is a trusted friend who always provides good suggestions and comfort whenever I am frustrated and upset. I owe my gratitude to Dr. Aryan Saadat Mehr who was my co-supervisor when I was in the University of Saskatchewan. We had many discussions and he gave valuable comments on my study, research, and writing.

I would like to thank all the thesis committee members, Prof. Afzal Suleman and Prof. Xiaodai Dong for their constructive comments. Special thanks go to Prof. Zuomin Dong for his extraordinary kindness and help whenever I was in need.

During my studies at the University of Saskatchewan and the University of Victoria, I always feel lucky to have a lot of groupmates, officemates and great friends around and I am grateful to their help and encouragement. Bo Yu taught me how to design the robust filter and gave me valuable suggestions on the deduction of linear matrix inequalities. Wutao Yin showed me the usage of LaTex and the programming of Hilbert Huang Transform. Ji Huang taught me how to use the hardware-in-the-loop simulation of the DC motor. Simon Parkinson gave me a lot of meaningful advices on the pronunciation and job hunting. Jian Wu shared his experience in the matrix operation with me. I really enjoyed the group meeting and discussion in ACIPL with Dr. Yang Shi, Dr. Yang Lin, Bo Yu, Huazhen Fang, Dr. Lili Han, Dr. Jie Ding, Jian Wu, Ji Huang, Qiao Zhang, Shurong Chen, Xianhao Yu, Huiping Li, Tina Hung, Xiaotao Liu, Mingxi Liu, Wenbai Li, Yanjun Liu, Ping Cheng, Fuqiang Liu, Bingxian

Mu, S. Doroudgar, Dr. Y. Zhao, Dr. F. Fang, Dr. L. Wei, and Prof. Zexu Zhang. With them, my research perspective becomes wide and my research is "reachable".

I gratefully acknowledge the financial support from the Department of Mechanical Engineering in the University of Saskatchewan, the Natural Sciences and Engineering Research Council of Canada (NSERC), the Department of Mechanical Engineering in the University of Victoria, the Faculty of Graduate Studies (FGS) and the Graduate Students' Society (GSS) in University of Victoria, the Heritage Office Furnishing Scholarship, the Robert W. Ford Graduate Scholarship, the B & C Food Distributors Scholarship, the Jarmila Vlasta Von Drak Thouvenelle Graduate Scholarship, the Albert Hung Chao Hong Scholarship, and the Chinese Government Award for Outstanding Self-financed Students Abroad.

Finally, and most importantly, I would like to thank my parents and my sister. I love them all very much.

List of Abbreviations

BMI	Bilinear Matrix Inequality
CAN	Controller Area Network
DCS	Distributed Control System
FIR	Finite Impulse Response
IAE	Integral of Absolute Error
IIR	Infinity Impulse Response
ISE	Integral of Square Error
ISI	Inter symbol interference
ITAE	Integral of Time-weighted Absolute Error
ITSE	Integral of Time-weighted Square Error
LMI	Linear Matrix Inequality
MIMO	Multiple-Input-Multiple-Output
NCS	Networked Control System
PID	Proportional-Integral-Derivative
QoS	Quality of Service
SISO	Single-Input-Single-Output
SOF	Static Output Feedback
SDS	Smart Distributed System
SMC	Sliding Mode Control
T-S	Takagi-Sugeno
TOD	Try-Once-Discard
VTOL	Vertical Take-Off and Landing
ZOH	Zero-Order Hold

Chapter 1

Introduction

1.1 Networked Control Systems

Networked control systems (NCSs) are known as distributed control systems (DCSs) which are based on traditional feedback control systems but closed via a real-time communication channel. The communication channel may be shared with other nodes outside the control system under consideration [3]. Figure 1.1 is a typical NCS architecture in industry. It can be seen that the controller nodes, the sensor nodes, the actuator nodes, and the monitoring terminal can exchange information mutually via the communication channel. The shared data (control signal or feedback signal) is transmitted over the network medium.

The communication network, acting as a bus, is the backbone of NCSs. It does not only connect each node, but also transmit the binary data to the specified node. Due to the requirement of the real-time implementation in applications, the quality of service (QoS) of NCSs depends on the network communication protocols. Categorizing by the protocol, the widely used networks in control systems are the Ethernet bus [4], with carrier sense multiple access and collision detection (CSMA/CD), token-passing

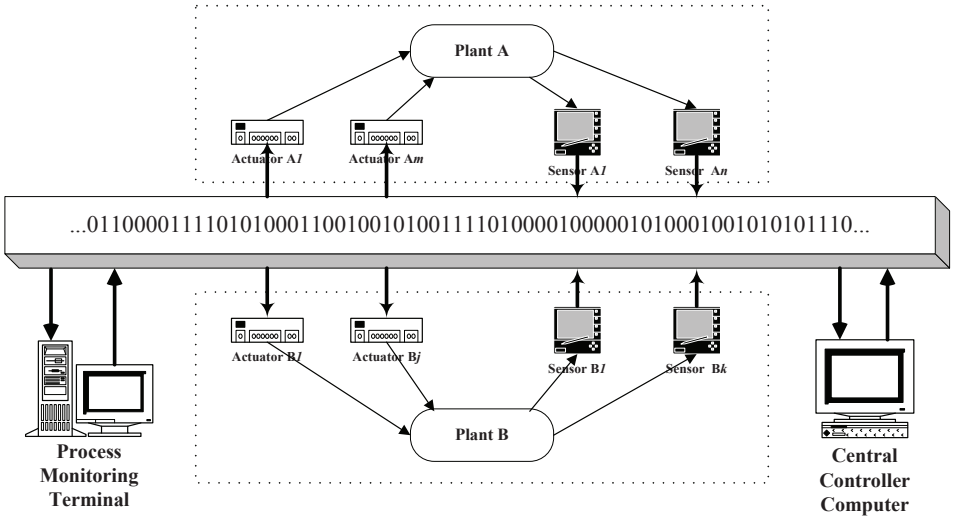

Figure 1.1: A typical NCS architecture in industry [1].

bus (e.g., ControlNet [5]), controller area network (CAN) bus [6, 7] (e.g., DeviceNet and smart distributed system (SDS) [8]), and other types of buses recently defined (e.g. try-once-discard (TOD) [9]).

Ethernet-based network uses the CSMA/CD mechanism, specified in the IEEE 802.3 network standard, for resolving contention on the communication medium [5]. A node occupies the network and transmits the data when the network is idle. When there are two or more nodes listening to the network and deciding to transmit a packet simultaneously, the messages planing to transmit collide. In this case, the messages are corrupted and one or some transmitting nodes stop the data transmission. After waiting for a random length of time, the failed node retries to occupy the network until the message is successfully transmitted [4]. The nodes in the token-passing bus network occupy the network and transmit the messages in an arranged logical order. If one node has no message to send when the token is at the node, it just passes the token to the successor node [5,10]. In this kind of protocol, the maximum waiting time

before sending a message frame can be calculated by the token rotation time [5], that is, the delay of the message is bounded and the network is a deterministic network. CAN was firstly developed and used for the automobile industry in the 1980s by a Germany company–Bosch [11]. It is a serial communication protocol and has been applied in all passenger cars in the world as well as some other time-critical industrial applications. Each node in CAN has a specific priority. If the network is idle, each node can access the network when the message is ready. When two nodes want to transmit the message simultaneously, the node with higher priority can access the network and the node with lower priority becomes a receiver of the node with higher priority. With the arbitration method, there is no congestion in the network and an ongoing transmission is never corrupted. The TOD protocol which employs the dynamic by scheduling allocating network resource based on the need was proposed in [9] for the stability analysis of NCSs. In a TOD network, the node with the greatest weighted error from the last reported value will win the competition for the network resource. If a data packet fails to win the competition for the network access, it will be discarded and new data will be used next time. The protocol was further employed in [12–14].

1.2 Literature Review

Early and comprehensive studies on the NCSs can be seen in [11, 15, 16]. Later, a special issue in IEEE Control Systems Magazine boosted the research on this subject; see the published papers in this issue [5, 17–19]. From then on, NCSs have been extensively investigated in the past ten years and there are a wide range of results in the literature, such as the recent books [20–22], graduation thesis [1, 8, 23–27], and surveys [28, 29]. The enormous attraction of NCSs is due to the emerging challenges

and the broad potential for many industry applications.

The classical feedback control originated from the 19th century [30]. In traditional point-to-point control systems, the components (sensors, actuators, controllers, and monitoring terminals) are locally connected and all the information is reliably transmitted to the monitors and controllers. However, in an NCS, the spatially distributed system components are connected via a communication network. Compared with the traditional point-to-point control (also called centralized control), the NCS has the following significant advantages:

- Reduced system wiring. A network replaces the direct connections among the involved components. Moreover, unnecessary wiring can be eliminated.
- Reduced weight and space. The network decreases the requirement on the space for the nodes. Recently, the trend toward using wireless network further reduces the constraint on the space.
- Effective data sharing and fusion. The controller can easily collect and fuse the collected information. Moreover, the cyber space and physical space are connected, which makes the remote data sharing achievable.
- Low cost and easy implementation. The network can effectively reduce the complexity of systems with economical investment [20].
- Ease of system diagnosis and maintenance and increased system agility [31].

Due to the above distinct advantages, NCSs have been attracting increasing attention and been recognized as one of the key future directions in the area of systems and control [32]. Application examples include, for example, froth flotation process [33], building automation [34,35], inverted pendulum, multi-agent systems and cooperative control [36–41], tele-surgery [42], haptics collaboration over Internet [43], unmanned

aerial vehicles [44], refineries [30], network controlled motors [45–50], automobiles [6], airplanes, and so on.

While enjoying the benefits and advantages brought by NCSs, we also need to consider the constraints induced by the inserted communication network. The major network-induced constraints are listed as follows.

- **Time delay**. The network-induced delay refers to the time difference between the instant when the data is collected and the instant when the data is released at the target node [51]. Since the processing time at the transmitter (pack the message) and the receiver (release the message) is too short compared to the waiting time and transmission time, it usually can be neglected. Thus, the network-induced delay can be obtained with the *time stamp* technique [52]. It is necessary to mention that the network-induced delay is unavoidable no matter which kind of protocol is used. The network-induced delay can be constant, time-varying, or stochastic. When a packet does not arrive at the target node due to the network congestion, the network-induced delay is not infinite since a buffer [53, 54] can be used and the latest available packet will be adopted. Usually, the delay is bounded and the upper bound of the delay can be obtained readily. Moreover, the distribution of the delay can be derived with the statistical information [11, 51, 55–57].

- **Packet dropout**. Packet dropouts arise from transmission errors in physical network links or from buffer overflows due to the network congestion [1, 29]. Sometimes, the packet is discarded in order to improve the QoS of the network. Along with the network-induced delay, packet dropouts could also degrade the performance or even destroy the stability of the closed-loop system. The packet dropouts should be considered especially when the transmission is subject to consecutive multiple packet dropouts [53, 58, 59].

- **Sampling and quantization**. In order to improve the approximation precision, the sampling frequency should be as large as possible. However, a high sampling frequency would increase the network load. A simple strategy is to adopt a low sampling frequency when the network is busy and a high sampling frequency when the network is not busy. Recently, a random sampling period scheme for NCSs was reported in [60]. Meanwhile, when a continuous-time signal is sampled, there is a quantization error between the real value and the sampled one. The quantization error can be modeled as a noise or an uncertainty to the system [61–68]. It is well-known that the uncertainty and noise can deteriorate the performance of designed controllers or filters [69].

- **Inter symbol interference**. Inter symbol interference (ISI) between neighboring symbols occurs in a digital communication system when the bandwidth of the channel is limited but the transmission rate is high [70]. In an ISI communication channel, the presence of ISI distorts the transmitted sequence and increases bit error rates (BERs) in the recovery of the transmitted sequence at the receiver [71]. The ISI is a challenge for the development of a reliable digital communication channel with high transmission rate. From the perspective of applications, it is paramountly important to minimize the negative effect of ISI. The study of mitigating the detrimental effect of ISI has attracted considerable attention during past decades; see [2, 72, 73] and the references therein. An effective yet simple attempt is to design a filter that takes the observations of the ISI channel and reconstructs the input signal. This filter is also called equalizer and the reconstruction process is named as equalization [2, 74–78].

- **Bandwidth limitation**. The bandwidth is the number of bits that an be transmitted per second [51]. Any communication network has a limited bandwidth. The limitation of the bandwidth poses significant constraints on the

operation of NCSs [29]. A great number of efforts have been devoted to determining the minimum bit rate that is needed to achieve the control and filtering objectives [79–88].

Generally, NCSs can be categorized into two types: Time-delay-sensitive NCSs and time-delay-insensitive NCSs [20]. In time-delay-insensitive NCSs, the network-induced delay is not critical for the application. However, when a physical system (especially a high speed system) is connected to a network, it is usually sensitive to the time delay. In this thesis, we focus on the study of time-delay-sensitive NCSs. Although there are many controllers or plants in a complex NCS, it is often common and practical to consider a single loop, that is, there are only one plant, one controller or one estimator in the system.

In the traditional point-to-point control, it is assumed that the signal transmission is ideal, that is, the signal from one component to another is instantaneous. Due to the insertion of the network, this assumption does not hold in NCSs. Hence, affluent results developed for traditional control systems, such as tracking control, robust control, adaptive control, and state estimation, can not be directly applied to NCSs. In the past few years, significant research efforts have been devoted to the problem of developing the control and filtering strategies for NCSs, which are briefly reviewed as follows.

- **Stability and stabilization.** The requirement of stability is the basic but the most important one for control systems. The early work on the stability and stabilization for NCSs were conducted under both continuous-time and discrete-time framework. In the discrete-time framework, there are two types. The first one is that the plant is a continuous-time system and the controller is a discrete-time controller [18]. In this case, the plant is firstly discretized by considering the the network-induced delay from the sensor to the controller [15, 89]. The

other one is that both the plant and the controller are in the discrete-time form; see the papers [31, 52, 55, 90, 91] and the references therein. In the continuous-time framework, the continuous-time plant with a sensor and a network link can be transformed into a continuous-time system with a delayed state [15, 92–99]. Specifically, by considering one or more emerging issues in the NCSs, the analysis of stability and stabilization is presented in [47, 100–115].

- **State estimation.** State estimation is the process of inferring the value of the state (or a combination of the states) of interest from indirect, often inaccurate and uncertain, measurements [116]. The problem of state estimation (also named filtering) is of importance since it has numerous applications in such diverse areas as control systems, fault detection [117–119], navigation and trajectory determination [116, 120], signal processing [121–123], to name a few. The state estimation over networks has other applications such as remote sensing, space exploration, and sensor networks [29]. Recently, the state estimation in a network environment has attracted considerable attention. By modeling the packet dropouts as a Bernoulli process, the Kalman filtering was applied in [124]. A critical value for the dropout rate was derived such that, when the dropout rate is larger than the critical value, the estimation error covariance would become unbounded. By assuming that only one sensor can use the channel at each time step, Kalman filtering for a network-based system with multiple outputs was investigated in [125]. In [126], the state estimation via a recursive Kalman filter for asynchronous communication channels was studied by considering irregular transmission times. The packet dropouts were characterized as a two-state Markov chain in [120, 127–129]. The phenomenon of multiple packet dropouts in the estimation problem was presented in [53, 58]. Since there is no bound on the multiple packet dropouts, an improved filter de-

sign was introduced in [59]. Both network-induced delay and packet dropouts were considered for the NCS filtering problem in [122, 130, 131].

- **Tracking control.** Beyond the requirement of stability, the plant is usually desired to achieve a tracking performance. However, the tracking problem has received relative less attention. In [99], a state-feedback controller was designed such that the output of the closed-loop networked control system can track the output of an virtual reference-generation model. Similar to the strategy in [99], an $\mathcal{H}_2$ output tracking for networked hydraulic system was studied in [132]. However, in practice, it is always required to directly track the specific reference input not the virtually generated output.

1.3 Research Motivations

Though there are numerous results on NCSs in the literature, the design problem for the tracking controller and the signal estimator are not fully studied. The motivations of this thesis are two-fold:

1. **Tracking control**. As mentioned, the tracking problem in the literature has gained relatively less attention. However, this is an important control problem in practical applications. The tracking control in a network environment deserves further research. The main techniques employed in the thesis include modified proportional-integral-derivative (PID) control, feedforward control, preview control, and predictive control. The tracking controllers will be designed for both linear and nonlinear plants. For linear systems, the main work is to modify and improve the controller design algorithms and strategies such that the tracking performance can be guaranteed when the systems are subject to network-induced constraints including the network-induced delays and missing

packets on both communication links from the sensors to the controllers and from the controllers to the actuators. For the nonlinear plant, we firstly utilize the Takagi-Sugeno (T-S) fuzzy model to approximate the nonlinear system. Compared with the linear NCSs, the challenge for nonlinear NCSs lies in that the T-S fuzzy model is involved in the closed-loop systems and should be considered in the stability and the tracking performance analysis.

2. **Signal estimation.** The signal estimation in this thesis consists of the state estimation and the signal reconstruction. Most of the results on the state estimation problem for NCSs are only sufficient conditions. This gives room for further improving the conditions, and thus enhancing the performance. To further reduce the conservativeness is meaningful for the application of state estimation. Since the network-induced delay presents a stochastic distribution property, the strategy for reducing the conservativeness of the filtering results is to incorporate the distribution property into the estimator design. In addition, for the data transmission over a communication channel, it is generally assumed that the control and feedback signals are not distorted. However, the ISI between neighboring symbols occurs in a digital communication system when the bandwidth of the channel is limited but the transmission rate is high [70]. When the phenomenon of ISI occurs, the received signal is not the same as the transmitted signal. The existing results on NCSs may not be effective any more. Therefore, from the perspective of applications and the implementation of NCSs, it is paramountly important to minimize the effect of ISI and reconstruct the input signal to the communication channel.

1.4 Thesis Organization

The thesis is organized as follows. Chapter 1 starts with reviewing the fundamentals of NCSs, the related work, and the research background, and then presents the motivations of the PhD thesis research.

Chapter 2 deals with the design problem of PID controllers for NCSs with polyhedral uncertainties. The load disturbance and measurement noise are both taken into account in the modeling in order to better reflect the practical scenario. By using a novel technique, the design problem of PID controllers is converted into a design problem of output feedback controllers. The goal of this chapter is two-fold: 1) To design the robust PID tracking controller for *practical* model; 2) to develop the robust $\mathcal{H}_\infty$ PID control such that load and reference disturbances can be attenuated with a prescribed level. Sufficient conditions are derived by employing advanced techniques for achieving delay dependence. The proposed controller can be readily designed based on an iterative suboptimal algorithm. Finally, design examples are presented to show the effectiveness of the proposed methods.

In Chapter 3, the combined feedback-feedforward tracking control problem for NCSs under the discrete-time framework is investigated. Network-induced delays, both network links from the sensor to the controller and from the controller to the actuator are considered. We assume that the probability for the occurrence of each delay within a known set is known. We use a predictive control scheme to compensate for the forward delay, and propose to design a controller for each network-induced delay. Using the augmentation technique twice, the tracking problem of NCSs is converted to a feedback control problem for stochastic systems without delays. The stochastic stability and $\mathcal{H}_\infty$ performance of the resulting closed-loop stochastic system are studied. These problems are formulated in terms of a linear matrix inequality (LMI) and a linear matrix equality (LME). Then, an approach of the controller design

is proposed by solving a nonlinear trace minimization problem. Finally, an example on the control of a helicopter model is given to illustrate the proposed design approach.

Chapter 4 is concerned with a tracking controller design problem for discrete-time networked predictive control systems. The control law used here is a combined state-feedback control and integral control. Since not all the states are available in practice, a local Luenberger observer is utilized to estimate the state vector. The measured output and the estimated state vector are packed together and transmitted to the tracking controller via a communication channel with limited capacity. Meanwhile, the control signal is also transmitted through a communication network. Networked-induced delays on both links are considered and modeled by Markov chains. Moreover, it is assumed that the elements in the Markov transition matrices are subject to uncertainties. In order to fully compensate for the network-induced delay, the controller generates a sequence of control signals which are dependent on each possible delays on the feedforward channel. With the augmenting technique twice, under the proposed control law, we obtain delay-free stochastic systems and the controlled output is the tracking error. Sufficient conditions are provided for assuring the energy-to-peak performance of the closed-loop systems. The feedback gains of the controller can be derived by solving a minimization problem. An illustrative example is given to show the effectiveness of the proposed design method.

The step tracking control problem for discrete-time nonlinear systems in a networked environment with a limited capacity is addressed in Chapter 5. The nonlinear system is represented by a T-S fuzzy system, and the network-induced delay is considered. In order to compensate for the delay effect and eliminate the tracking error, we employ advanced techniques including the predictive control and the integral control. Moreover, a quadratic cost function, including terms related to the performance of the system and the actuating capacity, is proposed. We assume that the lumped

network-induced delay lies within a known set, and that the occurrence probability for each element in the set is known *a priori*. Then, the delay information will be incorporated into the delay-dependent tracking controller. We consider the predictive and integral tracking controllers which are dependent on both the delay and the fuzzy-weighting-function. Then, an augmentation method will be used to convert the problem into designing state-feedback controllers for stochastic fuzzy systems with delayed states. In addition, the quadratic cost function is transformed into the 2-norm of a constructed controlled output. We study the exponential mean-square stability and $\mathcal{H}_\infty$ performance of the resulting stochastic system. It will be shown that the parameters of the tracking controller can be derived by solving an optimization problem. An example on an electro-mechanical system illustrates the efficacy of the proposed design method.

In Chapter 6, the robust weighted $\mathcal{H}_\infty$ filtering problem for networked systems with intermittent measurements under the discrete-time framework is studied. Multiple outputs of the plant are measured by separate sensors, each of which has a specific failure rate. Network-induced delays, packet dropouts and network-induced disorder phenomena are all incorporated in the modeling of the network link. The resulting closed-loop system involves both delayed noise and non-delayed noise. In order to make full use of the delayed information, we define a weighted $\mathcal{H}_\infty$ performance index. Sufficient delay-dependent and parameter-dependent conditions for the existence of the filter and the solvability of the addressed problem are given via a set of LMIs. Two simulation examples are presented to illustrate the relationship between the minimal performance level and the weighting factor, which shows the effectiveness of the proposed method.

Chapter 7 considers the state estimation problem for discrete-time systems in a network environment. Specifically, the network-induced delay from the sensor node to

the estimator node is modeled as a finite set of delays with corresponding occurrence probabilities. The design of $\mathcal{H}_\infty$ switched filters is proposed. The switching is performed according to the detected time delay. The occurrence probability of the delay is incorporated into the filter design, which can improve the filtering performance. Simulation studies and comparisons illustrate the effectiveness and the performance improvement of the proposed design method.

In Chapter 8, the problem of equalization for communication channels with ISI is investigated in this paper. One practical yet challenging constraint for a channel with high transmission rate is incorporated into the modeling of the equalization system: The communication channel is subject to uncertainties which are assumed to be within a polytope with finite vertices. By using the augmentation method, the filtering error system of the equalization problem is also characterized as a system with polytopic uncertainties. Sufficient conditions on the stability and the $\mathcal{H}_\infty$ performance for the filtering error system are obtained. A design method for the equalizer is proposed such that the filtering error system can achieve minimal $\mathcal{H}_\infty$ performance index even with the channel uncertainties. Two illustrative design examples demonstrate the design procedure and the effectiveness of the proposed method.

Chapter 9 summarizes the work in this thesis, and presents some potential future research directions.

Chapter 2

Robust $\mathcal{H}_\infty$ PID Control for Multivariable Networked Control Systems with Disturbance/Noise Attenuation

2.1 Introduction

The proportional-integral-derivative (PID) controller has dominated the feedback control applications in industry since its introduction in the 1940s. A survey showed that more than 90% of all control loops in use recently were PID-based, though considerable other advanced control theories and practical design techniques had been proposed [133]. The most significant advantage of PID controllers is their simplicity. PID controllers provide good performance for the majority of industrial plants, e.g. chemical processes, motor drives, automotive, magnetic and optic memories, flight vehicles, and so on. With the development of many new control design techniques

and applications, two questions arise: (1) How to develop a new robust PID control design technique while still enjoying the simplicity of the PID control structure and maintaining the existing PID control loops in applications? (2) How to apply the robust PID control to the emerging NCSs?

2.1.1 Background, Related Work and Motivations

There are two main approaches to finding a tuned PID controller for a process. (1) The first approach is based on the transfer function of the process, such as Integral of Time-weighted Absolute Error (ITAE), Internal Mode Control (IMC) and direct synthesis tuning methods. Most of these methods optimize the PID controller parameters based on the step response of a single loop [134]. However, in practice, many processes are multivariable, which makes the controller design even harder since the input and output variables are interacted. In this case, decentralized PID controllers are usually used via an iterative algorithm [133]. When the dimension of the process output is large, too many decentralized controllers would increase the cost of implementation, maintenance and energy supply. Furthermore, for this approach, it is difficult to consider simultaneously the uncertainty in the transfer function, the load disturbance and the measurement noise, which are inevitable in application processes. (2) The second approach to design a PID controller is based on the state-space model of the process. Based on the state-space model, it is convenient to deal with the model uncertainties and the external noise for multivariable systems. In the literature, the problem of PID controller design for continuous-time plants was transformed into a problem of static output feedback (SOF) controller design, and then the controller can be designed by using the well developed linear matrix inequality (LMI) technique; see [135–139]. In these papers, the reference signal was not incorporated into the controller design. However, in order to further enhance the tracking performance

with disturbance/noise attenuation, it is desirable to incorporate the reference signal, load disturbance, and measurement noise into the controller design.

On another industrial application frontier, NCSs have attracted increasing attention in the past few years, due to some distinct advantages over local control systems; see [31, 52, 94, 95, 131, 140, 141]. As many efforts from both academia and industry have been devoted to the wireless automation technologies, such as Wireless HART and ISA 100, NCSs will have a broad application future in industry. While welcoming and embracing new technologies, the lower implementation cost and less risk would be the first consideration by control practitioners in industry. Since most of the closed-loop control systems use the PID loops, it would be a great advantage if the newly developed NCSs could still make use of the existing PID control loops supplemented with improved design technique suitable for the network environment. The topic of PID control for NCSs has been tackled in [142, 143]. The existing work mainly used cost functions of the tracking error with criteria such as ITAE, Integral of Absolute Error (IAE), Integral of Square Error (ISE) or Integral of Time-weighted Square Error (ITSE). Nowadays, the technique of LMI has played an important role in the control theory and applications since it is convenient to deal with the uncertainties, time delays and external disturbance. However, there are few results on PID control for NCSs based on LMI technique. This motivates us to develop an approach to systematically tune the PID parameters such that the controller would work well in a network environment with network-induced constraints including delays and missing packets. To the best of our knowledge, the robust PID design for NCSs has not been fully studied in the literature, which is the focus of this chapter.

2.1.2 Research Objectives

In this chapter, we investigate the problem of robust $\mathcal{H}_\infty$ PID tracking control for NCSs. The main objective is to design the robust PID tracking control for *practical* models. In the control law, not only the reference (set point), but also the "anti-derivative kick" feature [134] is considered. To have a more realistic model, the load disturbance and measurement noise are both incorporated. For the modeling of the network, bothnetwork-induced delays and missing packets over the sensor-to-controller (S-C) link and the controller-to-actuator (C-A) link are considered. Each link has a buffer [53], which can make sure that the latest packet will be used at the controller or actuator node.

The chapter is organized as follows. The problem formulation for the robust $\mathcal{H}_\infty$ PID control problem in a network environment will be presented in Section 2.2. In Section 2.3, the stability is analyzed and the design methods of the robust PID controller for the stabilization and $\mathcal{H}_\infty$ control are developed. Four examples are presented in Section 2.4 and Section 2.5 concludes the chapter.

Notation: The notations used in this thesis are fairly standard. Superscript 'T' indicates matrix transposition; $\mathcal{E}\{\cdot\}$ stands for the expectation of the event $\{\cdot\}$; $\mathbb{R}^n$ denotes the n-dimensional Euclidean space; $l_2[0,\infty)$ is the space of square-summable infinite sequences, and for $\omega(k) \in l_2[0,\infty)$, the norm is given by $\|\omega\|_2 = \sqrt{\left(\sum_0^\infty |\omega(k)|^2\right)}$, which (its square) is associated with the energy of the sequence. In addition, in symmetric block matrices or long matrix expressions, we use $*$ as an ellipsis for the terms that are introduced by symmetry and $\text{diag}\{\cdots\}$ as a block-diagonal matrix. Matrices, if their dimensions may not be explicitly stated, are assumed to be compatible for algebraic operations.

2.2 Problem Formulation and Preliminaries

Consider a typical PID control system in a network environment as shown in Figure 2.1. The physical plant with parameter uncertainties is controlled by a remote

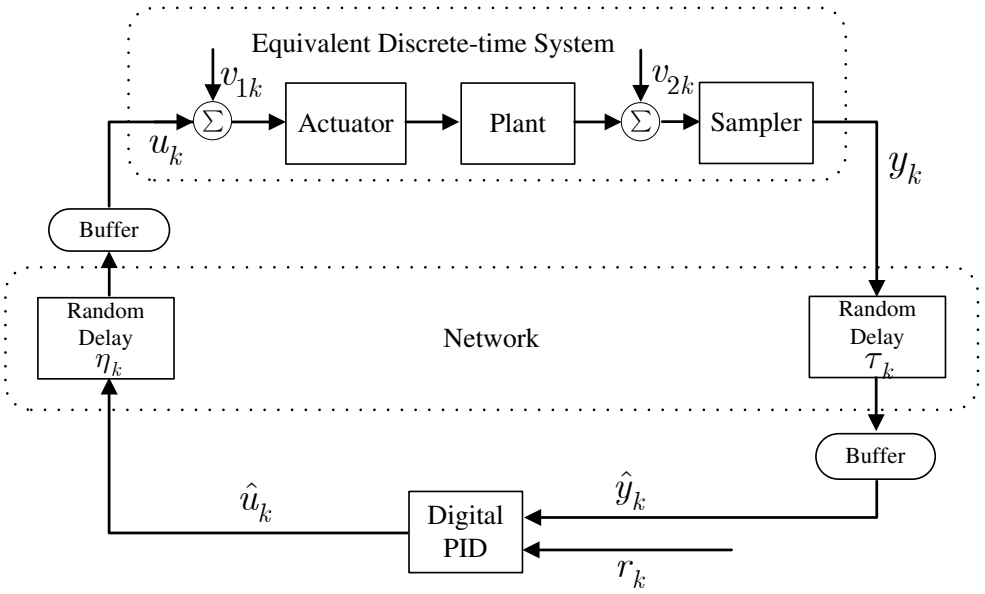

Figure 2.1: A typical PID control in a network environment.

digital PID controller via network links. The output of the plant is measured at a fixed sampling rate. Then the measured data is packed and transmitted through the network link to the PID controller. Two buffers are introduced to the NCS setup to store the received packets and provide the most recent packets to the controller and the actuator, respectively. In practice, it is inevitable to have the external disturbance on the actuator and the measurement noise on the sensor, therefore it is quite demanding to incorporate both of these factors to the system model. It is noticed that the actuator disturbance and the measurement noise have not been fully considered for NCSs in the literature. The equivalent discrete-time system can be represented

by the following linear system:

$$\begin{cases} x_{k+1} = A(\alpha)x_k + B(\alpha)(u_k + v_{1k}), \\ y_k = C(\alpha)x_k + v_{2k}, \end{cases} \tag{2.1}$$

where k is the sampling instant, $x_k \in \mathbb{R}^n$ is the state vector of the system, $y_k \in \mathbb{R}^p$ is the measurement of the plant output, $u_k \in \mathbb{R}^m$ is the control action, $v_{1k} \in \mathbb{R}^m$ is the disturbance or noise of the input at the actuator node, and $v_{2k} \in \mathbb{R}^p$ denotes the sequence of the measurement noise. Additionally, we assume that v_{1k} and v_{2k} are both $l_2[0,\ \infty)$ bounded.

Practical control systems unavoidably include model uncertainties due to inaccurate modeling, component aging or parameter variations. Assume that the matrices $A(\alpha), B(\alpha), \text{and } C(\alpha)$ are not precisely known, but lie within a given convex polyhedral uncertainties domain $\mathfrak{M}$ of s vertices. The domain $\mathfrak{M}$ is characterized using barycentric coordinates as:

$$\mathfrak{M} := \left\{ \Omega(\alpha) \,\middle|\, \Omega(\alpha) = \sum_{i=1}^{s} \alpha_i \Omega_i; \sum_{i=1}^{s} \alpha_i = 1, \alpha_i \geq 0 \right\}.$$

Note that $\Omega_i := (A_i, B_i, C_i),\ i = 1, \cdots, s$, representing the vertices of the polytope, are known matrices with compatible dimensions. The plant model with parameter uncertainties can be characterized by the combination of these vertices.

2.2.1 Modeling of the Network-induced Delays

Network-induced delays and packet dropouts are inevitable in NCSs because of limited bit rate of the communication channel, or signal processing and transmission. As shown in Figure 2.1, bounded random variables τ_k and η_k refer to the network-induced delay occurring on the S-C link and the C-A link, respectively. Thanks to the use of

the buffer, the controller and the actuator can obtain the most recent packets, that is,

$$\begin{cases} \hat{y}_k = y_{k-\tau_k}, \\ \tau_{k+1} \leq \tau_k + 1, \end{cases} \tag{2.2}$$

and

$$\begin{cases} u_k = \hat{u}_{k-\eta_k}, \\ \eta_{k+1} \leq \eta_k + 1, \end{cases} \tag{2.3}$$

where $\hat{y}_k$ is the packet that is adopted by the digital PID controller, τ_k denotes the delay between the current time instant k and the time stamp of the adopted packet at the controller node, $\hat{u}_k$ is the output sequence of the controller, and η_k represents the delay between the current time instant k and the time stamp of the adopted packet at the actuator node.

It is difficult to synchronize the plant and the controller for an NCS. Thus it is assumed that the controller is event-driven. When the controller receives a transmitted packet, the time instant information when this message was sent out by the sensor can be obtained from the time stamp. Define the tracking error as

$$\hat{e}_k = r_{k-\tau_k} - \hat{y}_k = r_{k-\tau_k} - y_{k-\tau_k}. \tag{2.4}$$

It is well known that a digital PID control law considering the "anti-derivative kick" is of the following form:

$$\hat{u}_k = K_p \hat{e}_k + K_i \sum_{i=0}^{k-1} \hat{e}_i + K_d(\hat{y}_{k-1} - \hat{y}_k). \tag{2.5}$$

Here, K_p, K_i, and K_d are proportional, integral, and derivative gains, respectively.

Remark 2.1. *In an NCS, the network-induced delay could result in the mixed order of packets. In this case, it is advantageous to use the most recent data which is stored*

in the buffer. When new packets arrive at the buffer, after a comparison, the most recent data, which may be previously stored data or newly received packets, would be stored in the buffer and sent to the controller or the actuator to update the input. Meanwhile, other old packets would be discarded. Although it is assumed that the delay occurring on each link is time-varying with equal probabilities, the delayed instants of the inputs at the controller node or actuator node show different probabilities. It follows from (2.2) and (2.3) that the delay of the used data at time $k+1$ is no larger than the delay at the time instant k plus 1. This property shows that the probability of large delays is less than that of small delays at the controller and the actuator nodes. In other words, the buffers can improve the reliability of the network. In the recent literature, similar analysis has been proposed, e.g. the modeling of packet dropouts was discussed in [53] and a logic zero-order hold (ZOH) was proposed in [90]. In this chapter, two buffers are employed to deal with the mixed order problem induced by the network.

Remark 2.2. *In the above problem formulation, only network-induced delays are considered. When several consecutive packets are lost in the transmission, the event-driven controller or the actuator will hold the lastly adopted signal. From this perspective, the phenomenon of the network-induced packet dropouts can be appropriately characterized by the model of network-induced delays.*

2.2.2 Transforming the PID Controller into an SOF Controller

In order to formulate the problem of PID controller design into a problem of SOF control for an augmented system, let us define a new state vector $\bar{x}_k^{\mathrm{T}} := \left[\begin{array}{ccc} x_k^{\mathrm{T}}, & \sum\limits_{i=0}^{k-1} e_i^{\mathrm{T}}, & y_{k-1}^{\mathrm{T}} \end{array} \right]$ and a new output sequence $\bar{y}_k^{\mathrm{T}} := \left[\begin{array}{ccc} e_k^{\mathrm{T}}, & \sum\limits_{i=0}^{k-1} e_i^{\mathrm{T}}, & (y_{k-1} - y_k)^{\mathrm{T}} \end{array} \right]$. Here, e_k represents

the tracking error of a system with a local PID controller, i.e., $e_k := r_k - y_k$. The augmented system can be written as the following compact form:

$$\begin{cases} \bar{x}_{k+1} = \bar{A}(\alpha)\bar{x}_k + \bar{B}(\alpha)u_k + \bar{B}_1(\alpha)\omega_k, \\ \bar{y}_k = \bar{C}(\alpha)\bar{x}_k + \bar{D}\omega_k, \end{cases} \tag{2.6}$$

where

$$\bar{A}(\alpha) = \begin{bmatrix} A(\alpha) & 0 & 0 \\ -C(\alpha) & I & 0 \\ C(\alpha) & 0 & 0 \end{bmatrix}, \ \bar{B}(\alpha) = \begin{bmatrix} B(\alpha) \\ 0 \\ 0 \end{bmatrix}, \bar{B}_1(\alpha) = \begin{bmatrix} 0 & B(\alpha) & 0 \\ I & 0 & -I \\ 0 & 0 & I \end{bmatrix},$$

$$\omega_k = \begin{bmatrix} r_k \\ v_{1k} \\ v_{2k} \end{bmatrix}, \ \bar{C}(\alpha) = \begin{bmatrix} -C(\alpha) & 0 & 0 \\ 0 & I & 0 \\ -C(\alpha) & 0 & I \end{bmatrix}, \ \bar{D} = \begin{bmatrix} I & 0 & -I \\ 0 & 0 & 0 \\ 0 & 0 & -I \end{bmatrix}.$$

Note that the control signal u_k is the delayed SOF of the augmented system, that is,

$$u_k = \hat{u}_{k-\eta_k} = K\bar{y}_{k-d_k}, \tag{2.7}$$

where $K := [K_p, \ K_i, \ K_d]$, and $d_k = \tau_k + \eta_k$. Here, the variable d_k, an integer, represents the overall network-induced delays on both S-C and C-A links. It is assumed that d_k is bounded and lies within an interval, i.e.,

$$0 \leq d_1 \leq d_k \leq d_2 < \infty.$$

Here, d_1 and d_2 are two known integers. Moreover, $\bar{d}$ is used to represent $d_2 - d_1$, that is, $\bar{d} := d_2 - d_1$. It follows from (2.2) and (2.3) that the time-varying d_k satisfies

$$d_{k+1} \leq d_k + 2. \tag{2.8}$$

2.2.3 $\mathcal{H}_\infty$ Optimization

The controlled output vector is chosen as

$$\bar{z}_k = \bar{E}\bar{x}_k + \bar{F}u_k, \tag{2.9}$$

where $\bar{E} := \bar{R}[\ 0 \quad I \quad 0\ ]$, $\bar{R}$ and $\bar{F}$ are weighting factors. Thus the design problem of the PID controller for the NCS reduces to the design of an SOF controller. By substituting (2.7) into (2.6) and combining (2.9), the closed-loop control system can be expressed as the following form

$$\begin{cases} \bar{x}_{k+1} = \bar{A}(\alpha)\bar{x}_k + \bar{B}(\alpha)K\bar{C}(\alpha)\bar{x}_{k-d_k} + \bar{B}(\alpha)K\bar{D}\omega_{k-d_k} + \bar{B}_1(\alpha)\omega_k, \\ \bar{z}_k = \bar{E}\bar{x}_k + \bar{F}K\bar{C}(\alpha)\bar{x}_{k-d_k} + \bar{F}K\bar{D}\omega_{k-d_k}, \\ \bar{x}_k = \phi_k, \quad k = -d_2,\ -d_2+1, \ldots 0, \end{cases} \tag{2.10}$$

where $\phi_k,\ k = -d_2,\ -d_2+1, \ldots 0$, are initial conditions.

Remark 2.3. *In (2.6), since $\alpha_1 + \alpha_2 + \cdots + \alpha_s = 1$, $\bar{A}(\alpha)$ can be rewritten as*

$$\begin{aligned} \bar{A}(\alpha) &= \begin{bmatrix} A(\alpha) & 0 & 0 \\ -C(\alpha) & I & 0 \\ C(\alpha) & 0 & 0 \end{bmatrix} = \begin{bmatrix} \sum_{i=1}^s \alpha_i A_i & \sum_{i=1}^s \alpha_i 0 & \sum_{i=1}^s \alpha_i 0 \\ -\sum_{i=1}^s \alpha_i C_i & \sum_{i=1}^s \alpha_i I & \sum_{i=1}^s \alpha_i 0 \\ \sum_{i=1}^s \alpha_i C_i & \sum_{i=1}^s \alpha_i 0 & \sum_{i=1}^s \alpha_i 0 \end{bmatrix} \\ &= \sum_{i=1}^s \alpha_i \begin{bmatrix} A_i & 0 & 0 \\ -C_i & I & 0 \\ C_i & 0 & 0 \end{bmatrix} = \sum_{i=1}^s \alpha_i \bar{A}_i. \end{aligned}$$

Thus, $\bar{A}(\alpha)$ linearly depends on the uncertainties. The augmentation does not increase the vertices of the polytope.

It is worthwhile noting that, in the closed-loop control system in (2.10), the time-

varying delay d_k is not only incorporated in the state, but also in the augmented noise. In addition, both delay-free and delayed noise vectors appear in the state equation of the system in (2.10). In order to take the delayed noise term into account, we introduce the following definition.

Definition 2.1. *Given a positive scalar γ, the closed-loop control system in (2.10) is said to be robustly asymptotically stable with a prescribed $\mathcal{H}_\infty$ performance γ, if it is asymptotically stable and*

$$\|\bar{z}\|_2^2 < \gamma^2 \|\omega\|_2^2 + \gamma^2 \|\omega_d\|_2^2 \tag{2.11}$$

for all nonzero $\omega_k \in l_2[0,\infty)$ subject to the zero initial condition and all admissible uncertainties, where $\|\bar{z}\|_2^2 := \sum_{k=0}^{\infty} \left(\bar{z}_k^{\mathrm{T}} \bar{z}_k\right)$, $\|\omega\|_2^2 := \sum_{k=0}^{\infty} \left(\omega_k^{\mathrm{T}} \omega_k\right)$, and $\|\omega_d\|_2^2 := \sum_{k=0}^{\infty} \left(\omega_{k-d_k}^{\mathrm{T}} \omega_{k-d_k}\right)$. Note that $\|\omega\|_2^2$ is associated with the energy of the augmented noise ω_k, and $\|\bar{z}\|_2^2$ is the energy of the controlled output. Hence it is also a type of energy-to-energy performance index.

The main objective of this chapter is to design a remote PID controller of the form in (2.5) such that, for all admissible polyhedral uncertainties and time-varying delays, the closed-loop control system in (2.10) is robustly asymptotically stable and a prescribed $\mathcal{H}_\infty$ performance γ is achieved. More specifically, the following two issues are to be discussed.

O1. *Robust PID stabilization*: To design a remote digital PID controller for an unstable networked control plant, such that the closed-loop system, subject to network-induced delays and missing packets, is asymptotically stable and robust against model uncertainties.

O2. *Robust $\mathcal{H}_\infty$ PID control*: Given a positive constant γ, to design a PID controller

for an NCS, such that the system in (2.10) is robustly asymptotically stable with $\mathcal{H}_\infty$ attenuate level γ.

2.3 Main Results

In this section, the problems of robust PID stabilization and robust $\mathcal{H}_\infty$ PID control for an unstable NCS with parameter uncertainties will be presented.

2.3.1 Robust PID Stabilization

In this subsection, we will derive sufficient conditions under which the closed-loop system in (2.10) is robustly asymptotically stable. Based on the stability analysis, an algorithm will be developed to design the remote PID controller to stabilize an unstable NCS in Figure 2.1.

Theorem 2.1. *Consider the PID control setup in a network environment, as shown in Figure 2.1. The unforced system in (2.10) is robustly asymptotically stable if there exist matrices* $P = P^{\mathrm{T}} > 0$, $Q(\alpha) = Q(\alpha)^{\mathrm{T}} > 0$, $Z = Z^{\mathrm{T}} > 0$, $S_1(\alpha)$, $S_2(\alpha)$, $M_1 = M_1^{\mathrm{T}} > 0$, $M_2 = M_2^{\mathrm{T}} > 0$ *and* K *such that the following condition is satisfied*

$$\mathcal{M}(\alpha) = \begin{bmatrix} \Phi_{11} & * & * & * & * \\ -S_1^{\mathrm{T}}(\alpha) + S_2(\alpha) & \Phi_{22} & * & * & * \\ S_1^{\mathrm{T}}(\alpha) & S_2^{\mathrm{T}}(\alpha) & -Z/d_2 & * & * \\ \bar{A}(\alpha) & \bar{B}(\alpha)K\bar{C}(\alpha) & 0 & -M_1 & * \\ \bar{A}(\alpha) - I & \bar{B}(\alpha)K\bar{C}(\alpha) & 0 & 0 & -M_2/d_2 \end{bmatrix} < 0, \quad (2.12)$$

where

$$\Phi_{11} = -P + (\bar{d}+2)Q(\alpha) + \mathrm{sym}(S_1(\alpha)),$$
$$\Phi_{22} = -\mathrm{sym}(S_2(\alpha)),$$
$$PM_1 = I \text{ and } ZM_2 = I.$$

Proof: Let $\nu_k := \bar{x}_{k+1} - \bar{x}_k$ and $\Theta_k := \left[\bar{x}_k^{\mathrm{T}}, \bar{x}_{k-1}^{\mathrm{T}}, \bar{x}_{k-2}^{\mathrm{T}}, \cdots, \bar{x}_{k-d_2}^{\mathrm{T}}\right]^{\mathrm{T}}$. Choose a Lyapunov functional candidate for the unforced state-noise-delayed system in (2.10) as follows:

$$V_k\left(\Theta_k\right) : = V_{1,k} + V_{2,k} + V_{3,k}, \tag{2.13}$$

where

$$V_{1,k} := \bar{x}_k^{\mathrm{T}} P \bar{x}_k,$$
$$V_{2,k} := \sum_{j=-d_2}^{-1} \sum_{i=k+j}^{k-1} \nu_i^{\mathrm{T}} Z \nu_i,$$
$$V_{3,k} := \sum_{i=k-d_k}^{k-1} \bar{x}_i^{\mathrm{T}} Q(\alpha) \bar{x}_i + \sum_{j=-d_2}^{-d_1} \sum_{i=k+j-1}^{k-1} \bar{x}_i^{\mathrm{T}} Q(\alpha) \bar{x}_i.$$

Here, $P > 0$, $Q(\alpha) > 0$ and $Z > 0$ are Lyapunov matrices to be determined. Under the assumption that the exogenous noise $\omega_k = 0$, the difference of the Lyapunov

functional candidate can be evaluated as follows.

$$
\begin{aligned}
\Delta V_{1,k} =& \bar{x}_k^{\mathrm{T}} \bar{A}(\alpha)^{\mathrm{T}} P \bar{A}(\alpha) \bar{x}_k + 2\bar{x}_k^{\mathrm{T}} A(\alpha)^{\mathrm{T}} P \bar{B}(\alpha) K \bar{C}(\alpha) \bar{x}_{k-d_k} \\
& - \bar{x}_k^{\mathrm{T}} P(\alpha) \bar{x}_k + \bar{x}_{k-d_k}^{\mathrm{T}} (\bar{B}(\alpha) K \bar{C}(\alpha))^{\mathrm{T}} P(\alpha) \bar{B}(\alpha) K \bar{C}(\alpha) \bar{x}_{k-d_k}, \\
\Delta V_{2,k} =& d_2 \nu_k^{\mathrm{T}} Z \nu_k - \sum_{i=k-d_2}^{k-1} \nu_i^{\mathrm{T}} Z \nu_i, \\
\Delta V_{3,k} =& \sum_{i=k+1-d_{k+1}}^{k} \bar{x}_i^{\mathrm{T}} Q(\alpha) \bar{x}_i - \sum_{i=k-d_k}^{k-1} \bar{x}_i^{\mathrm{T}} Q(\alpha) \bar{x}_i \\
& + \sum_{j=-d_2}^{-d_1} \left(\sum_{i=k+j}^{k} \bar{x}_i^{\mathrm{T}} Q(\alpha) \bar{x}_i - \sum_{i=k+j-1}^{k-1} \bar{x}_i^{\mathrm{T}} Q(\alpha) \bar{x}_i \right) \\
=& \bar{x}_k^{\mathrm{T}} Q(\alpha) \bar{x}_k + \bar{x}_{k-d_k-1}^{\mathrm{T}} Q(\alpha) \bar{x}_{k-d_k-1} + \sum_{i=k+1-d_{k+1}}^{k-1} \bar{x}_i^{\mathrm{T}} Q(\alpha) \bar{x}_i - \sum_{i=k-d_k-1}^{k-1} \bar{x}_i^{\mathrm{T}} Q(\alpha) \bar{x}_i \\
& + \sum_{j=-d_2}^{-d_1} \left(\bar{x}_k^{\mathrm{T}} Q(\alpha) \bar{x}_k - \bar{x}_{k+j-1}^{\mathrm{T}} Q(\alpha) \bar{x}_{k+j-1} \right) \\
\leq& \bar{x}_k^{\mathrm{T}} Q(\alpha) \bar{x}_k + \bar{x}_{k-d_k-1}^{\mathrm{T}} Q(\alpha) \bar{x}_{k-d_k-1} + (\bar{d}+1) \bar{x}_k^{\mathrm{T}} Q(\alpha) \bar{x}_k - \sum_{j=k-d_2-1}^{k-d_1-1} \bar{x}_j^{\mathrm{T}} Q(\alpha) \bar{x}_j \\
\leq& (\bar{d}+2) \bar{x}_k^{\mathrm{T}} Q(\alpha) \bar{x}_k.
\end{aligned}
\tag{2.14}
$$

Note that

$$
\nu_k = (\bar{A}(\alpha) - I) \bar{x}_k + \bar{B}(\alpha) K \bar{C}(\alpha) \bar{x}_{k-d_k}, \tag{2.15}
$$

for any matrices $S_1(\alpha)$ and $S_2(\alpha)$ with appropriate dimensions,

$$
\Xi_1 = \left(\bar{x}_k^{\mathrm{T}} S_1(\alpha) + \bar{x}_{k-d_k}^{\mathrm{T}} S_2(\alpha) \right) \left[\bar{x}_k - \bar{x}_{k-d_k} - \sum_{i=k-d_k}^{k-1} \nu_i \right] = 0, \tag{2.16}
$$

and

$$\Xi_2 = \sum_{i=k-d_k}^{k-1} \left(\bar{x}_k^{\mathrm{T}} S_1(\alpha) + \bar{x}_{k-d_k}^{\mathrm{T}} S_2(\alpha) + \nu_i^{\mathrm{T}} Z\right) Z^{-1} \left(\bar{x}_k^{\mathrm{T}} S_1(\alpha) + \bar{x}_{k-d_k}^{\mathrm{T}} S_2(\alpha) + \nu_i^{\mathrm{T}} Z\right)^{\mathrm{T}} \geq 0. \tag{2.17}$$

It follows from (2.13)-(2.17) that

$$\Delta V_k\left(\Theta_k\right) \leq \Delta V_{1,k} + \Delta V_{2,k} + \Delta V_{3,k} + \mathrm{sym}(\Xi_1) + \Xi_2 = \xi_k^{\mathrm{T}} \Pi \xi_k, \tag{2.18}$$

where

$$\begin{aligned}
\xi_k &= \begin{bmatrix} x_k \\ x_{k-d_k} \end{bmatrix}, \ \Pi = \begin{bmatrix} \Pi_{11} & * \\ \Pi_{21} & \Pi_{22} \end{bmatrix}, \\
\Pi_{11} =& \bar{A}^{\mathrm{T}}(\alpha) P \bar{A}(\alpha) - P + \mathrm{sym}(S_1(\alpha)) + d_2 S_1(\alpha) Z^{-1} S_1^{\mathrm{T}}(\alpha) \\
&+ d_2 (\bar{A}(\alpha) - I)^{\mathrm{T}} Z (\bar{A}(\alpha) - I) + (\bar{d} + 2) Q(\alpha), \\
\Pi_{21} =& (\bar{B}(\alpha) K \bar{C}(\alpha))^{\mathrm{T}} [P \bar{A}(\alpha) + d_2 Z(\alpha)(\bar{A}(\alpha) - I)] \\
&+ (-S_1(\alpha)^{\mathrm{T}} + S_2(\alpha)) + d_2 S_2(\alpha) Z^{-1} S_1^{\mathrm{T}}(\alpha), \\
\Pi_{22} =& (\bar{B}(\alpha) K \bar{C}(\alpha))^{\mathrm{T}} [P + d_2 Z] (\bar{B}(\alpha) K \bar{C}(\alpha)) \\
&+ d_2 S_2(\alpha) Z^{-1} S_2^{\mathrm{T}}(\alpha) + \mathrm{sym}(-S_2(\alpha)).
\end{aligned} \tag{2.19}$$

By using Schur complement, for any nonzero ξ_k, it can be seen that the condition in (2.12) implies

$$\Delta V_k\left(\Theta_k\right) < 0.$$

Therefore, if the condition in (2.12) holds, the unforced system in (2.10) is asymptotically stable. The proof is completed. □

Observe that, in Theorem 2.1, the matrices $Q(\alpha)$, and $S_l(\alpha)$, $l = 1, 2$, depend

on system uncertainties. Therefore, Theorem 2.1 can not be used to design the controller directly. A commonly used approach is to assume that these matrices are of the following form [144, 145],

$$Q(\alpha) = \sum_{i=1}^{s} \alpha_i Q_i \text{ and } S_l(\alpha) = \sum_{i=1}^{s} \alpha_i S_{l,i}. \tag{2.20}$$

Here, Q_i, and $S_{l,i}$, $\forall i = 1, \cdots, s,\ l = 1, 2$, are a set of corresponding matrices for each vertex of the polytope for the augmented system (2.10). Under this assumption, we have the following theorem.

Theorem 2.2. *Consider the PID control setup in a network environment, as shown in Figure 2.1. The unforced state-noise-delayed system in (2.10) is robustly asymptotically stable if there exist matrices* $P = P^{\mathrm{T}} > 0$, $Q_i = Q_i^{\mathrm{T}} > 0$, $Z = Z^{\mathrm{T}} > 0$, $S_{1,i}$, $S_{2,i}$, $M_1 = M_1^{\mathrm{T}} > 0$, $M_2 = M_2^{\mathrm{T}} > 0$ *and* K *such that the following condition is achievable*

$$\mathcal{M}_{i,j} + \mathcal{M}_{j,i} < 0, \forall\ i = 1, \cdots, s,\ j = i, \cdots, s, \tag{2.21}$$

where

$$\mathcal{M}_{i,j} = \begin{bmatrix} \Phi_{11} & * & * & * & * \\ -S_{1,i}^{\mathrm{T}} + S_{2,i} & \Phi_{22} & * & * & * \\ S_{1,i}^{\mathrm{T}} & S_{2,i}^{\mathrm{T}} & -Z/d_2 & * & * \\ \bar{A}_i & \bar{B}_i K \bar{C}_j & 0 & -M_1 & * \\ \bar{A}_i - I & \bar{B}_i K \bar{C}_j & 0 & 0 & -M_2/d_2 \end{bmatrix},$$

$$\Phi_{11} = -P + (\bar{d} + 2)Q_i + \mathrm{sym}(S_{1,i}),$$

$$\Phi_{22} = -\mathrm{sym}(S_{2,i}),$$

$$PM_1 = I \text{ and } ZM_2 = I.$$

Proof: Under the assumption in (2.20), we have

$$\mathcal{M}(\alpha) = \sum_{i=1}^{s} \alpha_i^2 \mathcal{M}_{i,i} + \sum_{i=1}^{s-1} \sum_{j=i+1}^{s} \alpha_i \alpha_j (\mathcal{M}_{i,j} + \mathcal{M}_{j,i}). \tag{2.22}$$

Condition (2.21) can guarantee the negative-definiteness of $\mathcal{M}_{i,i}$ and $\mathcal{M}_{i,j} + \mathcal{M}_{j,i}$, $\forall\ 1 \leq i \leq j \leq s$. Thus, it can be concluded that $\mathcal{M}(\alpha) < 0$. From Theorem 2.1, the closed-loop system in (2.10) is asymptotically stable. The proof is completed. □

In Theorem 2.2, the asymptotical stability of the closed-loop system in (2.10), whose system matrices lie in the polytope, can be guaranteed by those of the vertices of the polytope. Therefore, the remote PID controller for the stabilization of an unstable system in (2.1) with polyhedral uncertainties can be designed via Theorem 2.2. Note that the conditions stated in Theorem 2.2 are non-convex owing to the involved bilinear matrix equalities (BMEs). The problem of solving this kind of conditions can be formulated as a rank-constrained LMI problem. Over the past decades, well established iterative algorithms have been developed to solve the rank-constrained LMI problem [146, 147], among which the cone complementarity linearization (CCL) algorithm [148] and Newton-type search method [149] have been shown to be efficient.

In this chapter, the modified CCL algorithm is used to solve the robust PID stabilization problem by converting the non-convex problem in Theorem 2.2 into the following nonlinear minimization problem.

Robust PID Stabilization:

$$\min \text{ trace}\,(PM_1 + ZM_2)$$

subject to (2.21) and

$$\begin{bmatrix} P & I \\ I & M_1 \end{bmatrix} \geq 0, \quad \begin{bmatrix} Z & I \\ I & M_2 \end{bmatrix} \geq 0.$$

According to [148], if the solution of the minimization problem is $2(n + 2p)$, i.e., $\text{trace}\,(PM_1 + ZM_2) = 2(n + 2p)$, then the non-convex conditions in Theorem 2.2 are solvable.

In [148], it was shown that an optimal set of solution can be obtained by computing finite iterations of a set of LMIs for most of the cases. If the solution of the minimization problem is derived, the remote PID controller parameters for the stabilization problem can be readily obtained from the columns of K which is released from the solution space of the minimization problem.

2.3.2 Robust $\mathcal{H}_\infty$ PID Control

In the former subsection, the stability is analyzed for the unforced closed-loop system in (2.10). When the noise is taken into account, this subsection focuses on the development of robust PID control with guaranteed $\mathcal{H}_\infty$ performance.

Theorem 2.3. *Consider the PID control setup in a network environment, as shown in Figure 2.1. Assuming a positive γ is given, the state-noise-delayed system in (2.10) is robustly asymptotically stable with a prescribed disturbance attenuation level γ, if there exist matrices $P = P^{\mathrm{T}} > 0$, $Q(\alpha) = Q(\alpha)^{\mathrm{T}} > 0$, $Z = Z^{\mathrm{T}} > 0$, $S_1(\alpha)$, $S_2(\alpha)$, $S_3(\alpha)$, $S_4(\alpha)$, $M_1 = M_1^{\mathrm{T}} > 0$, $M_2 = M_2^{\mathrm{T}} > 0$ and K such that the following condition*

holds

$$\begin{bmatrix} \Phi_{11} & * & * & * & * & * & * & * \\ -S_1^{\mathrm{T}}(\alpha)+S_2(\alpha) & \Phi_{22} & * & * & * & * & * & * \\ S_3(\alpha) & -S_3(\alpha) & -\gamma^2 I & * & * & * & * & * \\ S_4(\alpha) & -S_4(\alpha) & 0 & -\gamma^2 I & * & * & * & * \\ S_1^{\mathrm{T}}(\alpha) & S_2^{\mathrm{T}}(\alpha) & S_3^{\mathrm{T}}(\alpha) & S_4^{\mathrm{T}}(\alpha) & -Z/d_2 & * & * & * \\ \bar{A}(\alpha) & \bar{B}(\alpha)K\bar{C}(\alpha) & \bar{B}(\alpha)K\bar{D} & \bar{B}_1(\alpha) & 0 & -M_1 & * & * \\ \bar{A}(\alpha)-I & \bar{B}(\alpha)K\bar{C}(\alpha) & \bar{B}(\alpha)K\bar{D} & \bar{B}_1(\alpha) & 0 & 0 & -M_2/d_2 & * \\ \bar{E} & \bar{F}K\bar{C}(\alpha) & \bar{F}K\bar{D} & 0 & 0 & 0 & 0 & -I \end{bmatrix} < 0, \tag{2.23}$$

where

$$\Phi_{11} = -P + (\bar{d}+2)Q(\alpha) + \mathrm{sym}(S_1(\alpha)),$$

$$\Phi_{22} = -\mathrm{sym}(S_2(\alpha)),$$

$$PM_1 = I \text{ and } ZM_2 = I.$$

Proof: To ensure the $\mathcal{H}_\infty$ performance for the closed-loop PID control system, assume the zero initial condition and consider the following objective function:

$$J := \Delta V_k(\Theta_k) + \bar{z}_k^{\mathrm{T}}\bar{z}_k - \gamma^2\omega_k^{\mathrm{T}}\omega_k - \gamma^2\omega_{k-d_k}^{\mathrm{T}}\omega_{k-d_k}. \tag{2.24}$$

For any nonzero noise, choose the similar Lyapunov functional candidate as defined in (2.13). The difference of the Lyapunov functional candidate can be obtained by following the similar lines as in (2.14) but with $w_k \neq 0$ and $w_{k-d_k} \neq 0$. Then, for any

matrices S_l, $l = 1, 2, 3, 4$, the following conditions hold

$$\Xi_3 = \left(\bar{x}_k^{\mathrm{T}} S_1(\alpha) + \bar{x}_{k-d_k}^{\mathrm{T}} S_2(\alpha) + \omega_{k-d_k}^{\mathrm{T}} S_3(\alpha) + \omega_k^{\mathrm{T}} S_4(\alpha)\right) \left[\bar{x}_k - \bar{x}_{k-d_k} - \sum_{i=k-d_k}^{k-1} \nu_i\right] = 0, \tag{2.25}$$

and

$$\begin{aligned}\Xi_4 = \sum_{i=k-d_k}^{k-1} & \left(\bar{x}_k^{\mathrm{T}} S_1(\alpha) + \bar{x}_{k-d_k}^{\mathrm{T}} S_2(\alpha) + \omega_{k-d_k}^{\mathrm{T}} S_3(\alpha) + \omega_k^{\mathrm{T}} S_4(\alpha) + \nu_i^{\mathrm{T}} Z(\alpha)\right) Z^{-1}(\alpha) \\ & \left(\bar{x}_k^{\mathrm{T}} S_1(\alpha) + \bar{x}_{k-d_k}^{\mathrm{T}} S_2(\alpha) + \omega_{k-d_k}^{\mathrm{T}} S_3(\alpha) + \omega_k^{\mathrm{T}} S_4(\alpha) + \nu_i^{\mathrm{T}} Z(\alpha)\right)^{\mathrm{T}} \geq 0.\end{aligned} \tag{2.26}$$

Substituting the difference of the Lyapunov functional, (2.25) and (2.26) into the index (2.24), we obtain

$$J \leq \begin{bmatrix} x_k \\ x_{k-d_k} \\ \omega_{k-d_k} \\ \omega_k \end{bmatrix}^{\mathrm{T}} \begin{bmatrix} \Omega_{11} & * & * & * \\ \Omega_{21} & \Omega_{22} & * & * \\ \Omega_{31} & \Omega_{32} & \Omega_{33} & * \\ \Omega_{41} & \Omega_{42} & \Omega_{43} & \Omega_{44} \end{bmatrix} \begin{bmatrix} x_k \\ x_{k-d_k} \\ \omega_{k-d_k} \\ \omega_k \end{bmatrix}, \tag{2.27}$$

where

$$\begin{aligned}\Omega_{11} =& \Pi_{11} + \bar{E}^{\mathrm{T}} \bar{E}, \\ \Omega_{21} =& \Pi_{21} + \bar{F} K \bar{C}(\alpha) \bar{E}, \\ \Omega_{22} =& \Pi_{22} + (\bar{F} K \bar{C}(\alpha))^{\mathrm{T}} \bar{F} K \bar{C}(\alpha), \\ \Omega_{31} =& (\bar{B}(\alpha) K \bar{D})^{\mathrm{T}} P \bar{A}(\alpha) + \bar{F} K \bar{D} \bar{E} + S_3(\alpha) \\ & + d_2 (\bar{B}(\alpha) K \bar{D})^{\mathrm{T}} Z (\bar{A}(\alpha) - I) + d_2 S_3(\alpha) Z^{-1} S_1^{\mathrm{T}}(\alpha),\end{aligned}$$

$$
\begin{aligned}
\Omega_{32} =&(\bar{B}(\alpha)K\bar{D})^{\mathrm{T}}[P+d_2Z]\bar{B}(\alpha)K\bar{C}(\alpha)-S_3(\alpha)\\
&+(\bar{F}K\bar{D})^{\mathrm{T}}\bar{F}K\bar{C}(\alpha)+d_2S_3(\alpha)Z^{-1}S_2^{\mathrm{T}}(\alpha),\\
\Omega_{33} =&(\bar{B}(\alpha)K\bar{D})^{\mathrm{T}}[P+d_2Z](\bar{B}(\alpha)K\bar{D})+d_2S_3(\alpha)Z^{-1}S_3^{\mathrm{T}}(\alpha)\\
&+(\bar{F}K\bar{D})^{\mathrm{T}}\bar{F}K\bar{D}-\gamma^2I,\\
\Omega_{41} =&\bar{B}_1^{\mathrm{T}}(\alpha)[P\bar{A}(\alpha)+d_2Z(\bar{A}(\alpha)-I))]+S_4(\alpha)+d_2S_4(\alpha)Z^{-1}S_1^{\mathrm{T}}(\alpha),\\
\Omega_{42} =&\bar{B}_1^{\mathrm{T}}(\alpha)[P+d_2Z](\bar{B}(\alpha)K\bar{C}(\alpha))-S_4(\alpha)+d_2S_4(\alpha)Z^{-1}S_2^{\mathrm{T}}(\alpha),\\
\Omega_{43} =&\bar{B}_1^{\mathrm{T}}(\alpha)[P+d_2Z](\bar{B}(\alpha)K\bar{D})+d_2S_4(\alpha)Z^{-1}S_3^{\mathrm{T}}(\alpha),\\
\Omega_{44} =&\bar{B}_1^{\mathrm{T}}(\alpha)[P+d_2Z]\bar{B}_1(\alpha)-\gamma^2I+d_2S_4(\alpha)Z^{-1}S_4^{\mathrm{T}}(\alpha).
\end{aligned}
$$

It can be seen from (2.23) that $J<0$ for any nonzero $[x_k^{\mathrm{T}},x_{k-d_k}^{\mathrm{T}},\omega_{k-d_k}^{\mathrm{T}},\omega_k^{\mathrm{T}}]^{\mathrm{T}}$. By summing up the objective function in (2.24) with respect to the time k, we have

$$\|\bar{z}\|_2^2<\gamma^2\|\omega\|_2^2+\gamma^2\|\omega_d\|_2^2+V_0(\Theta_0)-V_\infty(\Theta_\infty). \tag{2.28}$$

Noting that $V_0(\Theta_0)=0$ and $V_\infty(\Theta_\infty)\geq 0$, we can conclude

$$\|\bar{z}\|_2^2<\gamma^2\|\omega\|_2^2+\gamma^2\|\omega_d\|_2^2. \tag{2.29}$$

According to Definition 2.1, the closed-loop system in (2.10) is robustly asymptotically stable with a prescribed $\mathcal{H}_\infty$ attenuation level γ. This completes the proof. □

Note that uncertainty-dependent variables are incorporated in Theorem 2.3. Assuming that these matrices are linearly dependent on the uncertainty, a parameter-dependent theorem is established as follows.

Theorem 2.4. *Consider the PID control setup in a network environment, as shown in Figure 2.1. Assuming a positive γ is given, the state-noise-delayed system in (2.10) is robustly asymptotically stable with a prescribed disturbance attenuation level γ, if*

there exist matrices $P = P^{\mathrm{T}} > 0$, $Q_i = Q_i^{\mathrm{T}} > 0$, $Z = Z^{\mathrm{T}} > 0$, $S_{1,i}$, $S_{2,i}$, $S_{3,i}$, $S_{4,i}$, $M_1 = M_1^{\mathrm{T}} > 0$, $M_2 = M_2^{\mathrm{T}} > 0$ *and* K *such that the following conditions hold*

$$\mathcal{N}_{i,j} + \mathcal{N}_{j,i} < 0, \forall\ 1 \le i \le j \le s, \tag{2.30}$$

where

$$\mathcal{N}_{i,j} = \begin{bmatrix} \Phi_{11} & * & * & * & * & * & * & * \\ -S_{1,i}^{\mathrm{T}} + S_{2,i} & \Phi_{22} & * & * & * & * & * & * \\ S_{3,i} & -S_{3,i} & -\gamma^2 I & * & * & * & * & * \\ S_{4,i} & -S_{4,i} & 0 & -\gamma^2 I & * & * & * & * \\ S_{1,i}^{\mathrm{T}} & S_{2,i}^{\mathrm{T}} & S_{3,i}^{\mathrm{T}} & S_{4,i}^{\mathrm{T}} & -Z/d_2 & * & * & * \\ \bar{A}_i & \bar{B}_i K \bar{C}_j & \bar{B}_i K \bar{D} & \bar{B}_{1,i} & 0 & -M_1 & * & * \\ \bar{A}_i - I & \bar{B}_i K \bar{C}_j & \bar{B}_i K \bar{D} & \bar{B}_{1,i} & 0 & 0 & -M_2/d_2 & * \\ \bar{E} & \bar{F} K \bar{C}_i & \bar{F} K \bar{D} & 0 & 0 & 0 & 0 & -I \end{bmatrix},$$

$$\Phi_{11} = -P + (\bar{d} + 2) Q_i + \mathrm{sym}(S_{1,i}),$$

$$\Phi_{22} = -\mathrm{sym}(S_{2,i}),$$

$$PM_1 = I \text{ and } ZM_2 = I.$$

Proof: The proof is similar to the one of Theorem 2.2 and it is omitted here. □

To this end, the robust $\mathcal{H}_\infty$ PID controller can be designed by the following modified CCL algorithm.

Robust $\mathcal{H}_\infty$ PID Controller Design:

$$\min \text{ trace}\,(PM_1 + ZM_2)$$

subject to (2.30) and

$$\begin{bmatrix} P & I \\ I & M_1 \end{bmatrix} \geq 0, \quad \begin{bmatrix} Z & I \\ I & M_2 \end{bmatrix} \geq 0.$$

When the nonlinear optimization problem is solved and has a set of feasible solutions, the controller K can be readily determined from the derived solution space and the corresponding PID gains can be obtained from the columns of K.

Remark 2.4. *It is noticed that in (2.12) and (2.23), under the assumption of (2.20), some entries, e.g., P, I, $\bar{E}$, do not depend on the uncertainties and some other terms such as $\bar{B}(\alpha)$, $K\bar{C}(\alpha)$, $\bar{A}(\alpha)$ have a polynomial form of the uncertainties. To make all the entries have a homogeneous form of the uncertainties, the technique stated in Remark 2.3 is employed in the above proof.*

Remark 2.5. *For $\mathcal{H}_\infty$ control and filtering, the minimal γ is an important index to evaluate the system performance. Since the CCL method is an iterative algorithm and it depends on a given minimal scalar and a maximal iterative number, it is difficult to achieve the optimal γ [138].*

2.4 Illustrative Examples

In this section, four examples are presented to illustrate the proposed design methods of the robust PID stabilization and the robust $\mathcal{H}_\infty$ PID control. The first example is to robustly stabilize a two-input-two-output unstable plant. A PID controller will be designed to stabilize the NCS. The second one is to design a robust $\mathcal{H}_\infty$ PID controller. The third and the forth examples are for practical models.

Example 2.1: Robust PID Stabilization. Consider the NCS in Figure 2.1 with

system parameters as follows:

$$A = \begin{bmatrix} 0.8 & 0 \\ 0.05 & 1.1 \end{bmatrix}, \; B_1 = \begin{bmatrix} 0.5 & 0 \\ 0.2 & 0.1 \end{bmatrix},$$
$$B_2 = \begin{bmatrix} 0.5 & 0 \\ 0.4 & 0.1 \end{bmatrix}, \; C_1 = \begin{bmatrix} -2 & 0.1 \\ 0 & 0.34 \end{bmatrix}, \; C_2 = \begin{bmatrix} -2 & 0.1 \\ 0 & 0.36 \end{bmatrix}.$$

It can be seen that the plant is unstable and the polytope $\mathfrak{M}$ has 4 vertices. It is assumed that

$$1 \leq \tau_k \leq 3 \text{ and } 0 \leq \eta_k \leq 2.$$

The purpose is to design a remote PID controller such that the closed-loop system in (2.10) is asymptotically stable when the network characteristics are taken into account. By applying the proposed method, the gain matrix is designed as

$$K = \begin{bmatrix} -0.0124 & 0.0210 & -0.0104 & 0.0045 & 0.0030 & -0.0018 \\ -0.2766 & 4.8395 & 0.0246 & 0.0452 & -0.0518 & 0.0136 \end{bmatrix}.$$

Then, the parameters of the PID controller can be determined as

$$K_p = \begin{bmatrix} -0.0124 & 0.0210 \\ -0.2766 & 4.8395 \end{bmatrix}, \; K_i = \begin{bmatrix} -0.0104 & 0.0045 \\ 0.0246 & 0.0452 \end{bmatrix}, \; K_d = \begin{bmatrix} 0.0030 & -0.0018 \\ -0.0518 & 0.0136 \end{bmatrix}.$$

To verify that the closed-loop system is stable with the designed PID controller, the simulation results are shown in Figure 2.2. Although there exist uncertainties in the system model, the unstable plant is stabilized.

Example 2.2: Robust $\mathcal{H}_\infty$ PID Control. Consider the NCS in Figure 2.1 with

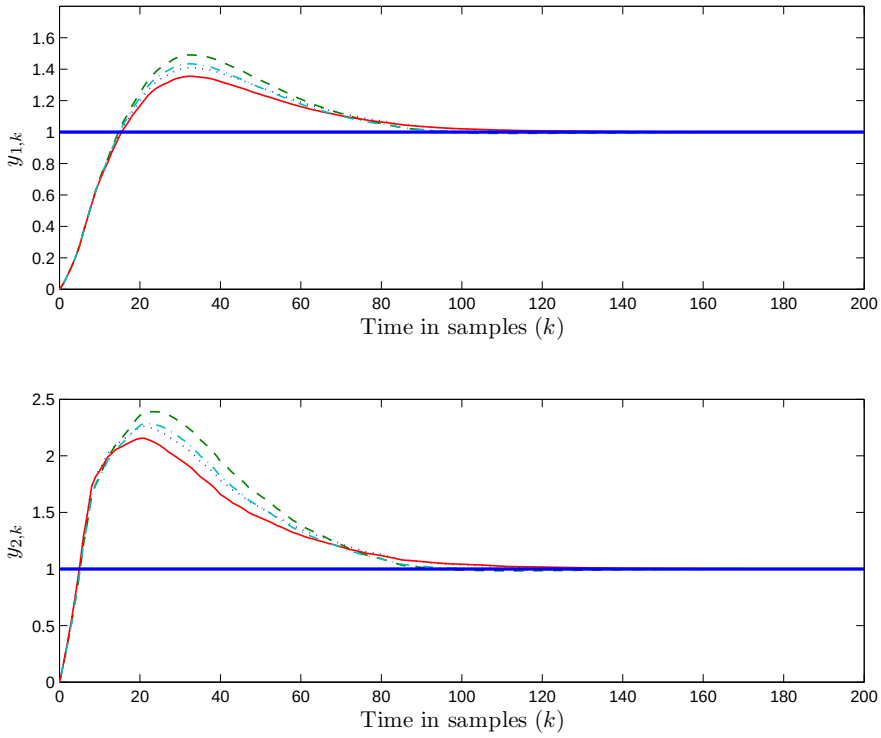

Figure 2.2: Measured output y_k for the four vertices and the references are all unit steps.

the following matrices

$$A_1 = \begin{bmatrix} 0.5 & 0 \\ 0 & 0.2 \end{bmatrix}, \; A_2 = \begin{bmatrix} 0.6 & 0 \\ 0 & 0.2 \end{bmatrix},$$
$$B = \begin{bmatrix} 0.8 & 1 \\ 0.3 & 0.5 \end{bmatrix}, C = \begin{bmatrix} 0.25 & 0.3 \\ 0.5 & 0.1 \end{bmatrix}.$$

Note that the plant is described by a two-vertex polytope. The network-induced delays are assumed to satisfy:

$$1 \leq \tau_k \leq 3 \text{ and } 0 \leq \eta_k \leq 2.$$

Given $\gamma = 30$, the parameters of the designed robust $\mathcal{H}_\infty$ PID controllers for different weighting matrices are listed in Table 2.1.

Table 2.1: PID parameters for different weighting factors.

	K_p	K_i	K_d
$\bar{R} = 1$ $\bar{F} = 0.1$	$\begin{bmatrix} -0.4352 & 0.4798 \\ 0.3532 & -0.1664 \end{bmatrix}$	$\begin{bmatrix} -0.6425 & 0.5107 \\ 0.5496 & -0.3267 \end{bmatrix}$	$\begin{bmatrix} 0.0913 & 0.0289 \\ -0.0709 & -0.0267 \end{bmatrix}$
$\bar{R} = 1$ $\bar{F} = 1$	$\begin{bmatrix} -1.5869 & 0.8320 \\ 1.2254 & -0.4470 \end{bmatrix}$	$\begin{bmatrix} -3.0585 & 1.6226 \\ 2.4248 & -1.1867 \end{bmatrix}$	$\begin{bmatrix} 0.3849 & 0.1131 \\ -0.2979 & -0.0937 \end{bmatrix}$

The quantization error is a major source for the measurement noise and each component of the quantization error is assumed to be uniform white noise with a covariance of 0.001, as illustrated in Figure 2.3. Since the reference is the unit

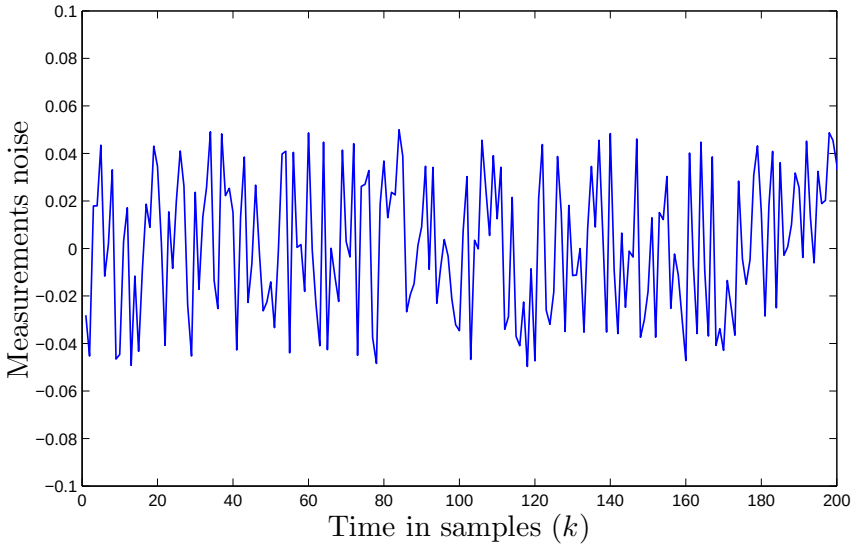

Figure 2.3: Random measurement noise.

step, the signal-to-noise ratio is around 30 dB. A Gaussian white noise with the zero mean and 0.001 variance is imposed onto each control action to simulate the load disturbance, as shown in Figure 2.4. The two reference input signals are both set as

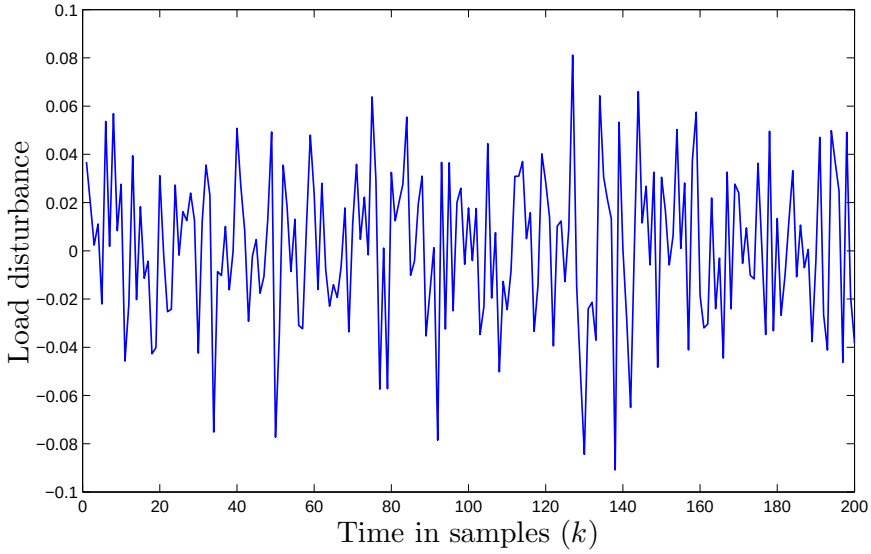

Figure 2.4: Random load disturbance.

unit steps. Figure 2.5 and Figure 2.6 show that, although there exist measurement

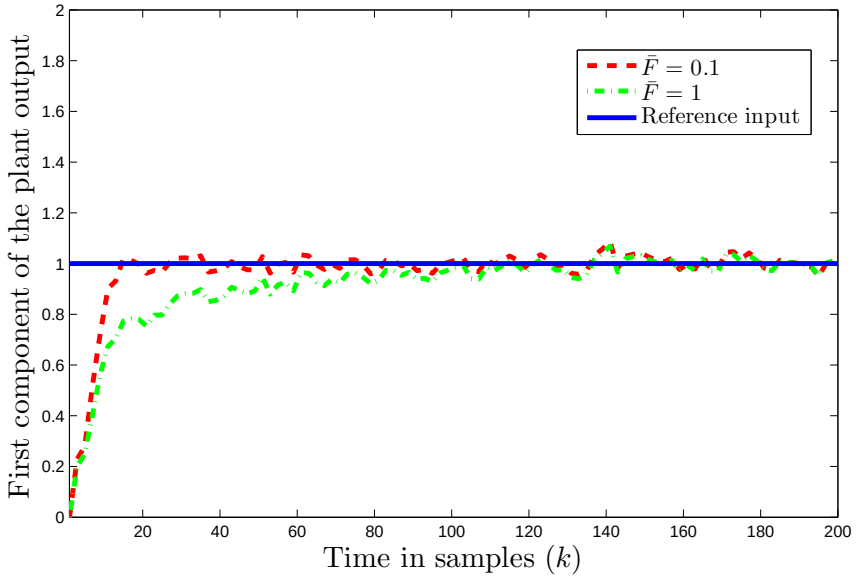

Figure 2.5: First component of the plant output for the vertex (A_1, B, C), when $\bar{R} = 1$.

noise and load disturbance, the plant outputs are smooth and they can both track the reference signals very well for all the weighting matrices. In particular, the overshoots

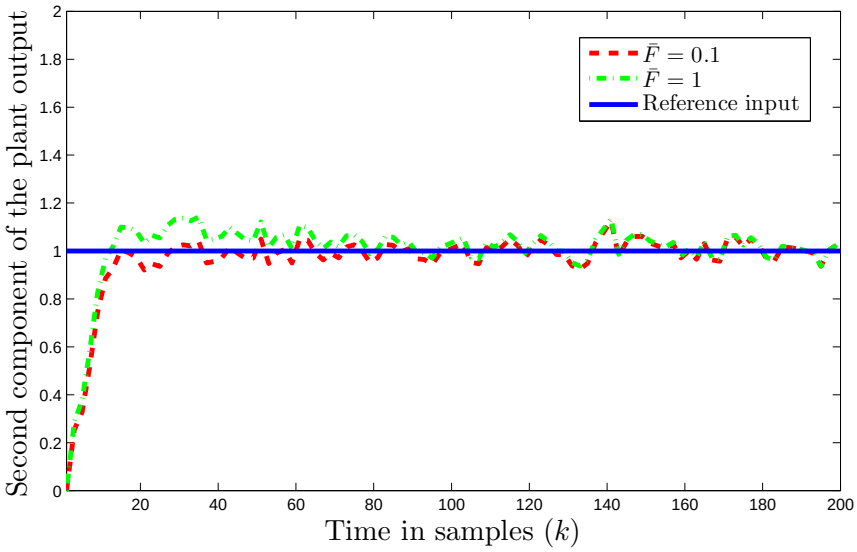

Figure 2.6: Second component of the plant output for the vertex (A_1, B, C), when $\bar{R} = 1$.

are small in the simulation.

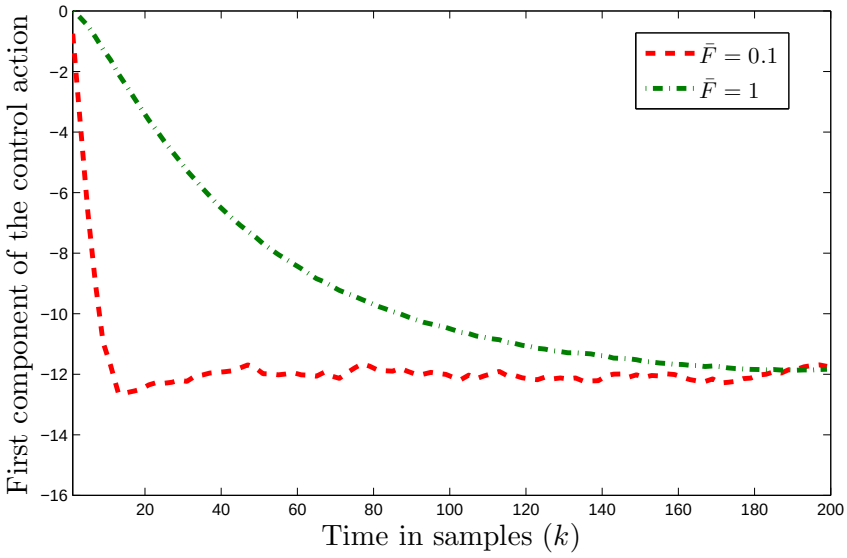

Figure 2.7: First component of the control actions of the closed-loop NCS with different $\bar{F}$, when $\bar{R} = 1$.

Finally, we examine how different weighting factors $\bar{R}$ and $\bar{F}$ will affect the control performance. Observe that the controlled equation (2.9) is a combination of the

summation of the tracking error and the control action. By changing the values for $\bar{R}$ and $\bar{F}$, the weighting factors of the error and the control action vary accordingly as illustrated in Figure 2.7 and Figure 2.8. When $\bar{R}$ keeps the same, a larger $\bar{F}$

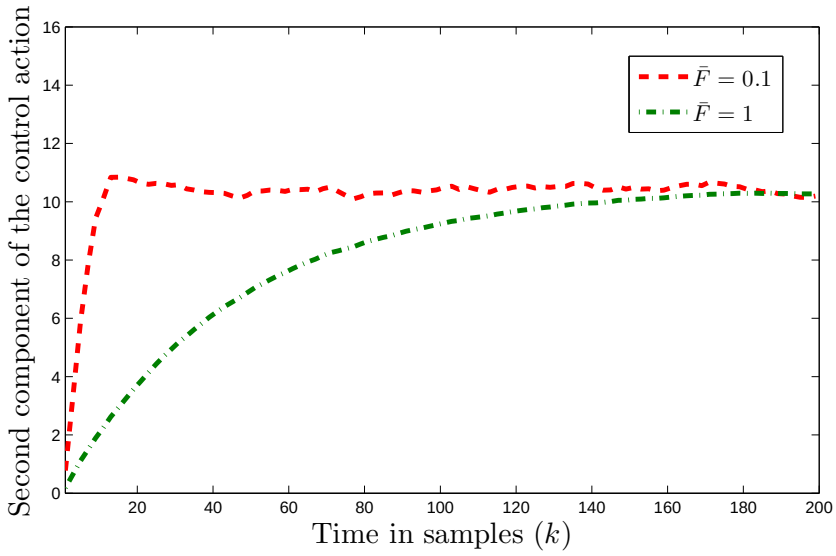

Figure 2.8: Second component of the control actions of the closed-loop NCS with different $\bar{F}$, when $\bar{R} = 1$.

'punishes' the control action, that is, the control action is softer. However, larger $\bar{F}$ deteriorates the tracking performance.

Example 2.3: Robust $\mathcal{H}_\infty$ PID Control for a VTOL Helicopter. Let us consider a practical design problem for a VTOL helicopter model from [150–152]. The discrete-time state-space model of the longitudinal motion of a helicopter is

shown below:

$$A = \begin{bmatrix} 0.9996+\sigma & 0.0003 & 0.0002 & -0.0046 \\ 0.0005 & 0.9900 & -0.0002 & -0.0400 \\ 0.0010 & 0.0036 & 0.9930 & 00141 \\ 0 & 0 & 0.0100 & 1.0001 \end{bmatrix},$$

$$B = \begin{bmatrix} 0.0044 & 0.0018 \\ 0.0353 & -0.0755 \\ -0.0549 & 0.0446 \\ -0.0003 & 0.0002 \end{bmatrix},\ C = \begin{bmatrix} 0 \\ 1 \\ 0 \\ 0 \end{bmatrix}^{\mathrm{T}}.$$

Here, the sampling period is $0.01s$, the value of σ lies in the range $[0,\ 0.02]$, and the four states of the helicopter are horizontal velocity, vertical velocity, pitch rate and pitch angle, respectively. The control inputs are collective pitch control action and longitudinal cyclic pitch control action. In fact, the VTOL model is unstable when the value for σ varies in the interval $[0,\ 0.02]$. It is noted that the VTOL model can be depicted by a 2-vertex polytope. In addition, we assume that the network-induced delay in this example is the same as the one in **Example 2.2**.

The weighting matrices $\bar{R}$ and $\bar{F}$ are chosen as I and $[0.1,\ 0.1]$, respectively. Employing the proposed robust $\mathcal{H}_\infty$ PID controller design approach, for $\gamma = 30$, the calculated SOF gain is

$$K = \begin{bmatrix} 0.2309 & 0.0165 & -0.0141 \\ -1.7116 & -0.1230 & 0.1043 \end{bmatrix}.$$

Then, the parameters of the PID controller can be extracted from each column of the

obtained SOF gain matrix as

$$K_p = \begin{bmatrix} 0.2309 \\ -1.7116 \end{bmatrix}, \; K_i = \begin{bmatrix} 0.0165 \\ -0.1230 \end{bmatrix}, \; K_d = \begin{bmatrix} -0.0141 \\ 0.1043 \end{bmatrix}.$$

Substituting the obtained PID parameters into (2.5), the control law is expressed as

$$\hat{u}_k = \begin{bmatrix} 0.2309 \\ -1.7116 \end{bmatrix} \hat{e}_k + \begin{bmatrix} 0.0165 \\ -0.1230 \end{bmatrix} \sum_{i=0}^{k-1} \hat{e}_i + \begin{bmatrix} -0.0141 \\ 0.1043 \end{bmatrix} (\hat{y}_{k-1} - \hat{y}_k).$$

In the simulation, the measurement noise is also a uniform random signal between $[-0.05, \; 0.05]$ and the load disturbance is a Gaussian distributed white noise with a variance of 0.001. Figure 2.9 shows the performance of the networked control VTOL

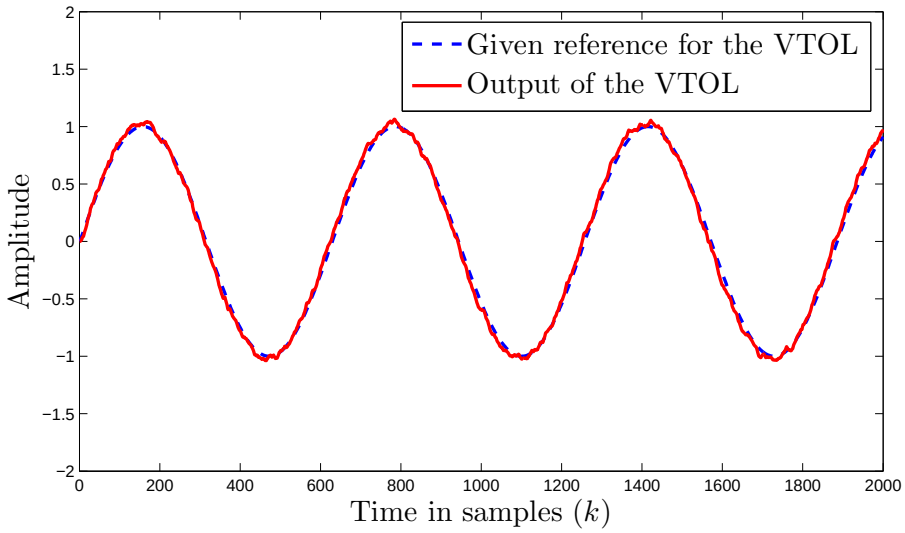

Figure 2.9: Tracking performance of the networked control VTOL under a sinusoidal reference.

($\sigma = 0.01$) when tracking a sinusoidal reference. Further, Figure 2.10 illustrates the tracking performance of the networked control VTOL under a unit step signal with a disturbance at $k = 1200$ whose magnitude is 0.4.

Now, we are going to show the robust performance of the designed controller

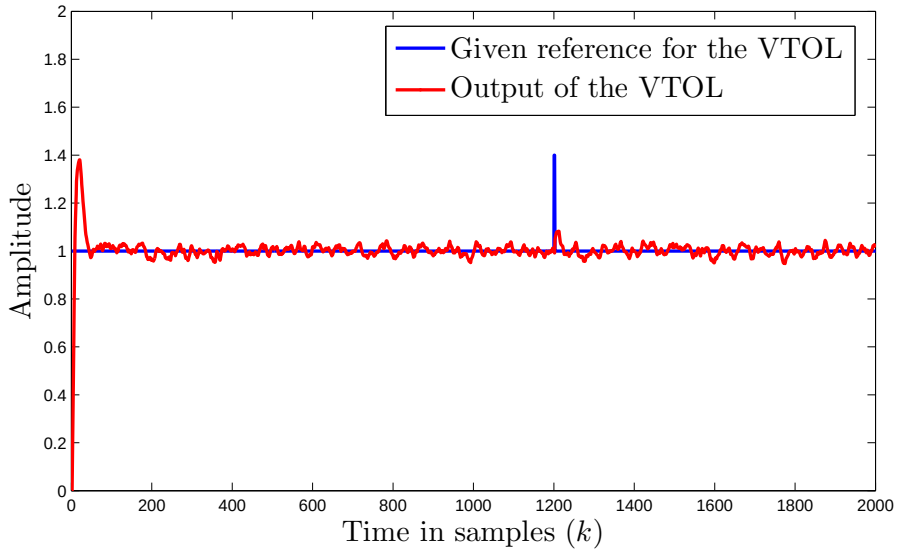

Figure 2.10: Tracking performance of the networked control VTOL under an unit step signal with a disturbance at $k = 1200$.

against the load disturbance and measurement noise. Suppose that the given reference and the measurement noise are zeros. In Figure 2.11, the output of the VTOL ($\sigma = 0.01$) and the load disturbance are both depicted. It can be seen from Figure 2.11 that

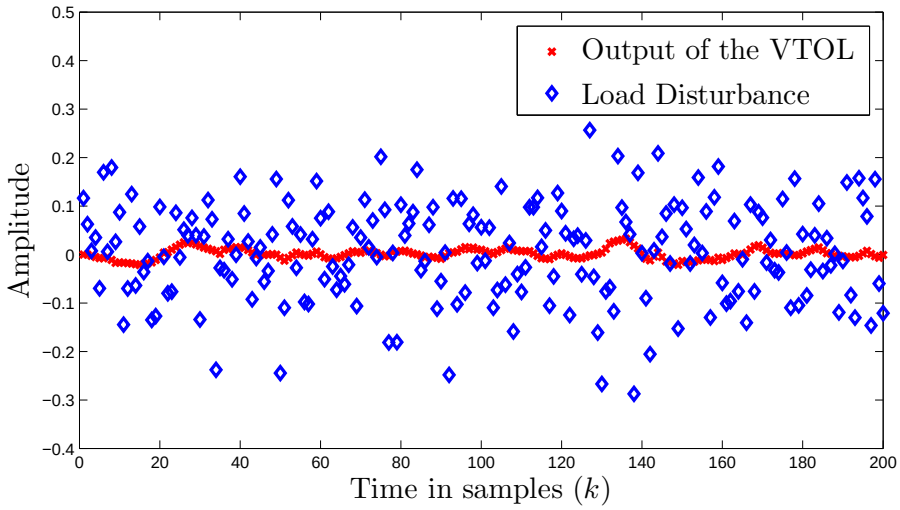

Figure 2.11: The output of the VTOL and the load disturbance.

the designed controller can attenuate the load disturbance well. When the simulation

time is 2000 steps ($20s$), the 2-norm and the ∞-norm of both signals are listed in the following table.

Table 2.2: Norms of the VTOL's output and the load disturbance.

Norms	2-norm	∞-norm
Output of the VTOL	0.6679	0.0576
Load disturbance	4.5554	0.3821

Example 2.4: Robust $\mathcal{H}_\infty$ PID Control for a Stirred Tank. The discretized version of a stirred tank [139] with the sampling period $0.1s$ is depicted by:

$$A = \begin{bmatrix} 0.9512 & 0 & 0 & 0 \\ 0 & 0.9048 & 0.0670 & 0.0226 \\ 0 & 0 & 0.8825 & 0 \\ 0 & 0 & 0 & 0.9048 \end{bmatrix},$$

$$B = \begin{bmatrix} 4.8771 & 4.8771 \\ -10.1895 & 3.5686 \\ 0 & 0 \\ 0 & 0 \end{bmatrix}, \; C = \begin{bmatrix} 0.01 & 0 \\ 0 & 1 \\ 0 & 0 \\ 0 & 0 \end{bmatrix}^{\mathrm{T}}. \tag{2.31}$$

The network-induced delays are assumed to be the same with the ones in **Example 2.2**, i.e.,

$$1 \leq \tau_k \leq 3, \quad 0 \leq \eta_k \leq 2.$$

In [139], the authors studied the $\mathcal{H}_\infty$ PID controller design for the stirred tank without any delays. When considering the influence of the network, the closed-loop system becomes unstable with the designed PID controller. Therefore, it is desired to employ the proposed design method for NCSs. The weighting matrices $\bar{R}$ and $\bar{F}$ are chosen

as I and $0.1I$, respectively. Then, for $\gamma = 80$, the SOF gain is calculated as

$$K = \begin{bmatrix} 1.0780 & -0.0248 & 0.0842 & -0.0021 & 0.0192 & 0.0293 \\ 0.3645 & 0.0210 & 0.0302 & 0.0030 & 0.0036 & -0.0040 \end{bmatrix}.$$

Thus, the obtained parameters of the robust $\mathcal{H}_\infty$ PID controller for the stirred tank are

$$K_p = \begin{bmatrix} 1.0780 & -0.0248 \\ 0.3645 & 0.0210 \end{bmatrix}, \; K_i = \begin{bmatrix} -0.0021 & 0.0192 \\ 0.0302 & 0.0030 \end{bmatrix}, \; K_d = \begin{bmatrix} 0.0192 & 0.0293 \\ 0.0036 & -0.0040 \end{bmatrix}.$$

In the simulation, assume that the measurement noise is an uniform white noise within $[-0.05,\ 0.05]$ and the load disturbance is a Gaussian white noise with the variance 0.0001. When the simulation time is 300 steps ($30s$), Figure 2.12 and Figure 2.13 illustrate the tracking performance of the designed controller under two unit step

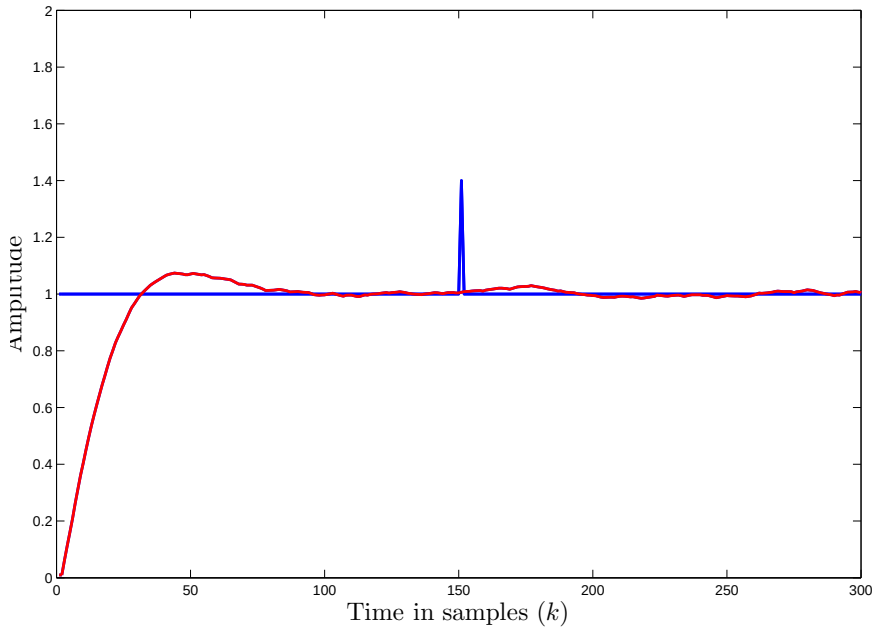

Figure 2.12: The first output of the stirred tank (red curve).

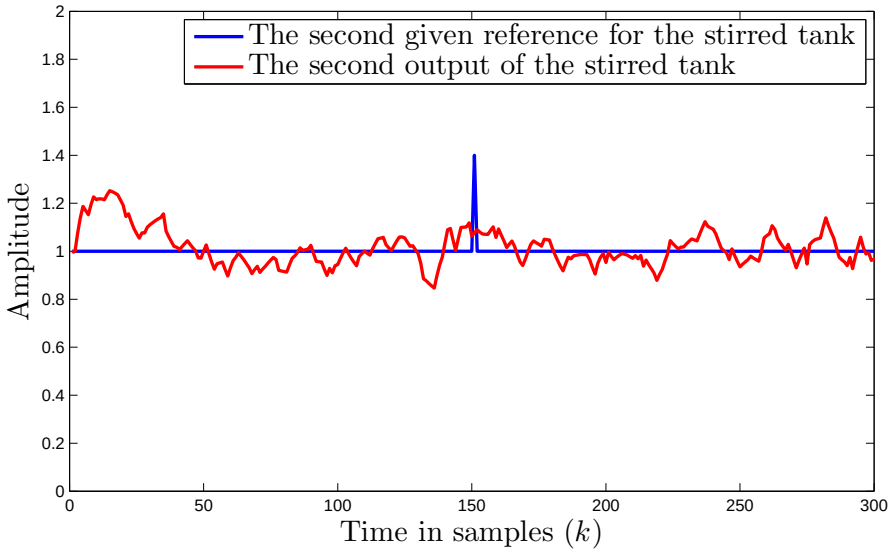

Figure 2.13: The second output of the stirred tank.

set points. Notice that the second output is more sensitive to the load disturbance compared with the first output. The reason is that the second output is only 1% of the first state. This can be found from the $(2, 1)$ component of the matrix C.

2.5 Conclusions

The design problem of remote PID controllers for multivariable NCSs has been investigated in this chapter. Compared with the existing work, the new features of the NCS model used are: (1) The reference, load disturbance and measurement noise are all incorporated into the closed-loop state-space model; (2) two buffers are employed to supply the newest information; (3) delay-free and delayed state and external noise are considered in the model. By using the robust control, the design methods of PID controllers for robust stabilization and $\mathcal{H}_\infty$ control are developed. Finally, the examples show, by applying the proposed methods, the developed robust PID controller achieves acceptable performance in a network environment.

Chapter 3

Combined Feedback-feedforward Tracking Control for Networked Control Systems with Probabilistic Delays

3.1 Introduction

In Chapter 2, the tracking control with PID controllers has been investigated. The illustrative examples show that the proposed algorithms are effective for many cases. However, the obtained conditions in Chapter 2 are only sufficient ones. It is natural to ask whether the performance of the tracking controllers can be further improved with other control schemes.

In this chapter, we study the tracking problem for NCSs. A combined feedforward-feedback control configuration is employed. We utilize a modified proportional-integral-derivative control scheme in the feedback control loop. Note that the con-

troller does not know the time delay for the control signal transmitted from the controller node to the actuator node. In order to compensate for the time delay on the link from the controller to the actuator, a predictive control scheme [153] is employed, that is, a series of control signals which are dependent on each of the possible delay on the link from the controller to the actuator are generated. The generated control signals are packed together and sent to the actuator node. At the actuator node, it is easy to obtain the accumulated delays induced by the network links. We assume that each delay has an occurrence probability which is known *a priori*. The generated control signals are dependent on the delays and the occurrence probabilities. When the packed control signals arrive at the actuator node, the control signal is chosen according to the accumulated delay. Using the augmentation technique, we obtain a delay-free closed-loop system with stochastic parameters. The stochastic stability and $\mathcal{H}_\infty$ performance are studied for the closed-loop system. Controller gains can be derived by solving a nonlinear optimization problem.

3.1.1 Problem Formulation and Preliminaries

Consider a typical tracking control problem for NCSs, as shown in Figure 3.1. The output of the plant is transmitted to the tracking controller via a communication link. The tracking controller generates a series of control signals according to the network-induced delay characteristics, the desired set points, and the received packets. The generated control signals are also delivered by a communication link to the actuator. When the actuator receives the sequence of control signals, it chooses an appropriate one to control the plant.

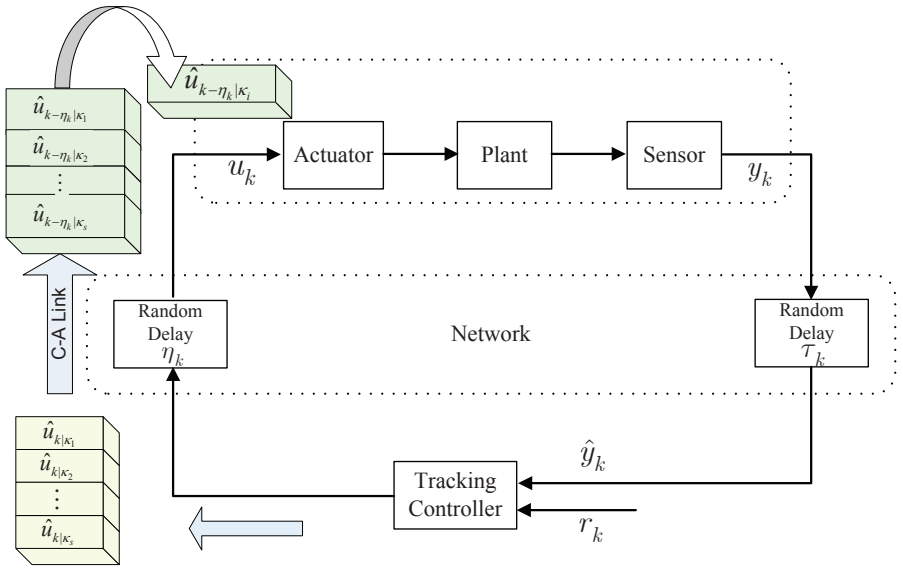

Figure 3.1: A typical tracking control system in a network environment.

The discrete-time system is represented by:

$$\begin{aligned} x_{k+1} &= Ax_k + Bu_k, \\ y_k &= Cx_k, \end{aligned} \tag{3.1}$$

where k is the sampling instant, $x_k \in \mathbb{R}^n$ is the state vector of the system, $y_k \in \mathbb{R}^p$ is the plant output, and $u_k \in \mathbb{R}^m$ is the control action. A, B and C are system matrices with appropriate dimensions.

In the traditional local control scheme, the observation of the output is always assumed to be exactly the measurement of the output and the control action is the same as the control signal generated by the controller. However, in an NCS with limited bandwidth, these assumptions do not hold. In practice, network-induced delays and packet dropouts are ubiquitous in NCSs because of the limited bandwidth of the communication channels, or limited buffer sizes. As depicted in Figure 3.1,

bounded random variables τ_k and η_k represent the network-induced delay occurring on the S-C link and the C-A link, respectively. It is assumed that we have the following *a priori* information and assumptions on the networked-induced delays on both communication links:

1. Let d_k denote the summation of τ_k and η_k, that is, $d_k = \tau_k + \eta_k$. The variable d_k is time-varying in the set $\mathcal{I} := \{\kappa_1, \cdots, \kappa_i, \cdots, \kappa_s\}$, where $\forall\ i = 1, \cdots, s$, κ_i is an integer and $0 < \kappa_1 < \cdots < \kappa_i < \cdots < \kappa_s$.

2. Define an indicator function

$$\alpha(k) = [\alpha_1(k), \cdots, \alpha_i(k), \cdots, \alpha_s(k)]^{\mathrm{T}}.$$

   For each sampling instant, the exact delay at the actuator node can be obtained by using the time-stamping technique. When the variable $\alpha_i(k)$ takes the value on 1, the lumped delay at the actuator node is κ_i, that is,

$$\begin{cases} \alpha_i(k) = 1, & d_k = \kappa_i, \\ \alpha_i(k) = 0, & d_k \neq \kappa_i. \end{cases} \tag{3.2}$$

   In the literature, it is common to simply assume that the delay d_k is time-varying. However, in many cases, the statistics of the time delay is available and employed to benefit the controller design, e.g., the Markovian delay in [31]. Suppose that the probability of $\alpha_i = 1$ is denoted by β_i, i.e.,

$$\begin{aligned} &\mathrm{Prob}\,\{\alpha_i = 1\} = \beta_i, \\ &\mathrm{Prob}\,\{\alpha_i = 0\} = 1 - \beta_i. \end{aligned} \tag{3.3}$$

3. The sensor is time driven, and the controller and the actuator are event driven.

The controller node and the actuator node can obtain the delay information by using the time-stamp technique [31].

3.1.2 Methodology and Contributions

Define the tracking error of the system as:

$$\hat{e}_k = r_{k-\tau_k} - \hat{y}_k = r_{k-\tau_k} - y_{k-\tau_k}, \tag{3.4}$$

where $\hat{y}_k$ is an input to the controller. The combined feedback-feedforward control law, when the accumulated delay at the actuator node is $\kappa_i \ \forall \ i = 1, \cdots, s$, has the following form:

$$\hat{u}_{k|\kappa_i} = K_{P|\kappa_i}\hat{e}_k + K_{I|\kappa_i}\sum_{j=0}^{k-1}\hat{e}_j + K_{D|\kappa_i}(\hat{y}_{k-1} - \hat{y}_k) + K_{F|\kappa_i}r_{k-\tau_k}. \tag{3.5}$$

Here, $K_{P|\kappa_i}$, $K_{I|\kappa_i}$, $K_{D|\kappa_i}$, and $K_{F|\kappa_i}$ are a set of delay-dependent matrix gains to be designed. As the controller does not know the delay on the C-A link when it generates the control signal, we group a sequence of control signals together in a packet, and send the packet to the actuator. When the controller receives a packet, the output of the controller is

$$\begin{bmatrix} \hat{u}_k|\kappa_1 \\ \vdots \\ \hat{u}_k|\kappa_s \end{bmatrix}.$$

By using the augmentation technique, we construct a new augmented system:

$$\begin{aligned} \bar{x}_{k+1} &= \bar{A}\bar{x}_k + \bar{B}_1 u_k + \bar{B}_2\omega_k, \\ \bar{y}_k &= \bar{C}\bar{x}_k + \bar{D}\omega_k, \end{aligned} \tag{3.6}$$

where

$$\bar{A} = \begin{bmatrix} A & 0 & 0 \\ -C & I & 0 \\ C & 0 & 0 \end{bmatrix} \in \mathbb{R}^{(n+2p)\times(n+2p)},\ \bar{x}_k = \begin{bmatrix} x_k \\ \sum_{j=0}^{k-1} e_j \\ y_{k-1} \end{bmatrix},\ \bar{B}_1 = \begin{bmatrix} B \\ 0 \\ 0 \end{bmatrix} \in \mathbb{R}^{(n+2p)\times m},$$

$$\omega_k = r_k,\ e_k = r_k - y_k,\ \bar{B}_2 = \begin{bmatrix} 0 \\ I \\ 0 \end{bmatrix} \in \mathbb{R}^{(n+2p)\times p},\ \bar{y}_k := \begin{bmatrix} e_k \\ \sum_{j=0}^{k-1} e_j \\ (y_{k-1} - y_k) \\ r_k \end{bmatrix},$$

$$\bar{C} = \begin{bmatrix} -C & 0 & 0 \\ 0 & I & 0 \\ -C & 0 & I \\ 0 & 0 & 0 \end{bmatrix} \in \mathbb{R}^{4p\times(n+2p)},\ \bar{D} = \begin{bmatrix} I \\ 0 \\ 0 \\ I \end{bmatrix} \in \mathbb{R}^{4p\times p}.$$

Though the controller sends a sequence of control signals via the communication link, upon each receipt, the actuator applies the control signal which is generated by $K_{P|\kappa_i}$, $K_{I|\kappa_i}$, $K_{D|\kappa_i}$, and $K_{F|\kappa_i}$, when $\alpha_i(k)$ is equal to one and d_k is equal to κ_i. It is noted from (3.6) that the control action u_k is the delayed static output feedback of the augmented system, that is,

$$u_k = \hat{u}_{k-\eta_k|\kappa_i} = \sum_{i=1}^{s} \alpha_i(k) K_{|\kappa_i} \bar{y}_{k-\kappa_i}, \tag{3.7}$$

where $K_{|\kappa_i} := [K_{P|\kappa_i},\ K_{I|\kappa_i},\ K_{D|\kappa_i},\ K_{F|\kappa_i}] \in \mathbb{R}^{m\times 4p}$.

In order to deal with the time-varying delay in the control action, we construct another augmented system as

$$\xi_{k+1} = \tilde{A}\xi_k + \tilde{B}_1 u_k + \tilde{B}_2 \omega_k, \tag{3.8}$$

where

$$\tilde{A} = \begin{bmatrix} \bar{A} & 0 & \cdots & 0 & 0 \\ \bar{C} & 0 & \cdots & 0 & 0 \\ 0 & I & \cdots & 0 & 0 \\ \vdots & \vdots & \ddots & \vdots & \vdots \\ 0 & 0 & \cdots & I & 0 \end{bmatrix} \in \mathbb{R}^{\mathcal{N}\times\mathcal{N}},\ \mathcal{N} = 4p \times \kappa_s + n + 2p,\ \xi_k = \begin{bmatrix} \bar{x}_k \\ \bar{y}_{k-1} \\ \vdots \\ \bar{y}_{k-\kappa_s+1} \\ \bar{y}_{k-\kappa_s} \end{bmatrix},$$

$$\tilde{B}_1 = \begin{bmatrix} \bar{B}_1 \\ 0 \\ \vdots \\ 0 \\ 0 \end{bmatrix} \in \mathbb{R}^{\mathcal{N}\times m}, \tilde{B}_2 = \begin{bmatrix} \bar{B}_2 \\ \bar{D} \\ 0 \\ \vdots \\ 0 \end{bmatrix} \in \mathbb{R}^{\mathcal{N}\times p}.$$

Now, the control action in (3.7) can be depicted as

$$u_k = \sum_{i=1}^{s} \alpha_i(k) K_{|\kappa_i} \tilde{C}_{|\kappa_i} \xi_k, \tag{3.9}$$

where $\tilde{C}_{|\kappa_i} = \begin{bmatrix} 0 & \cdots & 0 & I & 0 & \cdots & 0 \end{bmatrix} \in \mathbb{R}^{(n+2p)\times\mathcal{N}}$, and the $(\kappa_i + 1)$th block is a unit matrix. For the tracking problem, the primary objective is to minimize the tracking error. In this chapter, we want to minimize the summation of the tracking error, that is, the second state vector in $\bar{x}_k$. Therefore, the controlled output of the augmented system in (3.8) is chosen as

$$z_k = E\xi_k, \tag{3.10}$$

where $E = [0\ I\ 0\ 0\ \cdots\ 0] \in \mathbb{R}^{p\times\mathcal{N}}$ and the first zero matrix in E has the dimensions

of $p \times n$. In summary, the closed-loop system is expressed as

$$\begin{aligned} \xi_{k+1} &= \tilde{A}\xi_k + \tilde{B}_1 \sum_{i=1}^{s} \alpha_i(k) K_{|\kappa_i} \tilde{C}_{|\kappa_i} \xi_k + \tilde{B}_2 \omega_k, \\ z_k &= E\xi_k. \end{aligned} \tag{3.11}$$

Note that the tracking problem of the NCS in (3.1) with network-induced delay has now been converted into a feedback control problem of a delay-free system in (3.11). In addition, the objective of minimizing the tacking error has been equivalently converted into the minimization of the corresponding controlled output. In the following sections, the main objectives are to analyze the stability and the $\mathcal{H}_\infty$ performance of the stochastic system in (3.11), and to design the delay-dependent controllers. More specifically, the following issues are to be dealt with.

O1 To study the stochastic stability of the system in (3.11) with zero external input.

O2 To investigate the $\mathcal{H}_\infty$ performance of the stochastic system in (3.11) with l_2 bounded input r_k, that is, for a given $\gamma > 0$, find conditions such that

$$\|z\|_2 < \gamma \|\omega\|_2. \tag{3.12}$$

O3 To design a sequence of delay-dependent controllers to achieve the tracking objective based on the analysis results.

3.2 Stability Analysis and Controller Design

It is necessary to mention that the system in (3.11) is a stochastic system due to the existence of $\alpha_i(k)$. In order to deal with stochastic variables, we introduce the definition of stochastic stability.

Definition 3.1. *[52] The system in (3.11) is stochastically stable if for every finite* ξ_0 *and initial* α_i*, there exists a finite* $W > 0$ *such that the following condition holds:*

$$\mathcal{E}\left\{\sum_{k=0}^{\infty}\|\xi_k\|^2|\xi_0\right\} < \xi_0^{\mathrm{T}} W \xi_0. \tag{3.13}$$

The analysis of stochastic stability for the system in (3.11) is given in the following theorem.

Theorem 3.1. *Consider the tracking control problem for NCSs shown in Figure 3.1. Suppose that the sequence of controllers are known. The unforced system in (3.11) is stochastically stable if there exist matrices* $P = P^{\mathrm{T}} > 0$*, and* $Q = Q^{\mathrm{T}} > 0$ *such that the following conditions are satisfied*

$$\begin{bmatrix} \Omega_{11} & \Omega_{12} \\ * & -P \end{bmatrix} < 0, \tag{3.14}$$

and

$$PQ = I, \tag{3.15}$$

where

$$\Omega_{11} = \begin{bmatrix} -Q & 0 & \cdots & 0 \\ * & -Q & \cdots & 0 \\ * & * & \ddots & \vdots \\ * & * & * & -Q \end{bmatrix}, \ \Omega_{12} = \begin{bmatrix} \sqrt{\beta_1}(\tilde{A} + \tilde{B}_1 K_{|\kappa_1} \tilde{C}_{|\kappa_1}) \\ \sqrt{\beta_2}(\tilde{A} + \tilde{B}_1 K_{|\kappa_2} \tilde{C}_{|\kappa_2}) \\ \vdots \\ \sqrt{\beta_s}(\tilde{A} + \tilde{B}_1 K_{|\kappa_s} \tilde{C}_{|\kappa_s}) \end{bmatrix}.$$

Proof. Note that the matrix Q is the inverse of the matrix P. Thus the inequality (3.14) is equivalent to

$$\begin{bmatrix} \tilde{\Omega}_{11} & \tilde{\Omega}_{12} \\ * & -P \end{bmatrix} < 0, \tag{3.16}$$

where

$$\tilde{\Omega}_{11} = \begin{bmatrix} -P & 0 & \cdots & 0 \\ * & -P & \cdots & 0 \\ * & * & \ddots & \vdots \\ * & * & * & -P \end{bmatrix}, \ \tilde{\Omega}_{12} = \begin{bmatrix} \sqrt{\beta_1}P(\tilde{A} + \tilde{B}_1 K_{|\kappa_1} \tilde{C}_{|\kappa_1}) \\ \sqrt{\beta_2}P(\tilde{A} + \tilde{B}_1 K_{|\kappa_2} \tilde{C}_{|\kappa_2}) \\ \vdots \\ \sqrt{\beta_s}P(\tilde{A} + \tilde{B}_1 K_{|\kappa_s} \tilde{C}_{|\kappa_s}) \end{bmatrix}.$$

By using Schur complement, it is inferred from (3.16) that

$$\tilde{A}^{\mathrm{T}} P \tilde{A} + \sum_{i=1}^{s} \beta_i (\tilde{B}_1 K_{|\kappa_i} \tilde{C}_{|\kappa_i})^{\mathrm{T}} P (\tilde{B}_1 K_{|\kappa_i} \tilde{C}_{|\kappa_i}) - P < 0. \tag{3.17}$$

For the unforced system of (3.11), consider a quadratic Lyapunov function as

$$V(\xi_k, k) = \xi_k^{\mathrm{T}} P \xi_k, \tag{3.18}$$

where P is a Lyapunov weighting matrix. The difference of the quadratic Lyapunov function is defined as

$$\Delta V(\xi_k, k) = \mathcal{E}\left\{\xi_{k+1}^{\mathrm{T}} P \xi_{k+1} | \xi_k\right\} - \xi_k^{\mathrm{T}} P \xi_k. \tag{3.19}$$

Using the occurrence probabilities, $\Delta V(\xi_k, k)$ is evaluated as

$$\begin{aligned} \Delta V(\xi_k, k) &= \mathcal{E}\left\{\xi_{k+1}^{\mathrm{T}} P \xi_{k+1} | \xi_k\right\} - \xi_k^{\mathrm{T}} P \xi_k \\ &= \xi_k^{\mathrm{T}} \left[\tilde{A}^{\mathrm{T}} P \tilde{A} + \sum_{i=1}^{s} \beta_i (\tilde{B}_1 K_{|\kappa_i} \tilde{C}_{|\kappa_i})^{\mathrm{T}} P (\tilde{B}_1 K_{|\kappa_i} \tilde{C}_{|\kappa_i}) - P\right] \xi_k \\ &= \xi_k^{\mathrm{T}} \Omega \xi_k, \end{aligned} \tag{3.20}$$

where $\Omega = \tilde{A}^{\mathrm{T}} P \tilde{A} + \sum_{i=1}^{s} \beta_i (\tilde{B}_1 K_{|\kappa_i} \tilde{C}_{|\kappa_i})^{\mathrm{T}} P (\tilde{B}_1 K_{|\kappa_i} \tilde{C}_{|\kappa_i}) - P$. It follows from (3.17) that

$$\begin{aligned} \Delta V(\xi_k, k) &\leq -\lambda_{\min}(-\Omega) \xi_k^{\mathrm{T}} \xi_k \\ &\leq -c \xi_k^{\mathrm{T}} \xi_k \\ &= -c \|\xi_k\|^2. \end{aligned} \tag{3.21}$$

Here, we use c to denote $\lambda_{min}(-\prod)$. For any $k \geq 1$, it is inferred from (3.21) that

$$\begin{aligned} &\mathcal{E}\left\{V(\xi_{k+1}, k+1)\right\} - \mathcal{E}\left\{V(\xi_0, 0)\right\} \\ &\leq -c\mathcal{E}\left\{\sum_{j=0}^{k} \|\xi_j\|^2\right\}. \end{aligned} \tag{3.22}$$

As k approaches infinity, we have

$$\begin{aligned} &\mathcal{E}\left\{\sum_{j=0}^{\infty} \|\xi_j\|^2\right\} \\ &\leq \frac{1}{c}\left\{\mathcal{E}\left\{V(\xi_0, 0)\right\} - \mathcal{E}\left\{V(\xi_{k+1}, k+1)\right\}\right\} \\ &\leq \frac{1}{c}\mathcal{E}\left\{V(\xi_0, 0)\right\} = \frac{1}{c}\xi_0^{\mathrm{T}} P x_0 = \xi_0^{\mathrm{T}} W \xi_0. \end{aligned} \tag{3.23}$$

where W represents P/c. According to Definition 3.1, the unforced switched system of (3.11) is stochastically stable, and this completes the proof. □

Theorem 3.1 offers sufficient conditions for the unforced system in (3.11) by assuming that the external input of the plant is zero. For the combined feedback-feedforward tracking problem, we still need to study the attenuation level from the external input to the summation of the tracking error. The following theorem gives the results of the $\mathcal{H}_\infty$ performance of the closed-loop system (3.11).

Theorem 3.2. *Consider the tracking control problem for NCSs as shown in Fig-*

ure 3.1. Suppose that the parameters of the controllers are known. For a given positive constant γ, the closed-loop system in (3.11) is stochastically stable with a prescribed $\mathcal{H}_\infty$ attenuation level γ if there exist matrices $P = P^{\mathrm{T}} > 0$, and $Q = Q^{\mathrm{T}} > 0$ such that the following conditions are satisfied

$$\begin{bmatrix} \Omega_{11} & \Omega_{12} & \Omega_{13} & 0 \\ * & -P & 0 & E^{\mathrm{T}} \\ * & * & -I & 0 \\ * & * & * & -\gamma^2 I \end{bmatrix} < 0, \tag{3.24}$$

and

$$PQ = I, \tag{3.25}$$

where

$$\Omega_{13} = \begin{bmatrix} \sqrt{\beta_1}\tilde{B}_2 \\ \sqrt{\beta_2}\tilde{B}_2 \\ \vdots \\ \sqrt{\beta_s}\tilde{B}_2 \end{bmatrix}.$$

Proof. The proof can be obtained along the lines in Theorem 3.1 by evaluating the $\mathcal{H}_\infty$ performance function

$$\mathcal{J} = \Delta V(\xi_k, k) + z_k^{\mathrm{T}} z_k - \gamma^2 \omega_k^{\mathrm{T}} \omega_k, \tag{3.26}$$

for all l_2-bounded ω_k. □

In Theorem 3.1 and Theorem 3.2, by assuming that the controllers are given, we study the stability and $\mathcal{H}_\infty$ performance of the closed-loop system. Next, we will propose the design method of the feedback-feedforward tracking controllers.

Combined feedback-feedforward tracking controller design: For a given attenuation level γ, the optimized gains of the tracking control law in (3.5) can be derived by solving the following minimization problem:

$$\min \text{Trace}(PQ), \tag{3.27}$$

subject to (3.24) and

$$\begin{bmatrix} P & I \\ I & Q \end{bmatrix} \geq 0. \tag{3.28}$$

It is well known that several algorithms can solve the above nonlinear minimization problem. Among all the algorithms, the cone complementarity linearization (CCL) method [148] is regarded as one of the most effective approaches. When the nonlinear minimization problem is solved, the parameters of the delay-dependent controller can be determined from the solution set.

It is worthwhile to mention that the occurrence probability for each delay can not be known precisely. In order to consider the uncertainty in the probability, we assume that the occurrence probability for each delay is within an interval:

$$\beta_i \in [\underline{\beta_i},\ \overline{\beta_i}], \forall\ i = 1, \cdots, s. \tag{3.29}$$

Then, the $\mathcal{H}_\infty$ performance of the closed-loop system in (3.11) with uncertain probabilities for the stochastic variables is presented in the following corollary.

Corollary 3.1. *Consider the tracking control setup in a network environment shown in Figure 3.1. Suppose that the sequence of controllers are known. For a given positive constant γ, the closed-loop system in (3.11) with uncertain probabilities (3.29) for the stochastic variables is stochastically stable with a prescribed $\mathcal{H}_\infty$ attenuation level γ if*

there exist matrices $P > 0$, and $Q > 0$ such that the following conditions are satisfied

$$\begin{bmatrix} \Omega_{11} & \overline{\Omega}_{12} & \overline{\Omega}_{13} & 0 \\ * & -P & 0 & E^{\mathrm{T}} \\ * & * & -I & 0 \\ * & * & * & -\gamma^2 I \end{bmatrix} < 0, \tag{3.30}$$

and

$$PQ = I, \tag{3.31}$$

where

$$\overline{\Omega}_{12} = \begin{bmatrix} \sqrt{\overline{\beta}_1}(\tilde{A} + \tilde{B}_1 K_{|\kappa_1} \tilde{C}_{|\kappa_1}) \\ \sqrt{\overline{\beta}_2}(\tilde{A} + \tilde{B}_1 K_{|\kappa_2} \tilde{C}_{|\kappa_2}) \\ \vdots \\ \sqrt{\overline{\beta}_s}(\tilde{A} + \tilde{B}_1 K_{|\kappa_s} \tilde{C}_{|\kappa_s}) \end{bmatrix}, \ \overline{\Omega}_{13} = \begin{bmatrix} \sqrt{\overline{\beta}_1}\tilde{B}_2 \\ \sqrt{\overline{\beta}_2}\tilde{B}_2 \\ \vdots \\ \sqrt{\overline{\beta}_s}\tilde{B}_2 \end{bmatrix}.$$

Then the tracking controller can be designed by solving the minimization problem (3.27) subject to (3.30) and (3.28).

Remark 3.1. *In this work, the designed controller is not only dependent on a set of all possible delays, but also dependent on the occurrence probability for each delay. At the actuator node, a suitable control signal is chosen according to the accumulated delay. In other words, the controller switches among $K_{|\kappa_1}, \cdots, K_{|\kappa_s}$.*

3.3 Illustrative Example

Consider a practical design problem for a VTOL helicopter in Figure 3.1 [150, 151]. With the sampling period of $0.01s$, the parameters of the discrete-time state-space

model of the longitudinal motion of the VTOL helicopter are:

$$A = \begin{bmatrix} 0.9996 & 0.0003 & 0.0002 & -0.0046 \\ 0.0005 & 0.9900 & -0.0002 & -0.0400 \\ 0.0010 & 0.0036 & 0.9930 & 00141 \\ 0 & 0 & 0.0100 & 1.0001 \end{bmatrix},$$

$$B = \begin{bmatrix} 0.0044 & 0.0018 \\ 0.0353 & -0.0755 \\ -0.0549 & 0.0446 \\ -0.0003 & 0.0002 \end{bmatrix}, \; C = \begin{bmatrix} 0 \\ 1 \\ 0 \\ 0 \end{bmatrix}^{\mathrm{T}}.$$

The four states of the VTOL helicopter are horizontal velocity, vertical velocity, pitch rate and pitch angle, respectively. The control inputs are collective pitch control action and longitudinal cyclic pitch control action.

Suppose that the set $\mathcal{I} := \{1, 3, 5\}$, i.e., $\kappa_1 = 1, \; \kappa_2 = 3, \; \kappa_3 = 5$. The probability for each delay is 0.95, 0.025, and 0.025, respectively. By solving the minimization problem in (3.27) when the value for γ is 5, we obtain the controller gains as follows:

$$K_{|\kappa_1} = \begin{bmatrix} 4.4461 & 0.7929 & 2.0014 & -2.9241 \\ -4.0183 & -0.6792 & -0.7076 & 1.0519 \end{bmatrix},$$

$$K_{|\kappa_2} = \begin{bmatrix} 3.2917 & 1.3537 & 12.4305 & -1.3631 \\ -0.0120 & 0.1373 & 3.6939 & 0.7318 \end{bmatrix},$$

$$K_{|\kappa_3} = \begin{bmatrix} -2.7690 & 1.4206 & 90.5797 & 13.0911 \\ -1.3525 & -0.5934 & 39.1985 & 12.0436 \end{bmatrix}.$$

It is necessary to mention that the parameters for the control law in (3.5) can be readily obtained from the above designed gains. In the simulation, the reference

signal is set as a sinusoidal signal. The tracking output is depicted in Figure 3.2. It can be seen that although the system is subject to network-induced delays and the frequency of the reference signal is high, the output of the VTOL helicopter can track the reference well. Moreover, compared to the designed controller in Chapter 2 (**Example 2.3**), the tracking error is smaller by using the controller designed in this chapter.

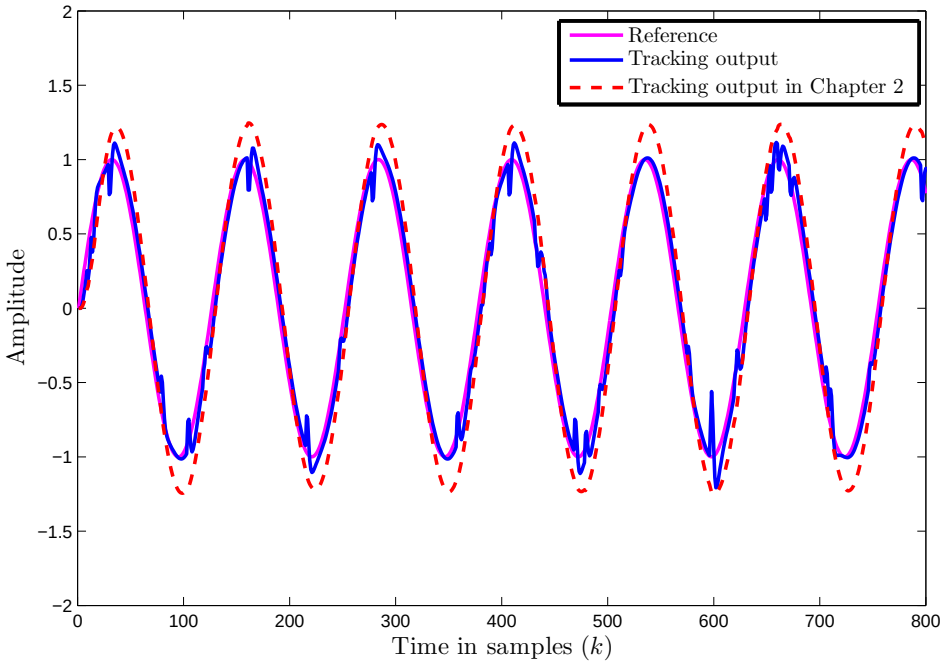

Figure 3.2: Simulation results of the tracking performance for the networked control VTOL under a sinusoidal reference signal.

3.4 Conclusions

In this work, we have proposed a design approach for combined feedback and feedforward tracking control of NCSs by considering network-induced delays. Assuming that each delay has an occurrence probability, delay-dependent controllers are designed for

each delay. The controller gains can be obtained by solving a nonlinear optimization problem. The tracking performance of a VTOL helicopter illustrated the effectiveness of the proposed design method.

Chapter 4

Observer-based Tracking Controller Design for Networked Predictive Control Systems with Uncertain Markov Delays

4.1 Introduction and Motivations

Among the rich literature on NCSs, there are relatively few results on the tracking controller design. The motivations of this chapter are two-fold: (1) To compensate for the network-induced delay by using more information of the delay and delay-predictive actions; (2) to apply the advanced tracking control strategy for NCSs. Specifically, in this chapter, we model the network-induced delay on each channel as a Markov chain. With the Markov chain model, the jump information of the delay can be incorporated into the controller design. Moreover, the Markov transition probability matrix is subject to uncertainties, which can be used to account for the inadequate statistical

information on the network characteristic and the variations during operations. In addition, the tracking controller generates a sequence of control signals which are not only dependent on the delay of the feedback channel but also dependent on all the possible delays of the feedforward channel.

This chapter is organized as follows. In Section 4.2, the problem formulation including the compensation and tracking schemes is introduced. Section 4.3 presents the derivation of sufficient conditions for the energy-to-peak control and the controller design algorithm. In Section 4.4, one example is given to show the design procedure and the efficacy of the proposed design method. Conclusions are summarized in Section 4.5.

4.2 Problem Formulation

The tracking control scheme with predictions used in this chapter is illustrated in Figure 4.1. The output of the plant in the NCSs is sampled by a sensor. Meanwhile, the measured output and the applied control signal are sent to a local Luenberger observer which is employed to estimate the state. The measured output and the estimated state are transmitted via a communication link (feedback channel) to the tracking controller with predictions. The tracking controller generates a sequence of control signals which are packed and transmitted to the actuator by another communication link (feedforward channel). When the control-signal package arrives at the actuator node, the smart actuator picks up a suitable control signal according to the delay between the controller and the actuator to drive the plant.

Consider the following discrete-time networked control systems:

$$\begin{cases} x(k+1) = Ax(k) + Bu(k), \\ \quad y(k) = Cx(k) + Du(k), \end{cases} \tag{4.1}$$

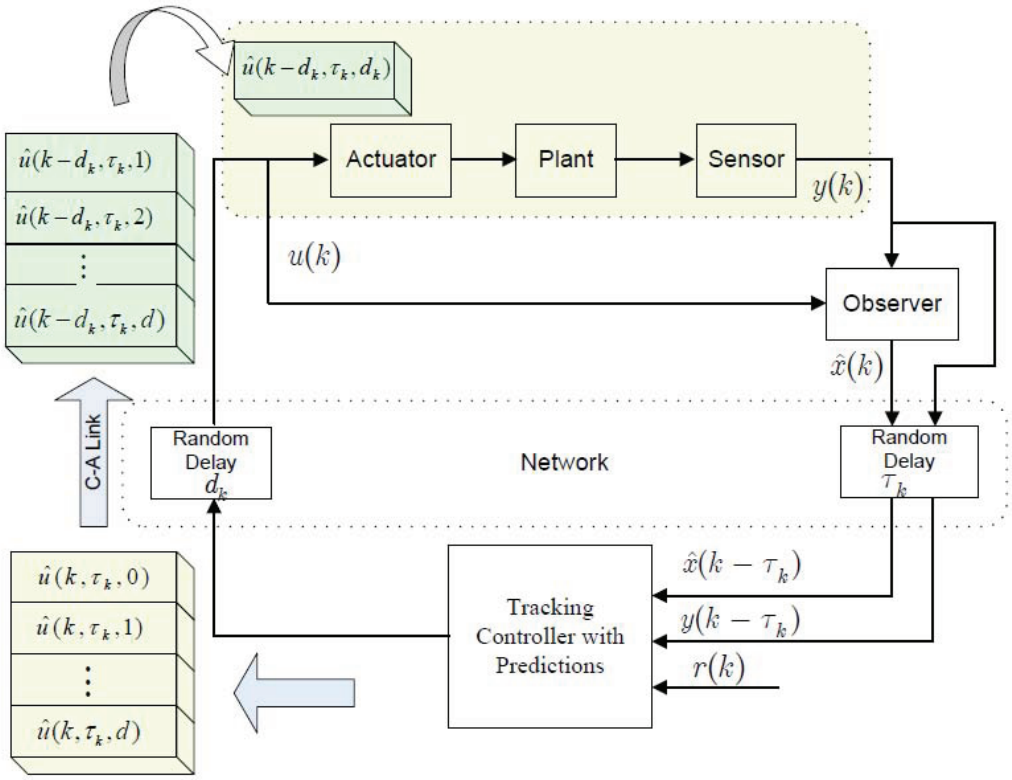

Figure 4.1: Tracking control scheme for a networked predictive control system.

where k is the sampling instant, $x(k) \in \mathbb{R}^n$ denotes the state of the system, $u(k) \in \mathbb{R}^m$ represents the control input, and $y(k) \in \mathbb{R}^q$ is the measured output. The matrices $A,\ B,\ C$ and D are constant with appropriate dimensions.

Before further proceeding, we make some assumptions on the system matrices. Based on these assumptions, we will present the estimator structure and the design procedure in the following sections.

Assumption 4.1. *The matrix set* $(A,\ B)$ *is stabilizable and the matrix set* $(C,\ A)$ *is detectable.*

Assumption 4.2. *The rank of the augmented matrix* $\begin{bmatrix} A-I & B \\ C & D \end{bmatrix}$ *is equal to* $n+m$.

In the tracking control, we propose to use the state vector to feedback. When

some elements in the state vector are not available, a Luenberger observer is utilized to estimate the state. The dynamic of Luenberger observer can be represented by

$$\hat{x}(k+1) = A\hat{x}(k) + Bu(k) + K(y(k) - C\hat{x}(k) - Du(k)), \tag{4.2}$$

where $\hat{x}(k)$ is the estimated state with the same dimension as $x(k)$ and K is a gain to be designed. The objective of the observer design is to design K such that $\hat{x}(k)$ can be estimated for the state $x(k)$ well. By defining the state tracking error as $x_e(k) := x(k) - \hat{x}(k)$, we have the dynamics of the state error as follows:

$$\begin{aligned} x_e(k+1) &= x(k+1) - \hat{x}(k+1) \\ &= (A - KC)x_e(k). \end{aligned} \tag{4.3}$$

The estimated state and the measured output are transmitted to the controller, and the control signals are delivered to the actuator via communication links with limited capacities. In this chapter, we consider the network-induced delays τ_k and d_k on both communication links as shown in Figure 4.1. We further assume that both τ_k and d_k are bounded, that is,

$$0 \leq \tau_k \leq \tau \text{ and } 0 \leq d_k \leq d.$$

In practice, the networked-induced delays can be obtained by using the time-stamp technique. In order to make use of more information on the delays, we can study the delay characteristics and model the random delays τ_k and d_k as two time-homogeneous Markov chains that take values in $\mathcal{M} = \{0, 1, \cdots, \tau\}$ and $\mathcal{N} = \{0, 1, \cdots, d\}$, respectively. The corresponding transition probability matrices are $\Lambda = [\lambda_{ij}^{\alpha^i}]$ and $\Pi = [\pi_{rs}^{\beta^r}]$. Different from the constant transition probability matrices in [52], it is assumed that the transition probability matrices are subject to uncertainties. That is, $\tau(k)$ and

$d(k)$ jump from mode i to j and from mode r to s, respectively, with probabilities $\lambda_{ij}^{\alpha^i}$ and $\pi_{ps}^{\beta^p}$, which are defined by

$$\begin{aligned} \lambda_{ij}^{\alpha^i} &= \Pr(\tau(k+1) = j | \tau(k) = i), \\ \pi_{ps}^{\beta^r} &= \Pr(d(k+1) = s | d(k) = p), \end{aligned} \tag{4.4}$$

where $\lambda_{ij}^{\alpha^i}$ and $\pi_{ps}^{\beta^p}$ are non-negative scalars and

$$\begin{aligned} \Lambda_i^{\alpha^i} &\in \left\{ \sum_{\mathscr{I}=1}^{\mathscr{S}_i} \alpha_{\mathscr{I}}^i \Lambda_i^{\mathscr{I}} \Big| \sum_{\mathscr{I}=1}^{\mathscr{S}_i} \alpha_{\mathscr{I}}^i = 1, \alpha_{\mathscr{I}}^i \geq 0 \right\}, \\ \Pi_p^{\beta^p} &\in \left\{ \sum_{\mathscr{J}=1}^{\mathscr{V}_p} \beta_{\mathscr{J}}^p \Pi_p^{\mathscr{J}} \Big| \sum_{\mathscr{J}=1}^{\mathscr{V}_p} \beta_{\mathscr{J}}^p = 1, \beta_{\mathscr{J}}^p \geq 0 \right\}, \end{aligned} \tag{4.5}$$

for all $i,\ j \in \mathcal{M}$ and $p,\ s \in \mathcal{N}$. Here, $\Lambda_i^{\alpha^i}$ and $\Pi_p^{\beta^p}$ represent the i^{th} row and the p^{th} row of the matrix Λ and Π, respectively. That is,

$$\begin{aligned} \Lambda_i^{\alpha^i} &= \begin{bmatrix} \lambda_{i0}^{\alpha^i} & \lambda_{i1}^{\alpha^i} & \cdots & \lambda_{i\tau}^{\alpha^i} \end{bmatrix}, \\ \Pi_p^{\beta^p} &= \begin{bmatrix} \pi_{p0}^{\beta^p} & \pi_{p1}^{\beta^p} & \cdots & \pi_{pd}^{\beta^p} \end{bmatrix}. \end{aligned} \tag{4.6}$$

Considering the network-induced delay from the estimator to the controller, the input of the tracking controller includes the delayed estimated state $\hat{x}(k-\tau_k)$, the delayed output $y(k-\tau_k)$ and the reference $r(k)$. Since the controller can determine the delay τ_k, we use $r(k-\tau_k)$ in the control law. In order to achieve a good tracking performance, we propose the delay-scheduling and mode-dependent tracking controller as:

$$\hat{u}(k, \tau_k, d_k) = K_S(\tau_k, d_k)\hat{x}(k-\tau_k) + K_I(\tau_k, d_k) \sum_{i=1}^{k-\tau_k-1} e(k-\tau_k), \tag{4.7}$$

where $e(k-\tau_k)$ is the tracking error defined as $e(k-\tau_k) = r(k-\tau_k) - y(k-\tau_k)$,

$K_S(\tau_k, d_k)$, and $K_I(\tau_k, d_k)$ are delay-dependent gains to be designed.

It is necessary to mention that: (1) The control law is a state-feedback control plus an integral control. The state-feedback control is used to stabilize the plant and the integral control can eliminate the tracking error; (2) the control signal is dependent on the randomly time-varying delays on both communication links. It is well known that, at the controller node, the time delay on the feedback link can be readily determined by using the time-stamp technique whereas the current time delay d_k is unknown. On the other hand, we know that the randomly time-varying delay d_k is bounded in the set $\mathcal{N}$ with finite elements. In this case, we adopt the predictive tracking controller from [154]. At each time k, the tracking controller with predictive actions generates a sequence of control signals $[\hat{u}^{\mathrm{T}}(k, \tau_k, 0), \cdots, \hat{u}^{\mathrm{T}}(k, \tau_k, d)]^{\mathrm{T}}$. These control signals are packed and transmitted to the actuator. By determining the network-induced delay d_k on the feedforward channel, the actuator picks up a suitable control signal $\hat{u}(k, \tau_k, d_k)$.

When considering the delays on both channels and the predictive control strategy, the utilized control signal at the actuator node is

$$u(k) = K_S(\tau_k, d_k)\hat{x}(k - \tau_k - d_k) + K_I(\tau_k, d_k) \sum_{i=1}^{k-\tau_k-d_k-1} e(k - \tau_k - d_k). \tag{4.8}$$

It is important to notice that the state-feedback control term in (4.8) is easy to be incorporated into the plant (4.1) whereas the second integration term is difficult to handle. In order to deal with the external input $r(k)$ and eliminate the output

tracking error, we introduce some new variables as

$$\begin{aligned}
\bar{u}(k) &= u(k+1) - u(k), \\
\bar{x}(k) &= \hat{x}(k+1) - \hat{x}(k), \\
\bar{y}(k) &= y(k+1) - y(k), \\
\bar{x}_e(k) &= x_e(k+1) - x_e(k), \\
\bar{r}(k) &= r(k+1) - r(k).
\end{aligned} \tag{4.9}$$

By considering these new variables, the tracking error $e(k)$ has the following dynamics:

$$\begin{aligned}
e(k+1) &= r(k+1) - y(k+1) \\
&= e(k) - C\bar{x}(k) - D\bar{u}(k) + \bar{r}(k).
\end{aligned} \tag{4.10}$$

Moreover, the expression of the observer (4.2) becomes

$$\bar{x}(k+1) = A\bar{x}(k) + B\bar{u}(k) + KC\bar{x}_e(k), \tag{4.11}$$

the dynamics of the state error becomes

$$\bar{x}_e(k+1) = (A - KC)\bar{x}_e(k). \tag{4.12}$$

and the difference of the utilized control signal is

$$\bar{u}(k) = K_S(\tau_k, d_k)\bar{x}(k - \tau_k - d_k) + K_I(\tau_k, d_k)e(k - \tau_k - d_k). \tag{4.13}$$

By defining a new state vector $\xi^{\mathrm{T}}(k) = [\bar{x}^{\mathrm{T}}(k),\ \bar{x}_e^{\mathrm{T}}(k),\ e^{\mathrm{T}}(k)]$ and considering from (4.10)–(4.12), we have the following augmented system:

$$\begin{aligned}\xi(k+1) &= \bar{A}\xi(k) + B_1 u(t) + B_2\bar{r}(k) \\ &= (A_0 + B_0 K C_0)\xi(k) + B_1\bar{u}(k) + B_2\bar{r}(k),\end{aligned} \tag{4.14}$$

where

$$\bar{A} = \begin{bmatrix} A & KC & 0 \\ 0 & A-KC & 0 \\ -C & 0 & I \end{bmatrix},\ A_0 = \begin{bmatrix} A & 0 & 0 \\ 0 & A & 0 \\ -C & 0 & I \end{bmatrix},$$

$$B_0 = \begin{bmatrix} I \\ -I \\ 0 \end{bmatrix},\ B_1 = \begin{bmatrix} B \\ 0 \\ -D \end{bmatrix}, B_2 = \begin{bmatrix} 0 \\ 0 \\ I \end{bmatrix},$$

$$C_0 = \begin{bmatrix} 0 & C & 0 \end{bmatrix}.$$

The difference of the utilized control signal in (4.13) can be rewritten as

$$\bar{u}(k) = \mathcal{K}(\tau_k, d_k)H\xi(k-\tau_k-d_k) + K_F(\tau_k, d_k)\bar{r}(k-\tau_k-d_k), \tag{4.15}$$

where $\mathcal{K}(\tau_k, d_k) = [K_S(\tau_k, d_k), K_I(\tau_k, d_k)]$ and $H = \begin{bmatrix} I & 0 & 0 \\ 0 & 0 & I \end{bmatrix}$. It is noted that the delayed state is involved in (4.15). In order to construct a delay-free closed-loop system, we define a new state-variable as

$$X^{\mathrm{T}}(k) = \begin{bmatrix} \xi^{\mathrm{T}}(k) & \xi^{\mathrm{T}}(k-1) & \cdots & \xi^{\mathrm{T}}(k-\tau-d) \end{bmatrix}. \tag{4.16}$$

The augmented system (4.14) with the utilized control signal (4.15) can be rewritten

as

$$\begin{aligned} X(k+1) =& \tilde{A}(\tau_k, d_k)X(k) + \tilde{B}w(k) \\ =& (\tilde{A}_0 + \tilde{B}_0 K \tilde{C}_0 + \tilde{B}_1 \mathcal{K}(\tau_k, d_k)\tilde{H})X(k) + \tilde{B}w(k), \\ X(0) =& [\Phi^{\mathrm{T}}(0)\ \Phi^{\mathrm{T}}(-1)\ \cdots \Phi^{\mathrm{T}}(-\tau - d)], \end{aligned} \tag{4.17}$$

where

$$\tilde{A}_0 = \begin{bmatrix} A_0 & 0 & \cdots & 0 & 0 \\ I & 0 & \cdots & 0 & 0 \\ 0 & I & \cdots & 0 & 0 \\ \vdots & \vdots & \ddots & \vdots & \vdots \\ 0 & 0 & \cdots & I & 0 \end{bmatrix},\ \tilde{B}_0 = \begin{bmatrix} B_0 \\ 0 \\ 0 \\ \vdots \\ 0 \end{bmatrix},$$

$$w(k) = \begin{bmatrix} \bar{r}(k) \end{bmatrix},\ \tilde{C}_0 = \begin{bmatrix} C_0 & 0 & 0 & \cdots & 0 \end{bmatrix},$$

$$\tilde{B} = \begin{bmatrix} B_2 \\ 0 \\ 0 \\ \vdots \\ 0 \end{bmatrix},\ \tilde{B}_1 = \begin{bmatrix} B_1 \\ 0 \\ 0 \\ \vdots \\ 0 \end{bmatrix},$$

$$\tilde{H} = \begin{bmatrix} 0 & \cdots & 0 & \underbrace{H}_{(\tau_k + d_k + 1)^{th}\text{block}} & 0 & \cdots & 0 \end{bmatrix}.$$

For the tracking control problem, we concern with the tracking error. Therefore, the controlled output is defined as:

$$z(k) = \tilde{E}X(k), \tag{4.18}$$

where $\tilde{E} = \begin{bmatrix} \begin{bmatrix} 0 & 0 & I \end{bmatrix} & 0 & \cdots & 0 & 0 \end{bmatrix}$. In summary, the closed-loop system with

the controlled output is

$$\begin{cases} X(k+1) = \tilde{A}(\tau_k, d_k)X(k) + \tilde{B}w(k), \\ \quad z(k) = \tilde{E}X(k), \\ \quad X(0) = [\Phi^{\mathrm{T}}(0)\ \Phi^{\mathrm{T}}(-1)\ \cdots \Phi^{\mathrm{T}}(-\tau - d)]. \end{cases} \tag{4.19}$$

It is necessary to emphasize that the tracking controller design problem has been transformed into the robust analysis of the closed-loop system in (4.19). Moreover, the closed-loop system in (4.19) is a stochastic system due to the existence of the stochastic variables τ_k and d_k.

In many practical applications, the overshoot of the output shall be constrained. Hence, by assuming that the external input $w(k)$ is l_2 bounded, we define the energy-to-peak performance for the closed-loop system.

Definition 4.1. *Given a positive scalar γ, the system in (4.19) is stochastically stable with an energy-to-peak performance γ when the initial state $X(0) = 0$, the closed-loop system in (4.19) is stochastically stable and the following condition is satisfied:*

$$\|z\|_{\mathcal{E}_\infty} < \gamma \|\omega\|_2, \tag{4.20}$$

for all nonzero $\omega(k) \in l_2[0, \infty)$, where

$$\begin{aligned} \|z\|_{\mathcal{E}_\infty} &:= \sup_{\tau(0)\in\mathcal{M}} \sup_{d(0)\in\mathcal{N}} \sup_k \sqrt{\mathcal{E}\left\{|z(k)|^2 \,\middle|\, \tau_0, d_0\right\}}, \\ \|\omega\|_2 &:= \mathcal{E}\left\{\sqrt{\sum\nolimits_{k=0}^{\infty} (\omega^{\mathrm{T}}(k)\omega(k))}\right\}. \end{aligned} \tag{4.21}$$

Note that the tracking controller design problem for the NCS with predictive actions in (4.1) subject to network-induced delays has now been converted into an output feedback control problem of a delay-free system (4.19) with stochastic variables.

In addition, the requirement on minimizing the tracking error has been equivalently converted into the minimization of the corresponding controlled output. In the following, the main objectives are to analyze the stochastic stability and the energy-to-peak performance of the stochastic system in (4.19), and to design the mode-dependent tracking controllers. More specifically, the following issues are to be tackled.

O1 By assuming the controllers are given, study the stochastic stability of the system in (4.19) with zero external input (zero reference).

O2 By assuming the controllers are given, investigate the energy-to-peak performance of the stochastic system in (4.19) with l_2 bounded input $w(k)$, that is, for a given $\gamma > 0$, find conditions such that

$$\|z\|_{\mathcal{E}_\infty} < \gamma \|\omega\|_2 . \tag{4.22}$$

O3 Based on the above results, design a sequence of mode-dependent controllers such that the closed-loop system in (4.19) is stochastically stable with an energy-to-peak performance γ.

Remark 4.1. *Recently, the research work on Markovian jump linear systems with unknown transition probabilities have received increasing attentions [155, 156]. The uncertain model of the transition matrix used in this chapter can characterize the phenomenon of unknown transition probabilities [157]. In this chapter, we employ the uncertain Markov chain to model the network-induced delay in NCSs. Since the statistic information of the network-induced delays may be incomplete, the delay description with an uncertain Markov chain is more practical and general.*

4.3 Main Results

4.3.1 Stability and Performance Analysis

In this subsection, we will present the stochastic stability and the energy-to-peak performance analysis results for the closed-loop system (4.19) by assuming the controllers proposed in (4.7) are given.

With Definition 3.1, the sufficient and necessary conditions of the stochastic stability for (4.7) are given in the following theorem.

Theorem 4.1. *With a zero external input ($w(k) = 0$), the closed-loop system (4.19) is stochastically stable if and only if there exist symmetric matrices $P(i,p) > 0$ such that the following matrix inequalities:*

$$\sum_{j=0}^{\tau}\sum_{s=0}^{d}\lambda_{ij}^{\alpha^i}\pi_{ps}^{\beta p}\tilde{A}^{\mathrm{T}}(i,p)P(j,s)\tilde{A}(i,p) - P(i,p) < 0 \tag{4.23}$$

hold for all $i \in \mathcal{M}$ and $p \in \mathcal{N}$.

Proof. Construct the following quadratic Lyapunov function:

$$V(X(k),k) = X^{\mathrm{T}}(k)P(i,p)X(k). \tag{4.24}$$

The difference of the quadratic Lyapunov function is defined as [52]:

$$\begin{aligned}\Delta V(X(k),k) =& \mathcal{E}\Big\{X^{\mathrm{T}}(k+1)P(j,s)X(k+1)\Big|X(k),\tau_k,d_k\Big\} \\ &- X^{\mathrm{T}}(k)P(i,p)X(k).\end{aligned} \tag{4.25}$$

The details are omitted since the theorem can be proved by following a similar line in [52] and [31]. □

Theorem 4.1 provides the sufficient and necessary conditions for the stochastic

stability of the closed-loop system by neglecting the external input. In order to evaluate the effect of the external input $w(k)$, we exploit the energy-to-peak performance of the closed-loop system in the following theorem.

Theorem 4.2. *Given a positive scalar γ, the closed-loop system (4.19) is stochastically stable with an energy-to-peak performance γ if there exist symmetric matrices $P(i,p) > 0$ such that the following matrix inequalities are satisfied:*

$$\begin{bmatrix} -\bar{P}(j,s) & \bar{P}(j,s)\tilde{A}(i,p) & \bar{P}(j,s)\tilde{B} \\ * & -P(i,p) & 0 \\ * & * & -I \end{bmatrix} < 0, \tag{4.26}$$

$$\begin{bmatrix} -P(i,p) & \tilde{E}^{\mathrm{T}} \\ * & -\gamma^2 I \end{bmatrix} < 0, \tag{4.27}$$

for all $i \in \mathcal{M}$ and $p \in \mathcal{N}$. Here, $\bar{P}(j,s) := \sum_{j=0}^{\tau}\sum_{s=0}^{d}\lambda_{ij}^{\alpha^i}\pi_{ps}^{\beta^p}P(j,s)$.

Proof. By using Schur complement, it implies from (4.26) that (4.23) in Theorem 4.1 is satisfied. Thus, the closed-loop system in (4.19) is stochastically stable. Reconsider the Lyapunov function (4.24) and the difference of the Lyapunov function in (4.25) for non-zero external input. The difference of the Lyapunov function in (4.25) can be re

evaluated as:

$$\mathcal{E}\Big\{\Delta V(X(k),k)\Big\} = \begin{bmatrix} X(k) \\ w(k) \end{bmatrix}^{\mathrm{T}} \begin{bmatrix} \Theta_{11} & \Theta_{12} \\ * & \Theta_{22} \end{bmatrix} \begin{bmatrix} X(k) \\ w(k) \end{bmatrix}, \tag{4.28}$$

where

$$\begin{aligned}\Theta_{11} &= \tilde{A}^{\mathrm{T}}(i,p)\bar{P}(j,s)\tilde{A}(i,p) - P(i,p),\\ \Theta_{12} &= \tilde{A}^{\mathrm{T}}(i,p)\bar{P}(j,s)\tilde{B},\\ \Theta_{22} &= \tilde{B}^{\mathrm{T}}\bar{P}(j,s)\tilde{B}.\end{aligned} \tag{4.29}$$

Subsequently, to establish the energy-to-peak performance for the closed-loop system, assume the zero initial condition and consider the following performance index:

$$J := \mathcal{E}\left\{V(X(k),k)\right\} - \mathcal{E}\left\{\sum_{\mathscr{G}=0}^{k-1} w^{\mathrm{T}}(\mathscr{G})w(\mathscr{G})\right\} \tag{4.30}$$

for any non-zero $w(k) \in l_2[0,\infty)$ and $k > 0$. Considering the external input $w(k)$ and the expression of the closed-loop system, we can obtain

$$\begin{aligned}J :=& \mathcal{E}\left\{V(X(k),k)\right\} - \mathcal{E}\left\{\sum_{\mathscr{G}=0}^{k-1} w^{\mathrm{T}}(\mathscr{G})w(\mathscr{G})\right\}\\ =& \mathcal{E}\left\{V(X(k),k)\right\} - \mathcal{E}\left\{V(X(0),0)\right\}\\ & - \mathcal{E}\left\{\sum_{\mathscr{G}=0}^{k-1} w^{\mathrm{T}}(\mathscr{G})w(\mathscr{G})\right\}\\ =& \mathcal{E}\left\{\sum_{\mathscr{G}=0}^{k-1} \Delta V(X(k),k) - \sum_{\mathscr{G}=0}^{k-1} w^{\mathrm{T}}(\mathscr{G})w(\mathscr{G})\right\}\\ =& \sum_{\mathscr{G}=0}^{k-1}\left\{\mathcal{E}\left\{\begin{bmatrix} X(\mathscr{G}) \\ w(\mathscr{G})\end{bmatrix}^{\mathrm{T}}\begin{bmatrix}\Theta_{11} & \Theta_{12}\\ * & \tilde{\Theta}_{22}\end{bmatrix}\begin{bmatrix} X(\mathscr{G}) \\ w(\mathscr{G})\end{bmatrix}^{\mathrm{T}}\right\}\right\},\end{aligned} \tag{4.31}$$

where

$$\tilde{\Theta}_{22} = -I + \tilde{B}^{\mathrm{T}}\bar{P}(j,s)\tilde{B}.$$

By using Schur complement again, the inequality (4.26) implies that $J < 0$, that

is, $\mathcal{E}\{V(X(k),k)\} < \mathcal{E}\left\{\sum_{\mathscr{G}=0}^{k-1} w^{\mathrm{T}}(\mathscr{G})w(\mathscr{G})\right\}$. From the expression of the Lyapunov function (4.24) and the above inequality, we can obtain

$$\mathcal{E}\left\{V(X(k),k) + w^{\mathrm{T}}(k)w(k)\right\} \leq \mathcal{E}\left\{\sum_{\mathscr{G}=0}^{k} w^{\mathrm{T}}(\mathscr{G})w(\mathscr{G})\right\}. \tag{4.32}$$

On the other hand, by using Schur complement, the LMI (4.27) is equivalent to

$$\tilde{E}^{\mathrm{T}}\tilde{E} < \gamma^2 P(i,p). \tag{4.33}$$

Then we can conclude that, for all time $k > 0$,

$$\begin{aligned}
&\mathcal{E}\left\{z^{\mathrm{T}}(k)z(k)\middle|\tau_0, d_0\right\} \\
&= \mathcal{E}\left\{X^{\mathrm{T}}(k)\tilde{E}^{\mathrm{T}}\tilde{E}X(k)\right\} \\
&\leq \mathcal{E}\left\{\gamma^2 X^{\mathrm{T}}(k)P(i,p)X(k)\right\} \\
&\leq \mathcal{E}\left\{\sum_{\mathscr{G}=0}^{k} w^{\mathrm{T}}(\mathscr{G})w(\mathscr{G})\right\} \leq \mathcal{E}\left\{\sum_{\mathscr{G}=0}^{\infty} w^{\mathrm{T}}(\mathscr{G})w(\mathscr{G})\right\}.
\end{aligned} \tag{4.34}$$

Taking the supremum over time $k > 0$ yields $\|z\|_{\mathcal{E}\infty} < \gamma \|w\|_2$ for all nonzero $w(k) \in l_2[0,\infty)$, which completes the proof.

□

In Theorem 4.2, sufficient conditions are derived for the energy-to-peak performance of the system in (4.19). However, the elements of the Markov transition matrices used in $\bar{P}(j,s)$ are subject to uncertainties. We can not directly employ Theorem 4.2 to evaluate the energy-to-peak performance and design the controller. It is assumed in (4.5) that each row of the transition matrices is described by a convex polytope. Thus, in the rest of this subsection, the conditions in Theorem 4.2 are

extended to each vertex of the polytopes.

Corollary 4.1. *Given a positive scalar γ, the closed-loop system (4.19) is stochastically stable with an energy-to-peak performance γ if there exist symmetric matrices $P(i,p) > 0$ such that the following matrix inequalities are satisfied:*

$$\begin{bmatrix} -\bar{P}^{\mathscr{I}\mathscr{J}}(j,s) & \bar{P}^{\mathscr{I}\mathscr{J}}(j,s)\tilde{A}(i,p) & \bar{P}^{\mathscr{I}\mathscr{J}}(j,s)\tilde{B} \\ * & -P(i,p) & 0 \\ * & * & -I \end{bmatrix} < 0, \tag{4.35}$$

$$\begin{bmatrix} -P(i,p) & \tilde{E}^{\mathrm{T}} \\ * & -I \end{bmatrix} < 0, \tag{4.36}$$

and

$$\bar{P}^{\mathscr{I}\mathscr{J}}(j,s) := \sum_{j=0}^{\tau}\sum_{s=0}^{d} \lambda_{ij}^{\alpha_{\mathscr{I}}^{i}} \Pi_{ps}^{\beta_{\mathscr{J}}^{p}} P(j,s,) \tag{4.37}$$

for all $i \in \mathcal{M}$, $p \in \mathcal{N}$, $\mathscr{I} = 1, \cdots, \mathscr{S}_i$, and $\mathscr{J} = 1, \cdots, \mathscr{V}_p$.

Proof. The proof can be done by using the convex combination as utilized in the extension of the robust control and filtering [123]. □

Remark 4.2. *In Theorem 4.2, we study the energy-to-peak performance for a Markovian jump linear system with uncertain transition matrices. The energy-to-peak control (known as generalized $\mathcal{H}_2$ [121, 158, 159] control) is one of the widely used strategies on evaluating and constraining the influence of the external input. In this chapter, by assuming that the increment of the reference signal $\bar{r}(k)$ is l_2 bounded, the main idea of energy-to-peak control is to constrain the gain from the 2 norm of the increment of the reference $\bar{r}(k)$ to the infinity norm of the tracking error.*

4.3.2 Controller Design

In Corollary 4.1, the energy-to-peak performance of the closed-loop system in (4.19) can be guaranteed by the conditions represented by the polytope vertices. Therefore, the tracking controller with predictive actions can be designed via Corollary 4.1. However, it is noted that the conditions stated in Corollary 4.1 are non-convex owing to the involved bilinear matrix terms. The problem of solving this kind of conditions can be formulated as a rank-constrained LMI problem. Firstly, we eliminate the bilinear terms in (4.35) in the next theorem.

Theorem 4.3. *Given a positive scalar γ, the closed-loop system (4.19) is stochastically stable with an energy-to-peak performance γ if there exist symmetric matrices $P(i,p) > 0$ and $\bar{Q}(i,p)$ such that the following matrix inequalities are satisfied:*

$$\begin{bmatrix} -\bar{Q}(i,p) & \tilde{A}(i,p) & \tilde{B} \\ * & -P(i,p) & 0 \\ * & * & -I \end{bmatrix} < 0, \tag{4.38}$$

$$\begin{bmatrix} -P(i,p) & \tilde{E}^{\mathrm{T}} \\ * & -\gamma^2 I \end{bmatrix} < 0, \tag{4.39}$$

and

$$\bar{Q}(i,p)\left\{\sum_{j=0}^{\tau}\sum_{s=0}^{d}\lambda_{ij}^{\alpha_{\mathscr{I}}^{i}}\Pi_{ps}^{\beta_{\mathscr{J}}^{p}}P(j,s)\right\} = I, \tag{4.40}$$

for all $i \in \mathcal{M}$, $p \in \mathcal{N}$, $\mathscr{I} = 1, \cdots, \mathscr{S}_i$, and $\mathscr{J} = 1, \cdots, \mathscr{V}_p$.

Proof. It is inferred from (4.40) that $\bar{Q}^{-1}(i,p) = \left\{\sum_{j=0}^{\tau}\sum_{s=0}^{d}\lambda_{ij}^{\alpha_{\mathscr{I}}^{i}}\Pi_{ps}^{\beta_{\mathscr{J}}^{p}}P(j,s)\right\}$. Performing a congruence transformation to (4.38) by $\mathrm{diag}\{Q^{-1}(i,p),\ I,\ I\}$, we derive the condition (4.35). The proof is completed. □

The main idea of the transformation is to utilize the fact that

$$Q(i,p)\left\{\sum_{j=0}^{\tau}\sum_{s=0}^{d}\lambda_{ij}^{\alpha_{\mathscr{I}}^{i}}\Pi_{ps}^{\beta_{\mathscr{J}}^{p}}P(j,s)\right\}=I,$$

if the rank of the product $\left\{Q(i,p)\left\{\sum_{j=0}^{\tau}\sum_{s=0}^{d}\lambda_{ij}^{\alpha_{\mathscr{I}}^{i}}\Pi_{ps}^{\beta_{\mathscr{J}}^{p}}P(j,s)\right\}\right\}$ is equal to the rank of $\left\{\sum_{j=0}^{\tau}\sum_{s=0}^{d}\lambda_{ij}^{\alpha_{\mathscr{I}}^{i}}\Pi_{ps}^{\beta_{\mathscr{J}}^{p}}P(j,s)\right\}$. Although this transformation is simple, it is still difficult to solve the involved rank conditions. Over the past decades, much work has been done and many iterative techniques have been developed to solve the rank-constrained LMI problem [146], such as the cone complementarity linearization (CCL) algorithm [148] and Newton-type search method [149].

In this chapter, we employ the CCL algorithm to solve the controller design problem by converting the non-convex problem in Theorem 4.3 into the following nonlinear minimization problem.

Tracking controller design:

$$\min \text{ trace}\left(\sum_{i=0}^{\tau}\sum_{p=0}^{d}\bar{Q}(i,p)\bar{P}^{\mathscr{I}\mathscr{J}}(j,s)\right)$$

subject to (4.38), (4.39) and

$$\begin{bmatrix}\bar{Q}(i,p) & I\\ I & \sum_{j=0}^{\tau}\sum_{s=0}^{d}\lambda_{ij}^{\alpha_{\mathscr{I}}^{i}}\Pi_{ps}^{\beta_{\mathscr{J}}^{p}}P(j,s)\end{bmatrix}\geq 0,$$

for all $i\in\mathcal{M}$, $p\in\mathcal{N}$, $\mathscr{I}=1,\cdots,\mathscr{S}_i$, and $\mathscr{J}=1,\cdots,\mathscr{V}_p$.

In [148], it was shown that an optimal set of solution can be obtained by computing finite iterations of a set of LMIs for most cases. If the solution of the minimization problem is derived, the parameters of the estimator and the tracking controller can be readily obtained from the solution set.

4.4 Numerical Example

Consider the tracking control for a DC motor in a network environment. The plant is a geared DC motor, being is a component of the MS150 Modular Servo System, with the following model:

$$\begin{cases} \dot{x}(t) = \begin{bmatrix} 0 & 1 \\ 0 & -3.5287 \end{bmatrix} x(t) + \begin{bmatrix} 0 \\ 172.38 \end{bmatrix} u(t), \\ y(t) = \begin{bmatrix} 1 & 0 \end{bmatrix} x(t), \end{cases} \tag{4.41}$$

where the input $u(t)$ is the power supply and $y(t)$ is the output (a rotary angle of the extended shaft). When the sampling period is $0.01s$, the equivalent discrete-time model is represented by

$$\begin{cases} \tilde{x}(k+1) = \begin{bmatrix} 1 & 0.0098 \\ 0 & 0.9653 \end{bmatrix} x(k) + \begin{bmatrix} 0.0085 \\ 1.6937 \end{bmatrix} u(k), \\ y(k) = \begin{bmatrix} 1 & 0 \end{bmatrix} x(k). \end{cases} \tag{4.42}$$

For the involved network channels, we assume that $\mathcal{M} = \{0,\ 1\}$ and $\mathcal{N} = \{0,\ 1\}$. The Markov transition matrix for the feedback channel is subject to uncertainties and is described by a 2-vertex polytope:

$$\Lambda^1 = \begin{bmatrix} 0.4 & 0.6 \\ 0.3 & 0.7 \end{bmatrix},\ \Lambda^2 = \begin{bmatrix} 0.6 & 0.4 \\ 0.3 & 0.7 \end{bmatrix}.$$

The transition matrix for the feedforward channel is expressed as

$$\Pi = \begin{bmatrix} 0.2 & 0.8 \\ 0.5 & 0.5 \end{bmatrix}.$$

By applying the tracking controller design algorithm, the derived controller gains are

$$K = \begin{bmatrix} 0.0041 \\ 0.0185 \end{bmatrix},$$

$$K_S(0,0) = \begin{bmatrix} -0.6145 & -0.3138 \end{bmatrix},\ K_I(0,0) = 0.0161,$$

$$K_S(0,1) = \begin{bmatrix} -0.0753 & 0.0059 \end{bmatrix},\ K_I(0,1) = 0.0009,$$

$$K_S(1,0) = \begin{bmatrix} -0.3049 & -0.1657 \end{bmatrix},\ K_I(1,0) = 0.0090,$$

$$K_S(1,1) = \begin{bmatrix} -0.1422 & -0.0624 \end{bmatrix},\ K_I(1,1) = 0.0042.$$

It is necessary to mention that the eigenvalues of the system matrix $A - KC$ are 0.9879 and 0.9733. Thus, the state error system (4.12) is stable.

In the simulation, we assume that the actual Markov transition matrix for the delay on the feedback channel is $\begin{bmatrix} 0.5 & 0.5 \\ 0.3 & 0.7 \end{bmatrix}$. Figure 4.2 shows the state estimation error for this example in a random simulation run. The tracking control performance is depicted in Figure 4.3 for a unit step reference. It can be seen that the estimator and the tracking controller work well.

4.5 Conclusions

In this chapter, we have exploited the tracking control problem for discrete-time networked predictive control systems. It is assumed that the networked-induced delays on both feedback and feedforward control channels are governed by Markov chains with uncertain transition matrices. By using the predictive control strategy, the tracking controller, consisting of a state-feedback control plus an integral control, is dependent on both networked-induced delay. Sufficient conditions are established for

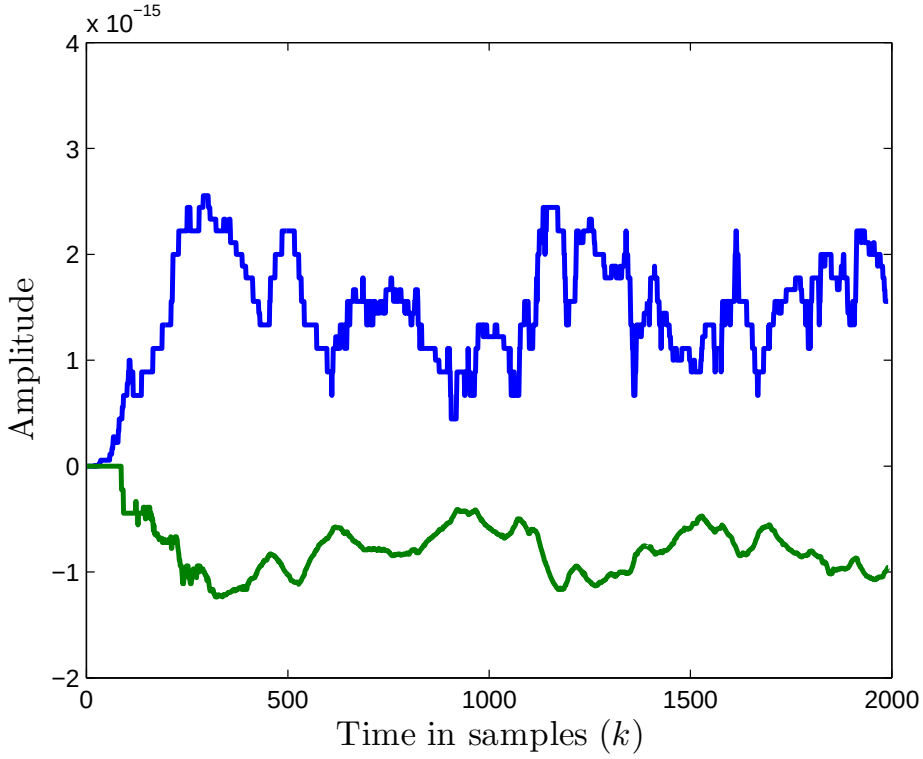

Figure 4.2: State estimation error of the DC motor example.

assuring the energy-to-peak performance of the closed-loop system. The controller can be designed by solving an LMI-based minimization problem. A DC motor example illustrates the effectiveness of the proposed design scheme.

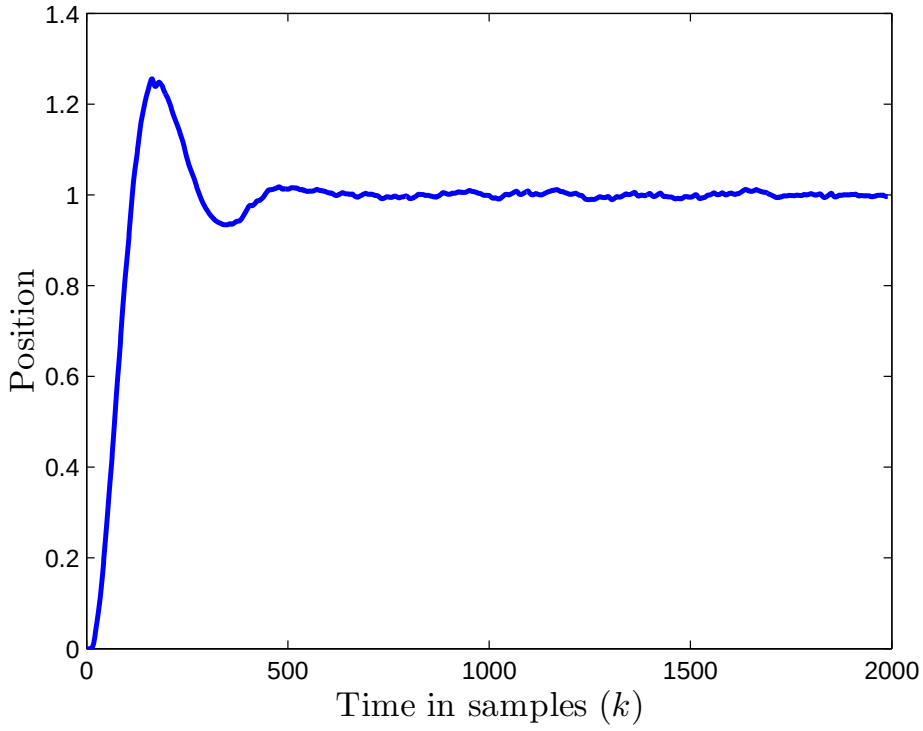

Figure 4.3: Tracking control performance of the networked predictive DC motor.

Chapter 5

$\mathcal{H}_\infty$ Step Tracking Control for Networked Discrete-time Nonlinear Systems with Integral and Predictive Actions

5.1 Introduction and Motivations

Smooth nonlinear systems can be universally approximated by T-S fuzzy linear models [160, 161]. Based on T-S models, we can study nonlinear systems using well-developed techniques in linear system theory. As T-S fuzzy models have been successfully used to model a wide range of practical nonlinear systems [162, 163], the control problem for nonlinear systems based on the T-S model have attracted considerable attention [164].

In the literature, although there are many research results on NCSs and T-S fuzzy systems, most of the works have been focused on the stability analysis, stabiliza-

tion [18, 52, 165, 166], and state estimation [124, 126, 167–169]. The tracking problem has received much less attention. Motivated by this, we study the tracking control problem for discrete-time nonlinear systems in a network environment with limited capacity. The nonlinear system is approximated by T-S fuzzy systems. The network-induced delay which is the main challenge in the design for NCSs is considered on both communication links from the sensor to the controller (S-C), and from the controller to the actuator (C-A). In order to compensate for the network-induced delay on the C-A link, the predictive control technique is applied. The control law is the state feedback plus the error integration. With the augmentation approach, the state-feedback and integral feedback controller design for the networked nonlinear system is transformed into a state-feedback controller design for a stochastic fuzzy system with delayed state. After investigating on the exponential mean-square stability and the $\mathcal{H}_\infty$ performance for the augmented system, the controller design approach is proposed.

This chapter is organized as follows. In Section 5.2, we formulate the step tracking control problem for the networked T-S fuzzy model (approximation of a nonlinear system) and present the control objectives. In Section 5.3, the stability and the $\mathcal{H}_\infty$ performance are investigated for the formulated stochastic system. Based on the obtained results, the controller design method is proposed. The delay-dependent and fuzzy-weighting-function-dependent feedback gains can be derived by solving a sequence of LMIs. In Section 5.4, a networked electro-mechanical system is used to show some features of the proposed control scheme. Section 5.5 concludes the chapter.

5.2 Problem Formulation

Consider the tracking control problem for a networked discrete-time nonlinear system as shown in Figure 5.1. The complex nonlinear discrete-time system can be repre-

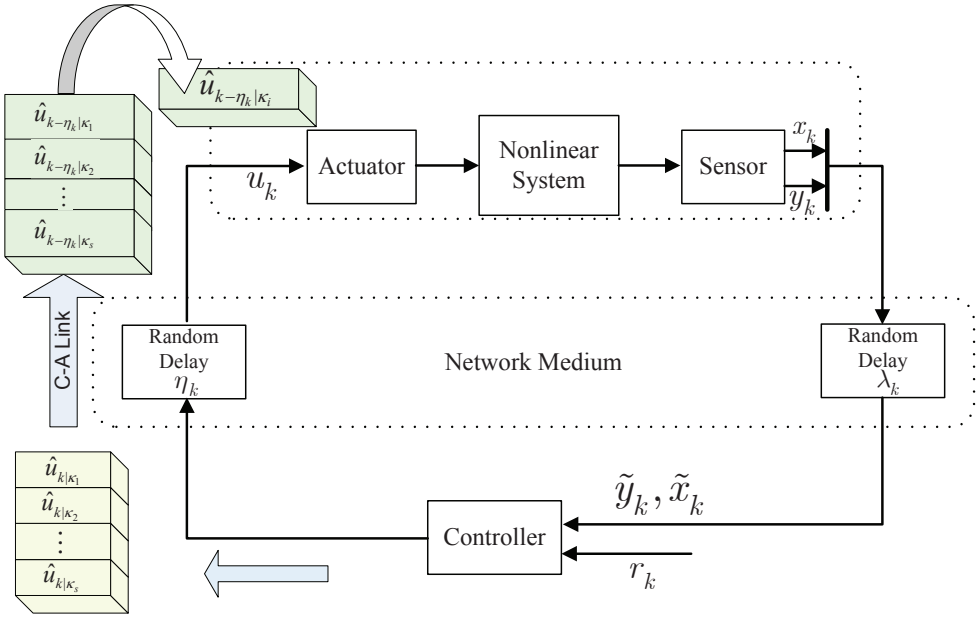

Figure 5.1: Networked tracking control for nonlinear systems.

sented by a T-S fuzzy model which characterizes the joint dynamics of each fuzzy rule by a linear system [160]. In this work, we consider a special case of the T-S fuzzy model in which the nonlinearity only occurs in the system matrix and input matrix, that is, the i^{th} rule of the model is

Plant rule i: **IF** $\theta_1(k)$ is $\mathcal{M}_{i1}$ and $\theta_2(k)$ is $\mathcal{M}_{i2}$ ... and $\theta_p(k)$ is $\mathcal{M}_{ip}$, **THEN**

$$\begin{aligned} x_{k+1} &= A_i x_k + B_i u_k, \\ y_k &= C x_k + D u_k, \\ i &\in \mathcal{R}, \end{aligned} \tag{5.1}$$

where $\mathcal{M}_{ij}$ for $j = 1, \cdots, p$ are the fuzzy sets, $\theta_k = [\theta_{1k},\ \theta_{2k},\ \ldots, \theta_{pk}]$ is the premise variable vector, $x_k \in \mathbb{R}^n$ represents the state of the system, $u_k \in \mathbb{R}^m$ denotes the control input, and $y_k \in \mathbb{R}^q$ is the output of the nonlinear system. $A_i,\ B_i,\ C$, and D are system matrices with appropriate dimensions. The normalized fuzzy weighting function for the i^{th} rule is defined as

$$h_i(\theta(k)) = \frac{\prod_{j=1}^{p} \mu_{ij}(\theta_j(k))}{\sum_{i=1}^{\tau} \prod_{j=1}^{p} \mu_{ij}(\theta_j(k))}, \tag{5.2}$$

where $\mu_{ij}(\theta_j(k))$ is the grade of the membership of $\theta_j(k)$ in the fuzzy rule i. Defining a vector as $\Theta_k = [h_1(\theta(k)), \cdots,\ h_\tau(\theta(k))]$, it is noted that the vector satisfies

$$\Theta_k \in \Upsilon := \Big\{\Theta \in \mathbb{R}^\tau | \sum_{i=1}^{\tau} h_i(\theta(k)) = 1, 0 \leq h_i(\theta(k)) \leq 1\Big\}. \tag{5.3}$$

With the normalized fuzzy weighting functions, the networked nonlinear system can be represented by

$$\begin{aligned} x_{k+1} &= \sum_{i=1}^{\tau} h_i(\theta(k))(A_i x_k + B_i u_k), \\ &= A(\Theta_k)x_k + B(\Theta_k)u_k, \\ y_k &= Cx_k + Du_k, \\ i &\in \mathcal{R} := \{1, \ldots, \tau\}, \end{aligned} \tag{5.4}$$

where

$$A(\Theta_k) = \sum_{i=1}^{\tau} h_i(\theta(k))A_i,\ B(\Theta_k) = \sum_{i=1}^{\tau} h_i(\theta(k))B_i.$$

As shown in Figure 5.1, the output and the state of the nonlinear system are transmitted to the tracking controller via a communication link. The control signal

is also transmitted to the actuator through a communication medium. Due to the limited bandwidth of the communication channels, or limited buffer sizes, in practice, network-induced delays and packet dropouts are unavoidable in an NCS. At the controller node, the exact delay information of the control signal is not known. In order to achieve a good tracking performance, a predictive control scheme is used in this work. The controller generates a series of control signals. Each one depends on the accumulated delay from the sensor to the controller (S-C) λ_k and the possible delay, which takes value in a known set, from the controller to the actuator (C-A) η_k. When the actuator receives the sequence of control signals, it chooses the most suitable signal to drive the nonlinear system.

Some assumptions are made next. These assumptions include general conditions on the system matrices and the characteristics of involved network links.

Assumption 5.1. *For each subsystem, the matrix set* $(A_i,\ B_i),\ \forall\ i \in \mathcal{R}$, *is stabilizable.*

Assumption 5.2. *Rank* $\begin{bmatrix} A_i - I & B_i \\ C & D \end{bmatrix} = n + m,\ \forall\ i \in \mathcal{R}.$

Assumption 5.3. *The vector* $\bar{r}_k$ *is bounded in the* l_2 *space, where* $\bar{r}_k = r_{k+1} - r_k$, *and* r_k *is the reference signal.*

Assumption 5.4. *Let* ν_k *denote the summation of* λ_k *and* η_k, *that is,* $\nu_k = \lambda_k + \eta_k$. *The variable* ν_k *is time-varying in the set* $\mathcal{I} := \{\kappa_1, \cdots, \kappa_i, \cdots, \kappa_s\}$, *where* $\forall\ i \in \mathcal{R}$, κ_i *is an integer, and* $0 < \kappa_1 < \cdots < \kappa_i < \cdots < \kappa_s$.

Assumption 5.5. *Define an indicator function*

$$\alpha(k) = [\alpha_1(k), \cdots, \alpha_i(k), \cdots, \alpha_s(k)]^{\mathrm{T}}.$$

For each sampling instant, the exact delay can be determined at the actuator node by the time-stamp technique [52]. When the variable $\alpha_i(k)$ equals to 1, the lumped delay at the actuator node is κ_i, that is,

$$\begin{cases} \alpha_i(k) = 1, & \nu_k = \kappa_i, \\ \alpha_i(k) = 0, & \nu_k \neq \kappa_i. \end{cases} \tag{5.5}$$

Suppose that the probability of $\alpha_i = 1$ is denoted by β_i, i.e.,

$$\begin{aligned} &\text{Prob}\{\alpha_i = 1\} = \beta_i, \\ &\text{Prob}\{\alpha_i = 0\} = 1 - \beta_i. \end{aligned} \tag{5.6}$$

Since each subsystem in the fuzzy system is linear, the system in (5.4) can be rewritten to an incremental form as

$$\begin{aligned} \bar{x}_{k+1} &= \sum_{i=1}^{\tau} h_i(\theta(k))(A_i\bar{x}_k + B_i\bar{u}_k), \\ i &= 1, \ldots, \tau, \end{aligned} \tag{5.7}$$

where $\bar{x}_k = x_{k+1} - x_k$, $\bar{u}_k = u_{k+1} - u_k$. Moreover, the tracking error $e_k := r_k - y_k$ has the following dynamics

$$e_{k+1} = e_k - C\bar{x}_k - D\bar{u}_k + \bar{r}_k, \tag{5.8}$$

where $\bar{r}_k = r_{k+1} - r_k$. Recalling (5.7) and (5.8), we obtain the following augmented system model

$$\xi_{k+1} = \bar{A}(\Theta_k)\xi_k + \bar{B}(\Theta_k)\bar{u}_k + \bar{B}_r\omega_k, \tag{5.9}$$

where

$$\xi_k = \begin{bmatrix} \bar{x}_k \\ e_k \end{bmatrix},\ \bar{B}_r = \begin{bmatrix} 0 \\ I \end{bmatrix},\ \omega_k = \bar{r}_k,$$

$$\bar{A}(\Theta_k) = \sum_{i=1}^{\tau} h_i(\theta(k))\bar{A}_i = \sum_{i=1}^{\tau} h_i(\theta(k)) \begin{bmatrix} A_i & 0 \\ -C & I \end{bmatrix},$$

$$\bar{B}(\Theta_k) = \sum_{i=1}^{\tau} h_i(\theta(k))\bar{B}_i = \sum_{i=1}^{\tau} h_i(\theta(k)) \begin{bmatrix} B_i \\ -D \end{bmatrix}.$$

In this work, the proposed controller u_k consists of two components: the state-feedback control and the integral control. When there are no delays on both communication links, the control signal can be represented by:

$$u_k = K_{SF}x_k + K_{IN}\sum_{i=1}^{k-1} e_i. \tag{5.10}$$

The increment of the control signal $\bar{u}_k$ is

$$\bar{u}_k = K_{SF}\bar{x}_k + K_{IN}e_k = K\xi_k, \tag{5.11}$$

where $K = [K_{SF},\ K_{IN}]$.

Considering the network-induced delay on both communication links, the received signals at the controller node become

$$\tilde{y}_k = y_{k-\lambda_k}, \text{and } \tilde{x}_k = x_{k-\lambda_k}. \tag{5.12}$$

The tracking error at the controller node is defined as:

$$\hat{e}_k = r_{k-\lambda_k} - \tilde{y}_k = r_{k-\lambda_k} - y_{k-\lambda_k}. \tag{5.13}$$

Suppose that the accumulated delay $\kappa_i \ \forall \ i = 1, \cdots, s$, at the actuator node is known for each sampling time k. The delay scheduling control law has the following representation:

$$\hat{u}_{k|\kappa_i} = K_{SF|\kappa_i} x_{k-\lambda_k} + K_{IN|\kappa_i} \sum_{i=1}^{k-\lambda_k-1} e_i. \tag{5.14}$$

Here, $K_{SF|\kappa_i}$ and $K_{IN|\kappa_i}$ are delay-scheduling matrix gains to be designed. For each delay κ_i, we need to design $K_{SF|\kappa_i}$ and $K_{IN|\kappa_i}$. As the controller does not know the delay on the C-A link when it generates the control signal, we design a sequence of control signals which are dependent on all the possible delays within a known set. The control signals are grouped together in a packet, and are sent to the actuator. When the controller receives a packet from the sensor, the output of the controller is $\begin{bmatrix} \hat{u}_k^{\mathrm{T}}|\kappa_1 & \cdots & \hat{u}_k^{\mathrm{T}}|\kappa_s \end{bmatrix}^{\mathrm{T}}$, and the increment of the output is $\begin{bmatrix} \bar{u}_k^{\mathrm{T}}|\kappa_1 & \cdots & \bar{u}_k^{\mathrm{T}}|\kappa_s \end{bmatrix}^{\mathrm{T}}$, where

$$\bar{u}_{k|\kappa_i} = K_{SF|\kappa_i} \bar{x}_{k-\lambda_k} + K_{IN|\kappa_i} e_{k-\lambda_k}. \tag{5.15}$$

When the actuator receives the packet, it chooses a suitable control signal according to the accumulated delay. If the accumulated delay is κ_i, the i^{th} segment of the packet is adopted as the control signal, that is denoted as

$$\bar{u}_k = K_{SF|\kappa_i} \bar{x}_{k-\kappa_i} + K_{IN|\kappa_i} e_{k-\kappa_i}. \tag{5.16}$$

Recalling the dynamics of the augmented system and the characteristics of the net-

work links, the resulting closed-loop system is rewritten as

$$\begin{aligned}\xi_{k+1} =&\bar{A}(\Theta_k)\xi_k + \sum_{i=1}^{s}\alpha_i(k)\bar{B}(\Theta_k)K_{|\kappa_i}\xi_{k-\kappa_i} + \bar{B}_r\omega_k,\\ =&\bar{A}(\Theta_k)\xi_k + \sum_{i=1}^{s}\alpha_i(k)\bar{B}_{|\kappa_i}(\Theta_k)\xi_{k-\kappa_i} + \bar{B}_r\omega_k,\end{aligned} \tag{5.17}$$

where

$$\bar{B}_{|\kappa_i}(\Theta_k) = \bar{B}(\Theta_k)K_{|\kappa_i}.$$

In the tracking control problem, the primary objective is to minimize the tracking error. In order to avoid the actuator saturation and achieve the trade-off between the tracking error and the control action, we adopt a quadratic form of the tracking error and the control signals as

$$\mathcal{J} = \sum_{i=0}^{\infty}(e_i^{\mathrm{T}}R_1e_i + \bar{u}_i^{\mathrm{T}}R_2\bar{u}_i), \tag{5.18}$$

where R_1 and R_2 are two positive definite weighting matrices. It is necessary to mention that the cost function $\mathcal{J}$ is equal to the 2-norm of the following constructed signal

$$z_k = \bar{C}\xi_k + \bar{D}\bar{u}_k, \tag{5.19}$$

where $\bar{C} = \begin{bmatrix} 0 & R_1^{1/2} \\ 0 & 0 \end{bmatrix}, \bar{D} = \begin{bmatrix} 0 \\ R_2^{1/2} \end{bmatrix}$. Note that Ω_k is bounded in the l_2 space. Introducing an $\mathcal{H}_\infty$ performance index γ such that $\mathcal{J} < \gamma^2\|\omega\|_2^2$, the optimization problem on the cost function $\mathcal{J}$ becomes an optimal $\mathcal{H}_\infty$ control problem for the

following system:

$$\begin{aligned}\xi_{k+1} =&\bar{A}(\Theta_k)\xi_k + \sum_{i=1}^{s}\alpha_i(k)\bar{B}_{|\kappa_i}(\Theta_k)\xi_{k-\kappa_i} + \bar{B}_r\omega_k,\\ z_k =&\bar{C}\xi_k + \sum_{i=1}^{s}\alpha_i(k)\bar{D}_{|\kappa_i}\xi_{k-\kappa_i},\end{aligned} \tag{5.20}$$

where

$$\bar{D}_{|\kappa_i} = \bar{D}K_{|\kappa_i}.$$

Remark 5.1. *In this work, we consider a special case of the T-S fuzzy model in which the nonlinearity only occurs in the system matrix and the input matrix, that is, the matrices in the output equation are constant. This assumption is reasonable since most of the nonlinearities occurs in the system matrices in practical applications.*

Remark 5.2. *For tracking control in a network environment, the authors in [99] designed a state-feedback controller such that the output of the closed-loop NCS can track the output of a virtual reference-generation model. $\mathcal{H}_2$ output tracking for networked hydraulic system was investigated in [132] with a strategy similar to that proposed in [99]. Although the results show a good tracking performance in a network environment, in practice, it is generally required to directly track a specified reference input. In this work, we focus on the reference tracking problem in the network environment.*

Remark 5.3. *Note that the external input is generally required to be bounded. However, here, it is only required that the increment of the external reference input $\bar{r}_k$ be bounded. Thus, Assumption 3) is a relaxed condition.*

It is necessary to mention that the closed-loop system in (5.20) is a stochastic system. To deal with the stochastic variables, we use the following definitions.

Definition 5.1. *The closed-loop stochastic system in* (5.20) *is said to be exponentially mean-square stable, if with* $\omega_k = 0$*, there exist constants* $\phi_1 > 0$ *and* $\phi_2 > 0$ *such that for* $k \geq 0$*, the following inequality is held:*

$$\mathcal{E}\left\{\|\xi_k\|^2\right\} \leq \phi_1 e^{-\phi_2 k}\mathcal{E}\left\{\sup_{-\kappa_s \leq i \leq 0}\|\xi_i\|^2\right\}. \tag{5.21}$$

Definition 5.2. *Given a scalar* $\gamma > 0$*, the closed-loop stochastic system in* (5.20) *is said to be exponentially mean-square stable with a prescribed* $\mathcal{H}_\infty$ *performance* γ *if it satisfies (5.21) and*

$$\|z\|_{\mathcal{E}2} < \gamma \|\omega\|_{\mathcal{E}2} \tag{5.22}$$

for all nonzero $\omega_k \in l_2[0,\infty)$ *subject to the zero initial condition, where* $\|z\|_{\mathbb{E}2} := \sqrt{\sum_{k=0}^{\infty}(\mathbb{E}|z_k|^2)}$ *and* $\|\omega\|_{\mathbb{E}2} := \sqrt{\sum_{k=0}^{\infty}(\mathbb{E}|\omega_k|^2)}$.

The step tracking problem for an NCS is to ensure that the output of the nonlinear system can follow a step reference in a network environment as shown in Figure 5.1. Note that the tracking problem of the networked nonlinear system subject to the network-induced delay has now been converted into a feedback control problem of a stochastic fuzzy system. In addition, the objective of minimizing the tacking error and the control action has been equivalently converted into the minimization of the corresponding controlled output. In the following sections, the main objectives are to analyze the stability and the $\mathcal{H}_\infty$ performance of the stochastic system in (5.20), and to design the delay-dependent and fuzzy-weighting-function-dependent controllers. More specifically, the following issues are to be dealt with.

O1 To study the exponential mean-square stability of the stochastic system in (5.20) with zero external input.

O2 To investigate the $\mathcal{H}_\infty$ performance of the stochastic system in (5.20) with l_2

bounded input increment r_k, that is, for a given $\gamma > 0$, find conditions such that

$$\|z\|_{\mathcal{E}2} < \gamma \|\omega\|_{\mathcal{E}2}\,. \tag{5.23}$$

O3 To design a sequence of delay-dependent and fuzzy-weighting-function-dependent controllers to achieve the tracking objective based on the analysis results.

5.3 Main Results

In the previous section, we have formulated the tracking control problem for discrete-time nonlinear networked system and derived the closed-loop system model with delayed state and stochastic variables. In this section, we will study the stability and $\mathcal{H}_\infty$ performance of the system in (5.20). Note that the closed-loop system is a stochastic system with delayed state. In order to deal with the stochastic variables and delayed state, and derive less conservative results, we introduce the following lemma.

Lemma 5.1. *Let* $\eta_k := \xi_{k+1} - \xi_k$ *and* $\Phi_k := [\xi_k^{\mathrm{T}}, \xi_{k-1}^{\mathrm{T}}, \xi_{k-2}^{\mathrm{T}}, \cdots, \xi_{k-\kappa_s}^{\mathrm{T}}]^{\mathrm{T}}$, *where* ξ_k *is the state vector of the closed-loop system in (5.20). Consider a Lyapunov-Krasovskii functional candidate*

$$\begin{aligned} V_k(\Phi_k) :&= V_{1k} + V_{2k} + V_{3k}, \\ V_{1k} &:= \xi_k^{\mathrm{T}} P \xi_k, \\ V_{2k} &:= \sum_{i=1}^{s} \sum_{j=k-\kappa_i}^{k-1} \xi_j^{\mathrm{T}} Q_i(\Theta_j) \xi_j, \\ V_{3k} &:= \sum_{i=1}^{s} \sum_{j=-\kappa_i}^{-1} \sum_{l=k+j}^{k-1} \eta_l^{\mathrm{T}} Z_i(\Theta_l) \eta_l, \end{aligned} \tag{5.24}$$

where $P = P^{\mathrm{T}} > 0$, $Q_j(\Theta_k) = Q_j^{\mathrm{T}}(\Theta_k) > 0$ *and* $Z_l(\Theta_k) = Z_l^{\mathrm{T}}(\Theta_k) > 0$. *If there exists*

a scalar $\psi > 0$ *such that*

$$\mathcal{E}\left\{V_{k+1}\left(\Phi_{k+1}\right)|\Phi_k\right\} - V_k\left(\Phi_k\right) < -\psi\left\|\xi_k\right\|^2, \tag{5.25}$$

then the dynamics of the process ξ_k *is exponentially mean-square stable.*

Proof. The proof can be carried out along the lines in [123]. Thus, it is omitted for brevity. □

5.3.1 Stability and $\mathcal{H}_\infty$ Performance Analysis

Assume that the controller in the closed-loop system (5.20) is given, that is, the delay-dependent controller parameters are known. Choose the above fuzzy-weighting-dependent Lyapunov-Krasovskii functional with the triple-summation term. The following theorem offers a condition for the exponential mean-square stability of the closed-loop system.

Theorem 5.1. *Consider the networked discrete-time nonlinear system in Figure 5.1 under the control law in (5.16). The closed-loop system in (5.20) without any external input is exponentially mean-square stable, if there exist fuzzy-weighting-dependent matrices* $P = P^{\mathrm{T}} > 0$, $Q_a(\Theta_k) = Q_a^{\mathrm{T}}(\Theta_k) > 0$, $Q_a(\Theta_{k-\kappa_a}) = Q_a^{\mathrm{T}}(\Theta_{k-\kappa_a}) > 0$, $Z_a(\Theta_k) = Z_a^{\mathrm{T}}(\Theta_k) > 0$, $Z_a(\Theta_{k-l_a}) = Z_a^{\mathrm{T}}(\Theta_{k-l_a}) > 0$, $M_a(\Theta_k)$, $\forall\ a = 1, \cdots, s, l_a \in \{1, \cdots, \kappa_a\}$, *satisfying*

$$\begin{bmatrix} \Pi_1^{\mathrm{T}}\Xi_1\Pi_1 + \Xi_2 + \Pi_2^{\mathrm{T}}\Xi_3\Pi_2 + \Xi_4 & \Xi_5^{\mathrm{T}} \\ * & \Xi_6 \end{bmatrix} < 0, \tag{5.26}$$

where

$$
\begin{aligned}
\Xi_1 =& \operatorname{diag}\left\{P, P, \ldots, P\right\}, \\
\Xi_2 =& \operatorname{diag}\Big\{ \sum_{a=1}^{s} Q_a(\Theta_k) - P, -Q_1(\Theta_{k-\kappa_1}), \cdots, -Q_s(\Theta_{k-\kappa_s}) \Big\}, \\
\Xi_3 =& \sum_{a=1}^{s} \operatorname{diag}\left\{\kappa_a Z_a(\Theta_k), \kappa_a Z_a(\Theta_k), \ldots, \kappa_a Z_a(\Theta_k)\right\}, \\
\Xi_4 =& \left[\sum_{a=1}^{s} M_a^{\mathrm{T}}(\Theta_k),\ -M_1^{\mathrm{T}}(\Theta_k),\ \cdots,\ -M_s^{\mathrm{T}}(\Theta_k) \right] \\
&+ \left[\sum_{a=1}^{s} M_a^{\mathrm{T}}(\Theta_k),\ -M_1^{\mathrm{T}}(\Theta_k),\ \cdots,\ -M_s^{\mathrm{T}}(\Theta_k) \right]^{\mathrm{T}}, \\
\Xi_5^{\mathrm{T}} =& \left[\kappa_1 M_1^{\mathrm{T}}(\Theta_k)\ \kappa_2 M_2^{\mathrm{T}}(\Theta_k) \cdots\ \kappa_s M_s^{\mathrm{T}}(\Theta_k)\right], \\
\Xi_6 =& \operatorname{diag}\left\{-\kappa_1 Z_1(\Theta_{k-l_1}), \ldots, -\kappa_s Z_s(\Theta_{k-l_s})\right\}, \\
\Pi_1 =& \begin{bmatrix}
\sqrt{\beta_1}\bar{A}(\Theta_k) & \sqrt{\beta_1}\bar{B}_{|\kappa_1}(\Theta_k) & 0 & \cdots & 0 \\
\sqrt{\beta_2}\bar{A}(\Theta_k) & 0 & \sqrt{\beta_2}\bar{B}_{|\kappa_2}(\Theta_k) & \cdots & 0 \\
\vdots & \vdots & \ddots & \ddots & \vdots \\
\sqrt{\beta_s}\bar{A}(\Theta_k) & 0 & \cdots & 0 & \sqrt{\beta_s}\bar{B}_{|\kappa_s}(\Theta_k)
\end{bmatrix}, \\
\Pi_2 =& \begin{bmatrix}
\sqrt{\beta_1}(\bar{A}(\Theta_k) - I) & \sqrt{\beta_1}\bar{B}_{|\kappa_1}(\Theta_k) & 0 & \cdots & 0 \\
\sqrt{\beta_2}(\bar{A}(\Theta_k) - I) & 0 & \sqrt{\beta_2}\bar{B}_{|\kappa_2}(\Theta_k) & \cdots & 0 \\
\vdots & \vdots & \ddots & \ddots & \vdots \\
\sqrt{\beta_s}(\bar{A}(\Theta_k) - I) & 0 & \cdots & 0 & \sqrt{\beta_s}\bar{B}_{|\kappa_s}(\Theta_k)
\end{bmatrix}.
\end{aligned}
$$

Proof. Choose the Lyapunov-Krasovskii functional candidate as in the form of (5.24). The difference of the Lyapunov-Krasovskii functional is defined as

$$
\mathcal{E}\left\{\Delta V_k | \Phi_k\right\} = \mathcal{E}\left\{V_{k+1}\left(\Phi_{k+1}\right) | \Phi_k\right\} - V_k\left(\Phi_k\right). \tag{5.27}
$$

Considering the dynamics of the closed-loop system in (5.20), the difference is evalu-

ated as:

$$
\begin{aligned}
\mathcal{E}\left\{\Delta V_{1k}|\Phi_k\right\} &= \xi_k^{\mathrm{T}}\bar{A}^{\mathrm{T}}(\Theta_k)P\bar{A}(\Theta_k)\xi_k + 2\sum_{a=1}^{s}\beta_a\xi_k^{\mathrm{T}}\bar{A}^{\mathrm{T}}(\Theta_k)P\bar{B}_{|\kappa_a}(\Theta_k)\xi_{k-\kappa_a} \\
&+ \sum_{a=1}^{s}\beta_a\xi_{k-\kappa_a}^{\mathrm{T}}\bar{B}_{|\kappa_a}^{\mathrm{T}}(\Theta_k)P\bar{B}_{|\kappa_a}(\Theta_k)\xi_{k-\kappa_a} - \xi_k^{\mathrm{T}}P\xi_k = \zeta_{1k}^{\mathrm{T}}\Pi_1^{\mathrm{T}}\Xi_1\Pi_1\zeta_{1k} - \xi_k^{\mathrm{T}}P\xi_k, \\
\mathcal{E}\left\{\Delta V_{2k}|\Phi_k\right\} &= \sum_{a=1}^{s}\left[\xi_k^{\mathrm{T}}Q_a(\Theta_k)\xi_k\right] - \sum_{a=1}^{s}\left[\xi_{k-\kappa_a}^{\mathrm{T}}Q_a(\Theta_{k-\kappa_a})\xi_{k-\kappa_a}\right] = \zeta_{1k}^{\mathrm{T}}\dot{\Xi}_2\zeta_{1k}, \\
\mathcal{E}\left\{\Delta V_{3k}|\Phi_k\right\} &= \mathcal{E}\left\{\sum_{a=1}^{s}\sum_{l=-\kappa_a}^{-1}\eta_k^{\mathrm{T}}Z_a(\Theta_k)\eta_k\Big|\Phi_k\right\} - \mathcal{E}\left\{\sum_{a=1}^{s}\sum_{l=-\kappa_a}^{-1}\eta_{k+l}^{\mathrm{T}}Z_a(\Theta_{k+l})\eta_{k+l}\Big|\Phi_k\right\} \\
&= \mathcal{E}\left\{\sum_{a=1}^{s}\sum_{l=-\kappa_a}^{-1}\eta_k^{\mathrm{T}}Z_a(\Theta_k)\eta_k\Big|\Phi_k\right\} - \mathcal{E}\left\{\sum_{a=1}^{s}\sum_{l=k-\kappa_a}^{k-1}\eta_l^{\mathrm{T}}Z_a(\Theta_{k-l_a})\eta_l\Big|\Phi_k\right\} \\
&= \xi_k^{\mathrm{T}}(\bar{A}(\Theta_k)-I)^{\mathrm{T}}\sum_{a=1}^{s}\kappa_a Z_a(\Theta_k)(\bar{A}(\Theta_k)-I)\xi_k \\
&\quad + 2\sum_{a=1}^{s}\beta_a\xi_k^{\mathrm{T}}(\bar{A}(\Theta_k)-I)^{\mathrm{T}}\sum_{b=1}^{s}\kappa_b Z_b(\Theta_k)\bar{B}_{|\kappa_a}(\Theta_k)\xi_{k-\kappa_a} \\
&\quad + \sum_{a=1}^{s}\beta_a\xi_{k-\kappa_a}^{\mathrm{T}}B_{|\kappa_a}^{\mathrm{T}}(\Theta_k)\sum_{b=1}^{s}\kappa_b Z_b(\Theta_k)\bar{B}_{|\kappa_a}(\Theta_k)\xi_{k-\kappa_a} \\
&\quad - \mathcal{E}\left\{\sum_{a=1}^{s}\sum_{l=k-\kappa_a}^{k-1}\eta_l^{\mathrm{T}}Z_a(\Theta_{k-l_a})\eta_l\Big|\Phi_k\right\} \\
&= \zeta_{1k}^{\mathrm{T}}\Pi_2^{\mathrm{T}}\Xi_3\Pi_2\zeta_{1k} - \mathcal{E}\left\{\sum_{a=1}^{s}\sum_{l=k-\kappa_a}^{k-1}\eta_l^{\mathrm{T}}Z_a(\Theta_{k-l_a})\eta_l\Big|\Phi_k\right\},
\end{aligned}
\tag{5.28}
$$

where

$$
\begin{aligned}
\zeta_{1k}^{\mathrm{T}} &= \left[\begin{array}{cccccc} \xi_k^{\mathrm{T}} & \xi_{k-\kappa_1}^{\mathrm{T}} & \xi_{k-\kappa_2}^{\mathrm{T}} & \cdots & \xi_{k-\kappa_s}^{\mathrm{T}} \end{array}\right], \\
\dot{\Xi}_2 &= \mathrm{diag}\left\{\sum_{a=1}^{s}Q_a(\Theta_k), -Q_1(\Theta_{k-\kappa_1}), \cdots, -Q_s(\Theta_{k-\kappa_s})\right\}.
\end{aligned}
$$

For any matrix $M_a(\Theta_k)$, $a \in \{1, \cdots, s\}$ with appropriate dimension,

$$\Psi_{1a} = \zeta_{1k}^{\mathrm{T}} M_a^{\mathrm{T}}(\Theta_k) \left[\xi_k - \xi_{k-\kappa_a} - \sum_{l=k-\kappa_a}^{k-1} \eta_l \right] = 0, \tag{5.29}$$

and

$$\begin{aligned} \Psi_{2a} =& \mathcal{E} \left\{ \sum_{l=k-\kappa_a}^{k-1} \left(\zeta_{1k}^{\mathrm{T}} M_a^{\mathrm{T}}(\Theta_k) + \eta_l^{\mathrm{T}} Z_a(\Theta_{k-l_a}) \right) \right. \\ & \left. Z_a^{-1}(\Theta_{k-l_a}) \left(\zeta_{1k}^{\mathrm{T}} M_a^{\mathrm{T}}(\Theta_k) + \eta_l^{\mathrm{T}} Z_a(\Theta_{k-l_a}) \right)^{\mathrm{T}} \right\} \geqslant 0. \end{aligned} \tag{5.30}$$

It follows from (5.27) to (5.30) that

$$\begin{aligned} \mathcal{E}\left\{\Delta V_k | \Phi_k\right\} \leqslant & \mathcal{E}\left\{\Delta V_{1k} | \Phi_k\right\} + \mathcal{E}\left\{\Delta V_{2k} | \Phi_k\right\} + \mathcal{E}\left\{\Delta V_{3k} | \Phi_k\right\} + \sum_{a=1}^{s} \left(\Psi_{1a} + \Psi_{1a}^{\mathrm{T}} + \Psi_{2a} \right) \\ =& \zeta_{1k}^{\mathrm{T}} (\Pi_1^{\mathrm{T}} \Xi_1 \Pi_1 + \Xi_2 + \Pi_2^{\mathrm{T}} \Xi_3 \Pi_2 + \Xi_4 + \Xi_5^{\mathrm{T}} \Xi_6^{-1} \Xi_5) \zeta_{1k} \\ :=& \zeta_{1k}^{\mathrm{T}} \Lambda \zeta_{1k}. \end{aligned} \tag{5.31}$$

By using Schur complement, for any nonzero ζ_{1k}, it can be seen that the inequality (5.26) implies that

$$\mathcal{E}\left\{\Delta V_k | \Phi_k\right\} < 0. \tag{5.32}$$

Thus, it is concluded that there exists a positive scalar ψ such that

$$\Lambda < \begin{bmatrix} -\psi I & 0 \\ 0 & 0 \end{bmatrix}. \tag{5.33}$$

Expanding the right-side of the inequality (5.33), one gets

$$\mathcal{E}\left\{\Delta V_k|\Phi_k\right\} < -\psi\xi_k^{\mathrm{T}}\xi_k = -\psi\|\xi_k\|^2. \tag{5.34}$$

Recalling the definition in (5.27), it is inferred from Lemma 5.1 that the nominal system in (5.20) is exponentially mean-square stable. The proof is completed. □

In Theorem 5.1, the exponential mean-square stability of the fuzzy stochastic system (5.20) was studied by assuming that the external input is zero. As the external reference has been incorporated in (5.20) and the reference can not be a constant zero, in the following, we investigate the effects of the external input on the controlled output.

Theorem 5.2. *Consider the networked discrete-time nonlinear system in Figure 5.1 under the control law in (5.16). For a given scalar γ, the closed-loop system in (5.20) without any external input is exponentially mean-square stable with an $\mathcal{H}_\infty$ performance index γ, if there exist fuzzy-weighting-dependent matrices $P = P^{\mathrm{T}} > 0$, $Q_a(\Theta_k) = Q_a^{\mathrm{T}}(\Theta_k) > 0$, $Q_a(\Theta_{k-\kappa_a}) = Q_a^{\mathrm{T}}(\Theta_{k-\kappa_a}) > 0$, $Z_a(\Theta_k) = Z_a^{\mathrm{T}}(\Theta_k) > 0$, $Z_a(\Theta_{k-l_a}) = Z_a^{\mathrm{T}}(\Theta_{k-l_a}) > 0$, $M_a(\Theta_k)$, $\forall\ a = 1, \cdots, s, l_a \in \{1, \cdots, \kappa_a\}$, satisfying*

$$\begin{bmatrix} \bar{\Pi}_1^{\mathrm{T}}\Xi_1\bar{\Pi}_1 + \bar{\Xi}_2 + \bar{\Pi}_2^{\mathrm{T}}\Xi_3\bar{\Pi}_2 + \bar{\Pi}_3^{\mathrm{T}}\bar{\Pi}_3 + \bar{\Xi}_4 & \bar{\Xi}_5^{\mathrm{T}} \\ * & \Xi_6 \end{bmatrix} < 0, \tag{5.35}$$

where

$$
\begin{aligned}
\bar{\Xi}_2 =& \mathrm{diag}\Big\{ \sum_{a=1}^{s} Q_a(\Theta_k) - P, -\gamma^2 I, -Q_1(\Theta_{k-\kappa_1}), \cdots, -Q_s(\Theta_{k-\kappa_s}) \Big\}, \\
\bar{\Xi}_4 =& \left[\sum_{a=1}^{s} N_a^{\mathrm{T}}(\Theta_k)\ 0\ -N_1^{\mathrm{T}}(\Theta_k)\ \cdots\ -N_s^{\mathrm{T}}(\Theta_k) \right] \\
&+ \left[\sum_{a=1}^{s} N_a^{\mathrm{T}}(\Theta_k)\ 0\ -N_1^{\mathrm{T}}(\Theta_k)\ \cdots\ -N_s^{\mathrm{T}}(\Theta_k) \right]^{\mathrm{T}}, \\
\bar{\Xi}_5^{\mathrm{T}} =& \left[\kappa_1 N_1^{\mathrm{T}}(\Theta_k)\ \kappa_2 N_2^{\mathrm{T}}(\Theta_k) \cdots\ \kappa_s N_s^{\mathrm{T}}(\Theta_k) \right],
\end{aligned}
$$

$$
\bar{\Pi}_1 = \begin{bmatrix}
\sqrt{\beta_1}\bar{A}(\Theta_k) & \sqrt{\beta_1}\bar{B}_r & \sqrt{\beta_1}\bar{B}_{|\kappa_1}(\Theta_k) & 0 & \cdots & 0 \\
\sqrt{\beta_2}\bar{A}(\Theta_k) & \sqrt{\beta_2}\bar{B}_r & 0 & \sqrt{\beta_2}\bar{B}_{|\kappa_2}(\Theta_k) & \cdots & 0 \\
\vdots & \vdots & \vdots & \ddots & \ddots & \vdots \\
\sqrt{\beta_s}\bar{A}(\Theta_k) & \sqrt{\beta_s}\bar{B}_r & \cdots & 0 & 0 & \sqrt{\beta_s}\bar{B}_{|\kappa_s}(\Theta_k)
\end{bmatrix},
$$

$$
\bar{\Pi}_2 = \begin{bmatrix}
\sqrt{\beta_1}(\bar{A}(\Theta_k) - I) & \sqrt{\beta_1}\bar{B}_r & \sqrt{\beta_1}\bar{B}_{|\kappa_1}(\Theta_k) & 0 & \cdots & 0 \\
\sqrt{\beta_2}(\bar{A}(\Theta_k) - I) & \sqrt{\beta_2}\bar{B}_r & 0 & \sqrt{\beta_2}\bar{B}_{|\kappa_2}(\Theta_k) & \cdots & 0 \\
\vdots & \vdots & \vdots & \ddots & \ddots & \vdots \\
\sqrt{\beta_s}(\bar{A}(\Theta_k) - I) & \sqrt{\beta_s}\bar{B}_r & \cdots & 0 & 0 & \sqrt{\beta_s}\bar{B}_{|\kappa_s}(\Theta_k)
\end{bmatrix},
$$

$$
\bar{\Pi}_3 = \begin{bmatrix}
\sqrt{\beta_1}\bar{C} & 0 & \sqrt{\beta_1}\bar{D}_{|\kappa_1} & 0 & \cdots & 0 \\
\sqrt{\beta_2}\bar{C} & 0 & 0 & \sqrt{\beta_2}\bar{D}_{|\kappa_2} & \cdots & 0 \\
\vdots & \vdots & \vdots & \ddots & \ddots & \vdots \\
\sqrt{\beta_s}\bar{C} & 0 & \cdots & 0 & 0 & \sqrt{\beta_s}\bar{D}_{|\kappa_s}
\end{bmatrix}.
$$

Proof. Considering the external input of the closed-loop system in (5.20), the differ-

ence of the Lyapunov-Krasovskii functional is evaluated as:

$$\begin{aligned}
\mathcal{E}\left\{\Delta V_{1k}|\Phi_k\right\} =& \zeta_{2k}^{\mathrm{T}}\bar{\Pi}_1^{\mathrm{T}}\Xi_1\bar{\Pi}_1\zeta_{2k} - \xi_k^{\mathrm{T}}P\xi_k, \\
\mathcal{E}\left\{\Delta V_{2k}|\Phi_k\right\} =& \zeta_{2k}^{\mathrm{T}}\hat{\Xi}_2\zeta_{2k}, \\
\mathcal{E}\left\{\Delta V_{3k}|\Phi_k\right\} =& \zeta_{2k}^{\mathrm{T}}\bar{\Pi}_2^{\mathrm{T}}\Xi_3\bar{\Pi}_2\zeta_{2k} - \mathcal{E}\left\{\sum_{a=1}^{s}\sum_{l=k-\kappa_a}^{k-1}\eta_l^{\mathrm{T}}G_a(\Theta_{k-l_a})\eta_l\Big|\Phi_k\right\},
\end{aligned} \tag{5.36}$$

where

$$\zeta_{2k}^{\mathrm{T}} = \begin{bmatrix} \xi_k^{\mathrm{T}} & \omega_k^{\mathrm{T}} & \xi_{k-\kappa_1}^{\mathrm{T}} & \xi_{k-\kappa_2}^{\mathrm{T}} & \cdots & \xi_{k-\kappa_s}^{\mathrm{T}} \end{bmatrix},$$

$$\hat{\Xi}_2 = \mathrm{diag}\left\{\sum_{a=1}^{s}Q_a(\Theta_k), 0, -Q_1(\Theta_k), \cdots, -Q_s(\Theta_k)\right\}.$$

For any matrix $N_a(\Theta_k)$, $a \in \{1, \cdots, s\}$ with appropriate dimension,

$$\Psi_{3a} = \zeta_{2k}^{\mathrm{T}}N_a^{\mathrm{T}}(\Theta_k)\left[\xi_k - \xi_{k-\kappa_a} - \sum_{l=k-\kappa_a}^{k-1}\eta_l\right] = 0, \tag{5.37}$$

and

$$\begin{aligned}
\Psi_{4a} =& \mathcal{E}\left\{\sum_{l=k-\kappa_a}^{k-1}\left(\zeta_{2k}^{\mathrm{T}}N_a^{\mathrm{T}}(\Theta_k) + \eta_l^{\mathrm{T}}Z_a(\Theta_{k-l_a})\right)\right. \\
& \left. Z_a^{-1}(\Theta_{k-l_a})\left(\zeta_{2k}^{\mathrm{T}}N_a^{\mathrm{T}}(\Theta_k) + \eta_l^{\mathrm{T}}Z_a(\Theta_{k-l_a})\right)^{\mathrm{T}}\right\} \geqslant 0.
\end{aligned} \tag{5.38}$$

The conditional expectation of the controlled output is

$$\mathcal{E}\left\{z_k^{\mathrm{T}}z_k\Big|\Phi_k\right\} = \zeta_{2k}^{\mathrm{T}}\bar{\Pi}_3^{\mathrm{T}}\bar{\Pi}_3\zeta_{2k}. \tag{5.39}$$

It follows from (5.36)-(5.39) that

$$\begin{aligned} J_1 &= \mathcal{E}\left\{\Delta V_k|\Phi_k\right\} + \mathcal{E}\left\{z_k^{\mathrm{T}} z_k \middle| \Phi_k\right\} - \gamma^2 I \\ &< \mathcal{E}\left\{\Delta V_{1k}|\Phi_k\right\} + \mathcal{E}\left\{\Delta V_{2k}|\Phi_k\right\} + \mathcal{E}\left\{\Delta V_{3k}|\Phi_k\right\} + \sum_{a=1}^{s}\left(\Psi_{1a} + \Psi_{1a}^{\mathrm{T}} + \Psi_{2a}\right) \\ &= \zeta_{2k}^{\mathrm{T}}(\bar{\Pi}_1^{\mathrm{T}}\Xi_1\bar{\Pi}_1 + \bar{\Xi}_2 + \bar{\Pi}_2^{\mathrm{T}}\Xi_3\bar{\Pi}_2 + \bar{\Pi}_3^{\mathrm{T}}\bar{\Pi}_3 + \bar{\Xi}_4 + \bar{\Xi}_5^{\mathrm{T}}\Xi_6^{-1}\bar{\Xi}_5)\zeta_{2k}. \end{aligned} \tag{5.40}$$

The inequality in (5.35) implies that J_1 is negative for all nonzero ζ_{2k}. By summing up the objective function J_1 with respect to the time instant k we have

$$\|z\|_{\mathcal{E}2}^2 < \gamma^2\|w\|_{\mathcal{E}2}^2 + V_0(\Phi_0) - V_\infty(\Phi_\infty). \tag{5.41}$$

Under the zero initial condition, and the fact $V_\infty(\Phi_\infty) \geq 0$, we conclude that

$$\|z\|_{\mathcal{E}2} < \gamma\|w\|_{\mathcal{E}2}. \tag{5.42}$$

Hence, if the condition in Theorem 5.2 is satisfied, the closed-loop system in (5.20) is exponentially mean-square stable with an $\mathcal{H}_\infty$ performance index γ. The proof is completed. □

Remark 5.4. *For the stability analysis of state-delayed systems, the choice of Lyapunov-Krasovskii functional is crucial. The Lyapunov-Krasovskii functional in (5.24) is inspired by the work in [91]. The authors in [91] studied the stabilization problem for networked linear systems. Here, we discuss not only the stability, but also the $\mathcal{H}_\infty$ performance for nonlinear plants using the Lyapunov-Krasovskii functional in (5.24).*

5.3.2 Controller Design

Note that the parameters to be designed in Theorem 5.2 are coupled. Moreover, the Lyapunov weighting matrices are functions of the fuzzy weighting functions. Therefore, Theorem 5.2 can not be directly used to design the controller. The following theorem extends the conditions in Theorem 5.2 to each subsystem of the T-S fuzzy system.

Theorem 5.3. *Consider the networked discrete-time nonlinear system in Figure 5.1 under the control law in (5.16). For a given scalar γ, the closed-loop system in (5.20) without considering the external input is exponentially mean-square stable with an $\mathcal{H}_\infty$ performance index γ, if there exist fuzzy-weighting-dependent matrices $G = G^{\mathrm{T}} > 0$, $\tilde{Q}_{a,i} = \tilde{Q}_{a,i}^{\mathrm{T}} > 0$, $X_{a,i} = X_{a,i}^{\mathrm{T}} > 0$, $Y_{|\kappa_a,i}$, $\tilde{N}_{a,i}$, $\forall\ a, b, c = \{1, \cdots, s\}$, $t, o_b, d_c \in \mathcal{R}$, satisfying*

$$\mathcal{L}_i^{t,o_b,d_c} < 0, i \in \mathcal{R}, \tag{5.43}$$

where

$$\mathcal{L}_i^{t,o_b,d_c} = \begin{bmatrix} \bar{\Xi}_{2,i}^{o_b} + \bar{\Xi}_{4,i} & \bar{\Xi}_{5,i}^{\mathrm{T}} & \bar{\Pi}_{1,i}^{\mathrm{T}} & \bar{\Pi}_{2,i}^{\mathrm{T}} & \cdots & \bar{\Pi}_{2,i}^{\mathrm{T}} & \bar{\Pi}_{3,i}^{\mathrm{T}} \\ * & \Xi_6^{d_c} & 0 & 0 & 0 & \cdots & 0 \\ * & * & -G \bigotimes \Xi_7 & 0 & 0 & \cdots & 0 \\ * & * & * & -X_{1,d_1} \bigotimes \Xi_7/\kappa_1 & \cdots & 0 & 0 \\ * & * & * & * & \ddots & 0 & 0 \\ * & * & * & * & * & -X_{s,d_s} \bigotimes \Xi_7/\kappa_s & 0 \\ * & * & * & * & * & * & -I \end{bmatrix},$$

$$\bar{\Xi}_{2,i}^{o_b} = \mathrm{diag}\Big\{ \sum_{a=1}^{s} \tilde{Q}_{a,i} - G, -\gamma^2 I, -\tilde{Q}_{1,o_1}, \cdots, -\tilde{Q}_{1,o_s} \Big\},$$

$$\bar{\Xi}_{4,i} = \left[\sum_{a=1}^{s} \tilde{N}_{a,i}^{\mathrm{T}},\ 0,\ -\tilde{N}_{1,i}^{\mathrm{T}},\ \cdots,\ -\tilde{N}_{s,i}^{\mathrm{T}}\right] + \left[\sum_{a=1}^{s} \tilde{N}_{a,i}^{\mathrm{T}},\ 0,\ -\tilde{N}_{1,i}^{\mathrm{T}},\ \cdots,\ -\tilde{N}_{s,i}^{\mathrm{T}}\right]^{\mathrm{T}},$$

$$\bar{\Xi}_{5,i}^{\mathrm{T}} = \left[\kappa_1 \tilde{N}_{1,i}^{\mathrm{T}}\ \kappa_2 \tilde{N}_{2,i}^{\mathrm{T}} \cdots\ \kappa_s \tilde{N}_{s,i}^{\mathrm{T}}\right],$$

$$\Xi_6^{d_c} = \mathrm{diag}\left\{\kappa_1(X_{1,d_1} - 2G), \ldots, \kappa_s(Z_{s,d_s} - 2G)\right\},$$

$$\Xi_7 = \mathrm{diag}\{I, I, \cdots, I\},$$

$$\bar{\Pi}_{1,i} = \begin{bmatrix} \sqrt{\beta_1}\bar{A}_i G & \sqrt{\beta_1}\bar{B}_r G & \sqrt{\beta_1}\bar{B}_i Y_{|\kappa_1} & 0 & \cdots & 0 \\ \sqrt{\beta_2}\bar{A}_i G & \sqrt{\beta_2}\bar{B}_r G & 0 & \sqrt{\beta_2}\bar{B}_i Y_{|\kappa_2} & \cdots & 0 \\ \vdots & \vdots & \vdots & \ddots & \ddots & \vdots \\ \sqrt{\beta_s}\bar{A}_i G & \sqrt{\beta_s}\bar{B}_r G & \cdots & 0 & 0 & \sqrt{\beta_s}\bar{B}_i Y_{|\kappa_s} \end{bmatrix},$$

$$\bar{\Pi}_{2,i} = \begin{bmatrix} \sqrt{\beta_1}(\bar{A}_i - I)G & \sqrt{\beta_1}\bar{B}_r G & \sqrt{\beta_1}\bar{B}_i Y_{|\kappa_1} & 0 & \cdots & 0 \\ \sqrt{\beta_2}(\bar{A}_i - I)G & \sqrt{\beta_2}\bar{B}_r G & 0 & \sqrt{\beta_2}\bar{B}_i Y_{|\kappa_2} & \cdots & 0 \\ \vdots & \vdots & \vdots & \ddots & \ddots & \vdots \\ \sqrt{\beta_s}(\bar{A}_i - I)G & \sqrt{\beta_s}\bar{B}_r G & \cdots & 0 & 0 & \sqrt{\beta_s}\bar{B}_i Y_{|\kappa_s} \end{bmatrix},$$

$$\bar{\Pi}_{3,i} = \begin{bmatrix} \sqrt{\beta_1}\bar{C}G & 0 & \sqrt{\beta_1}\bar{D}Y_{|\kappa_1} & 0 & \cdots & 0 \\ \sqrt{\beta_2}\bar{C}G & 0 & 0 & \sqrt{\beta_2}\bar{D}Y_{|\kappa_2} & \cdots & 0 \\ \vdots & \vdots & \vdots & \ddots & \ddots & \vdots \\ \sqrt{\beta_s}\bar{C}G & 0 & \cdots & 0 & 0 & \sqrt{\beta_s}\bar{D}Y_{|\kappa_s} \end{bmatrix}.$$

In addition, the controller parameters for the controller can be determined by $K_{|\kappa} = Y_{|\kappa}G^{-1}$.

Proof. By using Schur complement, the inequality (5.35) in Theorem 5.2 can be

written as

$$\begin{bmatrix} \bar{\Xi}_2+\bar{\Xi}_4 & \bar{\Xi}_5^{\mathrm{T}} & \bar{\Pi}_1^{\mathrm{T}} & \bar{\Pi}_2^{\mathrm{T}} & \cdots & \bar{\Pi}_2^{\mathrm{T}} & \bar{\Pi}_3^{\mathrm{T}} \\ * & \Xi_6 & 0 & 0 & \cdots & 0 & 0 \\ * & * & -G\bigotimes\Xi_7 & 0 & \cdots & 0 & 0 \\ * & * & * & -X_1(\Theta_{k-l_1})\bigotimes\Xi_7 & \cdots & 0 & 0 \\ * & * & * & * & \ddots & 0 & 0 \\ * & * & * & * & * & -X_s(\Theta_{k-l_s})\bigotimes\Xi_7 & 0 \\ * & * & * & * & * & * & -I \end{bmatrix} < 0, \tag{5.44}$$

where $GP = I$, and $Z_a(\Theta_{k-l_a})X_a(\Theta_{k-l_a}) = I$. Applying a congruence transformation to (5.44) by $\mathrm{diag}\{\Omega_1, G, I, I, \cdots, I, I\}$, one gets

$$\begin{bmatrix} \tilde{\Xi}_2+\tilde{\Xi}_4 & \tilde{\Xi}_5^{\mathrm{T}} & \tilde{\Pi}_1^{\mathrm{T}} & \tilde{\Pi}_2^{\mathrm{T}} & \cdots & \bar{\Pi}_2^{\mathrm{T}} & \bar{\Pi}_3^{\mathrm{T}} \\ * & \tilde{\Xi}_6 & 0 & 0 & \cdots & 0 & 0 \\ * & * & -G\bigotimes\Xi_7 & 0 & \cdots & 0 & 0 \\ * & * & * & -X_1(\Theta_{k-l_1})\bigotimes\Xi_7 & \cdots & 0 & 0 \\ * & * & * & * & \ddots & 0 & 0 \\ * & * & * & * & * & -X_s(\Theta_{k-l_s})\bigotimes\Xi_7 & 0 \\ * & * & * & * & * & * & -I \end{bmatrix} < 0, \tag{5.45}$$

where

$$
\begin{aligned}
\Omega_1 =&[G, I, G, \cdots, G],\\
\tilde{\Xi}_2 =&\mathrm{diag}\Big\{ \sum_{a=1}^{s} \tilde{Q}_a(\Theta_k) - G, -\gamma^2 I,\\
&\qquad - \tilde{Q}_1(\Theta_{k-\kappa_1}), \cdots, -\tilde{Q}_s(\Theta_{k-\kappa_s}) \Big\},\\
\tilde{\Xi}_4 =& \left[\sum_{a=1}^{s} \tilde{N}_a^{\mathrm{T}}(\Theta_k),\ 0,\ -\tilde{N}_1^{\mathrm{T}}(\Theta_k),\ \cdots,\ -\tilde{N}_s^{\mathrm{T}}(\Theta_k) \right]\\
&+ \left[\sum_{a=1}^{s} \tilde{N}_a^{\mathrm{T}}(\Theta_k),\ 0,\ -\tilde{N}_1^{\mathrm{T}}(\Theta_k),\ \cdots,\ -\tilde{N}_s^{\mathrm{T}}(\Theta_k) \right]^{\mathrm{T}},\\
\tilde{\Xi}_5^{\mathrm{T}} =& \left[\kappa_1 \tilde{N}_1^{\mathrm{T}}(\Theta_k)\ \kappa_2 \tilde{N}_2^{\mathrm{T}}(\Theta_k) \cdots\ \kappa_s \tilde{N}_s^{\mathrm{T}}(\Theta_k) \right],\\
\tilde{\Xi}_6 =&\mathrm{diag}\left\{ \kappa_1 (Z_1(\Theta_{k-l_1}) - 2P), \ldots, \kappa_s (Z_s(\Theta_{k-l_s}) - 2P) \right\},\\
\tilde{\Pi}_1 =& \begin{bmatrix}
\sqrt{\beta_1}\bar{A}(\Theta_k)G & \sqrt{\beta_1}\bar{B}_r G & \sqrt{\beta_1}\bar{B}(\Theta_k)Y_{|\kappa_1} \\
\sqrt{\beta_2}\bar{A}(\Theta_k)G & \sqrt{\beta_2}\bar{B}_r G & 0 \\
\vdots & \vdots & \vdots \\
\sqrt{\beta_s}\bar{A}(\Theta_k)G & \sqrt{\beta_s}\bar{B}_r G & \cdots
\end{bmatrix}\\
&\qquad \begin{bmatrix}
0 & \cdots & 0 \\
\sqrt{\beta_2}\bar{B}(\Theta_k)Y_{|\kappa_2} & \cdots & 0 \\
\ddots & \ddots & \vdots \\
0 & 0 & \sqrt{\beta_s}\bar{B}(\Theta_k)Y_{|\kappa_s}
\end{bmatrix},\\
\tilde{\Pi}_2 =& \begin{bmatrix}
\sqrt{\beta_1}(\bar{A}(\Theta_k) - I)G & \sqrt{\beta_1}\bar{B}_r G & \sqrt{\beta_1}\bar{B}(\Theta_k)Y_{|\kappa_1} \\
\sqrt{\beta_2}(\bar{A}(\Theta_k) - I)G & \sqrt{\beta_2}\bar{B}_r G & 0 \\
\vdots & \vdots & \vdots \\
\sqrt{\beta_s}(\bar{A}(\Theta_k) - I)G & \sqrt{\beta_s}\bar{B}_r G & \cdots
\end{bmatrix}\\
&\qquad \begin{bmatrix}
0 & \cdots & 0 \\
\sqrt{\beta_2}\bar{B}(\Theta_k)Y_{|\kappa_2} & \cdots & 0 \\
\ddots & \ddots & \vdots \\
0 & 0 & \sqrt{\beta_s}\bar{B}(\Theta_k)Y_{|\kappa_s}
\end{bmatrix},
\end{aligned}
$$

$$\tilde{\Pi}_3 = \begin{bmatrix} \sqrt{\beta_1}\bar{C}G & 0 & \sqrt{\beta_1}\bar{D}Y_{|\kappa_1} & 0 & \cdots & 0 \\ \sqrt{\beta_2}\bar{C}G & 0 & 0 & \sqrt{\beta_2}\bar{D}Y_{|\kappa_2} & \cdots & 0 \\ \vdots & \vdots & \vdots & \ddots & \ddots & \vdots \\ \sqrt{\beta_s}\bar{C}G & 0 & \cdots & 0 & 0 & \sqrt{\beta_s}\bar{D}Y_{|\kappa_s} \end{bmatrix},$$

$$\tilde{Q}_a(\Theta_k) = GQ_a(\Theta_k)G, \tilde{N}_a(\Theta_k) = GN_a(\Theta_k)G,$$

$$Y_{|\kappa_a} = X_{|\kappa_a}G.$$

Under the fact $-GZ_a(\Theta_{k-l_a})G \leq X_a(\Theta_{k-l_a}) - 2G$ and assuming that the unknown parameters are all linearly dependent on the fuzzy weighting functions, if Condition (5.43) is satisfied, then Inequality (5.44) holds. According to Theorem 2, the closed-loop system in (5.20) is exponentially mean-square stable with an $\mathcal{H}_\infty$ performance index γ. The proof is completed. □

If γ is minimized, then an optimal performance can be achieved. The following corollary can be used to solve the minimization problem.

Corollary 5.1. *The minimum $\mathcal{H}_\infty$ performance index γ for the closed-loop system in (5.20) can be found by solving the following convex optimization problem:*

$$\min \gamma^2.$$
$$s.\ t.\ \ (5.43)$$

5.4 Illustrative Example

Consider a networked inverted pendulum [170]. Here, the original nonlinear system model is approximately represented by a T-S fuzzy system with 2 subsystems. When the sampling time is $0.02s$, the parameters for the equivalent discrete-time model are:

$$A_1 = \begin{bmatrix} 1.0002 & 0.02 & 0.02 \\ 0.196 & 1.0001 & 0.0181 \\ -0.0184 & -0.1813 & 0.8170 \end{bmatrix}, \; A_2 = \begin{bmatrix} 1 & 0.02 & 0.0002 \\ 0 & 0.9981 & 0.0181 \\ 0 & -0.1811 & 0.8170 \end{bmatrix},$$

$$B_1 = B_2 = \begin{bmatrix} 0 \\ 0.0019 \\ 0.1811 \end{bmatrix}, \; C_1 = C_2 = \begin{bmatrix} 1 & 0 & 0 \end{bmatrix}.$$

Suppose that the nonlinear system is controlled by a remote controller and the communication link is subject to delays. The lumped network-induced delay ν_k is time-varying and takes value in the set $\{2, 4\}$. In addition, the occurrence probability for $\nu_k = 2$ is 0.6 and the occurrence probability for $\nu_k = 4$ is 0.4. When the weighting matrices $R_1 = I$ and $R_2 = I$, the derived minimum γ is 143.6371. The corresponding parameters for the controller are

$$K_{|2} = [-13.0845 \; -3.3614 \; -0.8982 \; 0.2769],$$
$$K_{|4} = [-11.2990 \; -2.9215 \; -0.6637 \; 0.2486].$$

It can be seen from Figure 5.2 that by using the designed controllers, the output tracks the reference well, when the nonlinear system is subject to the network-induced delay as shown in Figure 5.3. The control actions are illustrated in Figure 5.4. From the simulation results, we can check that the 2-norm of z_k is 9.0668 and the 2-norm of w_k is 70.7177. The energy-to-energy gain is 0.1282 which is smaller than the derived γ.

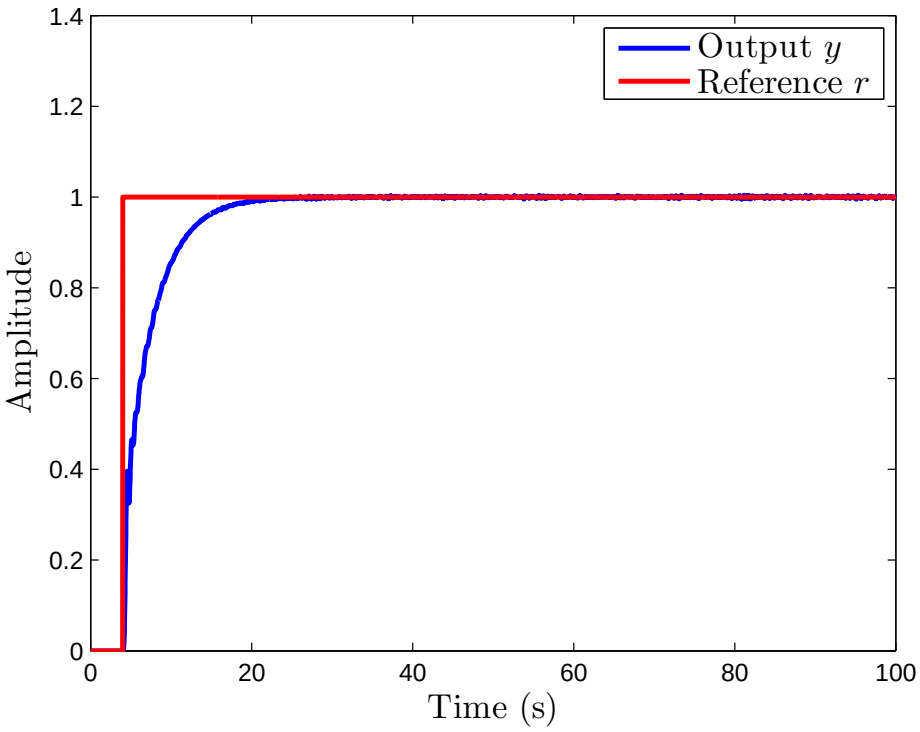

Figure 5.2: Tracking performance for a unit step signal.

5.5 Conclusions

In this work, the step tracking control problem for networked nonlinear systems has been investigated. The control signal is a combination of the state-feedback control and the integral control. The network-induced delay with *a priori* occurrence probability was considered in the modeling of the behavior of the communication link with a limited capacity. The design method was proposed for the delay-scheduling tracking controller. The parameters for the controller can be obtained by solving a set of LMIs. The proposed design method was applied to a networked inverted pendulum model. The simulation results illustrated the effectiveness of the proposed design scheme.

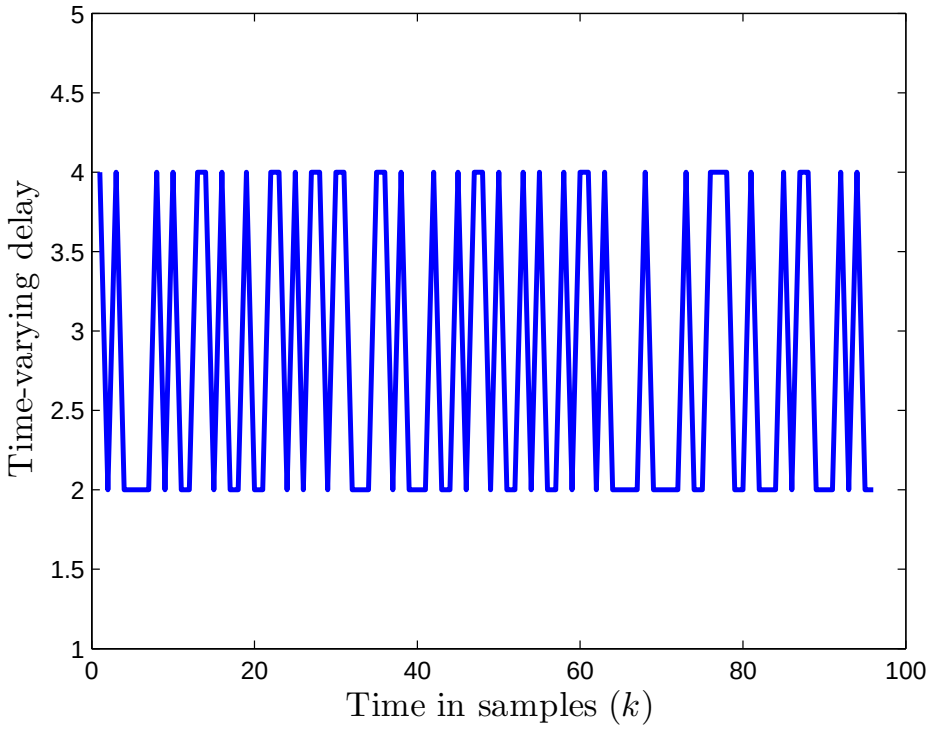

Figure 5.3: Time-varying network-induced delay.

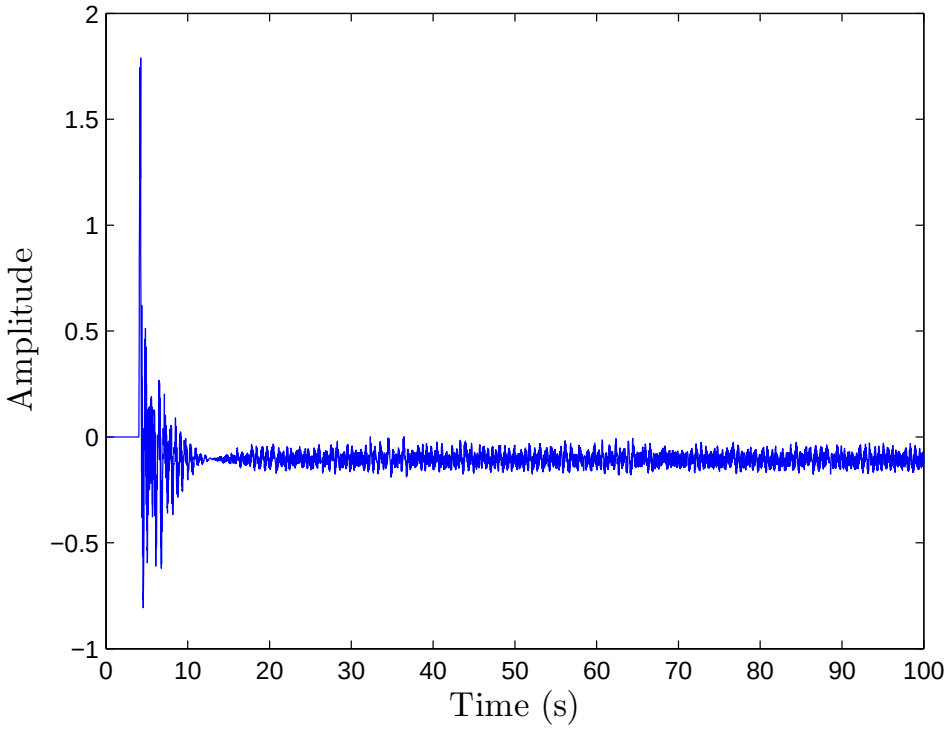

Figure 5.4: Control action in the simulation.

Chapter 6

Robust Weighted $\mathcal{H}_\infty$ Filtering for Networked Systems with Intermittent Measurements of Multiple Sensors

6.1 Introduction

Last decades have witnessed a renewed interest in the techniques for signal estimation. The estimation problem is very important from the application perspective in manufacturing, process control, mechatronics, biomedical systems, and so on [121,171–173]. In particular, Kalman filtering has been effectively applied to a wide range of applications. In general, the power spectral densities of the measurement noise and a precise system model are required to minimize the variance of the state estimation error. In most filtering problems, the system uncertainty, resulting from either inaccurate knowledge of the physical parameter values or from parameter variations during

operations [174], is unavoidable. Meanwhile, the assumption of knowing *a prior* statistical information about the exogenous noise is not always realistic [175]. Motivated by the need to accommodate significant modeling uncertainties and/or incomplete knowledge about the external noise in the filtering problems, increasing attention has been paid to the robust $\mathcal{H}_\infty$ filtering for linear and nonlinear systems with uncertain parameters; see [176, 177] for linear systems and [178, 179] for nonlinear systems, to name a few among many important results in the literature.

Standard filtering problems generally assume that the measurements of the sensors are completely available. In many practical applications, however, the sensors may have temporal failures during operation, and the observations from the sensors may be uncertain. The phenomenon of incomplete measurements, also called uncertain observations or missing measurements, was first addressed and modeled in [180]. Since sensors may fail more frequently in harsh industrial environment, the filtering problem considering sensor faults has attracted particular attention during the past few years [181–186]. The filtering problem considering partial observations and irregular time delays in the transmission was studied in [182]. In [184], multiple sensors with different failure rates were considered in the system model and the estimator design. The authors in [185] studied the robust filtering problem for systems with stochastic nonlinearities and multiple measurements. The robust filter design for a class of time-varying nonlinear systems with sector-bounded nonlinearity and probabilistic sensor gain faults was investigated in [186].However, there are few results on robust $\mathcal{H}_\infty$ filtering for systems with multiple sensor faults.

On another industrial application frontier, networked systems have received increasing attention in the past few years [52, 58]. As much effort from both academia and industry has been devoted to the wireless automation technologies, such as Wireless HART and ISA 100, network filtering will have broad applications in the future.

However, in the literature, there have been few results reported on robust $\mathcal{H}_\infty$ filtering for networked systems in the discrete-time framework, simultaneously considering network-induced delays, missing packets and out-of-order arrival of packets. This motivates the work in this chapter. Moreover, when taking the above phenomena into account, the delayed noise and non-delayed noise both exist in the resulting filtering error system. The delayed noise and non-delayed noise were often augmented into a new variable, in which the delay information does not appear explicitly [131]. In order to make full use of the delayed information (delayed states and delayed noises) and achieve better filtering performance, we choose not to lump the delayed noise and non-delayed noise together; instead, we propose to introduce a new weighted $\mathcal{H}_\infty$ performance index, which is another contribution of this chapter.

The remainder of the chapter is organized as follows. In Section 6.2, we formulate the robust filtering problem for networked systems by considering the incomplete measurements, network-induced delays and missing packets. Moreover, the definitions of the robust exponential mean-square stability and the weighted $\mathcal{H}_\infty$ filtering are introduced. The stability and robust weighted $\mathcal{H}_\infty$ performance for the filtering error system are then analyzed in Section 6.3. Based on the analysis results, the filter design method is proposed in Section 6.4. Numerical simulations are given in Section 6.5 to illustrate the effectiveness of the proposed method. Section 6.6 concludes the chapter.

6.2 Problem Formulation and Preliminaries

The filtering problem for a typical networked system with incomplete measurements in the discrete-time domain is shown in Figure 6.1.

Suppose that the physical plant, a linear time-invariant discrete-time system, is given by

$$\begin{aligned} x_{k+1} &= Ax_k + B\omega_k, \\ y_k &= Cx_k + D\omega_k, \\ z_k &= Lx_k + F\omega_k, \end{aligned} \tag{6.1}$$

where k is the sampling instant, $x_k \in \mathbb{R}^n$ is the state vector of the system, $y_k \in \mathbb{R}^m$ is the output of the plant, $\omega_k \in \mathbb{R}^q$ is the disturbance input which belongs to $l_2[0, \infty)$, and $z_k \in \mathbb{R}^p$ is the linear combination of the states and disturbance to be estimated. The system matrices A, B, C, D, L and F all have appropriate dimensions.

The uncertainty is unavoidable in practical systems due to inadequate knowledge of physical parameter values and parameter variations during operations [174]. Therefore, we consider the model uncertainties of the system in (6.1) and assume that the system matrices $(A,\ B,\ C,\ D,\ L,\ F) \in \mathfrak{M}$, where $\mathfrak{M}$ is a given convex bounded polyhedral domain described by s vertices:

$$\mathfrak{M} := \left\{ \Omega \middle| \Omega = \sum_{i=1}^{s} \alpha_i \Omega_i; \sum_{i=1}^{s} \alpha_i = 1, \alpha_i \geq 0 \right\}.$$

Here, $\Omega_i := (A_i,\ B_i,\ C_i,\ D_i,\ L_i,\ F_i),\ i = 1, \cdots, s$, represent the vertices of the polytope and are known matrices with compatible dimensions. The plant with parameter uncertainties can be determined by the combination of these vertices. The objective of filtering is to estimate z_k by using the measured outputs of the plant. Suppose a full-order estimator for the filtering problem is of the following form:

$$\begin{aligned} \hat{x}_{k+1} &= A_f \hat{x}_k + B_f \hat{y}_k, \\ \hat{z}_k &= L_f \hat{x}_k + F_f \hat{y}_k, \end{aligned} \tag{6.2}$$

where $\hat{x}_k$ is the filter state, $\hat{z}_k$ is the estimate of z_k, $\hat{y}_k$ is the input of the filter, and $(A_f,\ B_f,\ L_f,\ F_f)$ are appropriately dimensioned matrices to be designed.

In conventional filtering problems, the input of the filter is assumed to be equal to the output of the plant [158], i.e., $\hat{y}_k = y_k$. However, in many practical applications, the measurements may be incomplete because of sensor temporal failure and abrupt changes in the operation environment [180]. Thus, the problem of incomplete measurements is necessary to be considered from the application requirements. In addition, as shown in Figure 6.1, the measured outputs are transmitted via a network medium. The filtering problem for networked systems should consider the effect of the inserted network link. The network-induced delays, packet dropouts and out-of-order arrival of packets should be incorporated into the modeling and addressed in the design. In the following, we will model these network-induced issues with some practical assumptions.

- *Intermittent measurements*: Suppose m outputs of the plant are measured by m sensors separately and these sensors work separately. For each sensor, it is practical to assume that the scenario of random sensor faults can be characterized by a Bernoulli process with a probability for the available measurements [180], and the output of the sensor can be expressed as

$$y_{t,k} = \begin{cases} \Phi_t C x_k + \Phi_t D \omega_k, & \text{with probability } \beta_t, \\ \Phi_t D \omega_k, & \text{with probability 1-}\beta_t, \end{cases} \tag{6.3}$$

  where $y_{t,k}$ gives the measurement of t^{th} sensor at time k and

$$\Phi_t := \text{diag}\left\{0, \cdots, 0, 1, 0, \cdots, 0\right\},$$

  where the t^{th} entry on the diagonal is one and others are zeros, $\forall t = 1, \cdots, m$.

Equation (6.3) can be rewritten in a compact form by introducing Bernoulli variables $r_{t,k}$, $\forall t = 1, \cdots, m$, as

$$y_{t,k} = r_{t,k}\Phi_t C x_k + \Phi_t D\omega_k, \tag{6.4}$$

where $r_{t,k}$ is a Bernoulli distributed white sequence taking the value one with a probability of β_t and zero with a probability of $1 - \beta_t$ (the failure rate of the sensor). The measurement of the output at time instant k is characterized by

$$\tilde{y}_k = \sum_{t=1}^{m} r_{t,k}\Phi_t C x_k + D\omega_k. \tag{6.5}$$

- *Influence of the network:* Suppose that, at time instant k, the received data is $\widehat{y}_k$ and the transmission delay is τ_k at the buffer node. Then the relationship between $\widehat{y}_k$ and $\tilde{y}_k$ is

$$\widehat{y}_k = \tilde{y}_{k-\tau_k}.$$

It is assumed that the buffer is event-driven. When y_k is missing during the transmission, and thus it will not arrive at the buffer at time instant k, the buffer will not be updated if there are no other packets received. Therefore, the filter can only adopt the 'old' data (delayed data) at the time instant k. The influence of missing packets is similar as the effect of network-induced delays in the view of the buffer node. This problem was studied in the discrete-time framework in [187]. Since the effect of packet dropouts can be characterized by τ_k, we do not introduce another variable for this purpose.

The network-induced delays and packet dropouts may lead to the disorder of arriving packets. In this case, it is advantageous to use the most recent data [52]. The function of the buffer is to store the latest data that has the most recent

time stamp. When a new packet arrives at the buffer, if the time stamp of the data is greater than that of the data stored in the buffer, then the new data will be stored in the buffer and sent to the filter. Otherwise, the buffer does not send new data to the filter and the input of the filter remains the same. Meanwhile, the data in the buffer is not replaced by the newly received one. Considering the buffer node and network-induced delays, the relationship between the input of the filter $\hat{y}_k$ and the measurement $\tilde{y}_k$ is

$$\hat{y}_k = \tilde{y}_{k-d_k}. \tag{6.6}$$

Here, d_k represents the accumulated influence of the network-induced delays and packet dropouts, and satisfies

$$d_{k+1} \leq d_k + 1. \tag{6.7}$$

Since the delays and packet dropouts cannot be infinite, we further assume that d_k is bounded and lies within an interval, i.e.,

$$0 < d_1 \leq d_k \leq d_2 < \infty. \tag{6.8}$$

Considering the sensor faults and the influence of the inserted network medium, the input of the filter is described as

$$\hat{y}_k = \tilde{y}_{k-d_k} = \sum_{t=1}^{m} r_{t,k-d_k} \Phi_t C x_{k-d_k} + D\omega_{k-d_k}. \tag{6.9}$$

Define the filtering error as

$$e_k = z_k - \hat{z}_k.$$

Then construct the filtering error system by combining the system in (6.1) and the estimator system in (6.2) as follows:

$$\begin{aligned} \xi_{k+1} &= \bar{A}\xi_k + \bar{A}_d R\xi_{k-d_k} + \bar{A}_r R\xi_{k-d_k} + \bar{B}_1\omega_k + \bar{B}_2\omega_{k-d_k}, \\ e_k &= \bar{L}\xi_k + \bar{L}_d R\xi_{k-d_k} + \bar{L}_r R\xi_{k-d_k} + F\omega_k - F_f D\omega_{k-d_k}, \end{aligned} \tag{6.10}$$

where

$$\xi_k = \begin{bmatrix} x_k \\ \hat{x}_k \end{bmatrix},\ \bar{A} = \begin{bmatrix} A & 0 \\ 0 & A_f \end{bmatrix},\ \bar{B}_1 = \begin{bmatrix} B \\ 0 \end{bmatrix},$$

$$\bar{A}_d = \begin{bmatrix} 0 \\ B_f\Psi C \end{bmatrix},\ \bar{A}_r = \begin{bmatrix} 0 \\ B_f(\bar{\Psi} - \Psi)C \end{bmatrix},$$

$$\bar{L} = \begin{bmatrix} L & -L_f \end{bmatrix},\ \bar{B}_2 = \begin{bmatrix} 0 \\ B_f D \end{bmatrix},\ R = \begin{bmatrix} I & 0 \end{bmatrix},$$

$$\bar{L}_d = \begin{bmatrix} -F_f\Psi C \end{bmatrix},\ \bar{L}_r = \begin{bmatrix} -F_f(\bar{\Psi} - \Psi)C \end{bmatrix},$$

$$\bar{\Psi} = \text{diag}\left\{r_{1,k}, \cdots, r_{m,k}\right\},\ \text{and}\ \Psi = \mathcal{E}\{\bar{\Psi}\}.$$

It is noted that the stochastic variables $r_{t,k},\ \forall t = 1, \cdots, m$ are incorporated in (6.10). In order to deal with the random variables, we apply the stochastic stability in the mean square sense for the filtering error system. Moreover, the delayed noise and the non-delayed noise both appear in (6.10). In the literature, they were augmented into a new non-delayed noise variable [131]. However the delayed information was not fully used if such an augmentation method simple following. Therefore we seek to answer the following question: Is it possible to develop a more general approach in the filter design for networked systems, and to achieve better filtering performance if we explicitly incorporate the delayed noise information in the analysis

and design? The answer is positive, as seen soon in the following development. We first introduce the following definitions.

Definition 6.1. *The filtering error system in (6.10) is said to be exponentially mean-square stable, if with $\omega_k = 0$, there exist constants $\beta_1 > 0$ and $\beta_2 > 0$ such that for $k \geq 0$, the following inequality holds:*

$$\mathcal{E}\left\{\|\xi_k\|^2\right\} \leq \beta_1 e^{-\beta_2 k}\mathcal{E}\left\{\sup_{-d_2\leq i\leq 0}\|\xi_i\|^2\right\}.$$

□

Definition 6.2. *Given two scalars $\gamma > 0$ and $0 < \beta < 1$, the closed-loop control system in (6.10) is said to be robustly exponentially mean-square stable with a weighted $\mathcal{H}_\infty$ performance γ and a prescribed weighting factor β if it is exponentially mean-square stable and*

$$\mathcal{E}\left\{\|e\|_2^2\right\} < \beta\gamma^2\|\omega\|_2^2 + (1-\beta)\gamma^2\|\omega_d\|_2^2$$

for all nonzero $\omega_k \in l_2[0,\infty)$ subject to the zero initial condition and all admissible uncertainties, where $\mathcal{E}\left\{\|e\|_2^2\right\} := \mathcal{E}\left\{\sum_{k=0}^{\infty}\left(e_k^{\mathrm{T}}e_k\right)\right\}$, $\|\omega\|_2^2 := \sum_{k=0}^{\infty}\left(\omega_k^{\mathrm{T}}\omega_k\right)$, and $\|\omega_d\|_2^2 := \sum_{k=0}^{\infty}\left(\omega_{k-d_k}^{\mathrm{T}}\omega_{k-d_k}\right)$. □

Using Definition 6.1 and Definition 6.2, the main objective of this chapter can be cast as: To design robust weighted $\mathcal{H}_\infty$ filters of the form in (6.2) such that, for all admissible polytopic uncertainties, network-induced delay and incomplete measurements, the augmented filtering dynamics in (6.10) is exponentially mean-square stable with a weighted $\mathcal{H}_\infty$ performance γ for a prescribed weighting factor β.

6.3 Weighted $\mathcal{H}_\infty$ Filtering Performance Analysis

In this section, we will provide robust weighted $\mathcal{H}_\infty$ performance analysis results for the filtering error system in (6.10). Before proceeding further, we introduce the following lemma.

Lemma 6.1. *Let* $\eta_k := \xi_{k+1} - \xi_k$ *and* $\Theta_k := [\xi_k^{\mathrm{T}}, \xi_{k-1}^{\mathrm{T}}, \xi_{k-2}^{\mathrm{T}}, \cdots, \xi_{k-d_2}^{\mathrm{T}}]^{\mathrm{T}}$*, where* ξ_k *is the state vector of the filtering error system. Consider a Lyapunov functional candidate for the filtering error dynamic system in (6.10) in the following form:*

$$V_k(\Theta_k) := V_{1,k} + V_{2,k} + V_{3,k} + V_{4,k}, \tag{6.11}$$

$$\begin{aligned}
V_{1,k} &:= \xi_k^{\mathrm{T}} P \xi_k, \\
V_{2,k} &:= \sum_{i=k-d_k}^{k-1} \xi_i^{\mathrm{T}} R^{\mathrm{T}} Q R \xi_i, \\
V_{3,k} &:= \sum_{j=-d_2+1}^{-d_1+1} \sum_{i=k+j-1}^{k-1} \xi_i^{\mathrm{T}} R^{\mathrm{T}} Q R \xi_i, \\
V_{4,k} &:= \sum_{j=-d_2}^{-1} \sum_{i=k+j}^{k-1} \eta_i^{\mathrm{T}} R^{\mathrm{T}} Z R \eta_i,
\end{aligned}$$

where $P = P^{\mathrm{T}} > 0$*,* $Q = Q^{\mathrm{T}} > 0$*, and* $Z = Z^{\mathrm{T}} > 0$*. If there exists a scalar* $\psi > 0$ *such that*

$$\mathcal{E}\left\{V_{k+1}(\Theta_{k+1}) \,|\Theta_k\right\} - V_k(\Theta_k) < -\psi \|\xi_k\|^2, \tag{6.12}$$

then the dynamics of the process ξ_k *is exponentially mean-square stable.*

Proof. The proof can be done by following the similar lines of [123]. □

The following theorem will play a key role in the filter design.

Theorem 6.1. *Consider the filtering problem for a networked system, as shown in Figure 6.1. Suppose* A_f*,* B_f*,* L_f *and* F_f*,* γ *and* β *are given. The filtering error system*

in (6.10) is robustly exponentially mean-square stable, and the filter error e_k satisfies the weighted $\mathcal{H}_\infty$ disturbance attenuation level γ if there exist matrices $P = P^{\mathrm{T}} > 0$, $Q = Q^{\mathrm{T}} > 0$, $Z = Z^{\mathrm{T}} > 0$, S_1, S_2, S_3, and S_4 such that the following inequality is satisfied

$$\begin{bmatrix}
\Pi_{11} & * & * & * & * & * & * & * & * & * \\
-S_1^{\mathrm{T}} + S_2 R & \Pi_{22} & * & * & * & * & * & * & * & * \\
S_3 R & -S_3 & -\beta\gamma^2 I & * & * & * & * & * & * & * \\
S_4 R & -S_4 & 0 & (\beta-1)\gamma^2 I & * & * & * & * & * & * \\
d_2 S_1^{\mathrm{T}} & d_2 S_2^{\mathrm{T}} & d_2 S_3^{\mathrm{T}} & d_2 S_4^{\mathrm{T}} & -d_2 Z & * & * & * & * & * \\
P\bar{A} & P\bar{A}_d & P\bar{B}_1 & P\bar{B}_2 & 0 & -P & * & * & * & * \\
d_2 Z R(\bar{A}-I) & 0 & d_2 Z R \bar{B}_1 & 0 & 0 & 0 & -d_2 Z & * & * & * \\
\bar{L} & \bar{L}_d & F & -F_f D & 0 & 0 & 0 & -I & * & * \\
0 & \mathcal{A}_r & 0 & 0 & 0 & 0 & 0 & 0 & -\mathcal{P} & * \\
0 & \mathcal{L}_r & 0 & 0 & 0 & 0 & 0 & 0 & 0 & -I
\end{bmatrix} < 0. \tag{6.13}$$

Here,

$$\begin{aligned}
\Pi_{11} &= -P + (\bar{d}+2) R^{\mathrm{T}} Q R + \mathrm{sym}(S_1 R), \\
\Pi_{22} &= -Q - \mathrm{sym}(S_2), \\
A_{r,t} &= [0 \quad (B_f \Phi_t C)^{\mathrm{T}}]^{\mathrm{T}}, \\
\mathcal{A}_r &= [\sigma_1 A_{r,1}^{\mathrm{T}} P, \cdots, \sigma_m A_{r,m}^{\mathrm{T}} P]^{\mathrm{T}}, \\
\sigma_t &= \sqrt{\beta_t(1-\beta_t)}, \\
L_{r,t} &= [-F_f \Phi_t C], \\
\mathcal{L}_r &= [\sigma_1 L_{r,1}^{\mathrm{T}}, \cdots, \sigma_m L_{r,m}^{\mathrm{T}}]^{\mathrm{T}}, \\
\mathcal{P} &= \mathrm{diag}\left\{P, \cdots, P\right\}, \ \forall t = 1, \cdots, m.
\end{aligned}$$

Proof: Choose a Lyapunov functional candidate for the filtering error system in (6.10) in the form of (6.11). The difference of the Lyapunov function can be evaluated in the following:

$$\Delta V_k = \mathcal{E}\left\{V_{k+1}\left(\Theta_{k+1}\right)|\Theta_k\right\} - V_k\left(\Theta_k\right). \tag{6.14}$$

Under the assumption that the exogenous noise $\omega_k = 0$, the difference of the Lyapunov

functional candidate is given by:

$$
\begin{aligned}
\Delta V_{1,k} =& \mathcal{E}\left\{V_{1,k+1}\left(\Theta_{k+1}\right)|\Theta_k\right\} - V_{1,k}\left(\Theta_k\right) \\
=& \xi_k^{\mathrm{T}}\bar{A}^{\mathrm{T}}P\bar{A}\xi_k + 2\xi_k^{\mathrm{T}}\bar{A}^{\mathrm{T}}P\bar{A}_d R\xi_{k-d_k} + \xi_{k-d_k}^{\mathrm{T}}R^{\mathrm{T}}\bar{A}_d^{\mathrm{T}}P\bar{A}_d R\xi_{k-d_k} \\
& - \xi_k^{\mathrm{T}}P\xi_k + \xi_{k-d_k}^{\mathrm{T}}R^{\mathrm{T}}\mathcal{E}\left\{\bar{A}_r^{\mathrm{T}}P\bar{A}_r\right\}R\xi_{k-d_k}, \\
\Delta V_{2,k} =& \mathcal{E}\left\{V_{2,k+1}\left(\Theta_{k+1}\right)|\Theta_k\right\} - V_{2,k}\left(\Theta_k\right) \\
=& \sum_{i=k+1-d_{k+1}}^{k} \xi_i^{\mathrm{T}}R^{\mathrm{T}}QR\xi_i - \sum_{i=k-d_k}^{k-1} \xi_i^{\mathrm{T}}R^{\mathrm{T}}QR\xi_i \leq \xi_k^{\mathrm{T}}R^{\mathrm{T}}QR\xi_k, \\
\Delta V_{3,k} =& \mathcal{E}\left\{V_{3,k+1}\left(\Theta_{k+1}\right)|\Theta_k\right\} - V_{3,k}\left(\Theta_k\right) \\
=& \sum_{j=-d_2+1}^{-d_1+1} \left(\xi_k^{\mathrm{T}}R^{\mathrm{T}}QR\xi_k - \xi_{k+j-1}^{\mathrm{T}}R^{\mathrm{T}}QR\xi_{k+j-1}\right) \\
\leq& (\bar{d}+1)\xi_k^{\mathrm{T}}R^{\mathrm{T}}QR\xi_k - \sum_{j=k-d_2}^{k-d_1} \xi_j^{\mathrm{T}}R^{\mathrm{T}}QR\xi_j \\
\leq& (\bar{d}+1)\xi_k^{\mathrm{T}}R^{\mathrm{T}}QR\xi_k - \xi_{k-d_k}^{\mathrm{T}}R^{\mathrm{T}}QR\xi_{k-d_k}, \\
\Delta V_{4,k} =& \mathcal{E}\left\{V_{4,k+1}\left(\Theta_{k+1}\right)|\Theta_k\right\} - V_{4,k}\left(\Theta_k\right) \\
=& d_2\xi_k^{\mathrm{T}}(\bar{A}-I)^{\mathrm{T}}R^{\mathrm{T}}ZR(\bar{A}-I)\xi_k \\
& + 2d_2\xi_k^{\mathrm{T}}(\bar{A}-I)^{\mathrm{T}}R^{\mathrm{T}}ZR\bar{A}_d R\xi_{k-d_k} \\
& + d_2\xi_{k-d_k}^{\mathrm{T}}R^{\mathrm{T}}\bar{A}_d^{\mathrm{T}}R^{\mathrm{T}}ZR\bar{A}_d R\xi_{k-d_k} \\
& + d_2\xi_{k-d_k}^{\mathrm{T}}R^{\mathrm{T}}\mathcal{E}\left\{\bar{A}_r^{\mathrm{T}}R^{\mathrm{T}}ZR\bar{A}_r\right\}R\xi_{k-d_k} \\
& - \sum_{j=k-d_2}^{k-1} \eta_j^{\mathrm{T}}R^{\mathrm{T}}ZR\eta_j.
\end{aligned}
\tag{6.15}
$$

It is noted that

$$
\mathcal{E}\left\{\bar{A}_r^{\mathrm{T}}P\bar{A}_r\right\} = \sum_{t=1}^{m} \sigma_t^2 A_{r,t}^{\mathrm{T}}PA_{r,t}, \tag{6.16}
$$

$$
\mathcal{E}\left\{\bar{A}_r^{\mathrm{T}}R^{\mathrm{T}}ZR\bar{A}_r\right\} = 0, \tag{6.17}
$$

and

$$R\bar{A}_d = 0. \tag{6.18}$$

Moreover, for any matrices S_1 and S_2 with appropriate dimensions,

$$\Xi_1 = \left(\xi_k^{\mathrm{T}} S_1 + \xi_{k-d_k}^{\mathrm{T}} R^{\mathrm{T}} S_2\right) \left[R\xi_k - R\xi_{k-d_k} - R\sum_{i=k-d_k}^{k-1} \eta_i\right] = 0, \tag{6.19}$$

and

$$\Xi_2 = \sum_{i=k-d_k}^{k-1} \left(\xi_k^{\mathrm{T}} S_1 + \xi_{k-d_k}^{\mathrm{T}} R^{\mathrm{T}} S_2 + \eta_i^{\mathrm{T}} R^{\mathrm{T}} Z\right) Z^{-1} \left(\xi_k^{\mathrm{T}} S_1 + \xi_{k-d_k}^{\mathrm{T}} R^{\mathrm{T}} S_2 + \eta_i^{\mathrm{T}} R^{\mathrm{T}} Z\right)^{\mathrm{T}} \geq 0. \tag{6.20}$$

It follows from (6.15)-(6.20) that

$$\Delta V_k\left(\Theta_k\right) < \Delta V_{1,k} + \Delta V_{2,k} + \Delta V_{3,k} + \Delta V_{4,k} + \mathrm{sym}(\Xi_1) + \Xi_2 = \zeta_k^{\mathrm{T}} \Lambda \zeta_k, \tag{6.21}$$

where

$$\begin{aligned} \zeta_k &= \begin{bmatrix} \xi_k \\ R\xi_{k-d_k} \end{bmatrix}, \ \Lambda = \begin{bmatrix} \Lambda_{11} & * \\ \Lambda_{21} & \Lambda_{22} \end{bmatrix}, \\ \Lambda_{11} =& \bar{A}^{\mathrm{T}} P \bar{A} - P + \mathrm{sym}(S_1 R) + d_2 S_1 Z^{-1} S_1^{\mathrm{T}} \\ &+ d_2 (\bar{A} - I)^{\mathrm{T}} R^{\mathrm{T}} Z R (\bar{A} - I) + (\bar{d} + 2) R^{\mathrm{T}} Q R, \end{aligned} \tag{6.22}$$

$$\begin{aligned} \Lambda_{21} =& \bar{A}_d^{\mathrm{T}} P \bar{A} + (-S_1^{\mathrm{T}} + S_2 R) + d_2 S_2 Z^{-1} S_1^{\mathrm{T}}, \\ \Lambda_{22} =& \bar{A}_d^{\mathrm{T}} P \bar{A}_d + d_2 S_2 Z^{-1} S_2^{\mathrm{T}} - Q + \mathrm{sym}(-S_2) + \sum_{t=1}^{m} \sigma_t^2 A_{r,t}^{\mathrm{T}} P A_{r,t}. \end{aligned} \tag{6.23}$$

By using the Schur complement, for any nonzero ζ_k, it can be seen that Condi-

tion (6.13) implies

$$\Delta V_k\left(\Theta_k\right) < 0.$$

Therefore, there exists a positive scalar $\psi > 0$ such that

$$\Lambda < \begin{bmatrix} -\psi I & 0 \\ 0 & 0 \end{bmatrix}. \tag{6.24}$$

By considering (6.14), (6.21) and (6.24), we have the following inequality

$$\mathcal{E}\left\{V_{k+1}\left(\Theta_{k+1}\right)|\Theta_k\right\} - V_k\left(\Theta_k\right) < -\psi\xi_k^{\mathrm{T}}\xi_k = -\psi\left\|\xi_k\right\|^2. \tag{6.25}$$

According to *Lemma* 6.1, the filtering error system in (6.10) is exponentially mean-square stable.

To establish the weighted $\mathcal{H}_\infty$ performance for the filtering error system, assume the zero initial condition and consider the following objective function:

$$J := \Delta V_k\left(\Theta_k\right) + e_k^{\mathrm{T}}e_k - \beta\gamma^2\|\omega\|_2^2 - (1-\beta)\gamma^2\|\omega_d\|_2^2. \tag{6.26}$$

For any nonzero noise, choose the same Lyapunov functional candidate as defined in (6.11). The difference of the Lyapunov functional candidate can be obtained along similar lines as in (6.15) but with $w_k \neq 0$ and $w_{k-d_k} \neq 0$. Then, for any matrices S_l, $l = 1, 2, 3, 4$, the following conditions hold

$$\begin{aligned} \Xi_3 = &\left(\xi_k^{\mathrm{T}}S_1 + \xi_{k-d_k}^{\mathrm{T}}R^{\mathrm{T}}S_2 + \omega_k^{\mathrm{T}}S_3 + \omega_{k-d_k}^{\mathrm{T}}S_4\right) \\ &\left[R\xi_k - R\xi_{k-d_k} - R\sum_{i=k-d_k}^{k-1}\eta_i\right] = 0, \end{aligned} \tag{6.27}$$

and

$$\Xi_4 = \sum_{i=k-d_k}^{k-1} \left(\xi_k^{\mathrm{T}} S_1 + \xi_{k-d_k}^{\mathrm{T}} R^{\mathrm{T}} S_2 + \omega_{k-d_k}^{\mathrm{T}} S_3 + \omega_k^{\mathrm{T}} S_4 + \eta_i^{\mathrm{T}} R^{\mathrm{T}} Z\right) Z^{-1} \left(\xi_k^{\mathrm{T}} S_1 + \xi_{k-d_k}^{\mathrm{T}} R^{\mathrm{T}} S_2 + \omega_{k-d_k}^{\mathrm{T}} S_3 + \omega_k^{\mathrm{T}} S_4 + \eta_i^{\mathrm{T}} R^{\mathrm{T}} Z\right)^{\mathrm{T}} \geq 0. \tag{6.28}$$

Substituting the difference of the Lyapunov functional, (6.27) and (6.28) into (6.26) and using Schur complement, it is shown that if the inequality in (6.13) holds, then the objective function $J < 0$. By summing up the objective function J with respect to the time instant k, we have

$$\|e\|_2^2 < \beta\gamma^2 \|\omega\|_2^2 + (1-\beta)\gamma^2 \|\omega_d\|_2^2 + V_0(\Theta_0) - V_\infty(\Theta_\infty). \tag{6.29}$$

Noting that $V_0(\Theta_0) = 0$ and $V_\infty(\Theta_\infty) \geq 0$, we conclude

$$\|e\|_2^2 < \beta\gamma^2 \|\omega\|_2^2 + (1-\beta)\gamma^2 \|\omega_d\|_2^2 . \tag{6.30}$$

Hence, if the inequality in (6.13) holds, the filtering error system is exponentially mean-square stable and the filtering error achieves a given weighted $\mathcal{H}_\infty$ disturbance attenuation level γ with a weighting factor β. This completes the proof. □

Remark 6.1. *As seen from the above analysis, the information of the incomplete measurements has been incorporated in the filter performance analysis-see the condition stated in (6.13). When the expectations of the available measurements for all the sensors are identical, the special case was studied in [188] for systems with constant time-delays.*

In order to derive a less conservative result for the robust filtering design, two more slack variables will be introduced in the following theorem.

Theorem 6.2. *Consider the filtering problem for a networked system, as shown in Figure 6.1. Suppose A_f, B_f, L_f and F_f, γ and β are given. The filtering error system in (6.10) is robustly exponentially mean-square stable, and the filter error e_k satisfies the weighted $\mathcal{H}_\infty$ disturbance attenuation level γ if there exist matrices $P = P^{\mathrm{T}} > 0$, $Q = Q^{\mathrm{T}} > 0$, $Z = Z^{\mathrm{T}} > 0$, S_1, S_2, S_3, S_4, V and H such that the following inequality holds*

$$\mathscr{K} = \begin{bmatrix} \Pi_{11} & * & * & * & * & * & * & * & * & * \\ -S_1^{\mathrm{T}} + S_2 R & \Pi_{22} & * & * & * & * & * & * & * & * \\ S_3 R & -S_3 & -\beta\gamma^2 I & * & * & * & * & * & * & * \\ S_4 R & -S_4 & 0 & (\beta-1)\gamma^2 I & * & * & * & * & * & * \\ d_2 S_1^{\mathrm{T}} & d_2 S_2^{\mathrm{T}} & d_2 S_3^{\mathrm{T}} & d_2 S_4^{\mathrm{T}} & -d_2 Z & * & * & * & * & * \\ V\bar{A} & V\bar{A}_d & V\bar{B}_1 & V\bar{B}_2 & 0 & \mathcal{M} & * & * & * & * \\ d_2 HR(\bar{A}-I) & 0 & d_2 HR\bar{B}_1 & 0 & 0 & 0 & d_2\mathcal{Z} & * & * & * \\ \bar{L} & \bar{L}_d & F & -F_f D & 0 & 0 & 0 & -I & * & * \\ 0 & \mathcal{H}_r & 0 & 0 & 0 & 0 & 0 & 0 & \mathcal{H} & * \\ 0 & \mathcal{L}_r & 0 & 0 & 0 & 0 & 0 & 0 & 0 & -I \end{bmatrix} < 0, \tag{6.31}$$

where

$$\begin{aligned} \mathcal{M} &= P - \mathrm{sym}(V), \\ \mathcal{Z} &= Z - \mathrm{sym}(H), \\ \mathcal{H}_r &= [\sigma_1 A_{r,1}^{\mathrm{T}} V, \cdots, \sigma_m A_{r,m}^{\mathrm{T}} V]^{\mathrm{T}}, \\ \mathcal{H} &= \mathrm{diag}\left\{\mathcal{M}, \cdots, \mathcal{M}\right\}. \end{aligned}$$

Proof: By choosing $P = V = V^{\mathrm{T}}$ and $Z = H = H^{\mathrm{T}}$, we can obtain (6.31) from (6.13). On the other hand, if the condition in (6.31) holds, then $V + V^{\mathrm{T}} - P > 0$ and

$H + H^{\mathrm{T}} - Z > 0$. Noting that P and Z are positive-definite, we can confirm that V and H are nonsingular. It implies from the facts $(V-P)P^{-1}(V-P)^{\mathrm{T}} \geq 0$ and $(H-Z)Z^{-1}(H-Z)^{\mathrm{T}} \geq 0$ that $P-V-V^{\mathrm{T}} \geq -VP^{-1}V^{\mathrm{T}}$ and $Z-H-H^{\mathrm{T}} \geq -HZ^{-1}H^{\mathrm{T}}$, respectively. Then, we have

$$\begin{bmatrix}
\Pi_{11} & * & * & * & * & * & * & * & * & * \\
-S_1^{\mathrm{T}} + S_2 R & \Pi_{22} & * & * & * & * & * & * & * & * \\
S_3 R & -S_3 & -\beta\gamma^2 I & * & * & * & * & * & * & * \\
S_4 R & -S_4 & 0 & -(1-\beta)\gamma^2 I & * & * & * & * & * & * \\
d_2 S_1^{\mathrm{T}} & d_2 S_2^{\mathrm{T}} & d_2 S_3^{\mathrm{T}} & d_2 S_4^{\mathrm{T}} & -d_2 Z & * & * & * & * & * \\
V\bar{A} & V\bar{A}_d & V\bar{B}_1 & V\bar{B}_2 & 0 & \mathcal{M}_0 & * & * & * & * \\
d_2 HR(\bar{A}-I) & 0 & d_2 HR\bar{B}_1 & 0 & 0 & 0 & d_2\mathcal{Z}_0 & * & * & * \\
\bar{L} & \bar{L}_d & F & -F_f D & 0 & 0 & 0 & -I & * & * \\
0 & \mathcal{H}_r & 0 & 0 & 0 & 0 & 0 & 0 & \mathcal{H}_0 & * \\
0 & \mathcal{L}_r & 0 & 0 & 0 & 0 & 0 & 0 & 0 & -I
\end{bmatrix} < 0, \tag{6.32}$$

where

$$\begin{aligned}
\mathcal{M}_0 &= -VP^{-1}V^{\mathrm{T}}, \\
\mathcal{Z}_0 &= -HZ^{-1}H^{\mathrm{T}}, \\
\mathcal{H}_0 &= \mathrm{diag}\left\{\mathcal{M}_0, \cdots, \mathcal{M}_0\right\}.
\end{aligned}$$

Performing a congruence transformation $J := \mathrm{diag}\{I,\ I,\ I,\ I,\ I,\ V^{-\mathrm{T}}P,\ H^{-\mathrm{T}}Z,\ I,\ V^{-\mathrm{T}}P,\ \cdots,\ V^{-\mathrm{T}}P,\ I\}$ to (6.32), the inequality in (6.13) is obtained. This completes the proof. □

Remark 6.2. *In Theorem 6.2, two slack variables V and H, not being required to be positive definite, have been introduced to reduce the design conservativeness. The*

introduction of two slack variables can increase the flexibility in determining the matrices, and therefore, leads to less conservative results.

6.4 Robust Weighted $\mathcal{H}_\infty$ Filter Design

Based on the results in Section 6.3, we will propose a method to design the robust weighted $\mathcal{H}_\infty$ filter for the networked system in Figure 6.1.

Theorem 6.3. *Consider the filtering problem for the networked system in Figure 6.1. Suppose* $\Omega_i \in \mathfrak{M}$, $\forall i = 1, \cdots, s$, *are arbitrary, and let* $\gamma > 0$ *and* $0 < \beta < 1$ *be constant scalars. Then, there exists a weighted* $\mathcal{H}_\infty$ *filter in the form of (6.2) which can guarantee that the error system in (6.10) is robustly exponentially mean-square stable, and the filtering error* e_k *satisfies the given weighted* $\mathcal{H}_\infty$ *disturbance attenuation level* γ *for a prescribed weighting factor* β *for all admissible system uncertainties, if there exist matrices* $\tilde{P}_i = \tilde{P}_i^{\mathrm{T}} = \begin{bmatrix} \tilde{P}_{1,i} & \tilde{P}_{2,i} \\ * & \tilde{P}_{3,i} \end{bmatrix} > 0$, $\tilde{V}_i = \begin{bmatrix} \tilde{V}_{1,i} & \tilde{V}_2 \\ \tilde{V}_{3,i} & \tilde{V}_2 \end{bmatrix}$, $Q_i = Q_i^{\mathrm{T}} > 0$, $\tilde{S}_{1,i}$, $S_{2,i}$, $S_{3,i}$, $S_{4,i}$, $Z_i = Z_i^{\mathrm{T}} > 0$, H_i, $\tilde{A}_f$, $\tilde{B}_f$, $\tilde{L}_f$, *and* $\tilde{F}_f$, *such that*

$$\mathscr{M}_{i,j} + \mathscr{M}_{j,i} < 0, \ \forall\ 1 \le i \le j \le s, \tag{6.33}$$

where

$$\mathscr{M}_{i,j} = \begin{bmatrix} \tilde{\Pi}_{11,i} & * & * & * & * & * & * & * & * & * \\ -\tilde{S}_{1,i}^{\mathrm{T}} + S_{2,i}R & \tilde{\Pi}_{22,i} & * & * & * & * & * & * & * & * \\ S_{3,i}R & -S_{3,i} & -\beta\gamma^2 I & * & * & * & * & * & * & * \\ S_{4,i}R & -S_{4,i} & 0 & (\beta-1)\gamma^2 I & * & * & * & * & * & * \\ d_2\tilde{S}_{1,i}^{\mathrm{T}} & d_2 S_{2,i}^{\mathrm{T}} & d_2 S_{3,i}^{\mathrm{T}} & d_2 S_{4,i}^{\mathrm{T}} & -d_2 Z_i & * & * & * & * & * \\ \Upsilon_{1,i,j} & \Upsilon_{2,i} & \Upsilon_{3,i,j} & \Upsilon_{4,i} & 0 & \mathcal{M}_i & * & * & * & * \\ \Upsilon_{5,i,j} & 0 & \Upsilon_{6,i,j} & 0 & 0 & 0 & d_2\mathcal{Z}_i & * & * & * \\ \bar{L}_i & \bar{L}_{d,i} & F_i & -F_f D_i & 0 & 0 & 0 & -I & * & * \\ 0 & \mathcal{H}_{r,i} & 0 & 0 & 0 & 0 & 0 & 0 & \mathcal{H}_i & * \\ 0 & \mathcal{L}_{r,i} & 0 & 0 & 0 & 0 & 0 & 0 & 0 & -I \end{bmatrix},$$

$$\tilde{\Pi}_{11,i} = -\tilde{P}_i + (\bar{d}+2)R^{\mathrm{T}}Q_i R + \mathrm{sym}(\tilde{S}_{1,i}R),$$

$$\tilde{\Pi}_{22,i} = -Q_i - \mathrm{sym}(S_{2,i}),$$

$$\Upsilon_{1,i,j} = \begin{bmatrix} \tilde{V}_{1,i}A_j & \tilde{A}_f \\ \tilde{V}_{3,i}A_j & \tilde{A}_f \end{bmatrix}, \Upsilon_{2,i} = \begin{bmatrix} \tilde{B}_f\Psi C_i \\ \tilde{B}_f\Psi C_i \end{bmatrix},$$

$$\Upsilon_{3,i,j} = \begin{bmatrix} \tilde{V}_{1,i}B_j \\ \tilde{V}_{3,i}B_j \end{bmatrix}, \ \Upsilon_{4,i} = \begin{bmatrix} \tilde{B}_f D_i \\ \tilde{B}_f D_i \end{bmatrix},$$

$$\mathcal{M}_i = \tilde{P}_i - \mathrm{sym}(\tilde{V}_i), \ \mathcal{Z}_i = Z_i - \mathrm{sym}(H_i),$$

$$\Upsilon_{5,i,j} = \begin{bmatrix} d_2 H_i(A_j - I) & 0 \end{bmatrix}, \Upsilon_{6,i,j} = \begin{bmatrix} d_2 H_i B_j \end{bmatrix},$$

$$\bar{L}_i = \begin{bmatrix} L_i & -L_f \end{bmatrix},\ \bar{L}_{d,i} = \begin{bmatrix} -F_f \Psi C_i \end{bmatrix},$$

$$\tilde{A}_{r,t,i} = \begin{bmatrix} \tilde{B}_f \Phi_t C_i \\ \tilde{B}_f \Phi_t C_i \end{bmatrix},$$

$$\mathcal{H}_{r,i} = [\sigma_1 \tilde{A}^{\mathrm{T}}_{r,1,i}, \cdots, \sigma_m \tilde{A}^{\mathrm{T}}_{r,m,i}]^{\mathrm{T}},$$

$$\mathcal{H}_i = \mathrm{diag}(\mathcal{M}_i, \cdots, \mathcal{M}_i),\ L_{r,t,i} = [-F_f \Phi_t C_i],$$

$$\mathcal{L}_{r,i} = [\sigma_1 L^{\mathrm{T}}_{r,1,i}, \cdots, \sigma_m L^{\mathrm{T}}_{r,m,i}]^{\mathrm{T}},\ \forall\ t = 1,\ \cdots,\ m.$$

Furthermore, the parameters for the filter in (6.2) are determined as follows:

$$A_f = \tilde{V}_2^{-1} \tilde{A}_f,\ B_f = \tilde{V}_2^{-1} \tilde{B}_f,\ L_f = \tilde{L}_f,\ \textit{and}\ F_f = \tilde{F}_f. \tag{6.34}$$

Proof: Suppose that there exist matrices $P > 0$, $Q > 0$, $Z > 0$, S_1, S_2, S_3, S_4, V and H such that the condition in (6.31) holds. Then, the filtering error system is robustly exponentially stable with a weighted $\mathcal{H}_\infty$ attenuation level γ and with a prescribed weighting factor β. The $(6,6)$ block of $\mathscr{K}$ implies that $P - V - V^{\mathrm{T}}$ is negative-definite. Since P is positive-definite, the matrix V is a nonsingular matrix. Without loss of generality, we introduce the partition $V = \begin{bmatrix} V_1 & V_2 \\ V_3 & V_4 \end{bmatrix}$ and assume that V_2 is nonsingular. Observe that V_4 is invertible. Thus the product $V_2 V_4^{-1}$ is nonsingular. Define $J_1 = \begin{bmatrix} I & 0 \\ 0 & V_4^{-\mathrm{T}} V_2^{\mathrm{T}} \end{bmatrix}$ and $J_2 = \{J_1, I, I, I, I, J_1, I, I, J_1, \cdots, J_1, I, \cdots, I\}$. Then, performing congruence transformation to $\mathscr{K}$ in (6.31) by J_2 and introducing the following new variables:

$$\tilde{V} = \begin{bmatrix} \tilde{V}_1 & \tilde{V}_2 \\ \tilde{V}_3 & \tilde{V}_2 \end{bmatrix} = J_1^{\mathrm{T}} V J_1,\ \tilde{P} = \begin{bmatrix} \tilde{P}_1 & \tilde{P}_2 \\ * & \tilde{P}_3 \end{bmatrix} = J_1^{\mathrm{T}} P J_1 > 0,$$

$$\tilde{S}_1 = J_1^{\mathrm{T}} S_1,\ \tilde{A}_f = V_2 A_f V_4^{-\mathrm{T}} V_2^{\mathrm{T}},\ \tilde{B}_f = V_2 B_f,\ \tilde{L}_f = L_f V_4^{-\mathrm{T}} V_2^{\mathrm{T}},\ \text{and}\ \tilde{F}_f = F_f,$$

we obtain

$$\mathscr{M} = \begin{bmatrix} \tilde{\Pi}_{11} & * & * & * & * & * & * & * & * & * \\ -\tilde{S}_1^{\mathrm{T}} + S_2 R & \tilde{\Pi}_{22} & * & * & * & * & * & * & * & * \\ S_3 R & -S_{3,i} & -\beta\gamma^2 I & * & * & * & * & * & * & * \\ S_4 R & -S_4 & 0 & -(1-\beta)\gamma^2 I & * & * & * & * & * & * \\ d_2\tilde{S}_1^{\mathrm{T}} & d_2 S_2^{\mathrm{T}} & d_2 S_3^{\mathrm{T}} & d_2 S_4^{\mathrm{T}} & -d_2 Z & * & * & * & * & * \\ \Upsilon_1 & \Upsilon_2 & \Upsilon_3 & \Upsilon_4 & 0 & \mathcal{M} & * & * & * & * \\ \Upsilon_5 & 0 & \Upsilon_6 & 0 & 0 & 0 & d_2\mathcal{Z} & * & * & * \\ \bar{L} & \bar{L}_d & F & -F_f D & 0 & 0 & 0 & -I & * & * \\ 0 & \mathcal{H}_r & 0 & 0 & 0 & 0 & 0 & 0 & \mathcal{H} & * \\ 0 & \mathcal{L}_r & 0 & 0 & 0 & 0 & 0 & 0 & 0 & -I \end{bmatrix} < 0, \tag{6.35}$$

where

$$\begin{aligned}
&\tilde{\Pi}_{11} = -\tilde{P} + (\bar{d}+2)R^{\mathrm{T}}QR + \mathrm{sym}(\tilde{S}_1 R), \\
&\tilde{\Pi}_{22} = -Q - \mathrm{sym}(S_2), \\
&\Upsilon_1 = \begin{bmatrix} \tilde{V}_1 A & \tilde{A}_f \\ \tilde{V}_3 A & \tilde{A}_f \end{bmatrix}, \Upsilon_2 = \begin{bmatrix} \tilde{B}_f \Psi C \\ \tilde{B}_f \Psi C \end{bmatrix}, \\
&\Upsilon_3 = \begin{bmatrix} \tilde{V}_1 B \\ \tilde{V}_3 B \end{bmatrix}, \ \Upsilon_4 = \begin{bmatrix} \tilde{B}_f D \\ \tilde{B}_f D \end{bmatrix}, \\
&\mathcal{M} = \tilde{P} - \mathrm{sym}(\tilde{V}), \ \mathcal{Z} = Z - \mathrm{sym}(H), \\
&\Upsilon_5 = \begin{bmatrix} d_2 H(A-I) & 0 \end{bmatrix}, \Upsilon_6 = \begin{bmatrix} d_2 HB \end{bmatrix}, \\
&\bar{L} = \begin{bmatrix} L & -L_f \end{bmatrix}, \ \bar{L}_d = \begin{bmatrix} -F_f \Psi C \end{bmatrix},
\end{aligned}$$

$$\tilde{A}_{r,t} = \begin{bmatrix} \tilde{B}_f \Phi_t C \\ \tilde{B}_f \Phi_t C \end{bmatrix},$$

$$\mathcal{H}_r = [\sigma_1 \tilde{A}_{r,1}^{\mathrm{T}}, \cdots, \sigma_m \tilde{A}_{r,m}^{\mathrm{T}}]^{\mathrm{T}},$$

$$\mathcal{H} = \mathrm{diag}(\mathcal{M}, \cdots, \mathcal{M}),\ L_{r,t} = [-F_f \Phi_t C],$$

$$\mathcal{L}_r = [\sigma_1 L_{r,1}^{\mathrm{T}}, \cdots, \sigma_m L_{r,m}^{\mathrm{T}}]^{\mathrm{T}},\ \forall\ t = 1,\ \cdots,\ m.$$

Note that the system matrices in (6.35) are subject to system uncertainties and $\mathscr{M} < 0$ is not an LMI. In order to convert $\mathscr{M} < 0$ into a set of LMIs, we further assume that

$$\tilde{P} = \sum_{i=1}^{s} \alpha_i \tilde{P}_i = \sum_{i=1}^{s} \alpha_i \begin{bmatrix} \tilde{P}_{1,i} & \tilde{P}_{2,i} \\ * & \tilde{P}_{3,i} \end{bmatrix},\ Q = \sum_{i=1}^{s} \alpha_i Q_i,\ Z = \sum_{i=1}^{s} \alpha_i Z_i,$$

$$\tilde{S}_1 = \sum_{i=1}^{s} \alpha_i \tilde{S}_{1,i},\ S_l = \sum_{i=1}^{s} \alpha_i S_{l,i},\ H = \sum_{i=1}^{s} \alpha_i H_i,\ \tilde{V} = \sum_{i=1}^{s} \alpha_i \tilde{V}_i = \begin{bmatrix} \tilde{V}_{1,i} & \tilde{V}_2 \\ \tilde{V}_{3,i} & \tilde{V}_2 \end{bmatrix},$$

$\forall\ i = 1, \cdots, s,\ l = 2,\ 3,\ 4.$

Now, observe that, under the above assumptions, $\mathscr{M}$ can be rewritten as

$$\mathscr{M} = \sum_{i=1}^{s} \sum_{j=1}^{s} \alpha_i \alpha_j \mathscr{M}_{i,j} = \sum_{i=1}^{s} \alpha_i^2 \mathscr{M}_{i,i} + \sum_{i=1}^{s-1} \sum_{j=i+1}^{s} \alpha_i \alpha_j \left(\mathscr{M}_{i,j} + \mathscr{M}_{j,i} \right).$$

Thus, we can conclude that if $\mathscr{M}_{i,j} + \mathscr{M}_{j,i} < 0,\ \forall\ 1 \leq i \leq j \leq s$, $\mathscr{M}$ is negative-definite. According to Theorem 6.2, the filtering error system is robustly exponentially mean-square stable with a weighted $\mathcal{H}_\infty$ attenuation γ and a weighting factor β.

On the other hand, V_2 is assumed to be nonsingular. Meanwhile, the condition $\tilde{P}_3 = V_2 V_4^{-1} P_3 V_4^{-\mathrm{T}} V_2^{\mathrm{T}} > 0$ implies that V_2 is an invertible matrix. Further, it is noted

that the parameters of the filter satisfy the following equation

$$\begin{bmatrix} A_f & B_f \\ L_f & F_f \end{bmatrix} = \begin{bmatrix} V_2^{-1} & 0 \\ 0 & I \end{bmatrix} \begin{bmatrix} \tilde{A}_f & \tilde{B}_f \\ \tilde{L}_f & \tilde{F}_f \end{bmatrix} \begin{bmatrix} V_2^{-\mathrm{T}} V_4^{\mathrm{T}} & 0 \\ 0 & I \end{bmatrix}.$$

The discrete-time transfer function from $\hat{y}_k$ to $\hat{z}_k$ is represented by

$$\begin{aligned} T_{\hat{z}\hat{y}} &= L_f \left(zI - A_f\right)^{-1} B_f + F_f \\ &= \tilde{L}_f \left(zI - \tilde{V}_2^{-1}\tilde{A}_f\right)^{-1} \tilde{V}_2^{-1}\tilde{B}_f + \tilde{F}_f. \end{aligned} \tag{6.36}$$

Therefore, the parameters of the filter are given by

$$A_f = \tilde{V}_2^{-1}\tilde{A}_f,\ B_f = \tilde{V}_2^{-1}\tilde{B}_f,\ L_f = \tilde{L}_f, \text{ and } F_f = \tilde{F}_f.$$

The proof is completed. □

Remark 6.3. *In this chapter, to make full use of the delayed information, we establish the weighted $\mathcal{H}_\infty$ criterion (Definition 2) for the filtering system design. When the scalar β is set as* 0.5 *in Theorem 6.1 and Theorem 6.3, the criterion in Theorem 6.1 is equivalent to the $\mathcal{H}_\infty$ filtering, and the filter design method in Theorem 6.3 is the same as the $\mathcal{H}_\infty$ filter design. In this sense, the proposed weighted H_∞ filtering is more general in terms of two aspects: (1) It can explicitly employ the delayed noise term into the filtering performance analysis and the corresponding robust weighted $\mathcal{H}_\infty$ filter design; (2) the well established $\mathcal{H}_\infty$ filtering for networked systems can be regarded as a special case by fixing $\beta = 0.5$. The introduction of the constant β increases the flexible dimensions in the solution space for the $\mathcal{H}_\infty$ optimization.*

Corollary 6.1. *The minimal weighted $\mathcal{H}_\infty$ attenuation level γ with a prescribed*

weighting factor β in Theorem 6.3 can be derived by solving the optimization problem:

$$\min_{\tilde{P}_i,\tilde{Q}_i,\tilde{Z}_i,\tilde{V}_i,\tilde{H},\tilde{S}_{1,i},\tilde{S}_{2,i},\tilde{S}_{3,i},\tilde{S}_{4,i}} \gamma^2.$$

$$s.\ t. \ (6.33)$$

6.5 Numerical Examples

In this section, numerical examples are provided to show the effectiveness of the proposed method.

Example 6.1: Consider a networked system in (6.1) with system matrices as follow:

$$A = \begin{bmatrix} 0.7+\delta & 0 \\ 0 & 0.8 \end{bmatrix},\ B = \begin{bmatrix} 0.8 & 1 \\ 0.3 & 0.9 \end{bmatrix},$$
$$C = \begin{bmatrix} 1 & 0.3 \\ 0.5 & 0.1 \end{bmatrix},\ D = \begin{bmatrix} 1 & 0.5 \\ 0.4 & 0.8 \end{bmatrix},$$
$$L = \begin{bmatrix} 1 & 2 \\ 1 & 0.6 \end{bmatrix},\ F = \begin{bmatrix} 0.1 & -0.2 \\ 0.1 & 0.05 \end{bmatrix}.$$

Here, δ denotes the uncertainty in the system plant and it satisfies $|\delta| \leq 0.2$.

It is assumed that the bounds of network-induced delays are given by $d_1 = 1$, and $d_2 = 3$. In addition, we assume that the expectations of successful measurements for outputs are 0.9 and 0.8, that is, $\Psi = \begin{bmatrix} 0.9 & 0 \\ 0 & 0.8 \end{bmatrix}$. According to Corollary 6.1 and by using MATLAB LMI Toolbox, we obtain the relationship between the minimal γ and the weighting factor β, as shown in Figure 6.2.

It is observe that for $\beta \in [0.85,\ 0.95]$, smaller optimal γ is achieved for a larger β. Then we choose $\beta = 0.9$, and the determined parameters for the robust weighted $\mathcal{H}_\infty$ filter can be designed as follows:

$$A_f = \begin{bmatrix} 0.4443 & -0.8806 \\ -0.0773 & 0.2420 \end{bmatrix},\ B_f = \begin{bmatrix} -0.1697 & -0.1478 \\ -0.0363 & -0.1602 \end{bmatrix},$$
$$L_f = \begin{bmatrix} -0.1230 & -0.8212 \\ -0.4259 & 0.2197 \end{bmatrix},\ F_f = \begin{bmatrix} 0.3286 & 1.2806 \\ 0.2696 & 0.7803 \end{bmatrix}.$$

In order to illustrate the performance of the designed filter, we further assume that the initial states of the plant are equal to zeros and select the external input as $\begin{bmatrix} 1/(k+10) \\ 1/(k+10) \end{bmatrix}$, where k is the sampling instant. In the simulations, the influence of the inserted network d_k is generated randomly. For the first component of the output, the expectation of the complete measurements is 0.9, that is, the ratio of the incomplete measurements is 10%. For the second component of the output, the expectation of the complete measurements is 0.8 and the incomplete measurements also occur randomly. Figure 6.3 and Figure 6.4 depict the estimated signal, from which we can see that the designed filter can estimate the states well, even though the received measurements are *incomplete* due to the network transmission.

Example 6.2: Consider a networked system in the form of (6.1) with the following system matrices:

$$A = \begin{bmatrix} 0 & -0.5 \\ 1 & 1+\delta \end{bmatrix},\ B = \begin{bmatrix} -6 & 0 \\ 1 & 0 \end{bmatrix},$$
$$C = \begin{bmatrix} -100 & 10 \\ 100 & -5 \end{bmatrix},\ D = \begin{bmatrix} 0 & 1 \\ 1 & 0.1 \end{bmatrix},$$
$$L = \begin{bmatrix} 1 & 0 \\ 1 & 2 \end{bmatrix},\ F = \begin{bmatrix} 0 & 0 \\ 0 & 0 \end{bmatrix},$$

where $|\delta| \leq 0.45$. Note that the uncertain system can be described by a two-vertex polytope. Further, it is assumed that the bounds of network-induced delays are given by $d_1 = 1$, and $d_2 = 5$, the expectations of successful measurements for outputs are 0.9 and 0.95, that is, $\Psi = \begin{bmatrix} 0.9 & 0 \\ 0 & 0.95 \end{bmatrix}$.

In terms of Corollary 6.1, when the weighting factor β is equal to 0.9, the derived parameters of the designed filter are as follow:

$$A_f = \begin{bmatrix} -0.1038 & -0.1179 \\ 0.8288 & 0.6037 \end{bmatrix},\ B_f = \begin{bmatrix} 0.0067 & 0.0014 \\ -0.0133 & -0.0054 \end{bmatrix},$$
$$L_f = \begin{bmatrix} -0.8331 & -0.2744 \\ -1.5799 & -1.6311 \end{bmatrix},\ F_f = \begin{bmatrix} -0.0058 & -0.0013 \\ 0.0194 & 0.0110 \end{bmatrix}.$$

6.6 Conclusions

We have studied the filter design problem for networked systems with multiple sensor faults. It is assumed that the outputs of the plant are measured by multiple separated sensors with incomplete measurements due to the potential sensor faults. The

measured data is transmitted to the filter via a network medium and is simultaneously subject to network-induced delays, missing packets and mixed order of packets. Since the delayed and non-delayed noise terms are both incorporated into the filtering error system, in order to explicitly account for the delayed noise term and to achieve better filtering performance, we proposed to define the weighted $\mathcal{H}_\infty$ performance index. Further, we developed the robust weighted $\mathcal{H}_\infty$ filter design method. Numerical simulations illustrated the usefulness of the proposed filter design method.

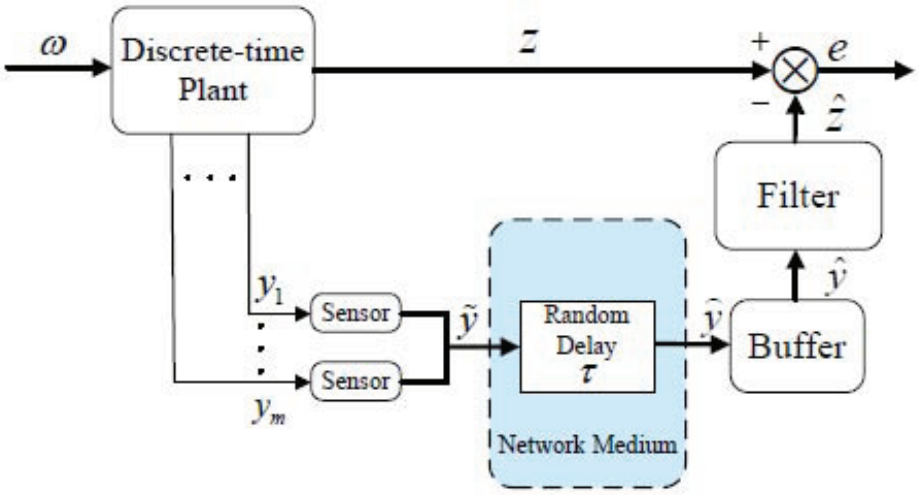

Figure 6.1: A typical filtering problem for a networked system with incomplete measurements, network-induced delays, and missing packets.

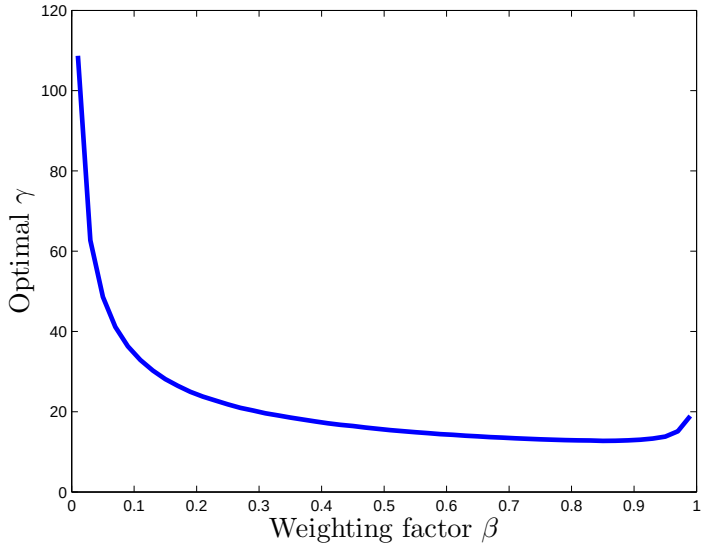

Figure 6.2: The relationship between the optimal γ and the weighting factor β.

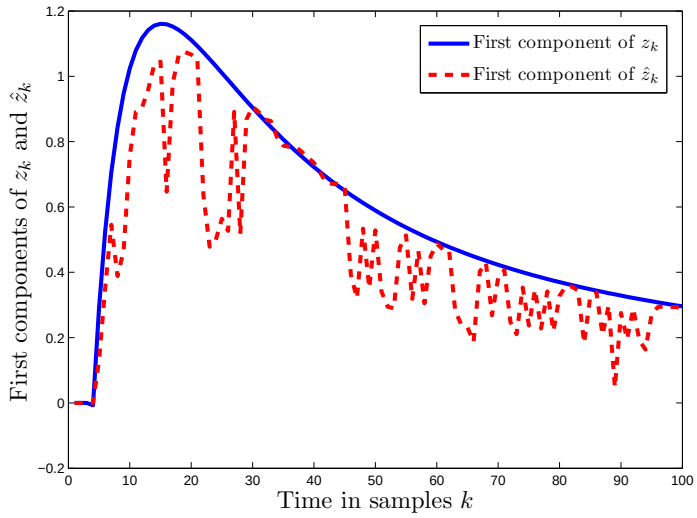

Figure 6.3: The first component of the estimated signal.

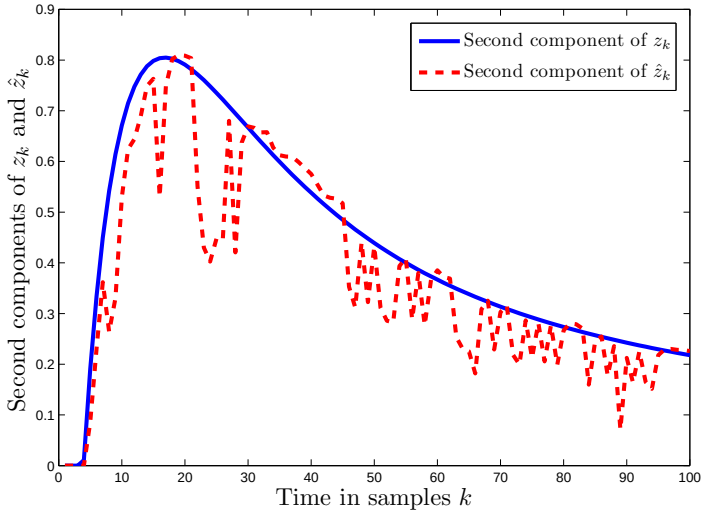

Figure 6.4: The second component of the estimated signal.

Chapter 7

$\mathcal{H}_\infty$ Switched Filtering for Networked Systems Based on Delay Occurrence Probabilities

7.1 Introduction

An estimator plays an important role in the filtering of the states for the synthesis or fault diagnosis, when system states of a system are unknown, but the outputs of the system are measurable. In a network environment, the estimation problem has stirred much research interest. The authors in [189] studied the filtering problem for network-based systems subject to Markov delays. Robust $\mathcal{H}_\infty$ estimation for networked systems with multiple state delays under the discrete-time framework was investigated in [190]. The measurement quantization, network-induced delay, and packet dropout were considered in the estimation problem [131]. Optimal $\mathcal{H}_\infty$ and $\mathcal{H}_2$ estimation for networked systems with multiple packet dropouts were exploited in [58] and [53], respectively. In [191], multiple-step measurement delays and multiple

packet dropouts were considered. Although the existing works have addressed the important issues in the estimation problem for networked systems, it is desirable to reduce the conservativeness and enhance the filtering performance.

Consider a stable discrete-time system represented by

$$\begin{aligned} x_{k+1} &= Ax_k + B\omega_k, \\ v_k &= Cx_k + D\omega_k, \\ z_k &= Ex_k, \end{aligned} \tag{7.1}$$

where $x_k \in \mathbb{R}^n$ is the state vector of the system, $y_k \in \mathbb{R}^p$ is the system output, $z_k \in \mathbb{R}^q$ is a combination of the system state, and $\omega_k \in \mathbb{R}^m$ is the external noise. A, B, C and D are system matrices with appropriate dimensions.

The state estimation problem in a network environment with a limited communication capacity is illustrated in Figure 7.1. The system output is sampled and

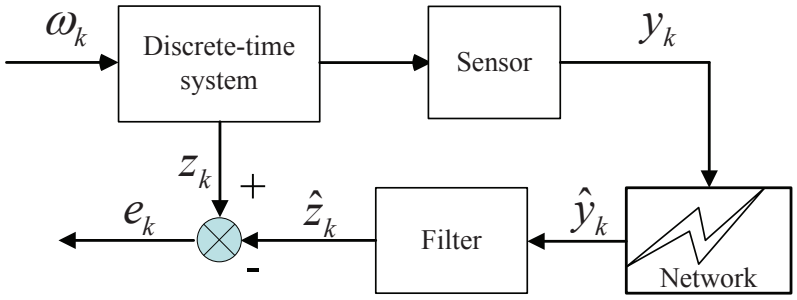

Figure 7.1: State estimation for a discrete-time system in a network environment.

transmitted over a network link. Due to the network-induced delay, the received signal at the filter node is

$$\hat{y}_k = y_{k-d(k)}, \tag{7.2}$$

where $d(k)$ is time-varying but takes a value from a set:

$$\mathscr{D} := [d_1, \cdots, d_i, \cdots, d_s], 0 < d_1 < \cdots < d_i < \cdots d_s.$$

Now define an indicator function

$$\alpha(k) = [\alpha_1(k), \cdots, \alpha_i(k), \cdots, \alpha_s(k)]^{\mathrm{T}}.$$

Note that, when the variable $\alpha_i(k)$ is equal to 1, the network-induced delay is d_i, $\forall\ i = 1, \cdots, s$. Suppose that the probability of $\alpha_i = 1$ is denoted by β_i, i.e.,

$$\begin{aligned} \text{Prob}\{\alpha_i = 1\} &= \beta_i, \\ \text{Prob}\{\alpha_i = 0\} &= 1 - \beta_i. \end{aligned} \tag{7.3}$$

An augmented discrete-time system incorporating the network-induced delays is represented by

$$\begin{aligned} \bar{x}_{k+1} &= \bar{A}\bar{x}_k + \bar{B}\omega_k, \\ \hat{y}_k &= \sum_{i=1}^{s} \alpha_i(k)\bar{C}_i\bar{x}_k, \\ z_k &= \bar{L}\bar{x}_k, \end{aligned} \tag{7.4}$$

where

$$\bar{x}_k = \begin{bmatrix} x_k \\ y_{k-1} \\ \vdots \\ y_{k-d_s} \end{bmatrix} \in \mathbb{R}^{n+d_s p},\ \bar{B} = \begin{bmatrix} B \\ D \\ \vdots \\ 0 \end{bmatrix} \in \mathbb{R}^{(n+d_s p)\times m},$$

$$\bar{A} = \begin{bmatrix} A & 0 & \cdots & 0 & 0 \\ C & 0 & \cdots & 0 & 0 \\ \vdots & \vdots & \ddots & \vdots & \vdots \\ 0 & 0 & \cdots & I & 0 \end{bmatrix} \in \mathbb{R}^{(n+d_s p)\times(n+d_s p)},$$

$$\bar{L} = L[I\ 0\ \cdots\ 0],\ \bar{C}_i = [0\ 0\ \cdots \underbrace{I}_{(d_i+1)^{th}\text{block}} \cdots 0].$$

Since the delay is detectable at the estimator node, we propose to design a sequence of delay-dependent full-order estimators taking the following form:

$$\begin{aligned} \hat{x}_{k+1} &= \sum_{i=1}^{s} \alpha_i(k) A_{fi}\hat{x}_k + \sum_{i=1}^{s} \alpha_i(k) B_{fi}\hat{y}_k, \\ \hat{z}_k &= \sum_{i=1}^{s} \alpha_i(k) C_{fi}\hat{x}_k + \sum_{i=1}^{s} \alpha_i(k) D_{fi}\hat{y}_k, \end{aligned} \tag{7.5}$$

where A_{fi}, B_{fi}, C_{fi}, and D_{fi}, $\forall\, i = 1, \cdots, s$, which are the estimators' system matrices to be designed. When the delay $d(k)$ is d_i, the implemented estimator will have the parameters: A_{fi}, B_{fi}, C_{fi}, and D_{fi}. Defining the estimation error as $e_k := z_k - \hat{z}_k$, we obtain the estimation error system as:

$$\begin{aligned} \underline{x}_{k+1} &= \underline{A}\underline{x}_k + \underline{B}\omega_k, \\ e_k &= \underline{L}\underline{x}_k, \end{aligned} \tag{7.6}$$

where

$$\underline{x}_k = \begin{bmatrix} \bar{x}_k \\ \hat{x}_k \end{bmatrix} \in \mathbb{R}^{2n+d_s p},\ \underline{B} = \begin{bmatrix} \bar{B} \\ 0 \end{bmatrix} \in \mathbb{R}^{(2n+d_s p)\times m},$$

$$\underline{A} = \sum_{i=1}^{s} \alpha_i(k) \begin{bmatrix} \bar{A} & 0 \\ B_{fi}\bar{C}_i & A_{fi} \end{bmatrix} \in \mathbb{R}^{(2n+d_s p)\times(2n+d_s p)},$$

$$\underline{L} = \sum_{i=1}^{s} \alpha_i(k)[\bar{L} - D_{fi}\bar{C}_i,\ -C_{fi}] \in \mathbb{R}^{q\times(2n+d_s p)}.$$

The main objective is to design estimators such that the estimation error system is exponentially mean-square stable with an $\mathcal{H}_\infty$ attenuation level γ.

7.2 $\mathcal{H}_\infty$ Switched Filter Design

In the following, we first study the stability of the filtering error system, and then propose the design method of the robust $\mathcal{H}_\infty$ estimator.

7.2.1 Stability and $\mathcal{H}_\infty$ Performance Analysis

Theorem 7.1. *Consider the discrete-time system in (7.1). Assuming that the delay-dependent estimators's system matrices and the performance index γ are known, the estimation error system in (7.6) is exponentially mean-square stable with an $\mathcal{H}_\infty$ attenuation level γ, if there exists a matrix $P = P^{\mathrm{T}} > 0$ such that the following condition is achieved:*

$$\begin{bmatrix} \Xi_1 & \Xi_2 & \Xi_3 & 0 \\ * & -P & 0 & \Xi_4 \\ * & * & -I & 0 \\ * & * & * & -\gamma^2 I \end{bmatrix} < 0, \tag{7.7}$$

where

$$\Xi_1 = \begin{bmatrix} -P & 0 & \cdots & 0 \\ * & -P & \cdots & 0 \\ * & * & \ddots & 0 \\ * & * & * & -P \end{bmatrix},\ \Xi_2 = \begin{bmatrix} \sqrt{\beta_1}\underline{A}_1 \\ \sqrt{\beta_2}\underline{A}_2 \\ \vdots \\ \sqrt{\beta_s}\underline{A}_s \end{bmatrix},$$

$$\Xi_3 = \begin{bmatrix} \sqrt{\beta_1}\underline{B} \\ \sqrt{\beta_2}\underline{B} \\ \vdots \\ \sqrt{\beta_s}\underline{B} \end{bmatrix},\ \Xi_4 = \begin{bmatrix} \sqrt{\beta_1}\underline{L}_1^{\mathrm{T}} & \sqrt{\beta_2}\underline{L}_2^{\mathrm{T}} & \cdots & \sqrt{\beta_s}\underline{L}_s^{\mathrm{T}} \end{bmatrix},$$

$$\underline{A}_i = \begin{bmatrix} \bar{A} & 0 \\ B_{fi}C_i & A_{fi} \end{bmatrix},\ \underline{L}_i = [\bar{L} - D_{fi}C_i,\ -C_{fi}],\ i \in [1,\ s].$$

Proof: Consider a Lyapunov function for the filtering error system (7.6) as

$$V(\underline{x}_k) = \underline{x}_k^{\mathrm{T}} P \underline{x}_k. \tag{7.8}$$

It follows from [192] that we need to prove, if the condition in Theorem 7.1 holds, then the following condition is fulfilled $\forall k > 0$

$$\mathcal{J} = \Delta V(\underline{x}_k) + \mathcal{E}\{e_k^{\mathrm{T}} e_k\} - \gamma^2 \omega_k^{\mathrm{T}} \omega_k < 0, \tag{7.9}$$

where

$$\Delta V(\underline{x}_k) := \mathcal{E}\{V(\underline{x}_{k+1}) | \underline{x}_k\} - V(\underline{x}_k). \tag{7.10}$$

Recalling the state-space model of (7.6), we have

$$\mathcal{J} = \begin{bmatrix} \underline{x}_k \\ \omega_k \end{bmatrix}^{\mathrm{T}} \begin{bmatrix} \Omega_{11} & \Omega_{12} \\ * & \Omega_{22} \end{bmatrix} \begin{bmatrix} \underline{x}_k \\ \omega_k \end{bmatrix}, \tag{7.11}$$

where

$$\begin{aligned} \Omega_{11} &= \sum_{i=1}^{s} \beta_i \underline{A}_i^{\mathrm{T}} P \underline{A}_i - P, \\ \Omega_{12} &= \sum_{i=1}^{s} \beta_i \underline{A}_i^{\mathrm{T}} P \underline{B}, \\ \Omega_{22} &= \sum_{i=1}^{s} \beta_i \underline{L}_i^{\mathrm{T}} \underline{L}_i + \underline{B}^{\mathrm{T}} \underline{B} - \gamma^2 I. \end{aligned} \tag{7.12}$$

Using the Schur compliment, the matrix inequality (7.7) ensures that $\mathcal{J} < 0$, and this completes the proof. □

In this subsection, the stability and the $\mathcal{H}_\infty$ performance of the filtering error system is studied. In the following, we will propose the design method for the delay-dependent switching estimators.

7.2.2 Filter Design via LMIs

Theorem 7.2. *Consider the discrete-time system in (7.1). Assuming that the performance index γ and a constant λ are given, the filtering error system in (7.6) is exponentially mean-square stable with an $\mathcal{H}_\infty$ attenuation level γ, if there exist matrices $P = P^{\mathrm{T}} = \begin{bmatrix} P_{11} & \lambda H P_{22} \\ * & P_{22} \end{bmatrix} > 0$, and $\left[\begin{array}{c|c} A_{Fi} & B_{Fi} \\ \hline C_{fi} & D_{fi} \end{array}\right]$ such that the following*

condition is satisfied:

$$\begin{bmatrix} \Xi_1 & \hat{\Xi}_2 & \hat{\Xi}_3 & 0 \\ * & -P & 0 & \Xi_4 \\ * & * & -I & 0 \\ * & * & * & -\gamma^2 I \end{bmatrix} < 0, \tag{7.13}$$

where

$$P_{11} \in \mathbb{R}^{(n+d_s p)\times(n+d_s p)},\ P_{22} \in \mathbb{R}^{n\times n},$$

$$\hat{\Xi}_2 = \begin{bmatrix} \sqrt{\beta_1}\hat{A}_1 \\ \sqrt{\beta_2}\hat{A}_2 \\ \vdots \\ \sqrt{\beta_s}\hat{A}_s \end{bmatrix},\ \hat{\Xi}_3 = \begin{bmatrix} \sqrt{\beta_1}\hat{B} \\ \sqrt{\beta_2}\hat{B} \\ \vdots \\ \sqrt{\beta_s}\hat{B} \end{bmatrix},$$

$$\hat{A}_i = \begin{bmatrix} P_{11}\bar{A} + \lambda H B_{Fi} C_i & \lambda H A_{Fi} \\ \lambda P_{22}^{\mathrm{T}} H^{\mathrm{T}} \bar{A} + B_{Fi} C_i & A_{Fi} \end{bmatrix},$$

$$\hat{B}_i = \begin{bmatrix} P_{11}\bar{B} \\ \lambda P_{22}^{\mathrm{T}} H^{\mathrm{T}} \bar{B} \end{bmatrix},$$

$$H = [I_{n\times n}\ 0 \cdots\ 0] \in \mathbb{R}^{n\times(n+d_s p)},\ i = 1, \cdots, s.$$

Moreover, the parameters C_{fi} and D_{fi} of the estimators can be obtained from the solution set of the LMI (7.13), and A_{fi} and B_{fi} can be computed by

$$A_{fi} = P_{22}^{-1} A_{Fi},\ B_{fi} = P_{22}^{-1} B_{Fi}.$$

Proof: Assume that the Lyapunov matrix P has a special form as

$$P = \begin{bmatrix} P_{11} & \lambda H P_{22} \\ * & P_{22} \end{bmatrix}. \tag{7.14}$$

By recalling the forms of $\underline{A}_i, \underline{B}_i$ and introducing two new variables $A_{Fi} = P_{22}A_{fi}$ and $B_{Fi} = P_{22}B_{fi}$, the matrix inequality (7.7) is equivalent to the linear matrix inequality (7.13). Moreover, if Condition (7.13) holds, then variable P_{22} will be nonsingular. Thus, the parameters of the estimators can be computed by

$$A_{fi} = P_{22}^{-1}A_{Fi},\ B_{fi} = P_{22}^{-1}B_{Fi}. \tag{7.15}$$

This completes the proof. □

In Theorem 7.2, the $\mathcal{H}_\infty$ attenuation level γ is assumed to be given. It is inferred from **Definition 2** that a smaller γ would result in a smaller expected filtering error. A suboptimal value for γ can be obtained by the following corollary.

Corollary 7.1. *The suboptimal $\mathcal{H}_\infty$ performance index γ for the state estimation problem can be found by solving the following convex optimization problem:*

$$\begin{aligned} &\min \gamma^2, \\ &s.\ t.\ \ (7.13) \end{aligned}$$

$\forall\ i = 1, \cdots, s$, *for a given* λ.

Remark 7.1. *Note that the condition in Theorem 7.2 is expressed in terms of an LMI. Moreover, the suboptimal γ may be different for different given λ. An optimal value for λ can be derived by using the linear search method.*

7.3 Numerical Example

Consider the following discrete-time system in (7.1) which has been studied in [189],

$$A = \begin{bmatrix} 0.2 & 0.05 \\ -0.02 & 0.3 \end{bmatrix},\ B = \begin{bmatrix} 0.1 \\ -0.2 \end{bmatrix},$$
$$C = \begin{bmatrix} 0.5 & -0.7 \end{bmatrix},\ D = 0.3,\ L = \begin{bmatrix} 1 & 0.6 \end{bmatrix}. \tag{7.16}$$

Note that in our work the minimum delay is assumed to be greater than zero. This is generally the case in a network environment. However, the minimum delay in [189] is zero. In order to compare our results with those in the above mentioned paper, we find the occurrence probability for a system in which the delay of zero and the delay of one is lumped as a single state with a delay of 1. Thus the following two tasks are tested for the purpose of comparison.

Task 1 Estimate the combination of the states z_k determined by (7.16). Assume that the network-induced delay is in the finite set [0, 2] and satisfies a Markov chain with the transition matrix given in [189]:

$$\Gamma = \begin{bmatrix} 0.5 & 0.25 & 0.25 \\ 0.4 & 0.2 & 0.4 \\ 0.58 & 0.14 & 0.28 \end{bmatrix}. \tag{7.17}$$

Task 2 Estimate the combination of the states z_k determined by (7.16). The network-induced delay is in the finite set [1, 2]. In addition, the occurrence probability for $d(k) = 1$ is 0.7101 and the occurrence probability for $d(k) = 2$ is 0.2899.

According to the transition matrix (7.17), the occurrence probabilities of the delays 0, 1, and 2 in Task 1 are 0.5024, 0.2077, and 0.2899, respectively. Note that the

occurrence probability of $d(k) = 1$ in Task 2 is the sum of the occurrence probabilities of $d(k) = 0$ and 1 in Task 1. It can be seen from Table 1 that by using the

Table 7.1: Suboptimal $\mathcal{H}_\infty$ performance indexes in different tasks

Task	γ
Task 1 using method in [189]	0.3
Task 2 using Corollary 1	0.0144 ($\lambda = 1$)
Task 2 using Corollary 1	0.0188 ($\lambda = 0$)

design method in this chapter, the suboptimal $\mathcal{H}_\infty$ attenuation level γ in Task 2 is significantly lower than the level in Task 1 using the design method in [189].

When the value for λ is equal to 1, the parameters of the designed estimators are

$$A_{f1} = \begin{bmatrix} 0.8774 & 0.3829 \\ -1.9704 & -0.8631 \end{bmatrix}, \; B_{f1} = \begin{bmatrix} -0.0320 \\ 0.2000 \end{bmatrix},$$
$$C_{f1} = \begin{bmatrix} -0.6684 & -0.3232 \end{bmatrix}, \; D_{f1} = \begin{bmatrix} -0.0757 \end{bmatrix},$$

$$A_{f2} = \begin{bmatrix} 0.7327 & 0.2634 \\ -1.8705 & -0.5487 \end{bmatrix}, \; B_{f2} = \begin{bmatrix} 0.0003 \\ 0.0560 \end{bmatrix},$$
$$C_{f2} = \begin{bmatrix} 0.0958 & -0.0112 \end{bmatrix}, \; D_{f2} = \begin{bmatrix} -0.0790 \end{bmatrix}.$$

Suppose that the external noise ω_k is a gaussian white noise with the mean value of zero and the covariance of one. Figure 7.2 depicts the estimation performance of the designed estimators. It can be seen from Figure 7.2 that although the system is subject to the network-induced delays, using the designed estimators the variable $\hat{z}_k$ tracks z_k pretty well.

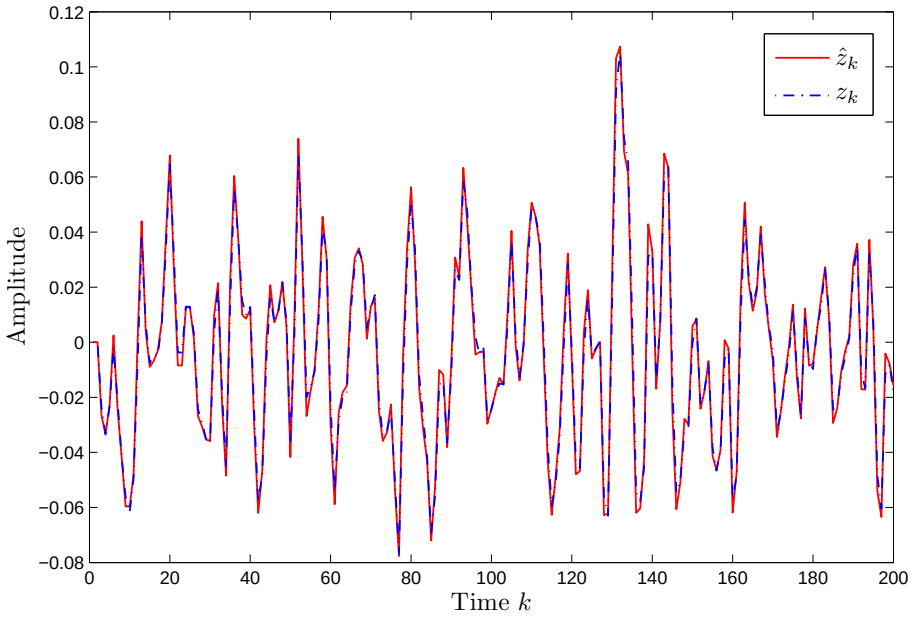

Figure 7.2: Estimation performance of the designed estimators.

7.4 Conclusions

In this chapter, we have studied the state estimation problem for discrete-time systems subject to network-induced delays. By considering the occurrence probability of the delay, the exponential mean-square stability and the $\mathcal{H}_\infty$ performance were exploited for the filtering error system. Delay-dependent estimators were designed by solving the derived LMI. Simulations and comparisons illustrated the usefulness and the advantage of the proposed design method.

Chapter 8

Robust Equalization for ISI Communication Channels

8.1 Introduction

The phenomenon of ISI between neighboring symbols occurs in a digital communication system when the bandwidth of the channel is limited but the transmission rate is high [70]. In an ISI communication channel, the presence of ISI distorts the transmitted sequence and increases bit error rates (BERs) in the recovery of the transmitted sequence at the receiver [71]. The ISI is a challenge for the development of a reliable digital communication channel with high transmission rate. From the perspective of applications, it is paramountly important to minimize the effect of ISI.

The study of mitigating the detrimental effect of ISI has attracted considerable attention during past decades; see [2, 72, 73] and the references therein. An effective but simple attempt is to design a filter that takes the observations of the ISI channel and reconstructs the input to the channel. This filter is also called equalizer and the reconstruction process is named as equalization. Under the framework of designing

an equalizer, there are many well-developed results in the past few years; see [2,74–78] and the references therein.

As the output measurements are always subject to noise, the equalizer design aims not only to reduce the effect of the channel but also to improve the robustness against the external noise. It is well known that the Kalman filter [171] is a powerful tool to filter the noise from the observation. However, it requires the priori information on the external noise. In the past several decades, an approach which assumes that the noise is bounded, but does not need the statistics of the noise, has gained popularity. As a result, the $\mathcal{H}_\infty$ filtering, the energy-to-peak filtering [123, 193], and the peak-to-peak filtering have been developed.

The authors in [2] employed the $\mathcal{H}_\infty$, mixed $\mathcal{H}_2/\mathcal{H}_\infty$ and minimum entropy criteria to tackle the FIR equalization problem. The $\mathcal{H}_2$ performance index was treated for the deconvolution problem of periodic digital channels in [194]. The authors in [195] studied how to recover MPSK-type (multiple phase-shift keying) modulus input signals against component-wise norm-bounded disturbances using an induced ∞-norm FIR filter. In addition, when the channel is imperfectly known or the parameter of the channel model varies, the results of robust equalization were proposed in [70, 72].

Uncertainty always occurs in practical systems. The uncertainty can be either from the modeling error or the slow variations during the operation. Without considering the uncertainty before the design, the uncertainty will degrade the performance of the designed equalizer or even deteriorate the equalizer. Therefore, it is demanding to consider the uncertainty in the model of the communication channel during the design of an equalizer. However, it is always assumed that the channel model is perfect. In the literature work, there exist relatively less works on the equalization problem by considering the uncertainty in the channel model, which motivates the research of this chapter.

We investigate the robust equalization problem for an communication channel with measurement noise. The contribution of this chapter can be organized as follows: (1) we study a general form of the equalization problem for communication channels with uncertainties; (2) compared with the existing results which were on the FIR equalizer, we adopt the IIR equalizer which is also a more general form; (3) in order to reduce the conservativeness of the design, we develop new conditions which bring more flexibility in the solution space the equalizer and study the relationship between the performance index and the order of the equalizer.

8.2 Problem Formulation and State-space Model

Figure 8.1 is the diagram of robust equalization for ISI communication channels with uncertainties. An input signal b_k is transmitted through an uncertain channel H subject to the phenomenon of ISI. We use y_k to denote the output of the channel. The observation $\hat{y}_k$ is contaminated by external noise v_k which is bounded. The aim of the equalization is to design an equalizer such that the reconstructed signals $\hat{z}_k$ approximates the input signal b_k, that is, the error signal e_k should be as small as possible under an evaluation criterion.

Consider a robust linear time-invariant channel H with single input and single output, and suppose that the channel has the following state-space model:

$$\begin{aligned} x_{k+1} &= A(\alpha)x_k + B(\alpha)b_k, \\ y_k &= C(\alpha)x_k + D(\alpha)b_k, \end{aligned} \tag{8.1}$$

where k is the sampling instant, $x_k \in \mathbb{R}^n$ is the state vector of the state-space model of the channel, $y_k \in \mathbb{R}$ is the ideal output of the channel, and $b_k \in \mathbb{R}$ is the input

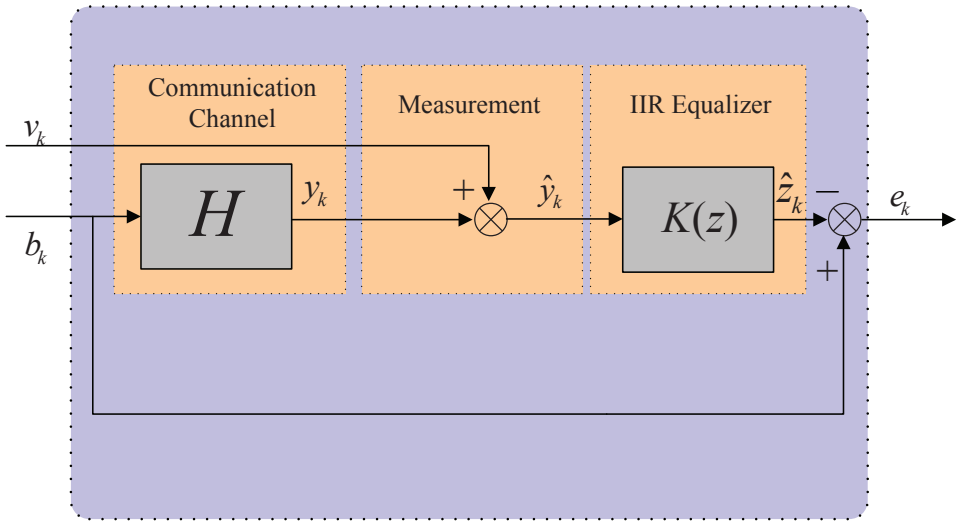

Figure 8.1: Equalization for a communication channel.

signal which belongs to $l_2[0, \infty)$.

Generally, the model for a practical communication channel may not be precise. The inaccuracy either arises from the modeling error, component aging or parameter variations during the operation. Therefore, it is necessary to consider the uncertainties for the system in (8.1). We assume that the matrices $(A(\alpha),\ B(\alpha),\ C(\alpha),\ D(\alpha))$ are within a given convex polyhedral uncertainties domain $\mathfrak{M}$ with s vertices. The domain $\mathfrak{M}$ is characterized using barycentric coordinates as:

$$\mathfrak{M} := \left\{ \Omega(\alpha) \,\middle|\, \Omega(\alpha) = \sum_{i=1}^{s} \alpha_i \Omega_i; \sum_{i=1}^{s} \alpha_i = 1, \alpha_i \geq 0 \right\}.$$

Note that $\Omega_i := (A_i,\ B_i,\ C_i,\ D_i),\ i = 1, \cdots, s$, representing the vertices of the polytope, are known matrices with compatible dimensions. The channel model with parameter uncertainties can be characterized by the combination of these vertices.

The principle of equalization is to utilize the output of the channel to reconstruct the input signal of the communication channel. However, the observation of the

output is inevitably subject to the measurement noise. As shown in Figure 8.1, the observation $\hat{y}_k$ is expressed as

$$\hat{y}_k = y_k + v_k = C(\alpha)x_k + D(\alpha)b_k + v_k, \tag{8.2}$$

where v_k is also assumed to be bounded in $l_2[0, \infty)$.

The objective of the equalization problem is to design an equalizer to estimate the input of the channel. The equalizer should be robust against the channel uncertainties and the measurement noise. In this chapter, we consider a general form of the equalizer: an $\mathcal{N}^{th}$-order IIR equalizer which has the following state-space model

$$\begin{aligned} x_{e(k+1)} &= A_e x_{ek} + B_e \hat{y}_k, \\ \hat{z}_k &= C_e x_{ek} + D_e \hat{y}_k. \end{aligned} \tag{8.3}$$

Here, A_e, B_e, C_e and D_e are parameters to be designed. It is well known that an FIR equalizer is a special form of an IIR equalizer. In the literature, most works focused on the FIR equalization. However, for equalizers with the same order, the IIR equalizer has more parameters to adjust such that the filtering error can be smaller. Therefore, it is demanding to develop the robust IIR equalization for ISI communication channels subject to uncertainties.

By defining the filtering error as $e_k := b_k - \hat{z}_k$, we obtain the filtering error system

$$\begin{aligned} \eta_{k+1} =& \bar{A}(\alpha)\eta_k + \bar{B}(\alpha)\omega_k, \\ e_k =& \bar{C}(\alpha)\eta_k + \bar{D}(\alpha)\omega_k, \end{aligned} \tag{8.4}$$

where

$$\eta_k = \begin{bmatrix} x_k \\ x_{ek} \end{bmatrix},\ \bar{A}(\alpha) = \begin{bmatrix} A(\alpha) & 0 \\ B_e C(\alpha) & A_e \end{bmatrix},$$
$$\bar{B}(\alpha) = \begin{bmatrix} B(\alpha) & 0 \\ B_e D(\alpha) & B_e \end{bmatrix},\ \omega_k = \begin{bmatrix} b_k \\ v_k \end{bmatrix},$$
$$\bar{C}(\alpha) = \begin{bmatrix} -D_e C(\alpha) & -C_e \end{bmatrix},$$
$$\bar{D}(\alpha) = \begin{bmatrix} I - D_e D(\alpha) & -D_e \end{bmatrix}.$$

Note that the parameters to be designed for the IIR equalizer exist in the system matrices of the filtering error system.

The filtering error system in (8.4) maps the external disturbance ω_k to the filtering error e_k. Next, the main focus is on the following objective: Design an $\mathcal{N}^{th}$-order IIR equalizer in (8.3) such that the filtering error system in (8.4) is robustly and asymptotically stable with a minimum $\mathcal{H}_\infty$ performance level γ^*, that is,

$$\|e\|_2 < \gamma^* \|\omega\|_2. \tag{8.5}$$

Remark 8.1. *We consider the SISO equalization problem for an ISI channel in this chapter. The modeling techniques can be extended to the MIMO case [71].*

8.3 IIR Equalizer Design

In Section 8.2, we formulated our design problem and derived a filtering error system with uncertainties. In this section, we will firstly analyze the stability and the $\mathcal{H}_\infty$ performance of the filtering error system. Based on the analysis results, we propose the design method of the equalizer.

Before proceeding, the following bounded real lemma, which is important for the subsequent discussion, is introduced.

Lemma 8.1. *Suppose that the IIR equalizer in (8.3) and a positive scalar γ are given. The filtering error system in (8.4) is robustly and asymptotically stable with an $\mathcal{H}_\infty$ attenuation level γ if and only if there exist matrices $P(\alpha) = P^{\mathrm{T}}(\alpha) > 0 \in \mathbb{R}^{\mathcal{I}\times\mathcal{I}}$, $G(\alpha) \in \mathbb{R}^{\mathcal{I}\times\mathcal{I}}$, and $F(\alpha) \in \mathbb{R}^{\mathcal{I}\times\mathcal{I}}$ such that the following condition is achievable*

$$\mathscr{M}(\alpha) = \begin{bmatrix} \Psi_1 & 0 & \Psi_2 & G(\alpha)\bar{B}(\alpha) \\ * & I & \bar{C}(\alpha) & \bar{D}(\alpha) \\ * & * & \Psi_3 & -F(\alpha)\bar{B}(\alpha) \\ * & * & * & \gamma^2 I \end{bmatrix} > 0, \tag{8.6}$$

where

$$\begin{aligned} \mathcal{I} &= n + \mathcal{N}, \\ \Psi_1 &= -P(\alpha) + G(\alpha) + G^{\mathrm{T}}(\alpha), \\ \Psi_2 &= G(\alpha)\bar{A}(\alpha) - F^{\mathrm{T}}(\alpha), \\ \Psi_3 &= P(\alpha) - F(\alpha)\bar{A}(\alpha) - (F(\alpha)\bar{A}(\alpha))^{\mathrm{T}}. \end{aligned}$$

Note that Lemma 8.1 offers a sufficient and necessary condition for assuring $\mathcal{H}_\infty$ performance of uncertain discrete-time systems. However the system matrices with uncertainties are involved in the sufficient condition. Therefore, Lemma 8.1 can not be directly used to design the equalizer. In the following, we propose an extension of Lemma 8.1.

Theorem 8.1. *Suppose that the IIR equalizer in (8.3) and a positive scalar γ are given. The filtering error system in (8.4) is robustly and asymptotically stable with an $\mathcal{H}_\infty$ attenuation level γ if there exist matrices $P_i = P_i^{\mathrm{T}} > 0 \in \mathbb{R}^{\mathcal{I}\times\mathcal{I}}$, $L_i \in \mathbb{R}^{\mathcal{I}\times\mathcal{I}}$,*

$Q_i \in \mathbb{R}^{\mathcal{I}\times\mathcal{I}}$, $M_i \in \mathbb{R}^{1\times\mathcal{I}}$, and $N_i \in \mathbb{R}^{2\times\mathcal{I}}$, such that the following conditions hold

$$\mathscr{M}_{ij} + \mathscr{M}_{ji} > 0,\ \forall\ 1 \le i \le j \le s, \tag{8.7}$$

where

$$\mathscr{M}_{ij} = \begin{bmatrix} \Psi_{1i} & 0 & \Psi_{2ij} & G_i\bar{B}_j \\ * & I & \bar{C}_i & \bar{D}_i \\ * & * & \Psi_{3ij} & -F_i\bar{B}_j \\ * & * & * & \gamma^2 I \end{bmatrix},$$

$$\Psi_{1i} = -P_i + G_i + G_i^{\mathrm{T}},$$

$$\Psi_{2ij} = G_i\bar{A}_j - F_i^{\mathrm{T}},$$

$$\Psi_{3ij} = P_i - F_i\bar{A}_j - (F_i\bar{A}_j)^{\mathrm{T}}.$$

Proof. Suppose that the Lyapunov weighting matrix $P(\alpha)$ and slack matrices $G(\alpha)$, and $F(\alpha)$ are linearly dependent on the uncertainties, that is,

$$P(\alpha) = \sum_{i=1}^{s} \alpha_i P_i,\ G(\alpha) = \sum_{i=1}^{s} \alpha_i L_i,\ F(\alpha) = \sum_{i=1}^{s} \alpha_i Q_i.$$

Under the above assumption, we have the following equation:

$$\mathscr{M}(\alpha) = \sum_{i=1}^{s} \alpha_i^2 \mathscr{M}_{ii} + \sum_{i=1}^{s-1} \sum_{j=i+1}^{s} \alpha_i\alpha_j(\mathscr{M}_{ij} + \mathscr{M}_{ji}). \tag{8.8}$$

Condition (8.7) can guarantee the negative definiteness of $\mathscr{M}_{ii}$ and $\mathscr{M}_{ij} + \mathscr{M}_{ji}$, $\forall\ 1 \le i \le j \le s$. Thus, we conclude that $\mathscr{M}(\alpha) < 0$. From Lemma 8.1, the filtering error system (8.4) is robustly and asymptotically stable. The proof is completed. □

Theorem 8.1 provides a sufficient condition for uncertain discrete-time systems.

Note that the Lyapunov weighting matrix is not coupled with the system matrices which contain the parameters to be designed. However, the slack matrices are coupled with the system matrices. In the following, we will show how to separate the slack matrices from the parameters to be designed. For the convenience of the further derivation, we define a new operation $\mathcal{T}(n,\mathcal{N})$ as follows:

$$\mathcal{T}(n,\mathcal{N}) = \begin{cases} \begin{bmatrix} I_{n,n} & 0_{n,\mathcal{N}-n} \end{bmatrix}, n \leq \mathcal{N}, \\ \begin{bmatrix} I_{\mathcal{N},\mathcal{N}} \\ 0_{n-\mathcal{N},\mathcal{N}} \end{bmatrix}, \qquad n > \mathcal{N}. \end{cases}$$

Theorem 8.2. *Suppose that a positive scalar γ and scalars ε_j, $\forall\ j = 1, \cdots, 3$, are given. The filtering error system in (8.4) is robustly and asymptotically stable with an $\mathcal{H}_\infty$ attenuation level γ if there exist matrices $P_i = P_i^{\mathrm{T}} = \begin{bmatrix} P_{11i} & P_{12i} \\ P_{12i}^{\mathrm{T}} & P_{22i} \end{bmatrix} > 0 \in \mathbb{R}^{\mathcal{I}\times\mathcal{I}}$, $G_i = \begin{bmatrix} G_{11i} & \mathcal{T}(n,\mathcal{N})G_{12} \\ G_{21i} & \varepsilon_1 G_{12} \end{bmatrix} \in \mathbb{R}^{\mathcal{I}\times\mathcal{I}}$, $F_i = \begin{bmatrix} F_{11i} & \varepsilon_2\mathcal{T}(n,\mathcal{N})G_{12} \\ F_{21i} & \varepsilon_3 G_{12} \end{bmatrix} \in \mathbb{R}^{\mathcal{I}\times\mathcal{I}}$, $A_F \in \mathbb{R}^{\mathcal{N}\times\mathcal{N}}$, $B_F \in \mathbb{R}^{\mathcal{N}\times 1}$, $C_e \in \mathbb{R}^{1\times\mathcal{N}}$, and $D_e \in \mathbb{R}^{1\times 1}$ such that the following conditions hold*

$$\mathscr{L}_{ij} + \mathscr{L}_{ji} > 0,\ \forall\ 1 \leq i \leq j \leq s, \tag{8.9}$$

where

$$\mathscr{L}_{ij} = \begin{bmatrix} \Psi_{1i} & 0 & \bar{\Psi}_{2ij} & \bar{\Psi}_{4ij} \\ * & I & \bar{C}_i & \bar{D}_i \\ * & * & \bar{\Psi}_{3ij} & \bar{\Psi}_{5ij} \\ * & * & * & \gamma^2 I \end{bmatrix},$$

$$\bar{\Psi}_{2ij} = \begin{bmatrix} G_{11i}A_j + \mathcal{T}(n,\mathcal{N})B_F C_j - F_{11i}^{\mathrm{T}} & \mathcal{T}(n,\mathcal{N})A_F - F_{21i}^{\mathrm{T}} \\ G_{21i}A_j + \varepsilon_1 B_F C_j - \varepsilon_2 G_{12}^{\mathrm{T}}\mathcal{T}^{\mathrm{T}}(n,\mathcal{N}) & \varepsilon_1 A_F - \varepsilon_3 G_{12}^{\mathrm{T}} \end{bmatrix},$$

$$\bar{\Psi}_{3ij} = \begin{bmatrix} P_{11i} - \mathrm{sym}(F_{11i}A_j + \varepsilon_2\mathcal{T}(n,\mathcal{N})B_F C_j) & P_{12i} - \varepsilon_2\mathcal{T}(n,\mathcal{N})A_F - A_j^{\mathrm{T}}F_{21i}^{\mathrm{T}} - \varepsilon_3 C_j^{\mathrm{T}}B_F^{\mathrm{T}} \\ * & P_{22i} - \varepsilon_3\mathrm{sym}(A_F) \end{bmatrix},$$

$$\bar{\Psi}_{4ij} = \begin{bmatrix} G_{11i}B_j + \mathcal{T}(n,\mathcal{N})B_F D_j & \mathcal{T}(n,\mathcal{N})B_F \\ G_{21i}B_j + \varepsilon_1 B_F D_j & \varepsilon_1 B_F \end{bmatrix},$$

$$\bar{\Psi}_{5ij} = \begin{bmatrix} -F_{11i}B_j - \varepsilon_2\mathcal{T}(n,\mathcal{N})B_F D_j & -\varepsilon_2\mathcal{T}(n,\mathcal{N})B_F \\ -F_{21i}B_j - \varepsilon_3 B_F D_j & -\varepsilon_3 B_F \end{bmatrix}.$$

Moreover, the parameters for the IIR filter are determined by

$$A_e = G_{12}^{-1}A_F,\ \ B_e = G_{12}^{-1}B_F, \tag{8.10}$$

and C_e and D_e can be obtained from the solution set.

Proof. We assume that the matrices P_i, G_i, and F_i have special structures in the statement of the theorem. By defining new variables $A_F = G_{12}A_e$, and $B_F = G_{12}B_e$, it is straightforward to achieve Condition (8.9) from Theorem 8.1. In addition, it follows from (8.9) that G_{12} is nonsingular. Therefore, the parameters of the IIR equalizer can be calculated from (8.10) once we get the solution set of (8.9). □

As mentioned in the formulation, the objective is to derive a minimum $\mathcal{H}_\infty$ attenuation level γ^* which means that the filtering error is smallest and the performance

of designed equalizers is the best from the perspective of the specific optimization criterion. The following corollary addresses the optimization method for seeking the best value.

Corollary 8.1. *The minimum $\mathcal{H}_\infty$ performance index γ^* in Theorem 8.2 can be found by solving the following convex optimization problem:*

$$\begin{array}{c} \beta = \min\ \gamma^2, \\ s.\ t.\ (8.9) \end{array} .$$

The corresponding minimum value for γ is $\gamma^* = \sqrt{\beta}$.

Remark 8.2. *Theorem 8.2 provides the design method for robust equalizers. Since we introduce two slack matrices in Theorem 8.1, the proposed design method can lead to less conservativeness results for communication channels with uncertainties. For precise channels, the proposed approach in Theorem 8.2 is also applicable. In order to reduce the computation effort, set $F_i = 0$ when designing the equalizers for the precise channels in Theorem 8.2.*

Remark 8.3. *In Theorem 8.2, there are three scalars ε_j, $\forall\ j = 1, \cdots, 3$, which provide extra flexibility in searching better solutions for the equalizers. The values for ε_j, $\forall\ j = 1, \cdots, 3$ can be set as random numbers or obtained by using the function* fminsearch *in MATLAB.*

8.4 Numerical Examples

In this section, two numerical examples are given to show the effectiveness of the proposed design method for IIR equalizers.

Example 7.1: Consider a communication channel as

$$H = 5 + z^{-1} + 2z^{-2} - z^{-3}.$$

The designed 3^{rd}-order $\mathcal{H}_\infty$ FIR equalizer in [74] is

$$K(z) = 0.1886 - 0.0706z^{-1} - 0.0380z^{-2} + 0.0240z^{-3}.$$

The corresponding minimal $\mathcal{H}_\infty$ performance γ^* is equal to 0.7367. As discussed, the IIR equalizer includes more parameters to adjust or tune such that it can achieve better filtering performance. Note that the channel has a precise model which is used for the purpose of comparison. Setting F_i as zero, the designed IIR equalizer by using Corollary 8.1 is

$$K(z) = \frac{0.1976z^3 - 0.0058z^2 - 0.0092z}{z^3 + 0.1629z^2 + 0.3142z - 0.1680},$$

when the scalar $\varepsilon_1 = 0.1$. The corresponding minimal $\mathcal{H}_\infty$ performance γ^* is equal to 0.4041 which is much less than 0.7367. To compare the equalization performance, we assume that the input signal b_k is a pulse signal with the amplitude of 2, the period of 20 seconds, the pulse width of 50% and the sampling period of 1 second. The measurement noise v_k is uniformly random between -0.5 and 0.5.

The equalization performance is shown in Figure 8.2. It can be seen that the equalizer designed in this chapter has a better equalization performance, which is consistent with the previous analysis.

Example 7.2: Consider an uncertain communication channel as

$$H = 4 + \sigma + z^{-1} + 0.5z^{-2} - z^{-3} + z^{-4},$$

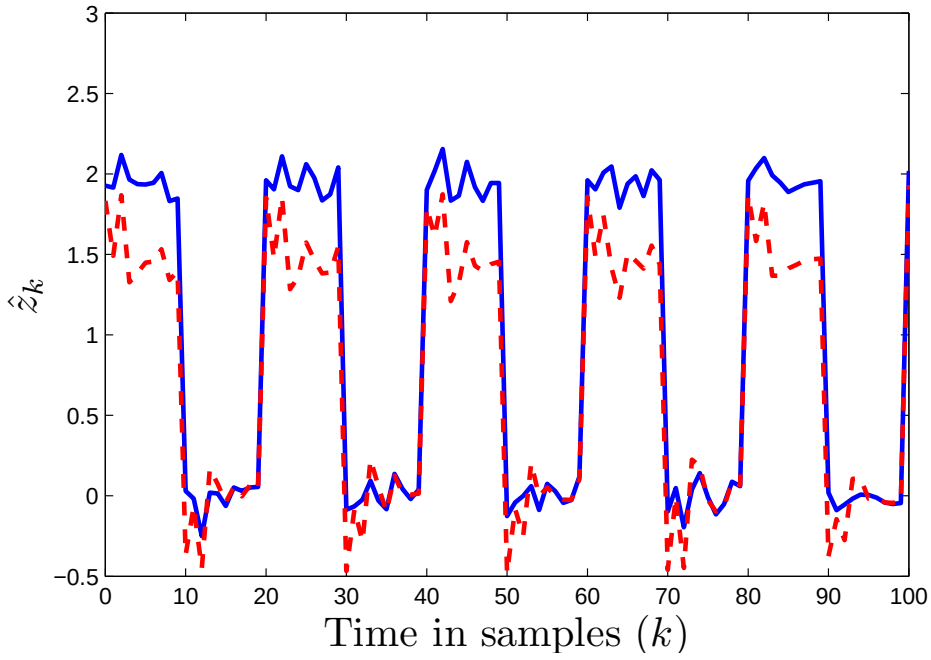

Figure 8.2: Equalization performance of different equalizers: The blue solid curve is the output of the equalizer designed in this chapter and the red dash curve is the output of the equalizer designed in [2].

where σ denotes the channel uncertainty and satisfies $\sigma \in [0,\ 1]$. It is noted that the uncertainty can be represented by a two-vertex polytope. By employing Corollary 8.1 when setting $\varepsilon_1 = 1$, $\varepsilon_2 = 0.1$ and $\varepsilon_3 = 0.3$, the relationship between the minimal $\mathcal{H}_\infty$ performance index γ^* and the order of the equalizer is shown in Figure 8.3. It can be observed from Figure 8.3 that the minimal performance index γ^* is monotonously decreasing as the order of the equalizer increases.

The corresponding 4^{th}-order IIR equalizer is

$$K(z) = \frac{0.2188z^4 + 0.0001z^3 + 0.0015z^2 + 0.001z + 0.0022}{z^4 + 0.2265z^3 + 0.11z^2 - 0.2035z + 0.2053}.$$

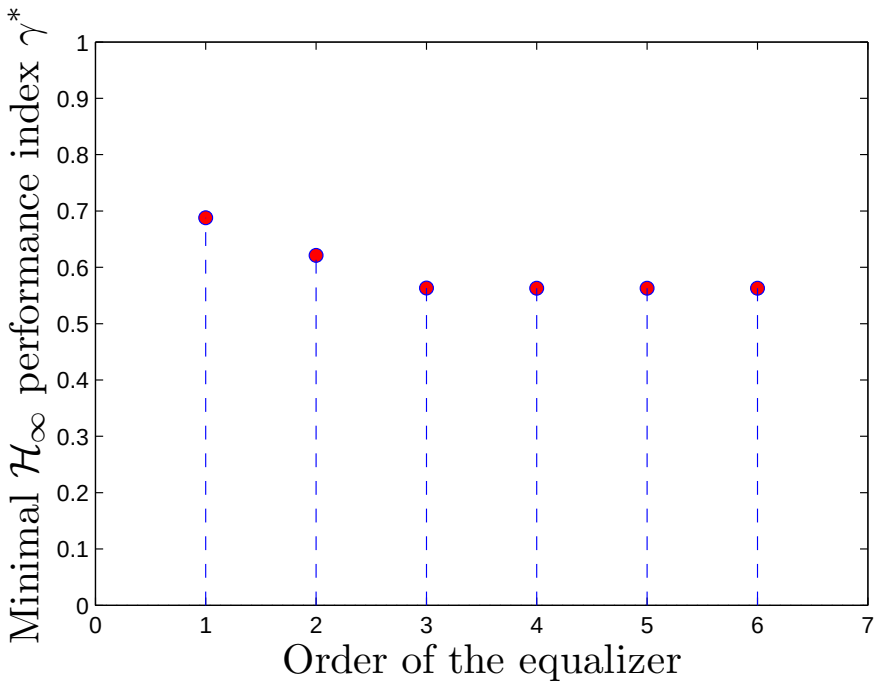

Figure 8.3: Relationship between the performance index and the order of the equalizer.

8.5 Conclusions

This chapter tackled the problem of designing an IIR equalizer for an ISI communication channel in the presence of uncertainties and measurement noise. An estimation error system was obtained by using an augmentation technique. Sufficient conditions for the robust and asymptotical stability were derived by employing a novel partition method. The design method for the equalizer was proposed on the basis of the analysis of robust stability and $\mathcal{H}_\infty$ performance. The usefulness of the proposed method was demonstrated by two numerical examples.

Chapter 9

Conclusions and Future Work

This thesis mainly focuses on two types of problems in the field of NCSs: Tracking control and signal estimation. The tracking controllers include the advanced PID controller, preview controller, combined feedback and feedforward controller, and observer-based controller. Both linear and nonlinear plants in a network environment have been investigated for the tracking problem. For the signal estimation problem, we have studied the state estimation and the signal reconstruction for networked systems. Different from the traditional peer-to-peer control systems, NCSs are inevitably subject to network-induced issues including the time delays, the packet losses, and the ISI. Without considering these issues, the performance of the designed tracking controllers, estimators, and equalizers via traditional methods may degrade. Therefore, in the setting of NCSs, it is desired to improve the traditional design methods and incorporate these network-induced constraints into the design.

9.1 Conclusions

The advanced $\mathcal{H}_\infty$ PID tracking controller design problem for NCSs subject to networked-induced delays and packet dropouts on both communication links from the sensor to

the controller (feedback loop) and from the controller to the actuator (feedforward loop) has been investigated in Chapter 2. It is assumed that there exists the load disturbance at the actuator node and the measurement noise at the sensor node. The designed controller demonstrates two features: (1) The measured output follows the expected reference well when the feedback loop and the feedforward loop are both subject to the network-induced delays and missing packets; (2) The load disturbance and the measurement noise are attenuated below a prescribed level satisfying the $\mathcal{H}_\infty$ performance index. It is worthy mentioning that the work in this chapter is *the first* to propose the algorithm on $\mathcal{H}_\infty$ PID controller design for discrete-time NCSs by considering the load disturbance and the measurement noise attenuation. The proposed control strategy can enjoy the merits of both NCSs and the PID controller without changing the structures of most existing industrial feedback controllers.

By further studying the network characteristics, it is shown that each delay in a bounded set has an occurrence probability. Compared with the Markov jump delay model in [52], it is more convenient to obtain the occurrence probability delay model. In Chapter 3, we have employed the delay occurrence probabilities to design the delay-scheduling tracking controller. The control law is essentially a combined feedback and feedforward control. Since the controller does not know the delay on the feedforward loop for the control signal to be transmitted, the idea of predictive control in which a sequence of control signals dependent on both communication links are transmitted to the actuator and the smart actuator will apply a suitable one to drive the plant is used. A comparative study on the VTOL helicopter model shows the advantage of the proposed design strategy over the modified PID in Chapter 2.

In many practical applications, the system states may not be always available or cannot be measured. In Chapter 4, an observer is firstly designed to estimate the states. For the modeling of the network-induced delays, we adopt the Markov jump

delay model, which is difference from the model in [52] in that the elements in the probability transition matrix are subject to uncertainties. Such a delay model is more general and practical. We have employed the energy-to-peak performance criteria to evaluate and attenuate the effect of the external inputs on the tracking error. For an SISO system, the minimization of the energy-to-peak performance index is equivalent to the optimization of the overshoot.

Generally, the linear state model is inadequate to represent most of the system dynamics. The nonlinearity always occurs in the system behavior. In order to extend the applications of the NCSs, we have investigated the tracking control problem for nonlinear systems in Chapter 5. The nonlinear system is approximated by T-S fuzzy linear models. The tracking control strategy is the modified PI control which can eliminate the tracking error for the step reference. We also adopt the probabilistic delay to model the network-induced delay. However, it is not required to augment the state-space model to obtain the delay-free system such that the dimension of the closed-loop system is much smaller than the one in Chapter 4.

We have presented a general filtering problem in Chapter 6. The output of the system is subject to multiple intermittent measurements. Then, the measured output is packed and transmitted to the filter via a communication link. A weighted $\mathcal{H}_\infty$ performance is defined to deal with the delayed noise and non-delayed noise. If there are not network-induced delays on the communication link, the studied problem is an estimator design problem for systems with intermittent measurements. Inspired by the tracking control problem in Chapter 3, we adopt the probabilistic delays to model the network-induced delays in Chapter 7. Another contribution of Chapter 7 is that we do not need to partition the Lyapunov weighting matrix. A comparative study shows that the estimation performance is greatly enhanced by using the proposed estimator design algorithm.

In Chapter 8, we have focused on the design of the robust equalizer to eliminate the effects of the ISI phenomenon and the parameter variations of the communication channel model. The channel model is not limited to an FIR channel, which can also represent an IIR channel. The measurement noise is required to be bounded in the $l_2[0,\infty)$ subspace. Additionally, we adopt the IIR form for the equalizer with $\mathcal{N}^{th}$ order since an IIR equalizer can obtain better results compared with a same order FIR equalizer.

9.2 Future Work

The research work in this thesis has solved emergying typical problems for NCSs and achieved applicable results. However, most of the obtained results are still based on sufficient conditions and some assumptions of the characteristics are ideal and strong. Therefore, it is believed that there is a further enhancement space for the control of NCSs by considering the control performance, the computation load and the control efforts. In the future research, we will investigate the following topics.

1: Robust Two-mode-dependent Controller Design for NCSs with Random Delays Modeled by Markov Chains with Partially Unknown Transition Probabilities. The controller design problem is illustrated in Figure 9.1. The state of the system is transmitted to the buffer via a feedback communication channel. Due to the network-induced delay, the state at the time k from the sensor can not arrive at the buffer simultaneously. The delay τ_k on the feedback channel is modeled by a Markov chain with partially unknown transition probabilities. The most recent packet at the buffer node is sent to the networked controller. The generated control signals are transmitted toward the actuator via another communication link which is subject to a Markovian delay d_k with partially unknown transition probabilities.

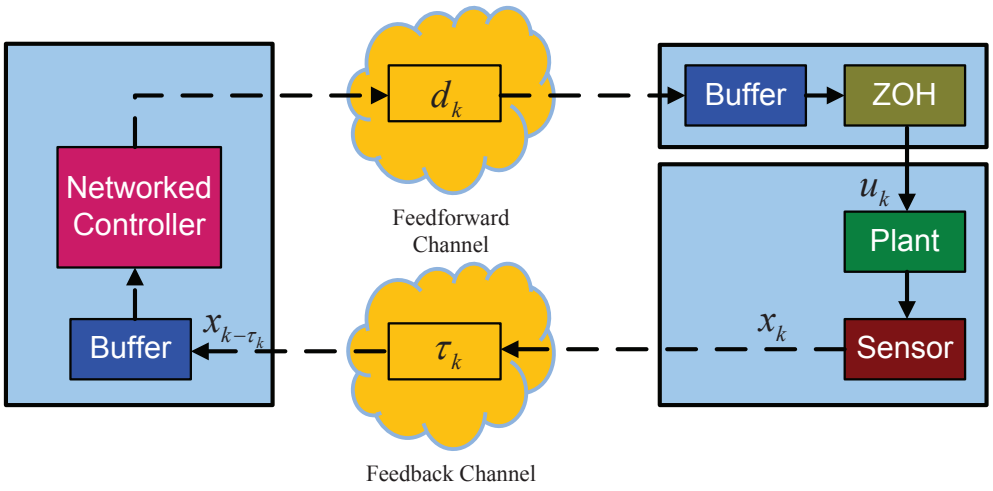

Figure 9.1: Diagram of a networked control system.

In order to utilize the delays on the feedforward channel, the authors in [52] developed the two-mode-dependent state-feedback control for the stabilization problem of NCSs by assuming that the previous delay d_{k-1} shall be obtained at the time k. The two-mode-dependent control refers to that the controller is dependent on the current delay on the feedback channel and the previous delay on the feedforward channel. However, the previous delay d_{k-1} can not be known at the controller node since it is subject to the current delay on the feedback channel. To modify the control scheme, a new two-mode-dependent compensation approach was exploited [31] in which $d_{k-\tau_k-1}$ was used to replace d_{k-1} in [52]. In this way, the modified two-mode-dependent control scheme is applicable.

However, the control scheme is still not perfect due to the following reasons: (1) In both papers [52] and [31], the augmentation technique was employed to transform the closed-loop systems into delay-free Markovian jump systems. When the delay upper bound is too large, the dimension of the resulting system matrix dimension will be accordingly large, leading to high computational complexity. (2) The probability transition matrices were set to constant in [52] and [31]. In practice, the probability

transition matrices are obtained by studying the characteristics of the network by using finite statistic information before the controller design. Therefore, it is natural that the matrices are subject to uncertainties which may be induced by the incomplete statistic information or the variations during the system operation. (3) The developed algorithms are LMI-based iterative ones which are well known as modified cone complementarity linearization (CCL) algorithm [148]. The computation time is unpredictable. (4) The delays d_{k-1} and $d_{k-\tau_k-1}$ were used to design the two-mode-dependent controllers in [52] and [31], respectively. Since both d_{k-1} and $d_{k-\tau_k-1}$ are old information for the controller at the time k, the best choice for the compensation is d_k. To the best of the authors' knowledge, the above four problems has not been fully investigated in two-mode-dependent controller design for NCSs, which motivates us to do the future work.

2: SMC for NCSs. Last two decades have witnessed the increasing attention to the SMC which is inherently robust against the system uncertainty, the external disturbance, and has a good transient response [196]. Therefore, SMC has been applied to many practical systems including electrical motors [197], power systems, suspension systems [198,199], robot manipulators [200], and underwater vehicles [201, 202]. In recent years, with the wide application of digital controllers, the discrete-time sliding-mode control (DT-SMC) has attracted more attention [203, 204]. Different from the continuous-time SMC [205, 206], it is challenging to drive the plant to the designed sliding-mode surface due to the finite sampling rate [207, 208] under the discrete-time framework. Thus, the study on the reaching law for the DT-SMC is of practical importance. The authors in [207] proposed a sufficient and necessary reaching law under which the closed-loop system would be driven toward the sliding-mode surface and the switching function should be strictly decreasing. The quasi sliding-mode and quasi sliding-mode band were defined for single-input systems and

multiple-input systems in [209] and [210], respectively. In addition, a linear reaching law was developed in [211].

In NCSs with limited communication capacities, the systems are subject to time-varying delays and missing packets. At the controller node, the received signals are delayed. In this case, the challenge is how to design the sliding-mode surface and how to determine the reaching law with the delayed information. In our future work, we will extend the definition of the sliding-mode surface by using the mean-square sense. A new control law will be proposed for the mean-square sliding mode surface.

Appendix A

Publications

- **Refereed journal papers that have been accepted**

J1. **H. Zhang**, A. Saadat Mehr, and Y. Shi, "Improved robust energy-to-peak filtering for uncertain linear systems," *Signal Processing*, vol. 90, no. 9, pp. 2667–2675, 2010.

J2. **H. Zhang**, Y. Shi and A. Saadat Mehr, "Robust energy-to-peak filtering for networked systems with time-varying delays and randomly missing data," *IET Control Theory & Applications*, vol. 4, no. 12, pp. 2921–2936, 2010.

J3. **H. Zhang**, Y. Shi and A. Saadat Mehr, "Robust weighted $\mathcal{H}_\infty$ filtering for networked systems with intermittent measurements of multiple sensors," *International Journal of Adaptive Control and Signal Processing,* vol. 4, no. 25, pp. 313–330, 2011.

J4. **H. Zhang**, Y. Shi and A. Saadat Mehr, "Robust $\mathcal{H}_\infty$ PID control for multivariable networked control systems with disturbance/noise attenuation," *International Journal of Robust and Nonlinear Control*, vol. 22, no. 2, pp. 183–204, 2012.

J5. **H. Zhang**, Y. Shi and A. Saadat Mehr, "Robust static output feedback control

and remote PID design for networked motor systems," *IEEE Transactions on Industrial Electronics*, vol. 58, no. 12, pp. 5396–5405, 2011.

J6. **H. Zhang**, Y. Shi and A. Saadat Mehr, "Robust non-fragile dynamic vibration absorbers with uncertain factors," *Journal of Sound and Vibration*, vol. 330, no. 4, pp. 559-566, 2011.

J7. **H. Zhang**, Y. Shi, A. Saadat Mehr, and H. Huang, "Robust energy-to-peak FIR equalization for time-varying communication channels with intermittent observations," *Signal Processing*, vol. 91, no. 7, pp. 1651–1658, 2011.

J8. **H. Zhang**, Y. Shi and A. Saadat Mehr, "Robust equalization for inter symbol interference communication channels," *IET Signal Processing*, vol. 6, no. 2, pp. 73–78, 2012.

J9. **H. Zhang**, Y. Shi and A. Saadat Mehr, "On $\mathcal{H}_\infty$ filtering for T-S fuzzy systems," *IEEE Transactions on Fuzzy Systems*, vol. 20, no. 2, pp. 396–401, 2012.

J10. **H. Zhang** and Y. Shi, "Observer-based $\mathcal{H}_\infty$ feedback control for arbitrarily time-varying discrete-time systems with intermittent measurements and input constraints," *ASME Transactions, Journal of Dynamic Systems, Measurement, and Control*, accepted and in press, 2011.

J11. **H. Zhang** and Y. Shi, "Delay-dependent stabilization of discrete-time systems with time-varying delay via switching technique," *ASME Transactions, Journal of Dynamic Systems, Measurement, and Control*, accepted and in press, 2011.

J12. **H. Zhang**, Y. Shi and A. Saadat Mehr, "Stability and stabilization of switched discrete-time systems with uncertain subsystem occurrence probabilities," *International Journal of Adaptive Control and Signal Processing*, accepted and in press, 2011.

J13. **H. Zhang**, Y. Shi and M. Liu, "$\mathcal{H}_\infty$ step tracking control for networked discrete-time nonlinear systems with integral and predictive actions," *IEEE Transactions on Industrial Informatics*, accepted and in press, 2012.

J14. **H. Zhang** and Y. Shi, "Parameter-dependent $\mathcal{H}_\infty$ filtering for linear parameter varying systems," *ASME Transactions, Journal of Dynamic Systems, Measurement, and Control*, accepted and in press, 2012.

- **Refereed conference papers that have appeared or been accepted**

C1. **H. Zhang**, Y. Shi and A. Saadat Mehr, "Robust $\mathcal{H}_\infty$ PID control for networked control systems with acceptable noise rejection," *29th American Control Conference*, Baltimore, Maryland, Missouri, USA, June 30–July 2, 2010.

C2. **H. Zhang**, A. Saadat Mehr and Y. Shi, "New results on energy-to-peak filtering for uncertain discrete-time systems," *29th American Control Conference*, Baltimore, Maryland, Missouri, USA, June 30–July 2, 2010.

C3. **H. Zhang**, Y. Shi and A. Saadat Mehr, "Robust weighted $\mathcal{H}_\infty$ filtering for NCS with multiple sensor faults," *8th World Congress on Intelligent Control and Automation*, Jinan, China, July 7–July 9, 2010.

C4. **H. Zhang**, Y. Shi and A. Saadat Mehr, "Optimal non-fragile dynamic vibration absorbers," Canadian Society for Mechanical Engineering Forum, Victoria, Canada, June 6–June 9, 2010.

C5. **H. Zhang**, Y. Shi, J. Zhang, Z. Wang and A. Saadat Mehr, "Fuzzy logic for autonomous garage parking of automobiles," Canadian Society for Mechanical Engineering Forum, Victoria, Canada, June 6–June 9, 2010.

C6. Y. Lin, **H. Zhang**, Y. Shi and R. Burton, "$\mathcal{H}_\infty$ PID plus feedforward controller design for an electrohydraulic actuator (EHA) system," Purdue PhD Symposium, 2010.

C7. X. Zhang, **H. Zhang**, M. Ahmadian, K. Guo, "Study on squeeze mode magneto-rheological engine mount with robust $\mathcal{H}_\infty$ control," *SAE 2011 World Congress & Exhibition*, Cobo Center Detroit, Michigan, USA, April 12–April 14, 2011.

C8. **H. Zhang** and Y. Shi, "Feedback and feedforward tracking control for networked control systems," The 23rd Canadian Congress of Applied Mechanics (CANCAM2011), Vancouver, BC, Canada, June 5–June 9, 2011.

C9. **H. Zhang** and Y. Shi, "Observer-based tracking controller design for networked predictive control systems with uncertain Markov delays," The 2012 American Control Conference (ACC 2012), Montreal, Canada, June 27–29, 2012.

Bibliography

[1] B. Yu, "Networked Control System Design and Parameter Estimation," Master's thesis, University of Saskatchewan, Saskatoon, Canada, 2008.

[2] A. T. Erdogan, B. Hassibi, and T. Kailath, "FIR $\mathcal{H}_\infty$ equalization," *Signal Process.*, vol. 81, no. 5, pp. 907–917, 2001.

[3] Networked Control Systems Repository, *Available at: http://filer.case.edu/org/ncs/basics.htm.* 24 Feburary 2011.

[4] A. S. Tanenbaum, *Computer Networks, 3rd ed.* Upper Englewood Cliffs, NJ: Prentice-Hall, 1996.

[5] F.-L. Lian, J. R. Moyne, and D. M. Tilbury, "Performance evaluation of control networks: Ethernet, ControlNet, and DeviceNet," *IEEE Control Syst. Mag.*, vol. 21, no. 1, pp. 66–83, 2001.

[6] J. Zhu, "The Study of Forward Simulation and Control Strategy for Fuel Cell Electric Vehicle Base on CAN Bus ," Master's thesis, Jilin University, Changchun, China, 2006.

[7] W. Lawrenz, *CAN System Engineering: From Theory to Practical Applications.* New York: Springer-Verlag, 1997.

[8] F.-L. Lian, " Analysis, Design, Modeling, and Control of Networked Control Systems," Ph.D. dissertation, University of Michigan, Ann Arbor, MI, 2001.

[9] G. C. Walsh, H. Ye, and L. G. Bushnell, "Stability analysis of networked control systems," *IEEE Trans. Contr. Syst. Technol.*, vol. 10, no. 3, pp. 438–446, 2002.

[10] J. D. Wheelis, "Process control communications: Token Bus, CSMA/CD, or Token Ring," *ISA Trans.*, vol. 32, no. 2, pp. 193–198, 1993.

[11] J. Nilsson, " Real-Time Control Systems with Delays," Ph.D. dissertation, Lund Institute of Technology, Lund, Sweden, 1998.

[12] G. C. Walsha, OctavianBeldiman, and L. G. Bushnell, "Error encoding algorithms for networked control systems," *Automatica*, vol. 38, no. 2, pp. 261–267, 2002.

[13] D. Necic and A. R. Teel, "Input-to-state stability of networked control systems," *Automatica*, vol. 40, no. 12, pp. 2121–2128, 2004.

[14] D. B. Dačić and D. Nešić, "Quadratic stabilization of linear networked control systems via simultaneous protocol and controller design," *Automatica*, vol. 43, no. 7, pp. 1145–1155, 2007.

[15] Karl J. Åström and B. Wittenmark, *Computer-Controlled Systems: Theory and Design, 3rd ed.* Englewood Cliffs, NJ: Prentice-Hall, 1997.

[16] S. C. Tatikonda, " Control under Communication Constraints," Ph.D. dissertation, Massachusetts Institute of Technology, Cambridge, MA, 2000.

[17] P. R. Kumar, "New technological vistas for systems and control: the example of wireless networks," *IEEE Control Syst. Mag.*, vol. 21, no. 1, pp. 24–37, 2001.

[18] W. Zhang, M. S. Branicky, and S. M. Phillips, "Stability of networked control systems," *IEEE Control Syst. Mag.*, vol. 21, no. 1, pp. 84–99, 2001.

[19] O. C. Imer, S. Compans, T. Basar, and R. Srikant, "Available bit rate congestion control in ATM networks," *IEEE Control Syst. Mag.*, vol. 21, no. 1, pp. 38–56, 2001.

[20] F.-Y. Wang and D. Liu, *Networked Control Systems Theory and Applications*. London Limited: Springer–Verlag, 2008.

[21] D. Huang and S. K. Nguang, *Robust Control for Uncertain Networked Control Systems with Random Delays*. Berlin Heidelberg: Springer-Verlag, 2009.

[22] A. Bemporad, M. Heemels, and M. Johansson, *Networked Control Systems*. Berlin Heidelberg: Springer-Verlag, 2010.

[23] L. Zhang, "Access Scheduling and Controller Design in Networked Control Systems," Ph.D. dissertation, University of Maryland, College Park, MD, 2005.

[24] M. Posthumus-Cloosterman, " Control over Communication Networks: Modeling, Analysis, and Synthesis," Ph.D. dissertation, Eindhoven University of Technology, Eindhoven, Netherlands, 2008.

[25] O. C. Imer, " Optimal Estimation and Control under Communication Network Constraints," Ph.D. dissertation, University of Illinois at Urbana-Champaign, Urbana, Illinois, 2005.

[26] H. Fang, "State Estimation, System Identification and Adaptive Control for Networked Systems," Master's thesis, University of Saskatchewan, Saskatoon, Canada, 2009.

[27] P. S. Padmasola, "Tradeoffs and Limitations in Networked Control Systems," Master's thesis, Iowa State University, Ames, Iowa, 2006.

[28] Y. Tipsuwan and M.-Y. Chow, "Control methodologies in networked control systems," *Control Eng. Pract.*, vol. 11, no. 10, pp. 1099–1111, 2003.

[29] J. P. Hespanha, P. Naghshtabrizi, and Y. Xu, "A survey of recent results in networked control systems," *Proc. IEEE*, vol. 95, no. 1, pp. 138–162, 2007.

[30] J. Baillieul and P. J. Antsaklis, "Control and communication challenges in networked real-time systems," *Proc. IEEE*, vol. 95, no. 1, pp. 9–28, 2007.

[31] Y. Shi and B. Yu, "Output feedback stabilization of networked control systems with random delays modeled by Markov chains," *IEEE Trans. Autom. Contr.*, vol. 54, no. 7, pp. 1668–1674, 2009.

[32] R. M. Murray, K. J. Åström, S. P. Boyd, R. W. Brockett, and G. Stein, "Future directions in control in an information-rich world," *IEEE Control Syst. Mag.*, vol. 23, no. 2, pp. 20–33, 2003.

[33] P. Park, "Modeling, Analysis, and Design of Wireless Sensor Network Protocols," Ph.D. dissertation, KTH Royal Institute of Technology, Stockholm, Sweden, 2011.

[34] O. P. Vidal, " Smart office: wireless sensor network for energy monitoring and user profiling," Stockholm, Sweden, 2010.

[35] E. Witrant, P. D. Marco, P. Park, and C. Briat, "Limitations and performances of robust control over WSN: UFAD control in intelligent buildings," *IMA J. Math Control Info.*, vol. 27, no. 4, pp. 527–543, 2010.

[36] Z. Qu, J. Wang, and R. A. Hull, "Cooperative control of dynamical systems with application to autonomous vehicles," *IEEE Trans. Autom. Contr.*, vol. 53, no. 4, pp. 894–911, 2008.

[37] E. Fiorelli, N. E. Leonard, P. Bhatta, D. A. Paley, R. Bachmayer, and D. M. Fratantoni, "Multi-AUV control and adaptive sampling in monterey bay," *IEEE J. Oceanic Eng.*, vol. 31, no. 4, pp. 935–948, 2006.

[38] P. Lin, Y. Jia, and L. Li, "Distributed robust $\mathcal{H}_\infty$ consensus control in directed networks of agents with time-delay," *Syst. Contr. Lett.*, vol. 57, no. 8, pp. 643–653, 2008.

[39] R. M. Murray, "Recent research in cooperative control of multivehicle systems," *ASME J. Dyn. Syst. Meas. Contr.*, vol. 129, no. 5, pp. 571–583, 2007.

[40] R. Olfati-Saber, "Flocking for multi-agent dynamic systems: Algorithms and theory," *IEEE Trans. Autom. Contr.*, vol. 51, no. 3, pp. 401–420, 2006.

[41] P. Ögren, E. Fiorelli, and N. E. Leonard, "Cooperative control of mobile sensor networks: Adaptive gradient climbing in a distributed environment," *IEEE Trans. Autom. Contr.*, vol. 49, no. 8, pp. 1292–1302, 2004.

[42] C. Meng, T. Wang, W. Chou, S. Luan, Y. Zhang, and Z. Tian, "Remote surgery case: robot-assisted teleneurosurgery," in *IEEE Int. Conf. Robot. and Auto.*, New Orleans. LP, USA, 2004, pp. 819–823.

[43] K. Hikichi, H. Morino, I. Arimoto, K. Sezaki, and Y. Yasuda, "The evaluation of delay jitter for haptics collaboration over the internet," in *Proc. IEEE Global Telecomm. Conf.*, Taipei, ROC, 2002, pp. 1492–1496.

[44] P. Seiler and R. Sengupta, "An $\mathcal{H}_\infty$ approach to networked control," *IEEE Trans. Autom. Contr.*, vol. 50, no. 3, pp. 356–364, 2005.

[45] Y. Xia, X. Liu, G. ping Liu, and D. Rees, "Stabilization analysis and implementation for MIMO NCS with time-varying delays," *Int. J. Robust Nonlinear Contr.*, in press, 2011.

[46] W. Hu, G.-P. Liu, D. Rees, and Y. Qiao, "Design and implementation of web-based control laboratory for test rigs in geographically diverse locations," *IEEE Trans. Ind. Electron.*, vol. 55, no. 6, pp. 2343–2354, 2008.

[47] Y.-B. Zhao, G.-P. Liu, and D. Rees, "Design of a packet-based control framework for networked control systems," *IEEE Trans. Contr. Syst. Technol.*, vol. 17, no. 4, pp. 859–865, 2009.

[48] W. Hu, G. Liu, and D. Rees, "Event-driven networked predictive control," *IEEE Trans. Ind. Electron.*, vol. 54, no. 3, pp. 1603–1613, 2007.

[49] Y.-B. Zhao, G.-P. Liu, and D. Rees, "Packet-based deadband control for internet-based networked control systems," *IEEE Trans. Contr. Syst. Technol.*, vol. 18, no. 5, pp. 1057–1067, 2010.

[50] R. Wang, G.-P. Liu, W. Wang, D. Rees, and Y.-B. Zhao, "Guaranteed cost control for networked control systems based on an improved predictive control method," *IEEE Trans. Contr. Syst. Technol.*, vol. 18, no. 5, pp. 1226–1232, 2010.

[51] J. R. Moyne and D. M. Tilbury, "The emergence of industrial control networks for manufacturing control, diagnostics, and safety data," *Proc. IEEE*, vol. 95, no. 1, pp. 29–47, 2007.

[52] L. Zhang, Y. Shi, T. Chen, and B. Huang, "A new method for stabilization of networked control systems with random delays," *IEEE Trans. Autom. Contr.*, vol. 50, no. 8, pp. 1177–1181, 2005.

[53] J. Wu and T. Chen, "Design of networked control systems with packet dropouts," *IEEE Trans. Autom. Contr.*, vol. 52, no. 7, pp. 1314–1319, 2007.

[54] J. Wu, L. Zhang, and T. Che, "Model predictive control for networked control systems," *Int. J. Robust Nonlinear Contr.*, vol. 19, no. 9, pp. 1016–1035, 2009.

[55] L. Xiao, A. H. Jonathan, and P. How, "Control with random communication delays via a discrete-time jump system approach," in *Proc. 2000 Amer. Contr. Conf.*, Chicago, Illinois, 2000, pp. 2199–2204.

[56] C. Peng, Y.-C. Tian, and M. O. Tadé, "State feedback controller design of networked control systems with interval time-varying delay and nonlinearity," *Int. J. Robust Nonlinear Contr.*, vol. 18, no. 12, pp. 1285–1301, 2008.

[57] C. Peng, D. Yue, and Y.-C. Tian, "Delay distribution based robust $\mathcal{H}_\infty$ control of networked control systems with uncertainties," *Asian J. Control*, vol. 12, no. 1, pp. 46–57, 2010.

[58] M. Sahebsara, T. Chen, and S. L. Shah, "Optimal $\mathcal{H}_\infty$ filtering in networked control systems with multiple packet dropouts," *Syst. Contr. Lett.*, vol. 57, no. 9, pp. 696–702, 2008.

[59] S. Sun, L. Xie, W. Xiao, and N. Xiao, "Optimal filtering for systems with multiple packet dropouts," *IEEE Trans. Circuits Syst. II*, vol. 55, no. 7, pp. 695–696, 2008.

[60] H. Yang, Y. Xia, and P. Shi, "Stabilization of networked control systems with nonuniform random sampling periods," *Int. J. Robust Nonlinear Contr.*, in press, 2010.

[61] D. F. Delchamps, "Stabilizing a linear system with quantized state feedback," *IEEE Trans. Autom. Contr.*, vol. 35, no. 8, pp. 916–924, 1990.

[62] D. Liberzon, "Hybrid feedback stabilization of systems with quantized signals," *Automatica*, vol. 39, no. 9, pp. 1543–1554, 2003.

[63] R. W. Brockett and D. Liberzon, "Quantized feedback stabilization of linear systems," *IEEE Trans. Autom. Contr.*, vol. 45, no. 7, pp. 1279–1289, 2000.

[64] M. Fu and L. Xie, "The sector bound approach to quantized feedback control," *IEEE Trans. Autom. Contr.*, vol. 50, no. 11, pp. 1698–1711, 2005.

[65] ——, "Finite-level quantized feedback control for linear systems," *IEEE Trans. Autom. Contr.*, vol. 54, no. 5, pp. 1165–1170, 2009.

[66] H. Ishii and T. Başar, "Quantization in $\mathcal{H}_\infty$ parameter identification," *IEEE Trans. Autom. Contr.*, vol. 53, no. 9, pp. 2186–2192, 2008.

[67] D. F. Coutinho, M. Fu, and C. E. de Souza, "Input and output quantized feedback linear systems," *IEEE Trans. Autom. Contr.*, vol. 55, no. 3, pp. 761–766, 2010.

[68] H. Gao and T. Chen, "A new approach to quantized feedback control systems," *Automatica*, vol. 44, no. 2, pp. 534–542, 2008.

[69] M. Yan and Y. Shi, "Robust discrete-time sliding mode control for uncertain systems with time-varying state delay," *IET Contr. Theory Appl.*, vol. 2, no. 8, pp. 662–674, 2008.

[70] V. A. Ugrinovskii and I. R. Petersen, "Robust ISI equalization for uncertain channel via minimax optimal filtering," *Int. J. Adapt. Contr. Signal Process.*, vol. 20, no. 3, pp. 99–122, 2006.

[71] B. Hassibi, A. T. Erdogan, and T. Kailath, "MIMO decision feedback equalization from an $\mathcal{H}_\infty$ perspective," *IEEE Trans. Signal Process.*, vol. 52, no. 3, pp. 734–745, 2004.

[72] C.-W. Lin, B.-S. Chen, and T.-Y. Yang, "Robust decision-feedback equalizer design method under parameter perturbation in a transmission channel," *Signal Process.*, vol. 44, no. 1, pp. 39–49, 1995.

[73] R. Fischer, J. Huber, and C. Windpassinger, "Signal processing in decision-feedback equalization of intersymbol-interference and multiple-input/multiple-output channels: a unified view," *Signal Process.*, vol. 83, no. 8, pp. 1633–1642, 2003.

[74] B. Dumitrescu, "Bounded real lemma for FIR MIMO systems," *IEEE Signal Process. Lett.*, vol. 12, no. 7, pp. 496–499, 2005.

[75] R. Venkataramani and Y. Bresler, "Filter design for MIMO sampling and reconstruction," *IEEE Trans. Signal Process.*, vol. 51, no. 12, pp. 3164–3176, 2003.

[76] Y. Guo and B. C. Levy, "Robust MSE equalizer design for MIMO communication systems in the presence of model uncertainties," *IEEE Trans. Signal Process.*, vol. 54, no. 5, pp. 1840–1852, 2006.

[77] T.-J. Su and H.-W. Peng, "Robust finite impulse response equalisation for time-delay communication channels: linear matrix inequality approach," *IET Contr. Theory Appl.*, vol. 1, no. 1, pp. 226–232, 2007.

[78] S. Chen, L. Hanzo, and B. Mulgrew, "Decision-feedback equalization using multiple-hyperplane partitioning for detecting ISI-corrupted M-ary PAM signals," *IEEE Trans. Commun.*, vol. 49, no. 5, pp. 760–764, 2001.

[79] N. G. Dokuchaev and A. V. Savkin, "Recursive state estimation via limited capacity communication channels," in *Proc. 38th IEEE Conf. Decision Control*, Phoenix, AZ, 1999, pp. 4929–4932.

[80] K. Li and J. Baillieul, "Robust quantization for digital finite communication bandwidth (dfcb) control," *IEEE Trans. Autom. Contr.*, vol. 49, no. 9, pp. 1573–1584, 2004.

[81] X. Li and W. S. Wong, "State estimation with communication constraints," *Syst. Contr. Lett.*, vol. 28, no. 1, pp. 49–54, 1996.

[82] G. N. Nair and R. J. Evans, "Stabilization with data-rate-limited feedback: tightest attainable bounds," *Syst. Contr. Lett.*, vol. 41, no. 1, pp. 49–56, 2000.

[83] ——, "Exponential stabilisability of finite-dimensional linear systems with limited data rates," *Automatica*, vol. 39, no. 4, pp. 585–593, 2000.

[84] ——, "Stabilizability of stochastic linear systems with finite feedback data rates," *SIAM J. Control Optim.*, vol. 43, no. 2, pp. 413–436, 2004.

[85] W. S. Wong and R. W. Brockett, "Systems with finite communication bandwidth constraints Part I: State estimation problems," *IEEE Trans. Autom. Contr.*, vol. 42, no. 9, pp. 1294–1299, 1997.

[86] ——, "Systems with finite communication bandwidth constraints-II stabilization with limited information feedback," *IEEE Trans. Autom. Contr.*, vol. 44, no. 5, pp. 1049–1053, 1999.

[87] S. Tatikonda and S. Mitter, "Control under communication constraints," *IEEE Trans. Autom. Contr.*, vol. 49, no. 7, pp. 1056–1068, 2004.

[88] J. H. Braslavsky, R. H. Middleton, and J. S. Freudenberg, "Feedback stabilization over signal-to-noise ratio constrained channels," *IEEE Trans. Autom. Contr.*, vol. 52, no. 8, pp. 1056–1068, 2007.

[89] M. B. G. Cloosterman, N. van de Wouw, W. P. M. H. Heemels, and H. Nijmeijer, "Stability of networked control systems with uncertain time-varying delays," *IEEE Trans. Autom. Contr.*, vol. 54, no. 7, pp. 1575–1580, 2009.

[90] J. Xiong and J. Lam, "Stabilization of networked control systems with a logic ZOH," *IEEE Trans. Autom. Contr.*, vol. 54, no. 2, pp. 358–363, 2009.

[91] H. Gao, X. Meng, and T. Chen, "Stabilization of networked control systems with a new delay characterization," *IEEE Trans. Autom. Contr.*, vol. 53, no. 9, pp. 2142–2148, 2008.

[92] E. Fridman, A. Seuret, and J.-P. Richard, "Robust sampled-data stabilization of linear systems: an input delay approach," *Automatica*, vol. 40, no. 8, pp. 1441–1446, 2004.

[93] M. Yu, L. Wang, and T. Chu, "Sampled-data stabilisation of networked control systems with nonlinearity," *IEE Proc.-Control Theory Appl.*, vol. 152, no. 6, pp. 609–614, 2005.

[94] X. Meng, J. Lam, and H. Gao, "Network-based $\mathcal{H}_\infty$ control for stochastic systems," *Int. J. Robust Nonlinear Contr.*, vol. 19, no. 3, pp. 295–312, 2009.

[95] D. Yue, Q.-L. Han, and J. Lam, "Network-based robust $\mathcal{H}_\infty$ control of systemswith uncertainty," *Automatica*, vol. 41, no. 5, pp. 999–1007, 2005.

[96] Y. He, G.-P. Liu, D. Rees, and M. Wu, "Improved stabilisation method for networked control systems," *IET Contr. Theory Appl.*, vol. 1, no. 6, pp. 1580–1585, 2007.

[97] H. Gao and T. Chen, "A new delay system approach to network-based control," *Automatica*, vol. 44, no. 1, pp. 39–52, 2008.

[98] D. Yue, Q.-L. Han, and C. Peng, "State feedback controller design of networked control systems," *IEEE Trans. Circuits Syst. II*, vol. 51, no. 11, pp. 640–644, 2004.

[99] H. Gao and T. Chen, "Network-based $\mathcal{H}_\infty$ output tracking control," *IEEE Trans. Autom. Contr.*, vol. 53, no. 3, pp. 655–667, 2008.

[100] J. Yu, L. Wang, and M. Yu, "Switched system approach to stabilization of networked control systems," *Int. J. Robust Nonlinear Contr.*, in press, 2010.

[101] X. Jiang, Q.-L. Han, S. Liu, and A. Xue, "A new $\mathcal{H}_\infty$ stabilization criteria for networked control systems," *IEEE Trans. Autom. Contr.*, vol. 53, no. 4, pp. 1025–1032, 2008.

[102] W.-A. Zhang and L. Yu, "Modelling and control of networked control systems with both network-induced delay and packet-dropout," *Automatica*, vol. 44, no. 12, pp. 3206–3210, 2008.

[103] J. Xiong and J. Lam, "Stabilization of linear systems over networks with bounded packet loss," *Automatica*, vol. 43, no. 1, pp. 80–87, 2007.

[104] S. Hu and W.-Y. Yan, "Stability of networked control systems under a multiple-packet transmission policy," *IEEE Trans. Autom. Contr.*, vol. 53, no. 7, pp. 1706–1711, 2008.

[105] D. Huang and S. K. Nguang, "State feedback control of uncertain networked control systems with random time delays," *IEEE Trans. Autom. Contr.*, vol. 53, no. 3, pp. 829–834, 2008.

[106] X.-M. Sun, G.-P. Liu, W. Wang, and D. Rees, "Stability analysis for networked control systems based on average dwell time method," *Int. J. Robust Nonlinear Contr.*, vol. 20, no. 15, pp. 1774–1784, 2010.

[107] L. A. Montestruque and P. Antsaklis, "Stability of model-based networked control systems with time-varying transmission times," *IEEE Trans. Autom. Contr.*, vol. 49, no. 9, pp. 1562–1572, 2004.

[108] W.-A. Zhang and L. Yu, "A robust control approach to stabilization of networked control systems with time-varying delays," *Automatica*, vol. 45, no. 10, pp. 2440–2445, 2009.

[109] R. Wang, G.-P. Liu, W. Wang, D. Rees, and Y.-B. Zhao, "$\mathcal{H}_\infty$ control for networked predictive control systems based on the switched Lyapunov function method," *IEEE Trans. Ind. Electron.*, vol. 57, no. 10, pp. 3565–3571, 2010.

[110] M. Tabbara, D. Nešić, and A. R. Teel, "Stability of wireless and wireline networked control systems," *IEEE Trans. Autom. Contr.*, vol. 52, no. 9, pp. 1615–1630, 2007.

[111] Y.-B. Zhao, G.-P. Liu, and D. Rees, "Modeling and stabilization of continuous-time packet-based networked control systems," *IEEE Trans. Syst., Man, Cybern. B*, vol. 39, no. 6, pp. 1646–1652, 2009.

[112] D. Carnevale, A. R. Teel, and D. Nešić, "A lyapunov proof of an improved maximum allowable transfer interval for networked control systems," *IEEE Trans. Autom. Contr.*, vol. 52, no. 5, pp. 892–897, 2007.

[113] D. Nešić and A. R. Teel, "Input-output stability properties of networked control systems," *IEEE Trans. Autom. Contr.*, vol. 49, no. 10, pp. 1650–1667, 2004.

[114] G.-P. Liu, Y. Xia, D. Rees, and W. Hu, "Design and stability criteria of networked predictive control systems with random network delay in the feedback channel," *IEEE Trans. Syst., Man, Cybern. C*, vol. 37, no. 2, pp. 173–184, 2007.

[115] X. M. Sun, G. P. Liu, W. Wang, and D. Rees, "Stability analysis for networked control systems based on event-time-driven mode," *Int. J. Control*, vol. 82, no. 12, pp. 2260–2266, 2009.

[116] M. Shakeri, K. R. Pattipati, and D. L. Kleinman, "Optimal measurement scheduling for state estimation," *IEEE Trans. Aerospace Electronic Syst.*, vol. 31, no. 2, pp. 716–729, 1995.

[117] D. Huang and S. K. Nguang, "Robust fault estimator design for uncertain networked control systems with random time delays: An ILMI approach," *Inf. Sci.*

[118] D. Sauter, S. Li, and C. Aubrun, "Robust fault diagnosis of networked control systems," *Int. J. Adapt. Contr. Signal Process.*, vol. 23, no. 8, pp. 722–736, 2009.

[119] X. He, Z. Wang, Y. D. Ji, and D. H. Zhou, "Network-based fault detection for discrete-time state-delay systems: a new measurement model," *Int. J. Adapt. Contr. Signal Process.*, vol. 22, no. 5, pp. 510–528, 2008.

[120] M. Huang and S. Dey, "Stability of Kalman filtering with Markovian packet losses," *Automatica*, vol. 43, no. 4, pp. 598–607, 2007.

[121] H. Zhang, A. Saadat Mehr, and Y. Shi, "Improved robust energy-to-peak filtering for uncertain linear systems," *Signal Process.*, vol. 90, no. 9, pp. 2667–2675, 2010.

[122] H. Zhang, Y. Shi, and A. Saadat Mehr, "Robust weighted $\mathcal{H}_\infty$ filtering for networked systems with intermitted measurements of multiple sensors," *Int. J. Adapt. Contr. Signal Process.*, vol. 25, no. 4, pp. 313–330, 2011.

[123] ——, "Robust energy-to-peak filtering for networked systems with time-varying delays and randomly missing data," *IET Contr. Theory Appl.*, vol. 4, no. 12, pp. 2921–2936, 2010.

[124] B. Sinopoli, L. Schenato, M. Franceschetti, K. Poolla, M. I. Jordan, and S. S. Sastry, "Kalman filtering with intermittent observations," *IEEE Trans. Autom. Contr.*, vol. 49, no. 9, pp. 1453–1464, 2004.

[125] V. Gupta, T. H. Chung, B. Hassibi, and R. M. Murray, "On a stochastic sensor selection algorithm with applications in sensor scheduling and sensor coverage," *Automatica*, vol. 42, no. 2, pp. 251–260, 2006.

[126] A. S. Matveev and A. V. Savkin, "The problem of state estimation via asynchronous communication channels with irregular transmission times," *IEEE Trans. Autom. Contr.*, vol. 48, no. 4, pp. 670–676, 2003.

[127] S. C. Smith and P. Seiler, "Estimation with lossy measurements: Jump estimators for jump systems," *IEEE Trans. Autom. Contr.*, vol. 48, no. 12, pp. 2163–2171, 2003.

[128] N. Xiao, L. Xie, and M. Fu, "Kalman filtering over unreliable communication networks with bounded Markovian packet dropouts," *Int. J. Robust Nonlinear Contr.*, vol. 19, no. 16, pp. 1770–1786, 2009.

[129] W.-A. Zhang, L. Yu, and H. Song, "$\mathcal{H}_\infty$ filtering of networked discrete-time systems with random packet losses," *Inf. Sci.*, vol. 179, no. 22, pp. 3944–3955, 2009.

[130] L. Schenato, "Optimal estimation in networked control systems subject to random delay and packet drop," *IEEE Trans. Autom. Contr.*, vol. 53, no. 5, pp. 1311–1317, 2008.

[131] H. Gao and T. Chen, "$\mathcal{H}_\infty$ estimation for uncertain systems with limited communication capacity," *IEEE Trans. Autom. Contr.*, vol. 52, no. 11, pp. 2070–2084, 2007.

[132] B. Yu, Y. Shi, and Y. Lin, "Discrete-time $\mathcal{H}_2$ output tracking control of wireless networked control systems with Markov communication models," *Wireless Comm. Mob. Comput.*, in press, 2011.

[133] K. J. Åström and T. Hägglund, "The future of PID control," *Control Eng. Pract.*, vol. 9, no. 11, pp. 1163–1175, 2001.

[134] Karl J. Åström and Tore Hägglund, *PID Controllers: Theory, Design, and Tuning*. 2nd ed., Instrument Society of America, 1995.

[135] M. Ge, M.-S. Chiu, and Q.-G. Wang, "Robust PID controller design via LMI approach," *J. Process Contr.*, vol. 12, no. 1, pp. 3–13, 2002.

[136] F. Zheng, Q.-G. Wang, and T. H. Lee, "On the design of multivariable PID controllers via LMI approach," *Automatica*, vol. 38, no. 3, pp. 517–526, 2002.

[137] C. Lin, Q.-G. Wang, and T. H. Lee, "An improvement on multivariable PID controller design via iterative LMI approach," *Automatica*, vol. 40, no. 3, pp. 519–525, 2004.

[138] Y. He and Q.-G. Wang, "An improved ILMI method for static output feedback control with application to multivariable PID control," *IEEE Trans. Autom. Contr.*, vol. 51, no. 10, pp. 1678–1683, 2006.

[139] L. S. Lim and Y. Il Lee, "Design of discrete-time multivariable PID controllers via LMI approach," in *International Conference on Control, Automation and System*, Seoul, Korea, 2008, pp. 1867–1871.

[140] X.-L. Zhu and G.-H. Yang, "State feedback controller design of networked control systems with multiple-packet transmission," *Int. J. Control*, vol. 82, no. 1, pp. 86–94, 2009.

[141] Y. Shi, H. Fang, and M. Yan, "Kalman filter based adaptive control for networked systems with unknown parameters and randomly missing outputs," *Int. J. Robust Nonlinear Contr.*, vol. 19, no. 18, pp. 1976–1992, 2009.

[142] L. Eriksson and H. N. Koivo, "Tuning of discrete-time PID controllers in sensor network based control systems," in *Proceedings of the 6th IEEE International Symposium on Computational Intelligence in Robotics and Automation*, Espoo, Finland, 2005.

[143] L. E. Mikael Pohjola and H. Koivo, "Tuning of PID controllers for networked control systems," in *Proceedings of the 32nd Annual Conference of the IEEE Industrial Electronics Society*, Paris, France, 2006, pp. 4650–4655.

[144] P. J. de Oliveira, R. C. L. F. Oliveria, V. J. S. Leite, V. F. Montagner, and P. L. D. Peres, "$\mathcal{H}_\infty$ guanranteed cost computation by means of parameter-dependent Lyapunov functions," *Automatica*, vol. 40, no. 6, pp. 1053–1061, 2004.

[145] Z. Duan, J. Zhang, C. Zhang, and E. Mosca, "Robust $\mathcal{H}_2$ and $\mathcal{H}_\infty$ filtering for uncertain linear systems," *Automatica*, vol. 42, no. 11, pp. 1919–1926, 2006.

[146] S.-J. Kim, Y.-H. Moon, and S. Kwon, "Solving rank-constrained LMI problems with application to reduced-order output feedback stabilization," *IEEE Trans. Autom. Contr.*, vol. 52, no. 9, pp. 1737–1741, 2007.

[147] Y. He, M. Wu, G.-P. Liu, and J.-H. She, "Output feedback stabilization for a discrete-time system with a time-varying delay," *IEEE Trans. Autom. Contr.*, vol. 53, no. 10, pp. 2372–2377, 2008.

[148] L. El Ghaoui, F. Oustry, and M. AitRami, "A cone complementarity linearization algorithm for static output-feedback and related problems," *IEEE Trans. Autom. Contr.*, vol. 42, no. 8, pp. 1171–1176, 1997.

[149] R. Orsi, U. Helmke, and J. B. Moore, "A newton-like method for solving rank constrained linear matrix inequalities," *Automatica*, vol. 42, no. 11, pp. 1875–1882, 2006.

[150] L. H. Keel, S. P. Bhattacharyya, and J. W. Howze, "Robust control with structure perturbations," *IEEE Trans. Autom. Contr.*, vol. 33, no. 1, pp. 68–78, 1988.

[151] Y.-Y. Cao, J. Lam, and Y.-X. Sun, "Static output feedback stabilization: An ILMI approach," *Automatica*, vol. 34, no. 12, pp. 1641–1645, 1998.

[152] B. Yu, Y. Shi, and J. Huang, "Step tracking control with disturbance rejection for networked control systems with random time delays," in *Proc. 48th IEEE Conf. Decision Control*, Shanghai, China, 2009, pp. 4951–4956.

[153] G.-P. Liu, "Predictive controller design of networked systems with communication delays and data loss," *IEEE Trans. Circuits Syst. II*, vol. 57, no. 6, pp. 481–485, 2010.

[154] R. Wang, B. Wang, G.-P. Liu, W. Wang, and D. Rees, "$\mathcal{H}_\infty$ controller design for networked predic control systems based on the average dwell-time approach," *IEEE Trans. Circuits Syst. II*, vol. 57, no. 4, pp. 310–314, 2010.

[155] L. Zhang and E.-K. Boukas, "Mode-dependent $\mathcal{H}_\infty$ filtering for discrete-time Markovian jump linear systems with partly unknown transition probabilities," *Automatica*, vol. 45, no. 6, pp. 1462–1467, 2009.

[156] ——, "Stability and stabilization of Markovian jump linear systems with partly unknown transition probabilities," *Automatica*, vol. 45, no. 2, pp. 463–468, 2009.

[157] A. P. C. Goncalves, A. R. Fioravanti, and J. C. Geromel, "Filtering of discrete-time Markov jump linear systems with uncertain transition probabilities," *Int. J. Robust Nonlinear Contr.*, vol. 21, no. 6, pp. 613–624, 2011.

[158] R. M. Palhares and P. L. D. Peres, "Robust filtering with guaranteed energy-to-peak performance-an LMI approach," *Automatica*, vol. 36, no. 6, pp. 851–858, 2000.

[159] H. Gao and C. Wang, "Robust energy-to-peak filtering with improved LMI representation," *IEE Proc.-Control Theory Appl.*, vol. 150, no. 2, pp. 82–89, 2003.

[160] T. Takagi and M. Sugeno, "Fuzzy identification of systems and its applications to modeling and control," *IEEE Trans. Syst., Man, Cybern.*, vol. 15, no. 1, pp. 116–132, 1985.

[161] J. Zhang and Y. Xia, "New LMI approach to fuzzy $\mathcal{H}_\infty$ filter designs," *IEEE Trans. Circuits Syst. II*, vol. 56, no. 9, pp. 739–743, 2009.

[162] H. Gao, Y. Zhao, and T. Chen, "$\mathcal{H}_\infty$ fuzzy control of nonlinear systems under unreliable communication links," *IEEE Trans. Fuzzy Syst.*, vol. 17, no. 2, pp. 265–278, 2009.

[163] K. Tanaka and H. O. Wang, *Fuzy Control Systems Design and Analysis: A Linear Matrix Inequality Approach.* New York: Wiley, 2001.

[164] S. K. Nguang and P. Shi, "$\mathcal{H}_\infty$ fuzzy output feedback control design for nonlinear systems: An LMI approach," *IEEE Trans. Fuzzy Syst.*, vol. 11, no. 3, pp. 331–340, 2003.

[165] H. Dong, Z. Wang, D. W. C. Ho, and H. Gao, "Robust $\mathcal{H}_\infty$ fuzzy output-feedback control with multiple probabilistic delays and multiple missing measurements," *IEEE Trans. Fuzzy Syst.*, vol. 18, no. 4, pp. 712–725, 2010.

[166] H. Gao, X. Liu, and J. Lam, "Stability analysis and stabilization for discrete-time fuzzy systems with time-varying delay," *IEEE Trans. Syst., Man, Cybern. B*, vol. 39, no. 2, pp. 306–317, 2009.

[167] H. Gao, Y. Zhao, J. Lam, and K. Chen, "$\mathcal{H}_\infty$ fuzzy filtering of nonlinears ystems with intermittent measurements," *IEEE Trans. Fuzzy Syst.*, vol. 17, no. 2, pp. 291–300, 2009.

[168] J. Qiu, G. Feng, and J. Yang, "A new design of delay-dependent robust $\mathcal{H}_\infty$ filtering for discrete-time T-S fuzzy systems with time-varying delay," *IEEE Trans. Fuzzy Syst.*, vol. 17, no. 5, pp. 1044–1058, 2009.

[169] G. Feng, M. Chen, D. Sun, and T. Zhang, "Approaches to robust filtering design of discrete time fuzzy dynamic systems," *IEEE Trans. Fuzzy Syst.*, vol. 16, no. 2, pp. 331–340, 2008.

[170] S.Kawamoto, "Nonlinear control and rigorous stability analysis based on fuzzy system for inverted pendulum," in *Proceedings of the Fifth IEEE International Conference on Fuzzy Systems*, vol. 2, 1996, pp. 1427–1432.

[171] R. E. Kalman, "A new approach to linear filtering and prediction problems," *Trans. ASME, J. Basic Eng.*, vol. 82, no. D, pp. 35–45, 1960.

[172] P. Neveux and G. Thomas, "Robust fltering for uncertain systems," *Signal Process.*, vol. 81, no. 4, pp. 809–817, 2001.

[173] K. A. Barbosa, C. E. de Souza, and A. Trofino, "Robust $\mathcal{H}_2$ filtering for uncertain linear systems: LMI based methods with parametric Lyapunov functions," *Syst. Contr. Lett.*, vol. 54, no. 3, pp. 251–262, 2005.

[174] P. Apkarian and P. Gahinet, "A convex characterization of gain-scheduled $\mathcal{H}_\infty$ controllers," *IEEE Trans. Autom. Contr.*, vol. 40, no. 5, pp. 853–864, 1995.

[175] B. Yu, Y. Shi, and H. Huang, "$l_2 - l_\infty$ filtering for multirate systems based on lifted models," *Circuits Syst. Signal Process.*, vol. 27, no. 5, pp. 699–711, 2008.

[176] U. Shaked, "$\mathcal{H}_\infty$-minimum error state estimation of linear stationary processes," *IEEE Trans. Autom. Contr.*, vol. 35, no. 5, pp. 554–558, 1990.

[177] M. Basin, P. Shi, D. Calderon-Alvarez, and J. Wang, "Central suboptimal $\mathcal{H}_\infty$ filter design for linear time-varying systems with state or measurement delay," *Circuits Syst. Signal Process.*, vol. 28, no. 2, pp. 305–330, 2009.

[178] W. M. McEneaney, "Robust/$\mathcal{H}_\infty$ filtering for nonlinear systems," *Syst. Contr. Lett.*, vol. 33, no. 5, pp. 315–325, 1998.

[179] S. Xu and P. V. Dooren, "Robust $\mathcal{H}_\infty$ filtering for a class of non-linear systems with state delay and parameter uncertainty," *Int. J. Control*, vol. 75, no. 10, pp. 766–774, 2002.

[180] N. E. Nahi, "Optimal recursive estimation with uncertain observation," *IEEE Trans. Inform. Theory*, vol. 15, no. 4, pp. 457–462, 1969.

[181] A. V. Savkin, I. R. Petersen, and S. O. R. Moheimani, "Model validation and state estimation for uncertain continuous-time systems with missing discrete-continuous data," *Comput. Electr. Eng.*, vol. 25, no. 1, pp. 29–43, 1999.

[182] A. S. Matveev and A. V. Savkin, "The problem of state estimation via asynchronous communication channels with irregular transmission times," *IEEE Trans. Autom. Contr.*, vol. 48, no. 4, pp. 670–676, 2003.

[183] Z. Wang, D. W. C. Ho, and X. Liu, "Variance-constrained filtering for uncertain stochastic systems with missing measurements," *IEEE Trans. Autom. Contr.*, vol. 48, no. 7, pp. 1254–1258, 2003.

[184] F. O. Hounkpevi and E. E. Yaz, "Robust minimum variance linear state estimators for multiple sensors with different failure rates," *Automatica*, vol. 43, no. 7, pp. 1274–1280, 2007.

[185] G. Wei, Z. Wang, and H. Shu, "Robust filtering with stochastic nonlinearities and multiple missing measurements," *Automatica*, vol. 45, no. 3, pp. 836–841, 2009.

[186] X. He, Z. Wang, and D. Zhou, "Robust $\mathcal{H}_\infty$ filtering for time-delay systems with probabilistic sensor faults," *IEEE Signal Process. Lett.*, vol. 16, no. 5, pp. 442–445, 2009.

[187] M. Yu, L. Wang, T. Chu, and F. Hao, "An LMI approach to networked control systems with data packet dropout and trasmission delays," in *Proc. 43th IEEE Conf. Decision Control*, Paradise Island, Bahamas, 2004, pp. 3545–3550.

[188] Z. Wang, F. Yang, D. W. C. Ho, and X. Liu, "Robust $\mathcal{H}_\infty$ filtering for stochastic time-delay systems with missing measurements," *IEEE Trans. Signal Process.*, vol. 54, no. 7, pp. 2579–2587, 2006.

[189] H. Song, L. Yu, and W.-A. Zhang, "$\mathcal{H}_\infty$ filtering of network-based systems with random delay," *Signal Process.*, vol. 89, no. 4, pp. 615–622, 2009.

[190] X. He, Z. Wang, and D. Zhou, "Robust $\mathcal{H}_\infty$ filtering for networked systems with multiple state delays," *Int. J. Control*, vol. 80, no. 8, pp. 1217–1232, 2007.

[191] M. Moayedi, Y. K. Foo, and Y. C. Soh, "Filtering for networked control systems with single/multiple measurement packets subject to multiple-step measurement delays and multiple packet dropouts," *International Journal of Systerms Science*, vol. 42, no. 3, pp. 335–348, 2011.

[192] Z. Wang, F. Yang, D. W. C. Ho, and X. Liu, "Robust $\mathcal{H}_\infty$ filtering for stochastic time-delay systems with missing measurements," *IEEE Trans. Signal Process.*, vol. 54, no. 7, pp. 2579–2587, 2006.

[193] H. Zhang, Y. Shi, A. Saadat Mehr, and H. Huang, "Robust energy-to-peak FIR equalization for time-varying communication channels with intermittent observations," *Signal Process.*, vol. 91, no. 7, pp. 1651–1658, 2011.

[194] H. Zhou, L. Xie, and C. Zhang, "A direct approach to $\mathcal{H}_2$ optimal deconvolution of periodic digital channels," *IEEE Trans. Signal Process.*, vol. 50, no. 7, pp. 1685–1698, 2002.

[195] P. Park and S. W. Yun, "Induced ∞-norm FIR filter for recovering MPSK-type modulus signals," *Signal Processing*, vol. 88, no. 11, pp. 2731 – 2737, 2008.

[196] V. Utkin, J. Guldner, and J. Shi, *Sliding Mode Control in Electromechanical Systems*. Boca Raton, FL: CRC Press, 1999.

[197] V. I. Utkin, "Sliding mode control design principles and applications to electric drives," *IEEE Trans. Ind. Electron.*, vol. 40, no. 1, pp. 23–36, 1993.

[198] S.-J. Huang and H.-Y. Chen, "Adaptive sliding controller with self-tuning fuzzy compensation for vehicle suspension control," *Mechatronics*, vol. 16, no. 10, pp. 607–622, 2006.

[199] Y. M. Sam, J. H. S. Osman, and M. R. A. Ghani, "A class of proportional-integral sliding mode control with application to active suspension system," *Syst. Contr. Lett.*, vol. 51, no. 3-4, pp. 217–223, 2004.

[200] V. Parra-Vega and G. Hirzinger, "Chattering-free sliding mode control for a class of nonlinear mechanical systems," *Int. J. Robust Nonlinear Contr.*, vol. 11, no. 12, pp. 1161–1178, 2001.

[201] L. Wu, P. Shi, and H. Gao, "State estimation and sliding-mode control of Markovian jump singular systems," *IEEE Trans. Autom. Contr.*, vol. 55, no. 5, pp. 1213–1219, 2010.

[202] L. Wu and D. W. C. Ho, "Sliding mode control of singular stochastic hybrid systems," *Automatica*, vol. 46, no. 4, pp. 779–783, 2010.

[203] J.-L. Chang, "Robust discrete-time model reference sliding-mode controller design with state and disturbance estimation," *IEEE Trans. Ind. Electron.*, vol. 55, no. 11, pp. 4065–4074, 2008.

[204] N. O. Lai, C. Edwards, and S. K. Spurgeon, "On output tracking using dynamic output feedback discrete-time sliding-mode controllers," *IEEE Trans. Autom. Contr.*, vol. 52, no. 10, pp. 1975–1981, 2007.

[205] H. H. Choi, "On the existence of linear sliding surfaces for a class of uncertain dynamic systems with mismatched uncertainties," *Automatica*, vol. 35, no. 10, pp. 1707–1715, 1999.

[206] L. Wu and W. X. Zheng, "Passivity-based sliding mode control of uncertain singular time-delay systems," *Automatica*, vol. 45, no. 9, pp. 2120–2127, 2009.

[207] S. Z. Sarpturk, Y. Istefanopulos, and O. Kaynak, "On the stability of discrete-time sliding mode control systems," *IEEE Trans. Autom. Contr.*, vol. 32, no. 10, pp. 930–932, 1987.

[208] L. Ma, Z. Wang, Y. Niu, Y. Bo, and Z. Guo, "Sliding mode control for a class of nonlinear discrete-time networked systems with multiple stochastic communication delays," *Int. J. Syst. Sci.*, vol. 42, no. 4, pp. 661–672, 2011.

[209] W. Gao, Y. Wang, and A. Homaifa, "Discrete-time variable structure control systems," *IEEE Trans. Ind. Electron.*, vol. 42, no. 2, pp. 117–122, 1995.

[210] A. Bartoszewicz, "Remarks on discrete-time variable structure control systems," *IEEE Trans. Ind. Electron.*, vol. 43, no. 1, pp. 235–238, 1996.

[211] S. Hui and S. H. Źak, "On discrete-time variable structure sliding mode control," *Syst. Contr. Lett.*, vol. 38, no. 4-5, pp. 283–288, 1999.